European Journal of Anatomy

Volume 27 - Number 4 July 2023

ORIGINAL ARTICLES

CASE REPORTS

TEACHING IN ANATOMY

Gross congenital abnormalities induced by leflunomide in mice embryos

Krishna Pandey[1], Nishtha Singh[1], Amit Nayak[2], C. Mohanty[2]

[1] *Department of Anatomy, MLNMC, Prayagraj, India*
[2] *Department of Anatomy IMS, BHU, Varanasi, India*

SUMMARY

Leflunomide is an antirheumatic drug commonly used by females, as this disease is common in females and there are chances of pregnancy while taking this medication in initial months of pregnancy this commonly prescribed drug lacks studies related to its teratogenic potential. Present study was conducted to know about its teratogenicity in mice embryos. Pregnant mice were exposed to Leflunomide by oral route on gestational days 6 to 11 either as single dose in one of the gestational days or continuous doses. The embryos were collected on day 19 of gestation, were measured and examined for external anomalies. Findings suggested that Leflunomide was embryo lethal when given as continuous dose as there were 100% resorption of embryos. In the single dose group, maximum resorptions were found when was given in early pregnancy. Other anomalies included malrotated limbs, open eyes, kinking of tails, defect in anterior abdominal wall and visceroptosis and anencephaly. these anomalies were noted in embryos exposed to leflunomide only on gestational days 7 and 8.

The above findings suggest that leflunomide interferes with embryonic growth It also interferes with neural tube closure leading to anencephaly. Findings of open eyes and kinking tails suggest that the drug may affect epithelial and mesodermal growth. Leflunomide perhaps interferes with the lateral folding of the embryo leading to defect in the anterior abdominal wall and visceroptosis. The present study concludes that Leflunomide is teratogenic and embryolethal in mice and should be avoided in human pregnancy.

Key words: Leflunomide – Teratology – Gestation age – Malformation – Resorption

INTRODUCTION

Leflunomide is a disease modifying antirheumatic drug that has been approved by food and drug administration for the treatment of rheumatoid arthritis, approval was based on data from a double-blind, multicentre trials in the United States in which leflunomide was superior to placebo and similar to methotrexate (Strand et al., 1999). Leflunomide is a novel isoxazole immunomodulatory agent that inhibits de novo pyrimidine synthesis and is also having anti proliferative activity. After oral administration, it is rapidly metabolized to an active metabolite (A77 1726), possibly in the gut wall, plasma and in the liver, which is presumed to be the active drug in vivo. No epidemiological studies have been completed with regard to the teratogenicity of lefluno-

Corresponding author:
Dr. Krishna Pandey. Department of Anatomy, MLNMC, Prayagraj-211002, India. Phone: 8933976025. E-mail: kp260683@gmail.com

Submitted: December 10, 2022. **Accepted:** February 6, 2023

https://doi.org/10.52083/WNEI1659

mide, since the drug was introduced in 1998. Of the few women who have been exposed during pregnancy, most have decided to interrupt their pregnancies. The pharmacokinetic level of the active metabolite of leflunomide reached clinically in humans is in the range of exposure that results in teratogenesis in the rat and rabbit. It is evident that leflunomide effects vary with species and it appears that the rat and rabbit are more sensitive to leflunomide inhibition of pyrimidine synthesis. But it is difficult to predict that metabolic difference into differences in teratogenic potential, because studies related to leflunomide's effect on the human embryo is lacking. Therefore, the conservative approach is to be considered and it is presumed that therapeutic blood levels of the active metabolite of leflunomide represent a teratogenic risk (Brent, 2001). Approximately 500 and 1500 patients in New Zealand have been prescribed leflunomide, up to the end of 2003 (Aventis Pharma Pvt Ltd, 2004). The adverse reactions reported in New Zealand for this medicine are similar to those seen internationally. Examples of the more serious local cases include:

- Elevated hepatic enzymes, along with neutropenia, thrombocytopenia and diarrhoea.
- Sepsis leading to multi-organ failure and death; concomitant medicines were methotrexate, ketoprofen and triamcinolone.
- Hypersensitivity pneumonitis, resulting in life-threatening respiratory compromise. The patient was taking leflunomide and methotrexate but did not relapse when methotrexate was re-introduced.
- Multiple bullous eruptions occurring within three weeks of starting leflunomide, and resolving upon discontinuation.
- In spite of the clear warning that the drug should not be prescribed for pregnant women, approximately 30% women have become pregnant while taking leflunomide as of December 1999 (Brent, 1999).
- In reproduction studies with pregnant rats during organogenesis, Leflunomide was reported to be teratogenic (anophthalmia or microphthalmia and internal hydrocephalus). This also resulted in an increase in embryo death and a decrease in maternal and surviving embryo body weight. However, the reports are only few. The present study aims to elucidate the different teratological outcome of leflunomide, its mechanism of teratogenesis in the developing organs exposed to Leflunomide in pregnant mice.

MATERIAL AND METHODS

Forty-eight female albino mice of an average weight of 25-30 g and an average age of 80-100 days weeks were used in this study. Institutional Ethical committee approval was obtained before starting this study. Animals were housed in separate plastic cages in animal house on a light dark cycle of 12:12 hours. Mice were fed on diet pellets (Hindustan Liver Ltd, Mumbai, India) and tap water *ad libitum* and were treated with utmost aseptic care. Female mice were kept overnight with the males of same stock (female: male 3:1) at 16 hrs. In the next morning the vaginal smear was examined and if the presence of sperms was found in the smear it was considered as day "Zero" of pregnancy. The pregnant mice were weighed and kept individually in separate cages, date of pregnancy and weight of the pregnant mice was worked on the cage.

The leflunomide was administered orally with the help of sterile syringe either as single or continuous dose. The single dose was 50 mg/ kg body weight/day and continuous dose was 15 mg/ kg body weight/day from day 6-11 of gestation. Control mice were given equal volumes of normal saline. The pregnant mice were sacrificed with an overdose of ether anaesthesia on day 19 of pregnancy. The uterine horns were exteriorized after opening the abdomen by midline incision. The sacs were inspected for sites of resorption and viable embryos. The embryos were removed from the uterus and blotted on blotting paper. The weight and CRL of the embryo were recorded. These were examined for external abnormalities like cleft palate, limb and tail abnormalities. Embryo were fixed in 10% formalin solution and were preserved for histological examination. Controls were given equal volumes of normal saline. Anterior abdominal wall of the embryos was opened. The liver, lungs, kidney, heart and brain were dissected out and were examined for external mal-

formations. All the organs were washed and fixed in buffered formalin for tissue processing.

Experimental groups

Each group were having 6 pregnant mice, total 48 pregnant albino mice were taken for study.

Group A: (Control) received equal volume of normal saline.

Group B: 50 mg/kg single dose on gestational day 6 (GD 6).

Group C:50 mg/kg single dose on gestational day 7 (GD 7).

Group D: 50 mg/kg single dose on gestational day 8 (GD 8).

Group E: 50 mg/kg single dose on gestational day 9 (GD 9).

Group F: 50 mg/kg single dose on gestational day 10 (GD 10).

Group G: 50 mg/kg single dose on gestational day 11 (GD 11).

Group H: 15 mg/kg/ once a day as continuous dose from GD-6 to GD-11.

Statistical analyses

Data has been entered into an excel spread sheet. Mean, standard deviation and standard error were calculated.

RESULTS

Various gross congenital abnormalities were reported in our study.

Resorption of embryos

The rate of resorption in different treated groups are depicted in Table 1, Fig. 1. The resorption rate was around 67% when the pregnant mice were exposed to leflunomide on GD6. The resorption rate decreased to 50% on GD7 and 25% on GD8. However, there was no resorption when the mice were exposed to leflunomide on GD9, GD 10 and GD11 and in the control group. On the contrary, all the embryos were resorbed when the pregnant mice were exposed continuously from GD6 to GD11. Total implantation sites including resorptions (Table 1) were counted on pregnant mice in every group. Uterine implantations were ranging from minimum of 3 to maximum of 11 sites in different groups.

Table 1. Total implantation sites including rate of resorptions in the different groups.

Group	Total number of implantations/ Number of implantations in each pregnant mice	Resorption/ Implantations (Resorption %)
Group A – Control	41 7,6,7,5,7,9	0 %
Group B – GD-6	24 3,5,4,4,3,5	16 (66.6%)
Group C – GD-7	30 4,3,7,8,4,4	15(50%)
Group D – GD-8	32 6,5,5,8,5,3	8(25)
Group E – GD-9	35 7,4,3,8,9,4	35 (0%)
Group F – GD-10	40 11,9,8,5,5,2	40 (0%)
Group G – GD-11	40 10,7,8,5,6,4	40 (0%)
Group H – GD-6-11	0	0 (100%)

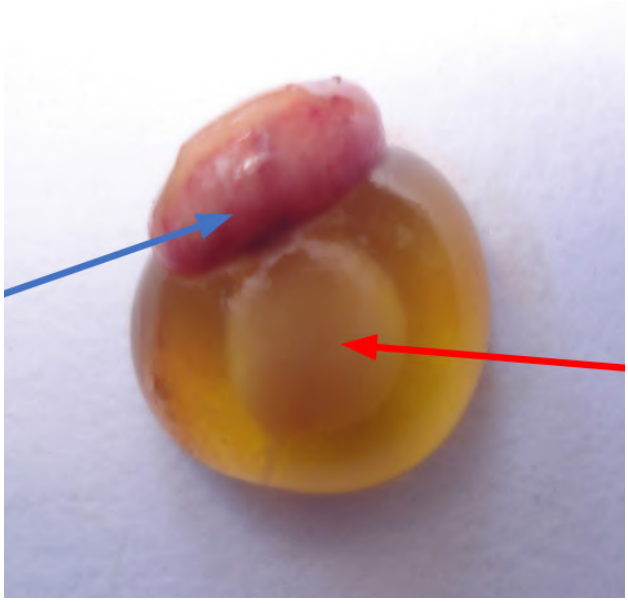

Fig. 1.- Fetal resorption Sac (red arrow - fetal resorption, blue arrow- placental site).

Fetal parameters (length & weight)

The mean embryonal weight in various treated groups ranged between 1.33 to 1.69 g, while the mean weight in control group was 2.11 g. There was significant reduction in weight of the treated embryos (p value<0.001). The treated embryos were also markedly reduced in size, as compared to the control group (p<0.001). Mean CR length in control group was 1.02 cm. while it ranged between 0.63 to 0.86 cm in different treated groups.

Gross malformations (Table 2)

- Large number of embryos showed haemorrhages either on forepaw or hind paw. About 52% embryos showed haemorrhages over forepaw while 58% showed haemorrhages over hind paw, when the pregnant mice were exposed to leflunomide on different gestational days. The forepaw haemorrhage rate ranged between 100% on GD6 to 40% on GD7. Similarly, the hind paw haemorrhage rates ranged from 75% on GD6 to 46.6% on GD7 (Table 2).
- Malrotated hindlimbs were found in 4.9 % embryos (Table 2). However, the findings were only confined to GD7 (20%) and GD8 (20.8%) groups.
- Open eye has been found in 3.7% embryos (Table 2) and confined to GD8 group.
- Kinking of tail was found in 2.4% embryos and only found in GD8 group (16.6%).
- Anterior abdominal wall defect and visceroptosis was found in 1.2% embryos and was limited to GD7 group (13.3%) (Table 2) (Fig. 1).
- Similarly, anencephaly was noted in 1.2% embryos and limited to GD7 group (13.3%). (Table 2, Fig. 1).

Gross examination of viscera

Brain, lung, kidney and liver were markedly reduced in size as compared to that of control group.

DISCUSSION

Fetal parameters (weight & length)

Growth retardation has been widely accepted as an expression of maldevelopment in both human beings (Grovenwald, 1961) and experimental animals (Mc Laren and Michie, 1960; Jensh and Brent, 1967; Wilson, 1973).

We reported significant reduction in the weight of exposed embryos. Fukushima et al. (2007, 2009) reported reduction in maternal as well as embryonic weight in leflunomide exposed mice. The embryonic weights were especially low when exposed on gestational day 7 and 9. The authors (Fukushima et al., 2009) demonstrated that the single administration of leflunomide on GD7, GD8 or GD9 caused severe embryo toxicity and reduced intrauterine growth. In our study, there were significant body weight reductions which suggests that leflunomide has a potential to affect the embryonic growth.

Skeletal malformations

Fukushima et al. (2009) reported 100% skeletal malformations in leflunomide treated embryos, and multiple malformations were reported such

Table 2. Various external malformations observed in leflunomide exposed mice fetuses.

MALFORMATION	Group B GD-6 8	Group C GD-7 15	Group D GD-8 24	Group E GD-9 35	Group F GD-10 40	Group G GD-11 40	Total malformed fetuses / Total no. of fetuses examined
Haemorrhage on forepaw	8(100%)	6(40%)	10(41.6%)	18(51.4%)	22(55%)	20(50%)	84/162(51.8)
Haemorrhage on hindpaw	6(75%)	7(46.6%)	12(50%)	19(54.2%)	20(50%)	30(75%)	94/162(58%)
Malrotated hind limbs		3(20%)	5(20.8%)				8(4.9%)
Kinking of tail			4(16.6)				42.46%)
Anterior abdominal wall defect & Visceroptosis		2(13.3)					2(1.23)
Anencephaly		2(13.3)					2(1.23%)
Open eye			6(25%)				6(3.70%)

as absent palatine bone and deformities of the skull bone, cervical to lumbar vertebrae, forelimb, ischium/pubis, and hindlimb were seen at significantly higher frequencies than in the control group. However, in the present study, no skeletal malformations were noted observed after alizarin staining to colour bones and cartilages. Only 2 embryos showed anencephaly when exposed to leflunomide on GD7. Absence of significant skeletal anomalies is difficult to explain in our study. It could be due to different doses used or due to species difference. Cleft lip and cleft palate were not observed in the present study but it has been reported by Fukushima et al. (2009).

In the present study, all the embryos were resorbed when the pregnant mice were exposed to leflunomide continuously from GD 6 to GD11. Fukushima et al. (2007), observed that at 70 mg/kg, all embryos were resorbed, and at 30 mg/Kg, leflunomide reduced embryonic viability and increased the incidence of multiple external malformations. These observations suggests that leflunomide has potential to affect growth and in continuous dosing it can completely stop embryonal development resulting in resorptions.

Visceral malformations

In previous study by Fukushima et al. (2009) the incidence of embryos with visceral malformations in the groups treated with leflunomide was significantly higher than that in control group. The malformations included membranous ventricular septal defects, overriding of aorta and diaphragmatic hernia. Other malformations included hydrocephaly, absent rhinencephalon, mishappen retina, right sided aortic arch, persistent truncus arteriosus, small thymus, absent accessory lobe of the lung, hydronephrosis and retrocaval ureter. In our study, small sized kidney, Liver, Lung and brain were observed.

External malformations

In the present study, majority of embryos showed malformations, predominantly haemorrhages on forelimb and hindlimbs, followed by malrotated limbs, open eye, kinking of tail, anterior abdominal wall defect along with visceroptosis and anencephaly. However, the haemorrhage rate was much higher in our study as compared to those observed by Fukushima et al. (2009). Ob-

Fig. 2.- Anencephaly (blue arrow) with visceroptosis (red arrow).

served haemorrhages on forepaw and hindpaw in maximum number of mice embryos from GD6-11 (84 and 94 respectively). In previous study by Fukushima et al. (2009) hematoma was observed in 2/40 embryos on GD9,15/84 embryos on GD10 and 5/104 embryos on GD11. Since this drug inhibits de novo pyrimidine synthesis producing toxicities in organs where rapidly proliferating cells are located such as haematopoietic system, immune system, pancreas and developing embryos. Observed haemorrhages in embryos could be due to toxic effects on bone marrow.

Malrotated hind limbs were observed on GD7 & GD8 in 3 & 5 embryos respectively. In previous study by Fukushima et al. (2009) anomalies of hind limb were reported on GD6 & GD10 in 1 & 10 embryos respectively. These results show that this drug affects skeletal development also.

We observed open eye in 6 embryos on GD8 treated group. In previous study by Fukushima et al. (2009) it was observed in 7 embryos on GD11. This defect shows that leflunomide has a potential to affect developing epithelium.

Kinking of tail was observed in 4 embryos on GD8, in previous study by Fukushima et al. (2009) it was observed in 5, 48 and 63 embryos on GD9, GD10 & GD11 respectively. In another study by Fukushima et al. (2009) its overall incidence was 63.3±28.5(38/62). Kinking of tail may be due to defect in musculature of tail, which is mesodermal in origin so it is hypothesized that this drug has effect on development of mesoderm also.

Anencephaly was observed in 2 embryos on GD7 (Fig. 2) treated group. In previous study by Fukushima et al. (2009) incidence of exencephaly was (12.5±25.0) reported on GD7 (1 out of total 12 examined). These results show that this drug has effect on embryonic neural tube closure during early embryonic stages.

Anterior abdominal wall defect along with visceroptosis was observed in 2 cases on GD7 (Fig. 2) this has not been reported previously in literature. Probable mechanism of action of leflunomide producing this defect may be due to producing disturbance in the lateral folding of embryo resulting in defective closure of anterior abdominal wall. Fukushima et al. (2009) stated that leflunomide is a proven teratogen in rats, rabbits and mice, it inhibits de novo pyrimidine nucleotide synthesis by inhibiting enzymes tyrosine kinase and dihydroorotate dehydrogenase (DHODH) leading to its embryotoxic and teratogenic influences. Its immunosuppressive effect also occurs via inhibition of these enzymes. Inhibition of de novo pyrimidine synthesis can be attributed to teratogenicity via the anti-proliferative activity of Leflunomide on embryonic cells. It is evident that leflunomide effects vary with the species, and it appears that the rat and rabbit are more sensitive to leflunomide inhibition of pyrimidine synthesis (Brent, 2001). Women who become pregnant while taking leflunomide are at risk of reproductive effects based on studies on rats and rabbit, because pharmacokinetic level of the active metabolite (A77 1726) of leflunomide reach clinically in humans in the range of exposure that results in teratogenesis in rat and rabbit.

ACKNOWLEDGEMENTS

It is my proud privilege to express my deepest sense of respect and gratitude to Dr. C. Mohanty, Professor, Department of Anatomy, IMS, BHU Prof. S.N. Shamal, Department of Anatomy Prof. IMS, BHU and Prof. S.K. Pandey Department of Anatomy, IMS, BHU, Varanasi for their guidance and support.

REFERENCES

AVENTIS PHARMA PTY LIMITED (2004) (Sponsor of Arava®) Data supplied, Australia in April 2004.

BRENT RL (1999) Utilization of developmental basic science principles in the evaluation of reproductive risks from pre- and postconception environmental radiation exposures. Presented at the 33th Annual Meeting of the National Council on Radiation Protection and Measurements. *The effects of pre- and postconception exposure to radiation*, April 2-3, 1997, Arlington, Virginia. *Teratology*, 59: 182-204.

BRENT RL (2001) Teratogen update: reproductive risks of leflunomide (Arava®); a pyrimidine synthesis inhibitor: counselling women taking leflunomide before or during pregnancy and men taking leflunomide who are contemplating fathering a child. *Teratology*, 63: 10612.

FOX RI, HERRMANN ML, FRANGOU CG, WAHL GM, MORRIS RE, STRAND V, KIRSCHBAUM BJ (1999) Mechanism of action for leflunomide in rheumatoid arthritis. *Clin Immunol*, 93(3): 198-208.

FUKUSHIMA R, KANAMORI S, HIRASHIBA M, HISHIKAWA A, MURANAKA R, KANETO M, KITAGAWA H (2007) Teratogenicity study of the dihydroorotate-dehydrogenase inhibitor and protein tyrosine kinase inhibitor leflunomide in mice. *Reprod Toxicol*, 24: 310-316.

FUKUSHIMA R, KANAMORI S, HIRASHIBA M, HISHIKAWA A, MURANAKA R, KANETO M, KITAGAWA H (2009) Critical periods for the teratogenicity of immune-suppressant leflunomide in mice. *Congenital Anomalies*, 49: 20-26.

JENSH RD, BRENT RL (1967) An analysis of the growth retarding effect of Trypan blue in the albino rat. *Anat Rec*, 159(4): 453-458.

MCLAREN, MICHIE D (1960) Congenital roots. In: Wolesterhome GEN, O'Connor CM (eds). *Ciba Foundation Symposium on Congenital Malformations*. Little Brown Company, Boston, pp 178-194.

WILSON (1973) Environment and birth defects. Academic Press, New York and London.

Variations in corpus and ramus measurements based on gonial angles in adult complete dentate mandibles

Ken Hiratsuka [a, 1], **Shigeo Osato** [a, 2]

[a] *Former Department of Oral Anatomy, The Nippon Dental University, School of Dentistry at Tokyo, 1-9-20 Fujimi, Chiyoda-ku, Tokyo 102-8159, Japan*

[1] *Hiratsuka Dental Clinic, #101, 1-16-8, Honcho, Toda, Saitama, 335-0023, Japan*

[2] *dento-Oral Science Institute, #2F Fukuoka 3rd Bldg, 1-4-7, Iidabashi, Chiyoda-ku, Tokyo, 102- 0072, Japan*

SUMMARY

This study aimed to reveal differences in the mandibular corpus and ramus measurements, volume (VOM), and gross weight of the mandible (GWOM) between the low and high gonial angles (L-GA and H-GA, respectively) in adult mandibles, and to evaluate the correlations between GAs and the measurement variables. Twenty-nine dried adult human complete dentate mandibles (L-GA ≤ 120°: 13 mandibles; H-GA: 125° ≥ GA: 16 mandibles) were measured using a lateral radiograph image-processing system, digital Vernier calipers, and an electric balance. The total length of the mandible (TLOM), corpus length (mental foramen–gonion [MeF'-Go'], mental foramen–mandibular foramen [MeF'-MaF'], and mandibular foramen–gonion [MaF'-Go']), inter-ramus (bicondylar, bicoronion, and bigonion) widths (BiCoW, BiCorW, and BiGoW), GA width (GAW), condylar perpendicular height (CPH), the VOM, and GWOM were measured. Data were assessed using the exact binomial test, Mann–Whitney U test and Pearson's correlation coefficient test. The MeF'-Go' and MaF'-Go', three inter-ramus widths, GAW, CPH, VOM, and GWOM in the L-GA group were significantly larger than those in the H-GA group. Significant negative correlations were found between GA size and multiple variables other than TLOM and BiCorW. Therefore, GA size was closely related to the enlarged morphometric dimensions of both the GA and the mandibular ramus in the posterior region of the mandibular corpus, as well as the volume and weight of the mandible, but it was not related to TLOM. These results indicate that the evaluation of GA size is useful for strategic dental treatment.

Key words: Forensic anthropology – Gonial angle – Lateral mandibular radiograph – Mandibular measurement – Mandibular volume and weight

INTRODUCTION

Over a person's lifetime, each area of the maxillofacial complex undergoes numerous changes. The morphological variations of the gonial angle (GA) depend on tooth growth (Larrazabal-Moron

Corresponding author:
Shigeo Osato. dento-Oral Science Institute, #2F Fukuoka 3rd Bldg, 1-4-7, Iidabashi, Chiyoda-ku, Tokyo, 102-0072, Japan. E-mail: osato-s@giga.ocn.ne.jp

Submitted: September 30, 2022. **Accepted:** February 14, 2023

https://doi.org/10.52083/AWYM4087

and Sanchis-Gimeno, 2018), aging (Leversha et al., 2016; Larrazabal-Moron and Sanchis-Gimeno, 2018), loss of teeth (Xie and Ainamo, 2004), presence or absence of dentures, and period of denture installation (Yanikoglu and Yilmaz, 2008).

The size of GA of the mandible is larger in women than in men (Huumonen et al., 2010; Joo et al., 2013; Fouda et al., 2019) and is more obtuse in edentulous patients than in dentulous patients (Xie and Ainamo, 2004; Huumonen et al., 2010; Joo et al., 2013). GA size is closely related to the functions of the masseter and internal pterygoid muscles, and is also affected by occlusal force (Kiliaridis et al., 1995; Sondang et al., 2003; Miwa et al., 2019). Notably, dentate patients with a small GA have well-developed masseter muscles. In addition, patients with a small GA have large mandibular cortical widths below the mandibular mental foramen (MeF) (Osato et al., 2012). Recently, the correlation of GA size with the prevalence of impacted lower third molars (Barone et al., 2021), frequency of mandibular and dental implant appliance fractures (Dhara et al., 2019; Murakami et al., 2020), and apnea syndrome severity (Gurgel et al., 2022) have been reported.

Many studies on GA size have been performed using lateral cephaloradiography (Sondang et al., 2003), dental panoramic radiography (DPR), and anatomohistological examination (Kingsmill and Boyde, 1998). Furthermore, a three-dimensional morphometric study using cone-beam computed tomography (CBCT) has been reported (Fouda et al., 2019). However, an electronic literature search did not find any studies on morphological changes in the body and mandibular ramus of the complete adult dentate mandible based on GA size. Therefore, this study was designed to identify areas in which morphological differences between the low and high GA groups (L-GA and H-GA, respectively) occur.

The purpose of this study was to investigate the GA-related morphometric differences in the mandibular corpus and ramus, bone weight, and the density of the adult complete dentate mandibles, as well as to evaluate correlations between the GA size and measurement variables.

MATERIALS AND METHODS

Twenty-nine dried adult human complete dentate mandibles that met the selection criteria for this investigation were used. The mandibles were selected and separated from several adult skull specimens of Indian origin. Indian adult specimens were used, because it was difficult to find Japanese specimens that met similar selection criteria. The upper and lower dentitions of these skull specimens had normal eruption of 32 permanent teeth, and normal dentition and occlusion. The skulls were collected in and around Kolkata from the early 1970s to the late 1980s, and were imported legitimately from India for academic research and education. As the identity of the specimens were not known; sex and age were estimated using forensic anthropological methods: sex, according to Krogman and Iscan (1986) and Singh et al. (2015), and age, according to Gazge et al. (2018). The GAs of these mandibular specimens were measured using a mandibulometer (GPM Anthropological Instruments, Zurich, Switzerland) and categorized into two groups: the L-GA group, where GA ≤ 120° (n = 13 mandibles), and the H-GA group, where GA ≥ 125° (n = 16 mandibles).

X-ray imaging and measurement methods

Lateral radiography

Two intra-oral X-ray films (DF-50 occlusal size, Kodak, Rochester, NY, USA) were used as a single sheet film. The two films were placed closely together and were attached with mending tape on the reverse side. After the X-ray film was temporarily adhered to a vertical plate, it was fixed so that the inside of the mandible was in contact with the film surface. Lateral radiography was performed on the right and left sides of the mandibles using a portable dental X-ray device (CK6105, Asahi Roentgen, Kyoto, Japan) with a tube voltage, tube current, and an exposure time of 65 kVp, 1.2–2.7s, and 10 mA, respectively. The focal film distance was 1 m. The X-ray films were processed using an automatic developing device (Max-Rhein, NIX, Tokyo, Japan).

The X-ray film image was converted to a JPG format using a scanner (GT-9800F, EPSON, To-

kyo, Japan). The image was pasted into Microsoft Office PowerPoint (Microsoft Corp, Redmond, WA, USA) on a Macintosh PC. Reference points and lines were drawn on the digital radiographs, which were then saved in TIFF format. The image was then transferred to a Windows PC.

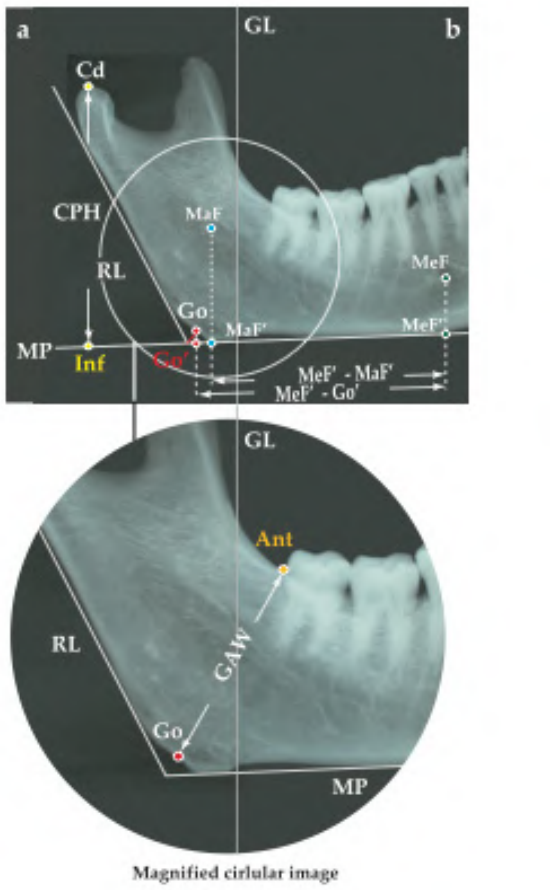

Fig. 1.- Lateral radiograph imaging and linear measurements of the adult human complete dentate mandible. Abbreviation: GL, gray line: border line of films **a** and **b**; MP, mandibular plane: the tangential line tied between the two most projected points on the mandibular inferior border; RL, ramus line: the tangential line connecting the two most projected points in the posterior margin of the ramus; MeF, mental foramen: the point at the middle of the lower border of the mental foramen; MaF, mandibular foramen: the point at the middle of the lower border of the mandibular foramen; Go, gonion: the point where the bisector of the angle formed by the mandibular plane and ramus line intersects the contour of the angle of the mandible; Cd, Condylion: the most superior point of the condyle of the mandible; Inf: the point where the perpendicular line passing through the Cd intersects the MP; MeF': the point where the perpendicular line passing through the MeF intersects the MP; MaF': the point where the perpendicular line passing through the MaF intersects the MP; Go': the point where the perpendicular line passing through the Go intersects the MP; CPH, condylar perpendicular height: the perpendicular distance from the Cd to the Inf; MaF'-MeF', the distance from MaF' to MeF'; MaF'-Go', the distance from MaF' to Go'; GAW, gonial angle width; the distance between the point where the bisector of the GA intersects the anterior margin of the ramus (Ant) and the Go. Measured in mm.

Compared to lateral cephalometric radiography, this method produces clearer and more reproducible projection images without overlap of left and right images. The horizontal distortion is smaller than that in the digital dental panoramic radiography (DPR), and metrology can be accurately measured. Moreover, it is a small and easy-to-carry device that is cost-effective compared to large and costly counterparts. Furthermore, the MeF, mandibular foramen (MaF), condylion (Cd, the most superior point of the condyle of the mandible), and the gonion (Go), which were used as anatomical landmarks, can be precisely positioned, and the measurement error of the distance between two points is very small.

Dental panoramic radiography

After fixing the dried mandible on a plastic structure, digital DPRs were taken on the chin rest of the X-ray equipment (Veraview epoc 3Df, MORITA, Kyoto, Japan) with the mandibular plane set at approximately 25°. The image was saved as a JPG file (Fig. 2).

Digital caliper measurements

The total length of the mandible (TLOM) and the inter-ramus widths (bicondylar width, BiCoW; bicoronion width, BiCorW; bimandibular foramen width, BiMaFW; and bigonion width, BiGoW) were measured by using digital Vernier calipers with 1/100 mm precision (CD-20AX, MITSUTOYO, Kawasaki, Japan) (Fig. 3).

Mandibular volume and weight measurements

The volume of the mandible (VOM; g/cm^3) was measured by hanging the mandible on a hook

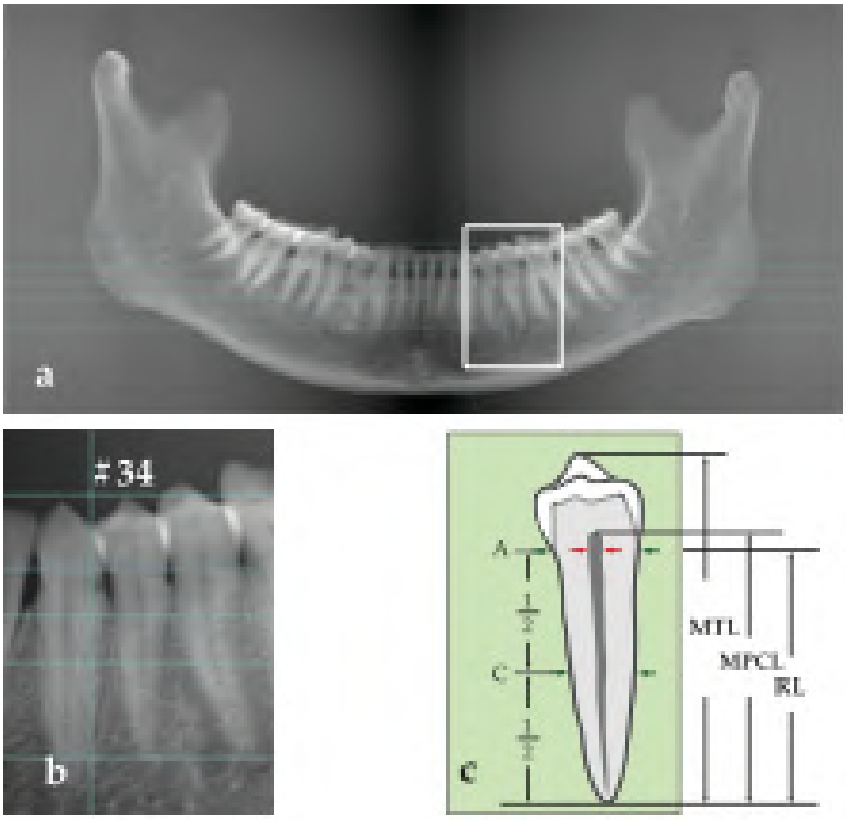

Fig. 2.- Measurement of tooth number #34 for the age estimation. **a:** A digital dental panoramic radiographic (digital DPR) image of mandible with a low gonial angle (L-GA; GA ≤ 120°). **b:** Enlarged view of #34 measured using DPR image and Photoshop's measurement tool. **c:** Drawing of tooth measurement (#34) and line measurement locations. MTL: Maximum tooth length; MPCL: Maximum pulp chamber length; RL: Root length on mesial surface. **d:** Multiple regression equations of Gazge et al. (2018) according to Kvaal's method (1995). Age = (81.1 × X1) + (180 × X2) – (69.6 × X4) – (1.7 × X3) + (3.7 × X5) – 36.6 [X1 = PW_A/RW_A, X2 = MPCL/MTL, X3 = RL, X4 = MPCL/RL, X5 = RW_C]. A: Root and pulp width (RW_A and PW_A, green and red arrows) at the cement-enamel junction (CEJ); C: Root width (RW_C, green arrow) at the midpoint between the root apex and level A.

of a digital hanging weight scale (SANKO, Tokyo, Japan) in a 15-cm square plastic case filled with water. The VOM was obtained by subtracting the value at the time of mandibular immersion from the gross weight of the mandible (GWOM). GWOM was measured using an electronic balance (ED-200, Shimadzu Corp, Kyoto, Japan).

Sex and age estimation

Sex was tentatively determined by observing the degree of development of the neurocranium and facial skeleton according to Krogman and Iscan (1986). Subsequently, sex was determined according to the criteria of Singh et al. (2015) for Indian mandibular evaluation using measurement parameters (BiCoW, male > 110 mm and female ≤ 110 mm; BiGoW, male ≥ 91 mm and female < 91 mm), and morphological parameters: the symphysis menti angle shape (square in males, and rounded in females), gonion flaring (everted in males, and inverted in females), muscular markings (more prominent in males, and less prominent in females) (Mobin and Vathsalya, 2018; Kanwar et al., 2021).

In this study, after the above thresholds were set, metric variables (BiCoW and BiGoW) were converted into nominal variables. Estimates for males and females were determined by sex, with at least three of the five geometrical characteristics. As a result of estimation, the sex of the 29 mandibles were 17 male and 12 female, with no significant difference in sex distribution ($P = 0.2291$).

Figure 2 shows the linear measurement sites for age estimation. The length and width of FDI #34 teeth and pulp chambers were measured using digital DPR images (in JPG format) and Photoshop (Adobe, Lehi, UT, USA) on a Mac PC. The measurement was performed by enlarging the image to 200–300%.

Age estimation was performed according to Gazge et al. (2018) concerning the methods of

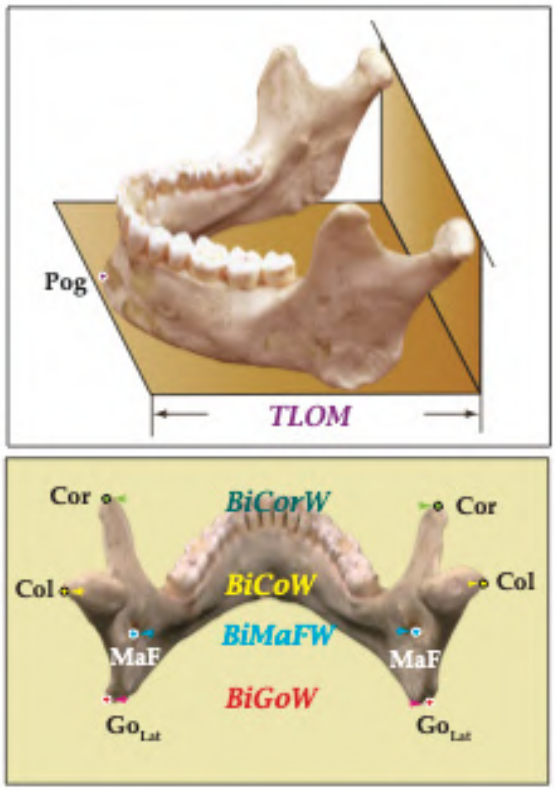

Fig. 3.- Measurements of the length and inter-ramus width of the complete dentate mandible using digital Vernier calipers. This photograph excluded a hand-fabricated mandibular fixation device (K.H.) and X-ray film. Abbreviations: TLOM, the total length of the mandibles: the distance from Pog to the posterior margin of the condylar of the mandible; Col, Condylion lateralis: the most lateral pole of the condyle of the mandible; Cor, Coronion: the tip of the coronoid processes of the mandible; MaF, mandibular foramen: point at the middle of the lower border of the mandibular foramen; Go_{Lat}, gonion: the lowest posterior and most lateral point of the angle of the mandible; Pog, pogonion: the most forward- projecting point on the anterior surface of the chin.

Gustafson (1950), Kvaal et al. (1995) and Cameriere et al. (2012). That is, the age evaluation was performed from the multiple regression equation of tooth #34 using the six-site measurements, which are considered optimal for age estimation. The 29 mandibles were estimated to be between 37 and 54 years. The mean age based on sex was 46.47 ± 4.27 years (37–54 years) for males and 46.43 ± 3.60 years (38-50 years) for females, and there was no significant difference between the sexes (P = 0. 9294).

Reproducibility of measurement and morphological evaluation

Five lateral radiograph images and five mandibular specimens were randomly selected, and linear measurements (MeF'-Go', MeF'-MaF', CPH) on the images and actual measurements (BiCoW, BiGoM, BiCorW, BiMaFW) with digital Vernier calipers were performed by a research assistant (T.S.) with more than 10 years of experience. The measurement reliability was evaluated from the intraclass correlation coefficient (ICC; 1, 1). The ICC (1, 1) for lateral radiographic imaging and digital caliper measurements of the mandibles was 0.99 and 0.99, respectively. Reliability results approximated studies with other Indian populations (Mobin and Vathsalya, 2018; Kanwar et al., 2021).

Sex was determined by two dentists (K.H. and S.O.) for the five geometrical features described above, after 12 mandibles were selected at random, and inter-rater reproducibility was evaluated from Cohen's kappa (κ) coefficient. The κ coefficient was 0.83. This result was comparable to that of another study (Mello-Gentil and Souza-Mello, 2022).

For age estimation, 12 digital DPR images were randomly selected. Two dentists (K.H. and S.O.) measured the six locations for #34 on the digital DPR images, and inter-rater reliability was confirmed from the ICC (2, 1). The ICC (2, 1) for #34 on digital DPR images was 0.99. The result was similar to results of other studies (Mobin and Vathsalya, 2018; Kanwar et al., 2021).

Statistical analysis

The average values of the right and left parameters were used for the linear measurement of mandibular corpus length (MeF'-Go', MeF'-MaF', MaF'-Go') and GAW. The linear and actual measured values obtained from the lateral radiograph images and dried mandibles were inputted into a Microsoft Excel Spread-sheet. The significant differences in the distribution of mandibular specimens between L-GA and H-GA groups and between males and females were evaluated with the exact binomial test, respectively. Similarly, the Mann-Whitney U test was used to analyze significant differences in the mean age between the two GA groups and between both sexes. The significance of the correlation between GA and each variable was determined using Pearson's correlation test. Statistical analyses were performed using Stat View 4.02 (Abacus, Berkeley, CA USA), open free js-STAR XR+ software, and the Microsoft Excel analysis tool.

RESULTS

Table 1 shows the mean values and standard deviations for the mandibular morphometric, VOM, and GWOM parameters in the L-GA and H-GA groups. There was no significant difference between the distribution of the number of mandibular specimens (13 vs. 16) and mean age in the L-GA and H-GA groups ($P = 0.3555$ and $P = 0.2635$, respectively). The GA was 12.14° and was significantly smaller in the L-GA group than that in the H-GA group ($P < 0.01$). When comparing the mean values of the parameters for mandibular corpus lengths, the MeF'-Go' and MaF'-Go' in the L-GA group were significantly larger, by 7.02 mm and 3.82 mm, respectively, than those in the H-GA group ($P < 0.01$). Similarly, the parameters for BiCoW, BiCorW, and BiMaFW were significantly larger in the L-GA group than those in the H-GA group by 4.03 mm, 2.96 mm, and 2.57 mm, respectively (all $P < 0.05$). BiGoW, GAW, CPH, and VOM were also significantly larger in the L-GA group than that in the H-GA group by 5.08 mm, 7.48 mm, 8.84 mm, and 9.62 cm^3, respectively (all $P < 0.01$). VOM and GWOM were significantly greater in the L-GA group than that in the H-GA group by 9.62 cm^3 and 13.02 g ($P < 0.05$ and $P < 0.01$, respectively). No significant differences in the parameters TLOM and MeF'-MaF' were observed between the groups.

Table 2 shows the correlations between the GA and each variable, and their statistical significance. Significant negative correlations were observed between the GA and mandibular corpus length variables (MeF'-Go' and MaF'-Go': $r = -0.63$ and $r = -0.65$, respectively).

Furthermore, significant moderate negative correlations of the GA with the BiCoW, BiGoW, VOM, and GWOM were observed ($r = -0.40$ and $r = -0.44$, $r = -0.53$, and $r = -0.44$, respectively) (all $P < 0.05$). Significant strong negative correlations of the GA with the GAW ($r = -0.79$) and CPH ($r = -0.61$) were observed (both $P < 0.01$). In contrast, no significant correlations of the GA with the TLOM, MeF'-MaF, BiCorW, and BiMaFW were observed.

DISCUSSION

To achieve the objectives of this study, we analyzed the relationship between GA and morphometric changes in the mandible by examining adult mandibles with 32 fully erupted teeth, a normal dental arch, and a normal occlusion. The mandibular specimens used in this study were categorized into the L-GA (GA ≤ 120°) and H-GA (GA ≥ 125°) groups, and comparisons were subsequently made between the two groups. It revealed that the three-dimensional morphology of the posterior mandibular corpus and ramus, as well as the mandibular volume and weight, was greater in the L-GA group than in the H-GA group. Based on the estimated age range (37–59 years) of the mandibles investigated and analyzed, these morphological changes are considered to be the effects of mastication and bite force in daily life during aging, rather than heredity, growth and development, time in which they lived or geographical influences.

The present study was one of a series of investigations on the differences in mandibular structure between the two GA groups. No statistically significant difference was observed in the number and mean ages between the 13 L-GA group (mean: 47.51 years) and the 16 H-GA group (mean: 45.43 years). Thus, the sample numbers and the mean ages were similar.

Table 1. Comparison of morphometric, bone volume, weight, and density measurements between L-GA and H-GA groups of the mandible.

Parameters		L-GA (n = 13) [#]		H-GA (n = 16) [#]				*P-value*
		mean ± SD	(95%CI)	mean ± SD	(95%CI)	Differences	%	
Age, yr	Age	47.51 ± 5.83	(36.53, 58.49)	45.43 ± 3.60	(38.59, 52.27)	2.08	4.38	0.2635
Gonial angle, degree								
	GA	115.73 ± 2.41	(111.19, 120.27)	127.88 ± 2.00	(124.07, 131.68)	-12.14	-10.49	**<0.0001****
Mandibular length, mm								
	TLOM	101.23 ± 5.71	(90.47, 111.99)	101.03 ± 5.82	(89.98, 112.08)	0.20	0.20	0.8953
Mandibular corpus length, mm								
	MeF'-Go'	62.74 ± 3.29	(56.55, 68.93)	55.72 ± 3.74	(48.61, 62.82)	7.02	11.19	**0.0001****
	MeF'-MaF'	56.41 ± 3.88	(49.10, 63.72)	54.79 ± 3.68	(47.81, 61.76)	1.62	2.87	0.2452
	MaF'-Go'	6.41 ± 2.07	(2.52, 10.31)	2.60 ± 1.32	(0.08, 5.11)	3.82	59.50	**<0.0001****
Inter-ramus width, mm								
	BiCoW	113.81 ± 4.33	(105.65, 121.97)	109.78 ± 3.90	(102.37, 117.19)	4.03	3.54	**0.0159***
	BiCorW	94.73 ± 3.76	(87.65, 101.82)	91.77 ± 3.71	(84.73, 98.82)	2.96	3.12	**0.0353***
	BiMaFW	79.39 ± 2.48	(74.71, 84.07)	76.82 ± 3.97	(69.28, 84.35)	2.57	3.24	0.0226*
	BiGoW	96.29 ± 4.37	(85.50, 106.16)	91.21 ± 4.03	(83.56, 98.86)	5.08	5.28	**0.0075****
Width of the angle, mm								
	GAW	39.70 ± 1.85	(36.22, 43.17)	32.22 ± 3.06	(26.40, 38.03)	7.48	18.85	**<0.0001****
Ramus height, mm								
	CPH	60.61 ± 3.77	(53.52, 67.70)	51.77 ± 6.50	(39.44, 64.10)	8.84	14.59	**0.0006****
Bone volume, cm^3								
	VOM	56.23 ± 7.78	(41.58, 70.88)	46.61 ± 7.3	(32.71, 60.52)	9.62	17.11	**0.0044****
Bone weight, g								
	GWOM	90.64 ± 13.33	(65.54, 115.74)	77.62 ± 11.17	(56.42, 98.82)	13.02	14.36	**0.0124***

L-GA and H-GA, low and high gonial angles; SD, standard deviation; CI, confidential interval; Significance: Exact binomial test and Mann-Whitney U test, *$P < 0.05$ and **$P < 0.01$ (bold text). Abbreviations: TLOM, the total length of the mandible; MeF'-Go', the distance from the mental foramen to the gonion on the mandibular plane (MP); MeF'-MaF', the distance from the mental foramen to the mandibular foramen on the MP; MaF'-Go', the distance from the mandibular foramen to the gonion on the MP; BiCoW, bicondylar width (Col-Col); BiCorW, bicoronoid width (Cor-Cor); BiMaFW (MaF-MaF), bimandibular foramen width; BiGoW, bigonion width (GoLat-GoLat); GAW, gonial angle width (Go-Ant); CPH, condylar perpendicular height: the perpendicular distance from the Cd to the Inf; VOM, the volume of the mandible; GWOM, gross weight of the mandible (See reference Figs. 1 and 3).
#: Testing significance using exact binomial test for distribution of number of L-GA (13) and H-GA group mandibles (16) ($P = 0.3555$).

In addition, no abnormalities were observed in the teeth and periodontal tissues in the mandibles, suggesting that they belonged to a population group with similar social activities, sociocultural levels, regions, habit, customs, and economics. Consequently, it was not necessary to adjust the results.

Cho et al. (2014) classified face configurations into brachyfacial and mesofacial groups, with a GA threshold of 120°. In this study, a gap of 5° was set to distinguish the L-GA and H-GA groups clearly (Osato et al., 2012). The result showed a significant difference (12.14°) in the mean GA between the groups ($P < 0.01$). Compared to the H-GA group, the L-GA group showed a significantly larger MeF'-Go', MaF'-Go', GAW, inter-ramus widths, CPH, VOM, and GWOM. Changes in the GA had a significant negative correlation with multiple variables, but did not correlate with TLOM and BiCroW.

Table 2. Pearson's correlation analysis between the gonial angles (GA) and **v**ariables of the mandible, as well as statistical assessments (n = 29).

Variables		*r*	*P-value*
Age, yr			
	Age	-0.235	0.2218
Mandibular length, mm			
	TLOM	0.113	0.5603
Mandibular corpus length, mm			
	MeF'-Go'	-0.626	**0.0003****
	MeF'-MaF'	-0.127	0.5121
	MaF'-Go'	-0.651	**0.0001****
Inter-ramus width, mm			
	BiCoW	-0.400	**0.0313***
	BiCorW	-0.296	0.1196
	BiMaFW	-0.267	0.1616
	BiGoW	-0.436	**0.018***
Width of the angle, mm			
	GAW	-0.791	**<0.0001****
Ramus height, mm			
	CPH	-0.611	**0.0004****
Bone volume, cm^3			
	VOM	-0.531	**0.0026****
Bone weight, g			
	GWOM	-0.439	**0.0171***

r: Pearson's correlation coefficients; Significance: Pearson's correlation test, *$P < 0.05$, **$P < 0.01$ (bold text). Abbreviations: TLOM, the total length of the mandible; MeF'-Go', the distance from the mental foramen to the gonion on the mandibular plane (MP); MeF'-MaF', the distance from the mental foramen to the mandibular foramen on the MP; MaF'-Go', the distance from the mandibular foramen to the gonion on the MP; BiCoW, bicondylar width (Col-Col); BiCorW, bicoronoid width (Cor-Cor); BiMaFW, bimandibular foramen width (MaF-MaF); BiGoW, bigonion width (Go_{Lat}-Go_{Lat}); GAW, gonial angle width (Go-Ant); CPH, condylar perpendicular height (Cd-Int); VOM, the volume of the mandible; GWOM, gross weight of the mandible.

Corpus and ramus dimensions of the mandible

The biomechanical load of mastication affects mandibular morphology (Mays, 2015). Occlusal force strongly depends on the relative size of jaw-closing muscles and is associated with mandibular morphological changes (Custodio et al., 2011). The GA in a mandible with multiple teeth was significantly smaller, while the mandibular ramus was larger, than that in a mandible with few teeth. Furthermore, the mandibular length of mandibles with few teeth was larger than that of mandibles with multiple teeth (Vinter et al., 1997). It has also been suggested that functional hyperactivity of the masticatory system may affect bony structures through increased stress (Kiliaridis et al., 1995).

This study revealed that the complete dentate mandibular corpus lengths (MeF'-Go' and MaF'-Go') in the L-GA group were significantly larger than those in the H-GA group. On the other hand, there was no significant difference in dimensions from the MeF' to the MaF' with the central corpus area in the L-GA group as compared to the H-GA group, indicating that this region was less susceptible to occlusal force. This interesting finding indicates that the influence of occlusal forces on the midcorpus is small.

Adult patients with a sharp GA, as compared to those with an obtuse GA, have a flaring Go and a significantly larger BiGoW (Hong et al., 2009). A reduced masticatory function is associated with decreased BiCoW and BiGoW (Rando et al., 2014). Based on these reports, it is considered that the occlusal force of the L-GA group was strongly applied to the lower (BiGoW), middle (BiMaFW), and upper (BiCoW and BiCorW) areas of the inter-ramus, which consequently expanded laterally.

A study on the relationship between the ramus width of the mandible around the MaF and GA size revealed that the ramus width in adult dentate patients was larger in the L-GA group than in the H-GA group (Ogawa et al., 2012). The ramus width measured using CBCT was 2.0 mm larger in the L-GA group (118.5°) than in the H-GA group (128.6°) in a previous study (Barone et al., 2021). Strong sexual dimorphism was also observed in these ramus widths (Leversha et al., 2016; Mehta et al., 2020). In this study, the GAW around the GA was also significantly greater in the L-GA group (by 7.48 mm [18.85%]) than in the H-GA group (Table 1). Thus, it is indicated that individuals with narrow GA may have increased masticatory muscle activity, greater occlusal force, and vigorous bone addition in a wide area from the Go to the retromolar triangle of the anterior margin of the mandibular ramus.

According to previous lateral cephalogram analyses regarding the ramus height of the mandible, patients with a small GA had a short face with a

shorter anterior (distance between nasion and menton, N-Me), and vertically larger posterior (sella to gonion, S-Go) facial heights, and a larger facial height ratio (S-Go/N-Me) (Karlsen, 1997). CBCT analysis also showed that the ramus height of a small GA was higher than that of a large GA (Barone et al., 2021). Furthermore, ramus height was higher in dentate patients than in completely edentulous patients (Okşayan et al., 2014) and was also higher in men than in women (Lopez-Capp et al., 2018). This investigation showed that the CPH was 8.84 mm (14.59%), which was significantly larger in the L-GA group than in the H-GA group (Table 1). Therefore, the skeletal facial configuration of individuals with a L-GA may involve a large posterior facial height (Tsai, 2000). Although it is clear from previous reports that masticatory muscle function and occlusal force are closely related to the difference in GAW and the mandibular ramus widths value between the two GA groups, it is necessary to investigate the relationship between GA and bite force in the same subject.

Mandibular volume and weight

There have been few reports on the volume of completely dentate mandibles. Based on the analysis using MRI, it has been reported that the volume of the mandible increased by 6,530 mm^3 (18.6%) during the growth period (age 7-13 years) (Maeda, 2018). Additionally, an investigation of maxillofacial morphology and mandibular volume used lateral cephalometry and CBCT, respectively. The mean volume of mandibles was 63.23 cm^3 in males and 53.92 cm^3 in females. No significant differences were observed in mandibular volumes among cases with Angle classes I, II, and III maxillofacial morphology. On the other hand, an inverse relationship between the mandibular plane angle (MPA) and mandibular volume was observed, and the hypodivergent (short face height, MPA: < 23°) group was larger than the hyperdivergent (long face height, MPA: > 30°) group (Nakawaki et al., 2016).

In this study, the Archimedes method was used to determine volume, revealing that the volume in the L-GA group (56.23 cm^3) was significantly larger (by 9.62 cm^3, 17.11%) than that in the H-GA group (46.61 cm^3), indicating that the decrease in GA size affected not only an increase in three-dimensional dimensions, but also in mandibular volume (Table 1). This change is thought to be the effect of bone remodeling associated with increased masticatory muscle function and occlusal force. The results of this study supported those of Nakawaki et al. (2016) mentioned above.

From a conventional report on the weight of the mandible, in patients with developed masticatory muscles, the mandibular weight was greater while the GA was smaller than in those with less muscle mass (Jensen and Palling, 1954). On the other hand, no studies have reported on the relationship between mandibular angle and mandibular weight. It has been reported that the mandibular weight and morphology in Indians are divided into three types, and the heavy and large group (30.0%) was most common in males, while the light and small group (12.5%) was most common in females. Bone weights were not described in that paper (Mobin and Vathsalya, 2018). The GWOM of dried, completely dentate adult mandibles in the L-GA group (90.64 g) was significantly heavier than that of the H-GA group (77.62 g), by 13.02 g (14.36%), in this study (Table 1). Therefore, it was conceivable that a decrease in GA size was associated with an increase in mandibular morphometric dimensions.

Correlations between GA and measured variables

In correlations between GA and craniofacial radiomorphometry, increasing GA changes the facial features from a brachyofacial to a dolicofacial pattern (Custodio et al., 2011). It is associated with a decreased ramus width and posterior ramus notch depth (Ogawa et al., 2012). Moreover, a smaller GA is associated with maximum occlusal force from the second premolars and first molars (Miwa et al., 2019). Notably, a reduced GA size is associated with a higher incidence of impacted lower third molars (Barone et al., 2021). GA also has a negative correlation with the growth of permanent teeth (Ashkenazi et al., 2011; Larrazabal-Moron et al., 2018), and positive correlations with tooth loss and aging (Vinter et al., 1997; Xie and Ainamo, 2004; Joo et al., 2013; Okşayan et al., 2014). In this study, the GA negatively and significantly contributed to bone apposition with

bone remodeling of the posterior mandibular area, MeF'-Go' and MaF'-Go'. Thus, changes in the GA size were considered to be closely associated with remodeling of the posterior region of the corpus length, while maintaining TLOM and corpus length from MeF' to MaF'.

Regarding the association between the dimensions of the right and left mandibular ramus and masticatory function, a previous study reported that BiGoW in patients with a small GA was positively correlated with masseter muscle volume (r = 0.37) (Hong et al., 2009), and that the occlusal force was strong (Kiliaridis et al., 1995; Sondang et al., 2003; Miwa et al., 2019). Generally, the BiGoW decreases with aging (Leversha et al., 2016). This study revealed negative moderate linear relationships between the GA size and the inter-ramus width variables of BiCoW and BiGoW (r = - 0.40 and r = -0.43, respectively) (Table 2), suggesting that occlusal force and mandibular bone morphology are related. Specifically, it was indicated that, when the masticatory muscle activity and occlusal force increased, the GA decreased, and the inter-ramus width spread laterally.

In a digital DPR analysis, the ramus width around the mandibular foramen was closely associated with a decreased GA, and an increase in GA contributed to reduced ramus width on lateral radiograph imaging (Ogawa et al., 2012; Cho et al., 2014). It was found that GA size had a significantly strong negative linear relationship with GAW (r = -0.79). In addition, the GA size strongly affected the MaF region, including the gonion process and anterior margin of the retromolar triangle, through bone apposition. Similar reports on the negative association between GA size and ramus width (BiGoW; r = -0.44) have been reported using CBCT analysis (Kronseder et al., 2020). The activities of the jaw-closing muscles and increased occlusal force are closely associated with enlargement of the GAW.

The ramus height generally decreases with age (Leversha et al., 2016). GA size showed significant negative correlations with the coronoid and ramus heights of the mandible (Huumonen et al., 2010; Joo et al., 2013). Therefore, as the occlusal force increases, the posterior facial height gradually increases, while GA size decreases (Sondang et al., 2003). This investigation observed a significantly negative moderate linear relationship between the GA and CPH (r = -0.61), which was similar to the previously reported results (Huumonen et al., 2010; Joo et al., 2013). The occlusal force of patients with a small GA is strong (Kiliaridis et al., 1995; Miwa et al., 2019), and contributes to bone apposition around the GA. In addition, a 10-year follow-up study also reported that the fracture risk of abutments in implant treatment was higher in male patients with a GA size less than 120° on digital DPR images (Murakami et al., 2020). These results indicate that careful consideration should be given to the strong occlusal force of patients with a GA ≤ 120° when designing and fabricating a prosthesis and that the evaluation of the GA is an important checkpoint for reducing oral rehabilitation risk (Osato et al., 2012). Further investigation into the relationship between the complications of implant-supported prosthetic treatment and GA size is warranted.

The volume of the mandibles increased in proportion to body weight in Norwegian schoolchildren (Maeda, 2018). In addition, a cephalometric investigation on the association between maxillofacial morphology (ANB, SNB, or MPA) and mandibular bone volume in patients with skeletal malocclusion reported that a significant weak linear relationship was found between GA and mandibular bone volume (Katayama et al., 2014). On the other hand, a significant correlation (r = 0.44) was observed with the length index (condylion to gonion; Cd-Go) (Katayama et al., 2014).

From this result, significant negative moderate correlations (r = -0.53 and r = -0.44) were observed between GA size with mandibular volume and weight, indicating that the two variables were closely related to the GA in adult mandibles.

Hence, these results suggest that the mandibular morphology (external trait) in a wide range from the mandibular posterior corpus to the mandibular ramus, centered on the attachment of the mouth-closing muscle, and the mandibular volume increased; the stimulus caused by mastication was also active. These may be associated with increased bone strength (endomorphic bone quality and bone mass) through bone remodeling.

CONCLUSIONS

In this study, morphometric measurements of sex- and age-estimated completely dentate mandibles of Indian revealed that the MeF'-Go' and MaF'-Go' of the posterior corpus, the inter-ramus widths, GAW, CPH, VOM and GWOM were significantly larger in the L-GA group compared to the H-GA group. GA size had a negative linear relationship with those variables, whereas no significant association found in TLOM and BiCorW. Hence, the results could reveal that the L-GA group compared to the H-GA group occurred in vigorous bone apposition in the three-dimensional directions around the Go and also had larger VOM and GWOM without changing the TLOM. These results suggest that the evaluation of GA size is helpful in the field of prospective dental medicine. Future studies should focus on the relationship between GA size and mandibular morphometry and occlusal forces in a large population of dentate and edentate individuals.

ACKNOWLEDGEMENTS

We would like to thank Ms. Kyoko Fujii, for her cooperation with the preparation for submission of this manuscript.

FUNDINGS

This study did not receive any specific funding.

CONFLICTS OF INTEREST STATEMENT

The authors declare no conflicts of interest associated with this article.

INFORMED CONSENT

The authors declare that informed consent was not required.

REFERENCES

ASHKENAZI M, TAUBMAN L, GAVISH A (2011) Age-associated changes of the mandibular foramen position in anteroposterior dimension and of the mandibular angle in dry human mandibles. *Anat Rec*, 294(8): 1319-1325.

BARONE S, ANTONELLI A, AVERTA F, DIODATI F, MURACA D, BENNARDO F, GIUDICE A (2021) Does mandibular gonial angle influence the Eruption pattern of the lower third molar? A three-dimensional study. *J Clin Med*, 10(18): 4057.

CAMERIERE R, DE LUCA S, ALEMÁN I, FERRANTE L, CINGOLANI M (2012) Age estimation by pulp/tooth ratio in lower premolars by orthopantomography. *Forensic Sci Int*, 214(1-3): 105-112.

CHO IG, CHUNG JY, LEE JW, YANG JD, CHUNG HY, CHO BC, CHOI KY (2014) Anatomical study of the mandibular angle and body in wide mandibular angle cases. *Aesthetic Plast Surg*, 38(5): 933-940.

CUSTODIO W, GOMES SG, FAOT F, GARCIA RC, DEL BEL CURY AA (2011) Occlusal force, electromyographic activity of masticatory muscles and mandibular flexure of subjects with different facial types. *J Appl Oral Sci*, 19(4): 343-349.

DHARA V, KAMATH AT, VINEETHA R (2019) The influence of the mandibular gonial angle on the occurrence of mandibular angle fracture. *Dent Traumatol*, 35(3): 188-193.

FOUDA SM, GAD MM, EL TANTAWI M, VIRTANEN JI, SIPILA K, RAUSTIA A (2019) Influence of tooth loss on mandibular morphology: a cone-beam computed tomography study. *J Clin Exp Dent*, 11(9): e814-e819.

GAZGE N, PACHIPULUSU B, CHANDRA P, GOVINDRAJU P, VASAN V (2018) Comparative analysis of Kvaal's and Cameriere's methods for dental age estimation: a panoramic radiographic study. *IJFO*, 3: 30.

GURGEL M, CEVIDANES L, PEREIRA R, COSTA F, RUELLAS A, BIANCHI J, CUNALI P, BITTENCOURT L, CHAVES JUNIOR C (2022) Three-dimensional craniofacial characteristics associated with obstructive sleep apnea severity and treatment outcomes. *Clin Oral Invest*, 26(1): 875-887.

GUSTAFSON G, ODONT MALMÖ D (1950) Age determinations on teeth. *JADA*, 41(1): 45-54.

HONG HJ, HONG JW, KOH SH, KIM YO, PARK BY (2009) A three-dimensional analysis of the relationship among lower facial width, bony width, and masseter muscle volume in subjects with prominent mandible angles. *J Craniofac Sur*, 20(4): 1114-1119.

HUUMONEN K, SIPILA B, HAIKOLA M, TAPIO M, SODERHOLM AL, REMES-LYLY T, OIKARINEN K, RAUSTIA AM (2010) Influence of edentateness on gonial angle, ramus and condylar height. *J Oral Rehabil*, 37(1): 34-38.

JENSEN E, PALLING M (1954) The gonial angle: a survey. *Am J Orthod*, 40(2): 120-133.

JOO JK, LIM YJ, KWON HB, AHN SJ (2013) Panoramic radiographic evaluation of the mandibular morphological changes in elderly dentate and edentulous subjects. *Acta Odontol Scand*, 71(2): 357-362.

KANWAR R, GAJBHIYE N, DHAKAR JS, KANWAR IS (2021) Sex determination of dry human mandible using metrical parameters in Mahakaushal region of Madhya Pradesh, India: a cross-sectional study. *IJARS*, 10(4): AO65-AO69.

KARLSEN AT (1997) Association between facial height development and mandibular growth rotation in low and high MP-SN angle faces: a longitudinal study. *Angle Orthod*, 67(2): 103-110.

KATAYAMA K, YAMAGUCHI T, SUGIURA M, HAGA S, MAKI K (2014) Evaluation of mandibular volume using cone-beam computed tomography and correlation with cephalometric values. *Angle Orthod*, 84(2): 337-342.

KILIARIDIS S, JOHANSSON A, HARALDSON T, OMAR R, CARLSSON GE (1995) Craniofacial morphology, occlusal traits, and bite force in persons with advanced occlusal tooth wear. *Am J Orthod Dentofacial Orthop*, 107(3): 286-292.

KINGSMILL VJ, BOYDE A (1998) Variation in the apparent density of human mandibular bone with age and dental status. *J Anat*, 192 (Pt 2): 233-244.

KROGMAN WM, ISCAN MY (1986) The human skeleton in Forensic Medicine. 2nd ed. CC Thomas, Springfield, Illinois.

KRONSEDER K, RUNTE C, KLEINHEINZ J, JUNG S, DIRKSEN D (2020) Distribution of bone thickness in the human mandibular ramus - a CBCT-based study. *Head Face Med,* 16(1): 13.

KVAAL SI, KOLLVEIT KM, THOMSEN IO, SOLHEIM T (1995) Age estimation of adults from dental radiographs. *Forensic Sci Int*, 74: 175-185.

LARRAZABAL-MORON C, SANCHIS-GIMENO JA (2018) Gonial angle growth patterns according to age and gender. *Ann Anat*, 215: 93-96.

LEVERSHA J, MCKEOUGH G, MYRTEZA A, SKJELLRUP-WAKEFILED H, WELSH J, SHOLAPURKAR A (2016) Age and gender correlation of gonial angle, ramus height and bigonial width in dentate subjects in a dental school in Far North Queensland. *J Clin Exp Dent*, 8(1): e49-e54.

LOPEZ-CAPP TT, RYNN C, WILKINSON C, DE PAIVA LAS, MICHEL-CROSATO E, BIAZEVIC MGH (2018) Discriminant analysis of mandibular measurements for the estimation of sex in a modern Brazilian sample. *Int J Legal Med*, 132(3): 843-851.

MAEDA J (2018) Jyudan-teki MRI deta o mochiita kagakukotsu no seicho ni kansuru kenkyu. *Osaka University Knowledge Archive,* https://doi.org/10.18910/69506 [in Japanese].

MAYS S (2015) Mandibular morphology in two archaeological human skeletal samples from northwest Europe with different masticatory regimes. *Homo*, 66(3): 203-215.

MEHTA H, BHUVANESHWARI S, SINGH MP, NAHAR P, MEHTA K, SHARMA T (2020) Gender determination using mandibular ramus and gonial angle on OPG. *J Indian Acad Oral Med Radiol*, 32(2): 154-158.

MELLO-GENTIL T, SOUZA-MELLO V (2022) Contributions of anatomy to forensic sex estimation: focus on head and neck bones. *Forensic Sci Res*, 7(1): 11-23.

MIWA S, WADA M, MURAKAMI S, SUGANAMI T, IKEBE K, MAEDA Y (2019) Gonial angle measured by orthopantomography as a predictor of maximum occlusal force. *J Prosthodont*, 28(1): e426-e430.

MOBIN N, VATHSALYA SK (2018) Sexual dimorphism in adult human mandibles: a Southern Indian study. *IJARS*, 7(4): AO15-AO21.

MURAKAMI H, IGARASHI K, FUSE M, KITAGAWA T, IGARASHI M, UCHIBORI S, KOMINE C, GOTOUDA H, OKADA H, KAWAI Y (2020) Risk factors for abutment and implant fracture after loading. *J Oral Sci*, 63(1): 92-97.

NAKAWAKI T, YAMAGUCHI T, TOMITA D, HIKITA Y, ADEL M, KATAYAMA K, MAKI K (2016) Evaluation of mandibular volume classified by vertical skeletal dimensions with cone- beam computed tomography. *Angle Orthod*, 86(6): 949-954.

OGAWA T, OSATO S, SHISHIDO Y, OKADA M, MISAKI K (2012) Relationships between the gonial angle and mandibular ramus morphology in dentate subjects: a panoramic radiophotometric study. *J Oral Implantol*, 38(3): 203-210.

OKŞAYAN R, ASARKAYA B, PALTA N, ŞIMŞEK İ, SÖKÜCÜ O, İŞMAN E (2014) Effects of edentulism on mandibular morphology: evaluation of panoramic radiographs. *Sci World J*, 2014; 254932.

OSATO S, KUROYAMA I, NAKAJIMA S, OGAWA T, MISAKI K (2012) Differences in 5 anatomic parameters of mandibular body morphology by gonial angle size in dentate Japanese subjects. *Ann Anat*, 194(5): 446-451.

RANDO C, HILLSON S, ANTOINE D (2014) Changes in mandibular dimensions during the mediaeval to post-mediaeval transition in London: a possible response to decreased masticatory load. *Arch Oral Biol*, 59(1): 73-81.

SINGH R, MISHRA SR, SUSHOBHANA, PASSEY SJ, KUMAR P SINGH S, SINHA P, GUPTA S (2015) Sexual dimorphism in adult human mandible of North Indian origin. *FMAR*, 3: 82-88.

SONDANG P, KUMAGAI H, TANAKA E, OZAKI H, NIKAWA H, TANNE K, HAMADA T (2003) Correlation between maximum bite force and craniofacial morphology of young adults in Indonesia. *J Oral Rehabil*, 30(11): 1109-1117.

TSAI HH (2000) Cephalometric studies of children with long and short faces. *J Clin Pediatr Dent*, 25(1): 23-28.

VINTER I, KRMPOTIĆ-NEMANIĆ J, IVANKOVIĆ D, JALSOVEC D (1997) The influence of the dentition on the shape of the mandible. *Coll Antropol*, 21(2): 555-560.

XIE QF, AINAMO A (2004) Correlation of gonial angle size with cortical thickness, height of the mandibular residual body, and duration of edentulism. *J Prosthet Dent*, 91(5): 477-482.

YANIKOGLU N, YILMAZ B (2008) Radiological evaluation of changes in the gonial angle after teeth extraction and wearing of dentures: a 3-year longitudinal study. *Oral Surg Oral Med Oral Pathol Oral Radiol Endod*, 105(6): e55-e60.

Anatomy of the buccal fat pad for structures at risk during bichatectomy

Andrea Moreno-Salinas[1β], José Luis Treviño-González[2β], Claudio A. Casas-Murillo[3], Kouatzin Aguilar-Morales[1], Ricardo Pinales-Razo[3], Miguel De La Parra-Marquez[4], Rodrigo E. Elizondo-Omaña[1], Santos Guzmán-Lopez[1], Alejandro Quiroga-Garza[1,4]

[1] Universidad Autonoma de Nuevo Leon, School of Medicine, Human Anatomy Department, Monterrey, Nuevo Leon, Mexico

[2] Universidad Autonoma de Nuevo Leon, University Hospital "Dr. José Eleuterio González", Otorhinolaryngology Department, Nuevo León, Mexico

[3] Universidad Autonoma de Nuevo Leon, University Hospital "Dr. José Eleuterio González", Radiology and Imaging Department, Monterrey, Nuevo Leon, Mexico

[4] Instituto Mexicano del Seguro Social, Unidad Medica de Alta Especialidad 21, Monterrey, Nuevo Leon, Mexico

[β] Both authors participated equally in the study, and are both in the position of first author.

SUMMARY

The buccal fat pad (BFP), is an adipose tissue located in the cheek, with complex morphology. Oral bichatectomy is a frequent aesthetic procedure with possible complications. Our objective was to determine the volume and its relationship with the upper 2nd molar and the facial artery (FA). A cross-sectional, observational study was performed. Computed tomography was used to obtain 3D images to determine volume, length, and width. Distances from the 2nd molar to each extension, and the nearest distance to the FA were measured. A total of 106 BFP (70 male) were included. The mean age was 51±21. The mean volume, length, and width were 13.8±5.4 ml, 72.9±10.7 mm, and 21.4±5.6 mm, respectively. The BFP extends mainly cephalically and caudally from the second molar, reaching upto 8.5 cm and 32 ml. The mean distance between the second molar and FA was 12.9 mm, but as close as 3 mm. The FA had a mean distance of 2.1mm to the nearest BFP extension, with 42.5% in intimate contact, and another 9.4% crossing the center of the masseter extension. There were no statistically significant differences between sexes. The BFP has a dynamic shape with highly variable size and volume. The FA is often at risk of damage during procedures due to proximity.

Key words: Buccal fat pad – Bichatectomy – Anatomy – Facial artery

INTRODUCTION

The buccal fat pad (BFP) or Bichat bag, was first described by Marie François Xavier Bichat as a trigone-shaped adipose tissue located on the cheek. It has a complex morphology and is made

Corresponding author:
Alejandro Quiroga-Garza and Santos Guzman-Lopez. Departamento de Anatomía Humana, Facultad de Medicina, Universidad Autonoma de Nuevo León. Ave. Madero y Aguirre Pequeño, Col. Mitras Centro, s/n, Col. Mitras Centro, Monterrey, Nuevo León, México, C.P. 64460. Phone: +52 81 8329 4171. E-mail: dr.aquirogag@gmail.com / dr.santos.anato@gmail.com

Submitted: January 11, 2023. **Accepted:** February 20, 2023

https://doi.org/10.52083/NSQZ9800

up of a main pad or body (that is crossed by the parotid gland duct), from which several extensions arise (Kahn et al., 2000). It is wrapped within a thin fascia that is located in the masticatory space between the buccinator and the masseter muscles (Bither et al., 2013). It differs from subcutaneous fat, as it is made up of univacuolar, white fat adult adipose cells with very few fibrous trabeculae through which the vessels pass. It is not subject to lipid metabolism, making it independent of total body weight. It has an approximate mean volume of 10 ml (Kahn et al., 2000; Bither et al., 2013).

BFP constitutes an important point of reference in the aesthetics of the face through its shape, location, and right-left symmetry. A prominent BFP causing a rounded or wide face has been a common indication for a bichatectomy (bichectomy or facial lipectomy) which involves its excision (De La Lima Stevaeo, 2015; Moura et al., 2018; Roman-Torres et al., 2020). This provides a masculinization of the face, reducing the prominence of the cheeks, with improved facial aesthetic results (Lee and Park, 2017; De La Lima Stevaeo, 2015; Matarasso, 1991; Rohrich et al., 2009). Clinical evaluation has been the primary method to indicate the surgical procedure (Dubin et al., 1989; De La Lima Stevaeo, 2015; Matarasso, 1991). The procedure may be done with local anesthetics and an intraoral incision near the level of the second superior molar, identifying the Stensen's duct (De La Lima Stevaeo, 2015; Moura et al., 2018), or during more complex procedures such as facelift surgery (Surek et al., 2021). However, the procedure is not without risk. Complications include damage to the buccal branch of the facial nerve, to the parotid ducts, uncontrolled bleeding, pathological scarring, among others (Hwang et al., 2005; Pimentel et al., 2021; Rácz et al., 1989). In some cases, surgeons may overestimate the amount of buccal fat, due to a lack of parameters and indications for the procedure (Jaeger et al., 2016). Anatomical knowledge of the area, familiarity with BFP morphology, and adequate surgical training are fundamental for safer patient management (Fernández-Reyes et al., 2022; Kahn et al., 2000; Quiroga-Garza et al., 2020; Tapia-Nañez et al., 2022; Yousuf et al., 2010). Our objective was to determine the volume parameters in different age groups, the size of extensions of the BFP, as well as its relation to the second superior molar and facial artery.

MATERIALS AND METHODS

A descriptive cross-sectional, observational, and retrospective study was designed. Imaging studies (computed tomography (CT)) were obtained from the database of the Radiology and Diagnostic Imaging Department of the University Hospital "Dr. José Eleuterio González", Monterrey, Mexico. All studies were performed using a 64-slice CT scanner (General Electric CT99 Light Speed VCT, Software 2978195VCT). CT parameters were: rotation 0.4s helicoidal acquisition, 20 mm detector covering, 120 Kv, 400+, 0.625 mm width slices, 0.53:1 mm/rot Pitch, and 22 to 23 cm FOV.

Measurements were made using the Volume Viewer program to process DICOM images (General Electric Healthcare V8.7.4a). Through multiplanar sections and with the selection of specific densities, a 3D image of each BFP was obtained (Fig. 1) and distances of points located in the same plane were measured. The maximum volume (ml), length (mm), and width (mm), were registered, as well as the distance from the second molar to each of its extensions, and the distance between the segment of the facial artery that was closest to an extension of each BFP. Measurements were performed by two observers with a kappa coefficient of 0.83 for intra-observer, and 0.78 for interobserver comparison. Each study was evaluated by 2 non-blinded observers with experience in radiology and anatomy.

Inclusion criteria were CTs from adult patients (age range 18 to 75 years), without gender distinction, and with adequate BFP visualization. Those with a history of surgical procedures on the facial or neck regions, structural alterations, tumors, or artifacts, were excluded. Those with low image quality or unidentifiable BFP were eliminated.

Statistical analysis

Descriptive statistics were performed, reporting the quantitative variables with measures of central tendency and dispersion, and absolute and relative frequencies for qualitative variables.

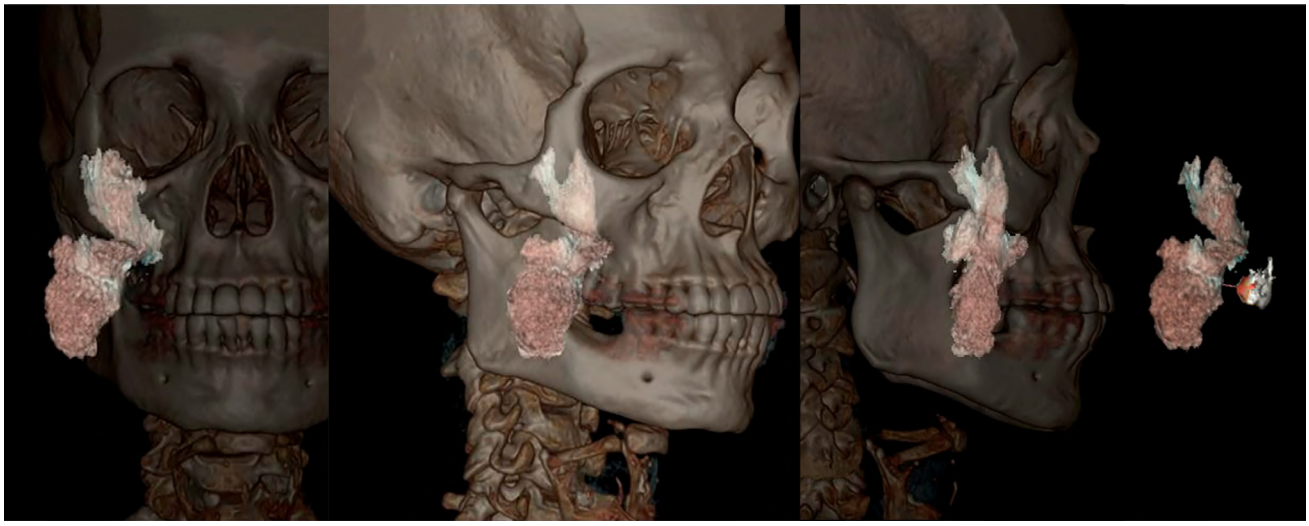

Fig. 1.- Frontal, oblique, and lateral 3D reconstruction views of the buccal fat pad. The reconstruction allows adequate visualization for plane selection for measurements in relation to structures such as the 2nd molar and the facial artery.

Quantitative variables are presented in means and standard deviations or median. Inferential statistics were also carried out by performing a normality test, resulting in a normal distribution with specific parametric tests for each variable; this was done with the SPSS IBM 24.0 program for Windows 10. The sample size was previously calculated based on the variability reported in the literature and a confidence of 95%. This resulted in a sample size of 106 BFP.

Ethical considerations

This study was previously reviewed and approved by the University's Ethics and Research Committees with the registration number AH18-00010, certifying it adheres to the guidelines of the General Health Law on Health Research in Human Beings of our country and the Declaration of Helsinki.

RESULTS

A total of 106 BFP (53 CT) were measured (66% males and 34% females). The mean age was 51±20.6 years. The morphometry measurements are shown in Table 1. The BFP extends primarily superiorly and inferiorly from the second molar, reaching ranges of up to 8.5cm and volumes of up to 32 ml. The mean distance between the 2nd molar and the facial artery was 12.9 mm but was reported as close as 3 mm. Anterior-inferior extensions of the BFP had a mean distance of 2.1 mm from the facial artery. Almost half (42.5%, n=45) of BFP were in intimate contact (less than 2 mm) with the facial artery, and another 9.4% (n=10) crossed the center of the masseteric extension. It was found at a distance from the closest portion of the BFP, a minimum of 1.6 mm, a maximum of 27.0 mm, and a mean of 10.4 (SD 5.9). The difference between genders was not statistically significant. Variables are stratified by age groups in Table 2. BFP volume did not change with age, although the age group 15 to 18 years of age had a significantly smaller size and standard deviation. There was a tendency to have a statistically longer BFP length with age, most notable in the masseteric, deep temporal, and pterygopalatine extensions.

DISCUSSION

With a mean volume of 14 ml, but ranging between 4.4 and 32.3 ml, the BFP is frequently close to or in contact with the facial artery. The FA is also 0.3 to 3 cm away from the second molar, the anatomical reference used to make the incision of the aesthetic procedure, BFP resection. This leaves the FA at risk of bleeding during surgical excision, when not considered.

Face and head aesthetic procedures are the most frequent (35.7%) worldwide, followed by breast (32.0%), and the body/extremities (32.2%) according to the 2019 survey by the International Society of Aesthetic Plastic Surgery (ISAPS, 2020). In Mexico, 580,659 aesthetic procedures

Table 1. Morphometric variables of the buccal fat pad.

		Mean (± SD)	Range	Males	Females	p
Volume (ml)		13.8 ± 5.4	4.4 – 32.3	14.5 ± 5.9	12.4 ± 3.8	0.533
Length (mm)		72.9 ± 10.7	46.7 – 96.3	74.0 ± 10.4	70.4 ± 11.2	0.481
Width (mm)		21.4 ± 5.6	6.0 – 37.4	21.2 ± 5.5	21.7 ± 5.2	0.881
Distance (mm)						
2º molar to	**BFP Extension**					
	Masseteric	32.3 ± 6.0	20.7 – 47.6	32.5 ± 6.0	31.6 ± 3.9	0.888
	Superficial temporal	59.3 ± 8.8	43.1 – 84.9	59.9 ± 8.9	56.4 ± 6.2	0.384
	Deep temporal	46.2 ± 7.3	17.6 – 76.9	46.5 ± 7.7	45.0 ± 7.5	0.228
	Pterygomandibular	30.9 ± 6.3	16.2 – 42.4	31.6 ± 5.9	28.5 ± 6.4	0.127
	Pterygopalatine	43.9 ± 7.8	25.7 – 62.6	43.8 ± 7.15	43.0 ± 9.4	0.767
	Lower orbital	39.4 ± 4.2	24.1 – 51.2	39.8 ± 3.7	37.3 ± 3.6	0.051
	Facial artery (FA)	12.9 ± 7.7	3.3 – 32.9	14.6 ± 8.5	11.9 ± 6.5	0.241
FA	Nearest	2.1 ± 1.0	1.0 – 3.0	1.84 ± 1.0	2.5 ± 0.8	

SD: standard deviation; FA: Facial artery; ml: milliliter; mm: millimeter. Statistical analysis was performed with the Kruskal-Wallis test for independent variables. *: statistical significance ($p < 0.05$).

were registered of which 38.9% were in the face and head area. A common procedure includes the bichatectomy, to improve facial contour. The procedure may be well under-reported, as it is performed by different surgical professionals ranging from dentists, maxilo-facial surgeons, and aesthetic plastic surgeons (Quiroga-Garza et al., 2022). The procedure, although simple and managed as out-patient, should be performed by trained personnel, as it can present important complications (Moura et al., 2018; Quiroga-Garza et al., 2020; Roman-Torres et al., 2020).

Hemorrhage is the most feared complication, due to the risk of hemorrhagic shock from lesions to the facial artery or other vessels derived from

Table 2. Variables measured by categorical age group division.

Age Group		**Mean (± SD)**							
		15-18	**19-30**	**31-40**	**41-50**	**51-60**	**61-70**	**>71**	**p**
Volume (ml)		11.1 ± 2.5	14.0 ± 2.9	13.2 ± 3.4	13.8 ± 5.1	15.7 ± 7.4	12.3 ± 2.5	14.6 ± 6.6	0.273
Length (mm)		65.5 ± 12.0	71.6 ± 18.3	66.8 ± 9.3	74.2 ± 7.4	76.2 ± 9.2	73.8 ± 7.2	75.6 ± 10.1	0.028*
Width (mm)		21.3 ± 5.4	23.2 ± 8.1	19.9 ± 5.1	23.1 ± 3.5	21.5 ± 7.2	21.7 ± 6.2	20.8 ± 4.0	0.800
Distance (mm)									
2º molar to	**BFP Extension**								
	Masseteric	32.9 ± 4.1	33.7 ± 10.0	28.7 ± 4.8	28.0 ± 5.1	33.7 ± 5.9	32.2 ± 6.0	34.1 ± 4.9	0.019*
	Superficial temporal	55.0 ± 9.6	53.8 ± 5.1	57.9 ± 7.0	63.6 ± 12.6	60.0 ± 10.8	58.3 ± 4.0	61.4 ± 7.0	0.092
	Deep temporal	43.6 ± 3.3	51.1 ± 13.5	48.4 ± 4.0	44.0 ± 5.4	45.1 ± 7.2	42.6 ± 8.4	48.7 ± 6.2	0.024*
	Pterygomandibular	27.6 ± 4.6	33.2 ± 3.3	29.5 ± 9.1	30.1 ± 6.7	30.8 ± 7.4	31.7 ± 5.7	32.6 ± 4.7	0.282
	Pterygopalatine	45.3 ± 8.5	45.0 ± 5.0	46.2 ± 8.6	45.8 ± 7.9	38.9 ± 7.6	41.8 ± 8.3	46.3 ± 5.9	0.016*
	Lower orbital	36.1 ± 6.3	39.9 ± 1.4	39.0 ± 3.7	40.9 ± 4.6	39.6 ± 3.6	40.0 ± 3.7	40.0 ± 3.9	0.109
	Facial artery (FA)	12.7 ± 7.1	9.8 ± 3.6	18.8 ± 9.6	16.2 ± 8.1	14.9 ± 8.9	9.4 ± 7.2	9.9 ± 4.0	0.003*
FA	Nearest	2.31 ± 0.9	1.25 ± 0.5	1.92 ± 1.0	2.0 ± 1.04	2.1 ± 1.0	2.0 ± 0.9	2.1 ± 1.0	

All values are expressed as mean ± standard deviation. Statistical analysis was performed with a one-way ANOVA test with Turkey adjustment. SD: standard deviation; ml: milliliter; mm: millimeter; *: statistical significance ($p < 0.05$).

the external carotid artery (Cepeda et al., 2019; Herrera-Nuñez et al., 2020; Roman-Torres et al., 2020; Vieira et al., 2019). Other complications include infection (Pimentel et al., 2021), lesions to the salivary parotid duct or fistula (De La Lima Stevao, 2015; Vieira et al., 2019), loss of nerve function (De La Lima Stevao, 2015), and incomplete removal (Dubin et al., 1989).

A pre-surgical imaging assessment of the BFP size should be recommended. With important anatomical structures in close proximity, a patient with a 34 ml BFP may be at risk of lesion, or incomplete removal. Procedures should be performed by highly trained medical professionals with an anatomical understanding of its morphometry and variability.

Jaeger et al. (2016) suggest the use of ultrasound to evaluate the BFP volume, although this method is operator-dependent, and may be difficult for untrained personnel. CT provided an objective and reproducible method of evaluating the BFP. This is also helpful not only in aesthetic procedure safety, but also in reconstructive surgery.

Knowledge of morphometric characteristics of the BFP is also useful in reconstructive procedures. Its vascularization and easy access make it a reliable tissue graft/flap for reconstruction of maxillofacial and oral defects (congenital, pathological, or neoplasic), as well as interpositioning material for temporomandibular joint reconstruction (Baumann and Ewers, 2000; Colella et al., 2004; Kim et al., 2017; Lucchetti et al., 2019; Mohan et al., 2012; Yang et al., 2018).

Limitations

The imaging technique selected allowed for precise morphometric measurements, but did not allow identification of nerve structures, so these could not be evaluated for risk of damage. Due to the retrospective design, BMI and patient characteristics can not be correlated with BFP.

CONCLUSIONS

The BFP has a dynamic shape with highly variable size and volume, extending primarily superiorly and inferiorly from the second molar, without statistical difference between sexes. The facial artery is frequently at risk of being damaged during the procedures due to its proximity as close as 3 mm.

REFERENCES

BAUMANN A, EWERS R (2000) Application of the buccal fat pad in oral reconstruction. *J Oral Maxillofac Surg*, 58(4): 389-392.

BITHER S, HALLI R, KINI Y (2013) Buccal fat pad in intraoral defect reconstruction. *J Maxillofac Oral Surg*, 12: 451-455.

CEPEDA LRS, VECCHIA JUNIO CPD, OVALLE DHM, GARCIA CP, DUARTE FO, BINS ELY J (2019) Hematoma pós-operatório de bichectomia: Relato de caso, revisão da literatura. *Rev Bras Cir Plástica – Brazilian J Plast Sugery*, 34.

COLELLA G, TARTARO GP, GIUDICE A (2004) The buccal fat pad in oral reconstruction. *Br J Plast Surg*, 57(4): 326-329.

DE LA LIMA STEVAO EL (2015) Bichectomy or Bichatectomy - A small and simple intraoral surgical procedure with great facial results. *Adv Dent Oral Heal,* 1(1): 1-4.

DUBIN B, JACKSON IT, HALIM A, TRIPLETT WW, FERREIRA M (1989) Anatomy of the buccal fat pad and its clinical significance. *Plast Reconstr Surg*, 83(2): 257-264.

FERNÁNDEZ-REYES BA, FLORES-GONZÁLEZ AK, ALVAREZ-LOZADA LA, GUERRERO-ZERTUCHE JT, ARRAMBIDE-GARZA FJ, QUIROZ-PERALES XG, QUIROGA-GARZA A, ELIZONDO-OMAÑA RE, GUZMÁN-LÓPEZ S (2022) The importance of simulation training in surgical sciences. *Int Surg J*, 9(6): 1289-1293.

HERRERA-NÚÑEZ M, MENCHACA-GUTIÉRREZ JL, PINALES-RAZO R, ELIZONDO-RIOJAS G, QUIROGA-GARZA A, FERNANDEZ-RODARTE BA, ELIZONDO-OMAÑA RE, GUZMÁN-LÓPEZ S (2020) Origin variations of the superior thyroid, lingual, and facial arteries: a computed tomography angiography study. *Surg Radiol Anat*, 42: 1085-1093.

HWANG K, CHO HJ, BATTUVSHIN D, CHUNG IH, HWANG SH (2005) Interrelated buccal fat pad with facial buccal branches and parotid duct. *J Craniofac Surg,* 16(4): 658-660.

ISAPS (2020) ISAPS International survey on aesthetic/cosmetic procedures 2020. URL: https://www.isaps.org/medical-professionals/isaps-global-statistics/.

JAEGER F, CASTRO CHBC DE, PINHEIRO GM, SOUZA ACRA DE, JUNIOR GTM, MESQUITA RA DE, MENEZES GB, SOUZA LN DE (2016) A novel preoperative ultrasonography protocol for prediction of bichectomy procedure. *Arq Bras Odontol*, 12(2): 1-6.

KAHN JL, WOLFRAM-GABEL R, BOURJAT P (2000) Anatomy and imaging of the deep fat of the face. *Clin Anat*, 13(5): 373-382.

KIM M-K, HAN W, KIM S-G (2017) The use of the buccal fat pad flap for oral reconstruction. *Maxillofac Plast Reconstr Surg*, 39(1): 5.

LEE TS, PARK S (2017) Use of pedicled buccal fat pad for midface augmentation. *J Craniofac Surg,* 28(8): 2133-2134.

LUCCHETTI D, PERELLI L, COLELLA F, SCOARUGHI G, BARBATO G (2019) Low intensity ultrasound can affect cell behavior and can promote drug delivery. *FASEB J*, 32(S1): 818.17.

MATARASSO A (1991) Buccal fat pad excision: Aesthetic improvement of the midface. *Ann Plast Surg*, 26(5): 413-418.

MATARASSO A (2003) Pseudoherniation of the buccal fat pad: A new clinical syndrome. *Plast Reconstr Surg*, 100(3): 723-730.

MOHAN S, KANKARIYA H, HARJANI B (2012) The use of the buccal fat pad for reconstruction of oral defects: review of the literature and report of cases. *J Maxillofac Oral Surg*, 11: 128-131.

MOURA LB, SPIN JR, SPIN-NETO R, PEREIRA-FILHO VA (2018) Buccal fat pad removal to improve facial aesthetics: an established technique? *Med Oral Patol Oral y Cir Bucal*, 23(4): 478-484.

PIMENTEL T, HADAD H, STATKIEVICZ C, ALCANTARA-JÚNIOR AG DE, VIEIRA EH, SOUZA FÁ, GARCIA-JÚNIOR IR (2021) Management of complications related to removal of the buccal fat pad. *J Craniofac Surg*, 32(3): 238-240.

QUIROGA-GARZA A, TERAN-GARZA R, ELIZONDO-OMAÑA RE, GUZMÁN-LÓPEZ S (2020) The use of clinical reasoning skills in the setting of uncertainty: a case of trial femoral head migration. *Anat Sci Educ*, 13(1): 102-106.

QUIROGA-GARZA A, GARZA-CISNEROS AN, ELIZONDO-OMAÑA RE, VILCHEZ-CAVAZOS JF, MONTES-DE-OCA-LUNA R, VILLARREAL-SILVA EE, GUZMAN-LOPEZ S, GONZALEZ-GONZALEZ JG (2022) Research barriers in the global South: Mexico. *J Glob Health*, 12: 03032.

RÁCZ L, MAROS TN, SERES-STURM L (1989) Structural characteristics and functional significance of the buccal fat pad (corpus adiposum buccae). *Morphol Embryol (Bucur),* 35(2): 73-77.

ROHRICH RJ, GHAVAMI A, LEMMON JA, BROWN SA (2009) The individualized component face lift: Developing a systematic approach to facial rejuvenation. *Plast Reconstr Surg*, 123(3): 1050-1063.

ROMAN-TORRES C, DOMINGUES NRAP, PIMENTEL AC, MARÃO HF, SENDYK WR (2020) Post-operative evaluation of the intra-oral buccal fat pad removal technique: a prospective study. *Open Dent J*, 14: 324-328.

SUREK CC, KOCHUBA AL, SAID SAD, SWANSON M, DURAES E, MCBRIDE J, DRAKE RL, ZINS JE (2021) External approach to buccal fat excision in facelift: anatomy and technique. *Aesthetic Surg J*, 41(5): 527-534.

TAPIA-NAÑEZ M, QUIROGA-GARZA A, GUERRERO-MENDIVIL FD, SALINAS-ALVAREZ Y, JACOBO-BACA G, DE-LA-FUENTE-VILLARREAL D, GUZMAN-LOPEZ S, ELIZONDO-OMAÑA E (2022). A review of the importance of research in Anatomy, an evidence-based science. *Eur J Anat,* 26(4): 477-486.

VIEIRA GM, JORGE FD, FRANCO EJ, CUNHA DIAS L DA, CARMO MACHADO GUIMARÃES M DO, OLIVEIRA LA DE (2019) Lesions of the parotid gland and buccal artery after buccal fat pad reduction. *J Craniofac Surg,* 30(3): 790-792.

YANG S, JEE Y-J, RYU D (2018) Reconstruction of large oroantral defects using a pedicled buccal fat pad. *Maxillofac Plast Reconstr Surg,* 40(1): 7.

YOUSUF S, TUBBS RS, WARTMANN CT, KAPOS T, COHEN-GADOL AA, LOUKAS M (2010) A review of the gross anatomy, functions, pathology, and clinical uses of the buccal fat pad. *Surg Radiol Anat,* 32: 427-436.

Morphology of carotid sinus wall under the influence of monosodium glutamate and following its withdrawal: an experimental study

Olha Sodomora[1], Lesia Mateshuk-Vatseba[1], Tetiana Harapko[2], Vasyl Kovalyhyn[3], Marta Kolishetska[4]

[1] *Department of Normal Anatomy, Danylo Halitskiy Lviv National Medical University, Ukraine*
[2] *Department of Human Anatomy and Histology, Uzhhorod National University, Medical Faculty, Ukraine*
[3] *Department of Histology, Cytology and Embryology, Danylo Halitskiy Lviv National Medical University, Ukraine*
[4] *Department of Pathologic Physiology, Danylo Halitskiy Lviv National Medical University, Ukraine*

SUMMARY

The aim of this experimental study was to evaluate micro- and ultrastructural changes of the carotid sinus wall during oral consumption of low doses of monosodium glutamate (MG) and following its withdrawal. Adult male albino rats (n=39) were enrolled into the study. Carotid sinus wall morphology was assessed by light and electron microscopy at the end of week 4 and week 8 of MG oral consumption, as well as 2 weeks after its withdrawal; the results were compared with the control group. After 8 weeks of MG consumption, the wall of the carotid sinus was disorganized, endothelial layer of intima deformed, often without clear margins, the media edematous and dissected with thickened elastic membranes, and the cells of the vascular wall were showing signs of apoptosis while extra fat was present in the adventitia. Upon discontinuation of MG after 4 weeks of its consumption, the structural organization of carotid sinus wall was partially preserved, whereas no compensatory processes were registered after 8 weeks of MG administration followed by 2 week-long withdrawal. Therefore, 8-week-long low-dose MG consumption resulted in pronounced changes of the micro- and ultra-structure of the carotid sinus wall of albino rats. Discontinuation of MG following 4 weeks of its administration partially improved the morphologic characteristics of the carotid sinus wall within 2 weeks. Withdrawal of MG after 8 weeks of its administration did not result in any improvement of the micro- and ultra-structure of the carotid sinus wall within 2 weeks.

Key words: Carotid sinus – Structural changes – Monosodium glutamate – Experimental study

INTRODUCTION

Widespread use of food additives, particularly MG, for the purpose of taste enhancement requires thorough morphological investigation of their possible effects on the structure of organs.

Corresponding author:
Olha Sodomora. Danylo Halitskiy Lviv National Medical University, Department of Normal Anatomy, 69 Pekarska str, Lviv, Ukraine, 79010. Phone: +380952773030 / +48881664791. E-mail: o.sodomora@gmail.com

Submitted: December 20, 2022. **Accepted:** February 21, 2023

https://doi.org/10.52083/EBSH2762

According to EFSA European Food Safety Authority Panel on Food Additives and Nutrient Sources added to Food, an acceptable daily intake (ADI) for MG was established at 30 mg/kg of body weight per day, expressed as glutamic acid, for glutamic acid and glutamates (E 620-625). The Panel noted that the exposure to glutamic acid and glutamates (E 620-625) exceeded not only the proposed ADI for all population groups at the high level (95th percentile) and at the mean level (except for the elderly), but also that these doses are associated with adverse effects in humans for some population groups. In the past, the Scientific Committee on Food established a group ADI for glutamic acid and its salts as 'not specified' in 1990; and the Joint FAO/WHO Expert Committee on Food Additives in 2006 maintained the previously established group ADI as 'not specified'. The European Commission considers revising the maximum permitted levels (Mortensen et al., 2017).

Despite the prevalence of the additives in food worldwide, scientific works dedicated to their effects on vascular morphology are scarce. Given the role of vascular pathology in the disability and mortality rates among patients of different ages, it continues to be an important medical and social problem in Ukraine and worldwide (Kyyak et al., 2019). Stroke is the fifth leading cause of death and is a leading cause of disability (Virani et al., 2020). Approximately 85% of strokes are ischaemic, they are predominantly caused by large artery disease (atherosclerosis), cardioembolism and cerebral small vessel disease. Extracranial internal carotid artery stenosis is a major cause of ischaemic stroke, as it is estimated to cause about 20% of all ischaemic strokes (Murphy et al., 2020). Atherosclerotic plaque occurs frequently at the carotid artery bifurcation and especially in the area of the carotid sinus – a slightly dilated zone in the internal carotid artery usually located cranially to carotid bifurcation and involved in hemodynamics regulation. Changes in carotid sinus size and position result in blood flow disturbances and can facilitate atherosclerotic plaque formation (Nagargoje, Gupta 2020), which is recognized as a leading cause of stroke in patients without other known cardiovascular risk factors (Cautinho et all., 2017).

MG consumption has been previously linked to obesity and arterial hypertension (Thongsepee et al., 2022), thus contributing to elevated risk of stroke, Alzheimer's disease (Fuchsberger et al., 2019; Saski-Hamada et al., 2021), developmental anomalies of the nervous system (Abdou at al., 2020), erosions of stomach wall (Chakraborty, 2019), as well as body weight increase (Konopelniuk at al., 2016). At the same time, data on the level of endogenous intoxication during long-standing MG consumption is not definitive (Bevzo, 2016). It was established that MG has toxic effects on the tissues of lymphatic nodes (Harapko et al., 2021), colon (Kolenchenko et al., 2017), and liver (Banergee et al., 2021); and it can also cause damage to the reproductive system (Mondal et al., 2018). Previous data show the ability of MG to induce oxidative stress in myocardial cells with the increase of marker enzymes, particularly lactate dehydrogenase, aspartate transaminase and alanine aminotransferase (Banergee et al., 2021). Additionally, in case of MG-induced obesity, extra fat is accumulated in the fatty tissue due to cholesterol level increase that leads to cardiovascular pathology (Airaodion et al., 2019). In recent studies, it was shown that low and moderate doses of MG increased serum levels of cholesterol, triglycerides and low density lipoproteins, as well as atherogenic index within one month of consumption (Hazzaa et al., 2020). Nevertheless, further studies are required to clarify the mechanisms of MG consumption effects on the morphology and function of blood vessels, particularly carotid arteries, when it comes to its role in development and progress of atherosclerosis as well as its direct effects on vascular walls.

MATERIALS AND METHODS

The materials constituted histologic and ultramicroscopic slides of the carotid sinus wall samples of 39 adult male albino rats, 3.5-5 months old, with initial body weight of 180-200 g, which were divided into experimental and control groups. The experimental group was further divided into three subgroups. Subgroup 1 (10 animals) received oral MG (10 mg/kg) daily for the duration of 8 weeks and had unrestricted access to standard vivarium food; subgroup 2 (10 animals) had the same

dose of MG discontinued after 4 weeks of the experiment, switching the animals to the standard vivarium diet for the next 2 weeks; subgroup 3 (10 animals) had MG withdrawn following 8 weeks of the experiment and their carotid sinuses studied 2 weeks later. The animals from the control group (9 animals) were on the standard vivarium diet for the entire duration of the experiment. MG was diluted in distilled water and 1 ml of the solution was administered orally by a syringe once daily (at 9 am) with subsequent unrestricted access to food and water. The dose of MG applied was selected on the basis of the utility patent for MG-induced obesity experimental model (Harapko et al., 2020), with the main focus on the dose to be low enough to create the possibility of results extrapolation on human population with regularly mild to moderate MG consumption. The animals from the control group were administered 1 ml of distilled water orally by a syringe once daily at approximately the same time.

All experimental animals were kept at the vivarium of Danylo Halitskiy Lviv National Medical University. The research was conducted in strict accordance with the European Convention for the Protection of Vertebrate Animals Used for Experimental and Other Scientific Purposes (Strasbourg, 1986), Council of Europe Directive 86/609/EEC (1986), the Law of Ukraine No. 3447-IV "On the Protection of Animals from Cruel Behavior" (2006), the General Ethical Principles on Animal Experimentation, approved by the First National Congress of Ukraine on Bioethics (2001).

The carotid sinuses of the experimental animals were harvested at the level of carotid bifurcation with cuts made 5 mm below and above it, with subsequent preparation of histological slides or paraffin blocks. While cutting the material, care was taken for cuts to be horizontal, i.e., perpendicular to the vascular axis.

For histologic studies, the specimens were stained with hematoxylin and eosin. The slides were studied using 400x and 1000x magnification of optic microscope, and computer system "Aver Media" was used for photographing the specimens.

Electron microscopy was also used for assessment of the specimens. Ultrathin slices of the carotid sinus wall were prepared with ultra-microtome using glass knives. Slices of silver or lemon color were selected for the study. The specimens were first contrasted in 2% solution of uranyl acetate, and then in lead citrate. The material was studied and photographed using electron microscope YEMV-100 K with acceleration voltage of 75 kV and magnification of 2000x-6000x.

RESULTS

After 8 weeks of continuous MG oral consumption (subgroup 1), the carotid sinus wall was noted to be disorganized, endothelial layer deformed, often without clear margins, sometimes interrupted; endothelial protrusions as well as endothelial proliferation were seen, and some endotheliocytes were dislodged into the carotid sinus lumen (Fig. 1a), while the endothelial layer of the carotid sinus wall in the control group did not show the aforementioned abnormalities (Fig. 1b). Subgroup 1 was remarkable for muscular bundles in the media layer that were separated with wide bands – thickened and sometimes deformed elastic membranes; some perivascular edema was present; occasional thrombi were noted in the vascular lumen (Fig. 1a).

Electron microscopy of the carotid sinus wall samples confirmed the presence of micro- and macroangiopathy following MG consumption. After 8 weeks of the experiment, considerable structural changes of the hemomicrocirculatory vessels of the carotid sinus wall were seen on the ultramicroscopic level (Fig .2a) compared to the control group (Fig. 2b). The endotheliocytes of the microcirculatory vessels were edematous with numerous mitochondria and free ribosomes in the cytoplasm. Chromatin blebs were seen on the periphery of the nuclei of endotheliocytes and pericytes, and their nucleoli were atrophied or disappearing. Apical plasmolemma was protruding in occasional places into the vessel's lumen and formed microvilli. The granular endoplasmic reticulum was fragmented; the Golgi complex contained vesicles that often proceeded to become microcysts, and mitochondria were noted to have clear matrix and scarce cristae, dissection and perforations.

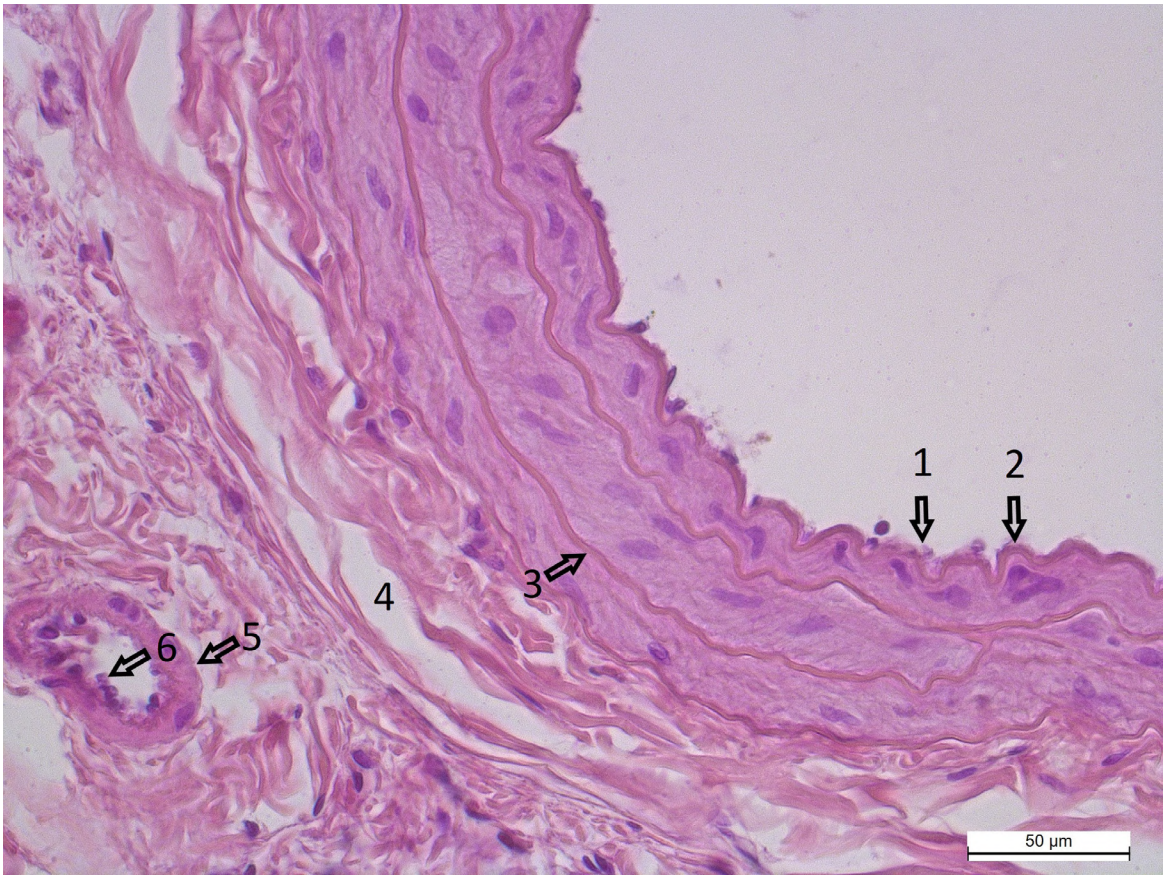

Fig. 1a.- A fragment of carotid sinus wall of an albino rat after 8 weeks of MG oral consumption. Staining with hematoxylin and eosin. Microphotograph. Magnification 400x. 1 – deformed layer of intima endotheliocytes; 2 – endothelial protrusion; 3 – thickened elastic membrane; 4 – perivascular edema; 5 – thickened arteriole wall; 6 – thrombus being formed next to the vascular wall.

Fig. 1b.- A fragment of carotid sinus wall of an albino of the control group. Staining with hematoxylin and eosin. Microphotograph. Magnification 1000x. 1 – intact layer of intima endotheliocytes; 2 – smooth intact elastic membrane.

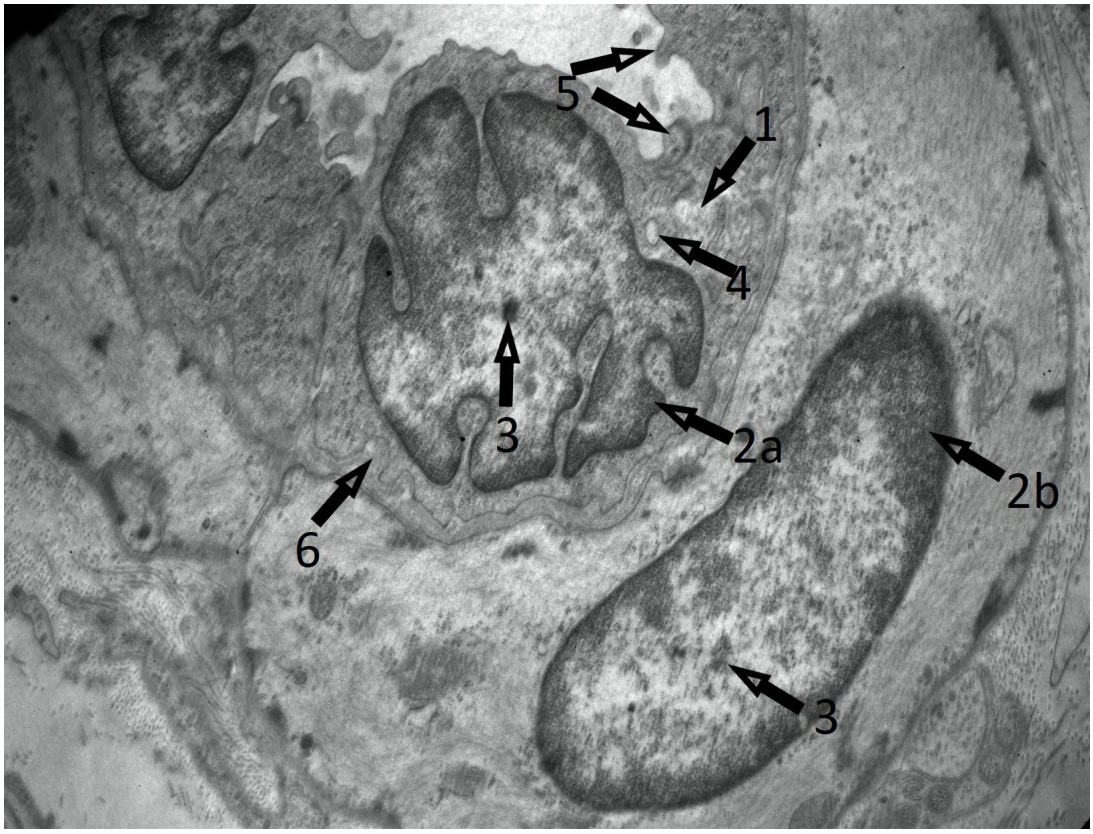

Fig. 2a.- An arteriole of the carotid sinus wall of an albino rat after 8 weeks of MG oral consumption. Magnification 6000x. 1 – vacuolated mitochondria in an endotheliocyte; 2 – chromatin accumulation at the periphery of the nucleus of an endotheliocyte (a) and pericyte (b); 3 – atrophied nucleolus; 4 – microcyst; 5 – protrusions inside the vascular lumen (microvilli) of apical plasmalemma; 6 – thickened, swollen, deformed basal membrane.

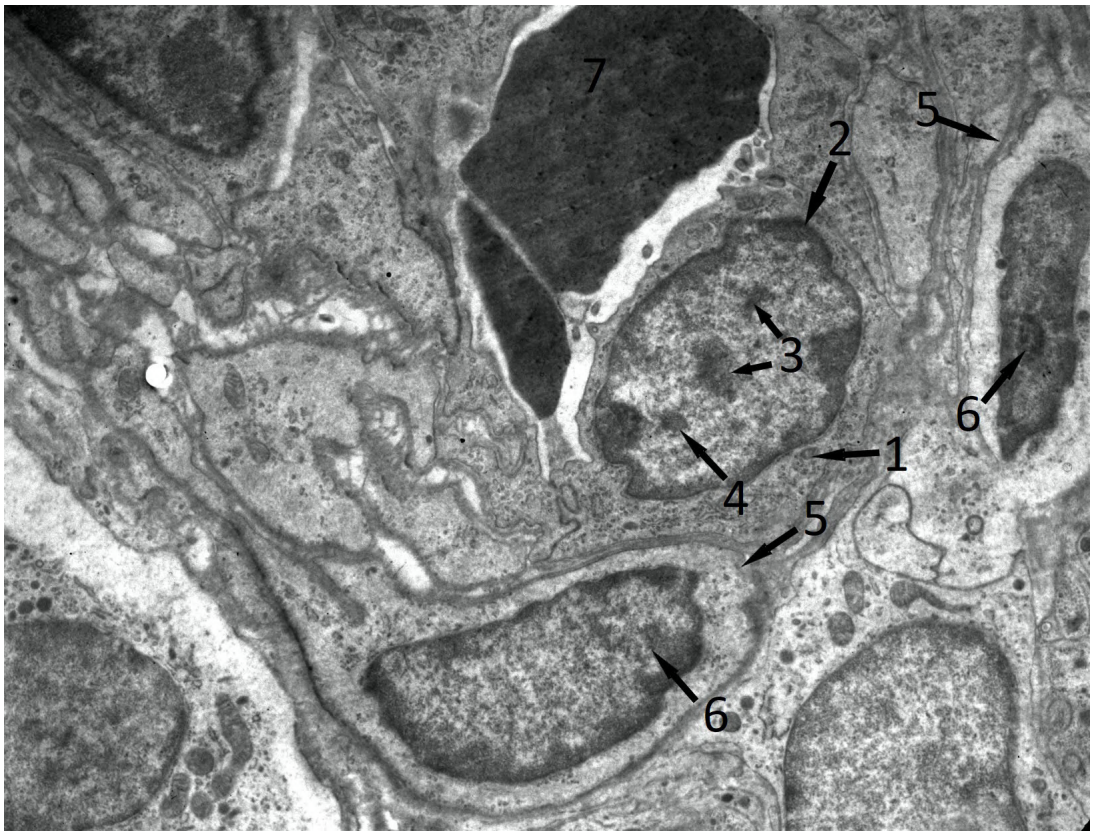

Fig. 2b.- A capillary of the carotid sinus wall of an albino rat of the control group. Magnification 4000x. 1 – intact mitochondria of an endotheliocyte; 2 – intact nucleus of a regular shape of an endotheliocyte; 3 – condensed chromatin within the nucleus; 4 – structured nucleolus within the nucleus; 5 – pericytes; 6 – structured nucleoli within the pericytes nuclei; 7 – erythrocyte in the microvascular lumen.

Regarding the structure of the carotid sinus intima after 8 weeks of the experiment, its endotheliocytes were considerably damaged, with their contours distorted and their shape bizarrely changed. The cytoplasm was edematous, with vacuoles and fused pinocytic vesicles seen within the endothelial cells, their mitochondria swollen with impaired cristae; the granular endoplasmic reticulum was damaged, and some nuclei contained condensed chromatin located peripherally, while other ones were translucent, their nuclear membrane featuring deep invaginations. Many nuclei showed signs of apoptosis and karyopycnosis. The media layer was also disorganized. Most nuclei of the smooth myocytes had irregular shape and their chromatin was represented by heterochromatin mostly located peripherally, perinuclear and pericellular spaces enlarged, mitochondria swollen, their cristae homogenized for the most part. Structureless areas of the cytoplasm were observed in the majority of the myocytes. Elastic membranes were thickened, fuzzy and without clear margins (Fig. 3a). The control group, however, showed no pathological changes in the morphology of intima or media structures (Fig. 3b). Hence, in the control group, micro- and ultra-structural organization of the carotid sinus wall was preserved and within the species norm if compared to subgroup 1, which that was subjected to oral consumption of MG and unrestricted access to food for the duration of 8 weeks, resulting in some morphological changes as described above.

In case of MG withdrawal and switching of the animals to the standard vivarium diet with evaluation of carotid sinus wall morphology 2 weeks upon MG discontinuation following the preceding period of 4 weeks (subgroup 2) and 8 weeks (subgroup 3) of MG oral consumption and unrestricted access to food, partial preservation of the carotid sinus wall structure was observed on assessment with light microscopy in subgroup 2 (Fig. 4a), while almost no improvement was noted in sub-

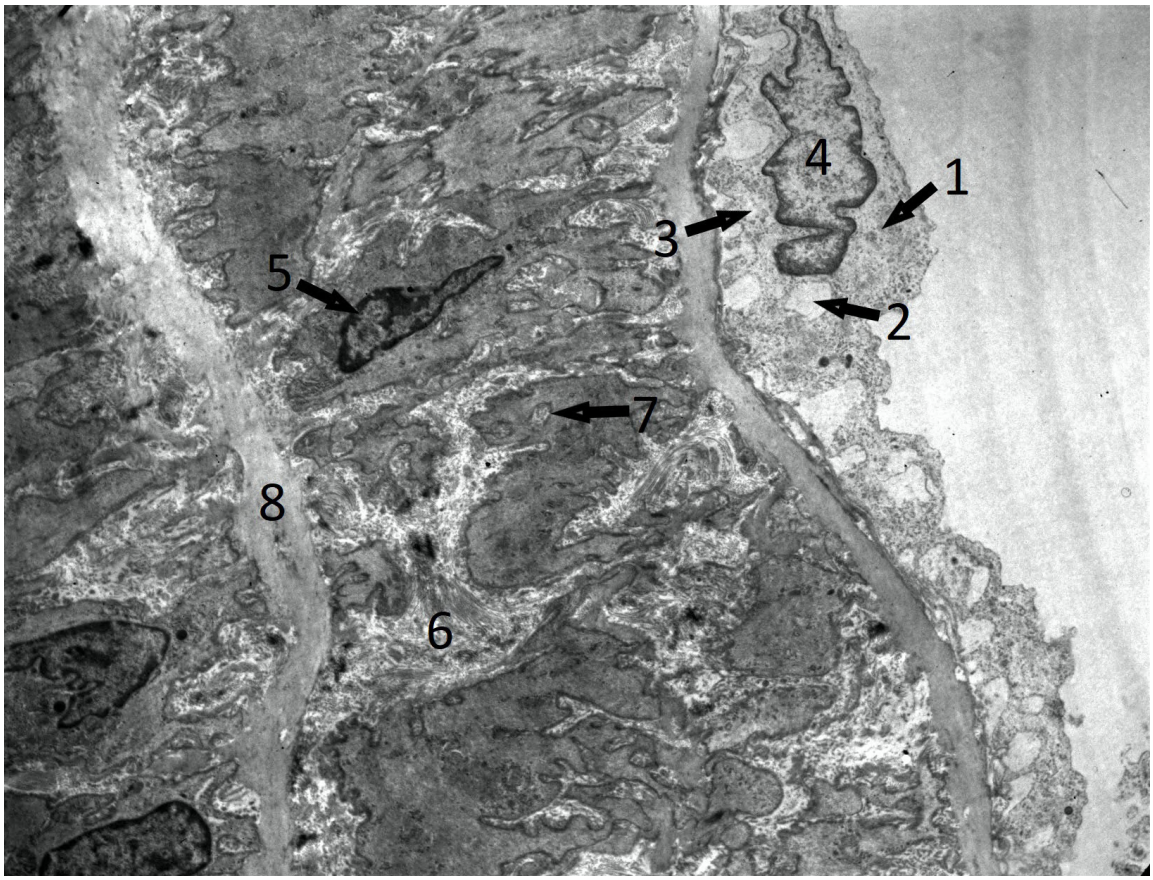

Fig. 3a.- A fragment of carotid sinus wall of an albino rat after 8 weeks of MG oral consumption. Magnification 2000x. 1 – translucent cytoplasm of an endotheliocyte of the carotid sinus wall intima; 2 – vacuole; 3 – swollen mitochondria with damaged cristae; 4 – translucent nucleus of an endotheliocyte with condensed chromatin located on the periphery of the nucleus; 5 – a smooth myocyte nucleus of irregular shape; 6 – dilated pericellular space; 7 – swollen mitochondria with homogenized cristae; 8 – thickened, disorganized elastic membrane lacking clear margins.

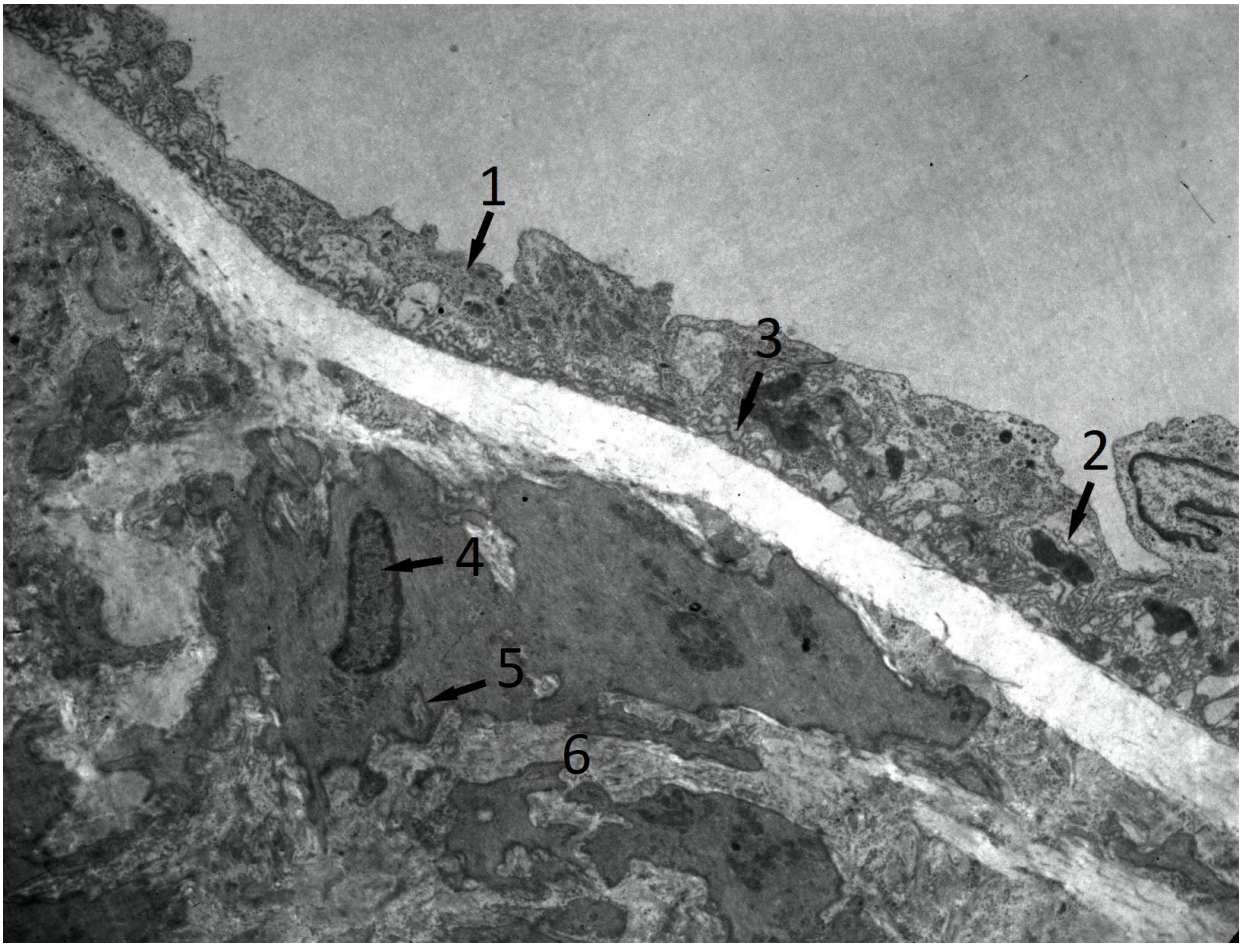

Fig. 3b.- A fragment of carotid sinus wall of an albino rat of the control group. Magnification 2000x. 1- intact endothelial layer; 2 – intact nucleus of an endotheliocyte featuring condensed chromatin; 3 – intact mitochondria of an endotheliocyte; 4 – intact nucleus of a myocyte; - intact mitochondria of a myocyte; 6 – intercellular space.

group 3 (Fig. 4b). For subgroup 2, signs of carotid sinus wall edema, fibrosis, hyperemia of adventitial capillaries, many of them with damaged walls, and additionally some diapedesis bleedings were noted (Fig. 4a), while in subgroup 3 destructive changes of the endothelium, as well as signs of connective tissue and perivascular edema, were seen along with microcirculatory vessels hyperemia (Fig. 4b).

While assessing the aforementioned experimental material with electron microscopy, carotid sinus morphology as well as vasa vasorum were found to be in satisfactory state in subgroup 2. However, some endotheliocytes were remarkable for karyopyknosis. Additionally, fibrosis of vascular walls was noted, as well as occasional cytoplasmic protrusions of endothelial cells into the lumen of micro- and macro-vessels. (Figs. 5, 6, 7).

In case of MG withdrawal after 8 weeks of oral consumption combined with unrestricted access to food, no compensatory processes were seen in the wall of carotid sinus of the experimental animals of subgroup 3 on electron microscopy (Fig. 8a) compared to the control group (Fig. 8b). Carotid sinus wall was notably thickened, intima showed signs of exudative-proliferative inflammatory processes, media was remarkable for the presence of vacuole-type dystrophy of myocytes, fibrotic and sclerotic changes and elastic membranes deformation. Adventitia showed structural changes of all hemomicrocirculatory vessels: hyperemia of capillaries and arterioles, formation of thrombi adjacent to vascular walls, dilation and thinning of venules' walls, perivascular edema as well as marked poikilocytosis of erythrocytes – fragmented cells, basket cells, degmacytes were seen in the microvascular lumen (Fig. 9a), while no significant changes in vascular or cellular morphology were observed in the control group (Fig. 9b, 9c), suggesting that structural impairment was less likely to regress over time in case of more prolonged exposure to MG and excessive food intake.

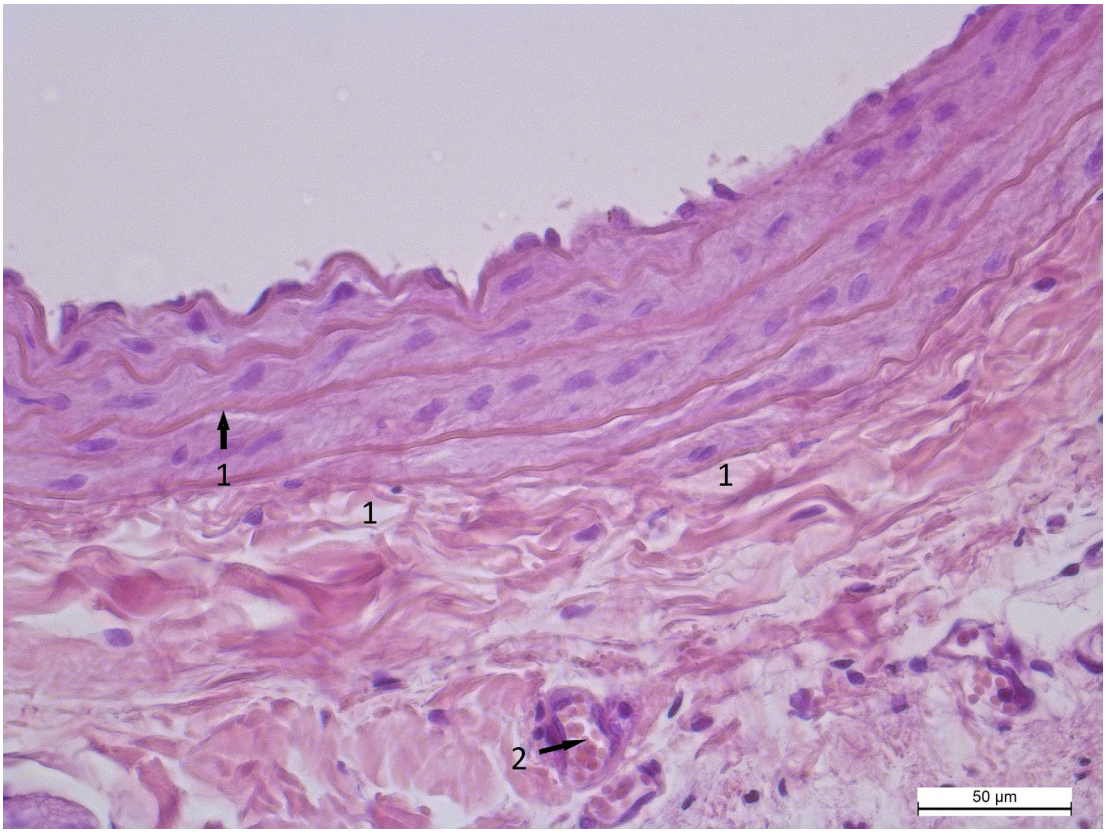

Fig. 4a.- A fragment of carotid sinus wall of an albino rat 2 weeks after withdrawal of MG following 4-week-long oral consumption. Hematoxylin & Eosin staining. Magnification 400x. 1 – signs of swelling in the carotid sinus wall; 2 – hyperemia of an adventitia capillary, damaged walls of the capillary and diapedesis bleeding.

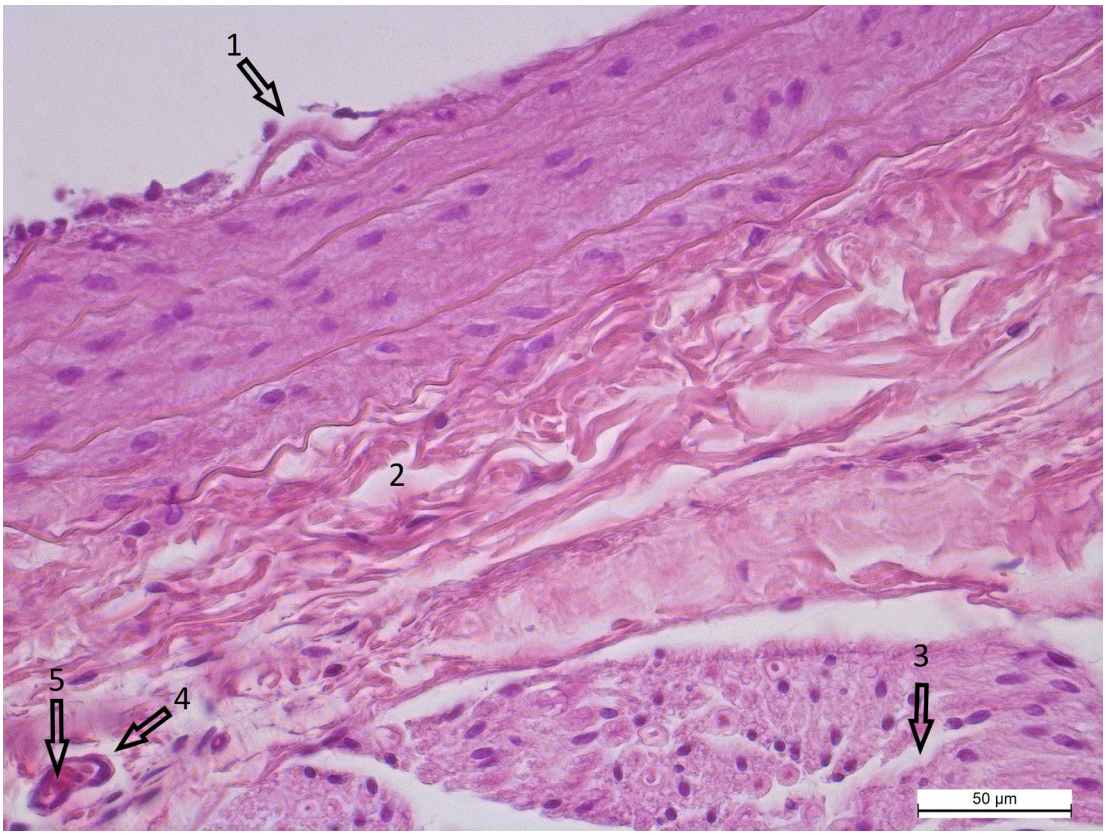

Fig. 4b.- A fragment of carotid sinus wall of an albino rat after 8 weeks of MG oral consumption and 2 week-long withdrawal. Hematoxylin & Eosin staining. Magnification 400x. 1 – de-structured endothelial layer; 2 – edematous connective tissue layers in the carotid sinus wall; 3 – widened connective tissue area in the carotid glomus; 4 – perivascular edema; 5 – hyperemia in a capillary of the carotid sinus wall.

Fig. 5.- An arteriole of carotid sinus wall of an albino rat following 4 weeks of MG oral consumption and 2 week-long withdrawal. Magnification 4000x. 1 – karyopyknosis in an endotheliosyte; 2 – intact perycite nucleus; 3 – endothelium; 4 – neurocyte nucleus, 5 – vascular lumen.

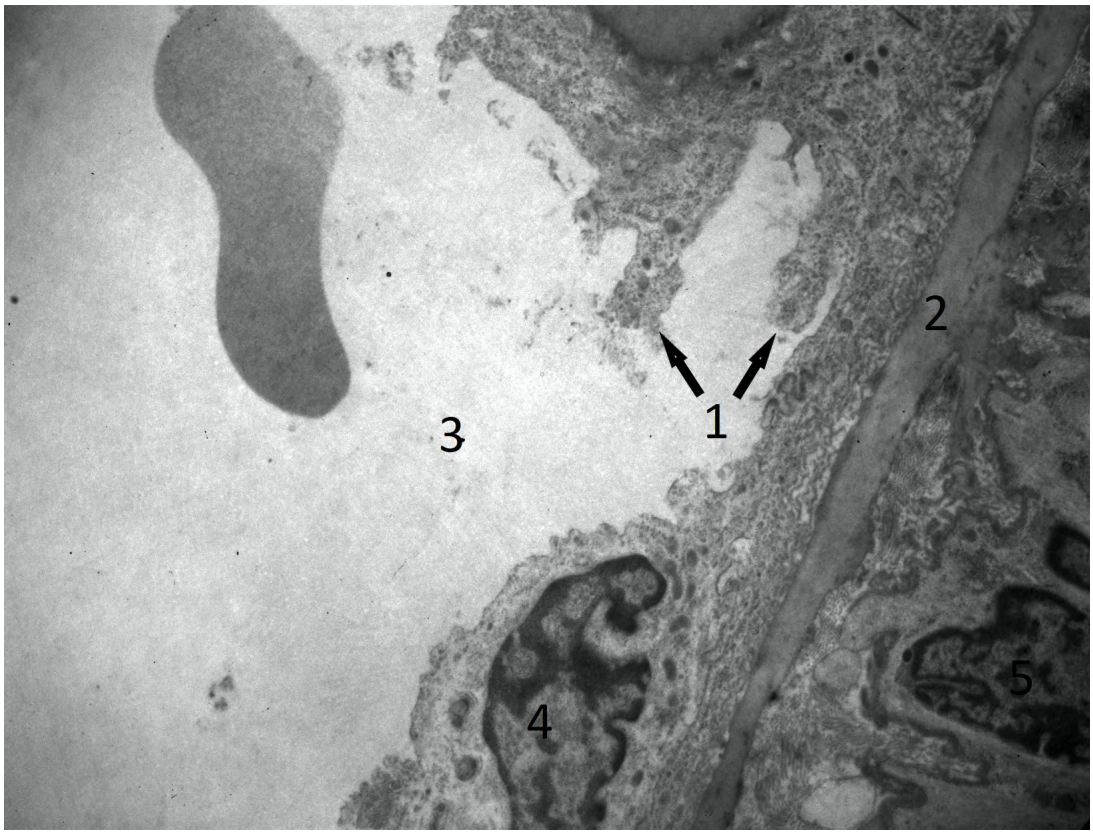

Fig. 6.- A fragment of carotid sinus wall of an albino rat following 4 weeks of MG oral consumption and 2 week-long withdrawal. Magnification 4000x. 1 – cytoplasmic protrusion of an endothelial cell into the macrovascular lumen; 2 – elastic membrane of media; 3 – macrovascular lumen; 4 – intact endotheliocyte nucleus; 5 – intact myocyte nucleus.

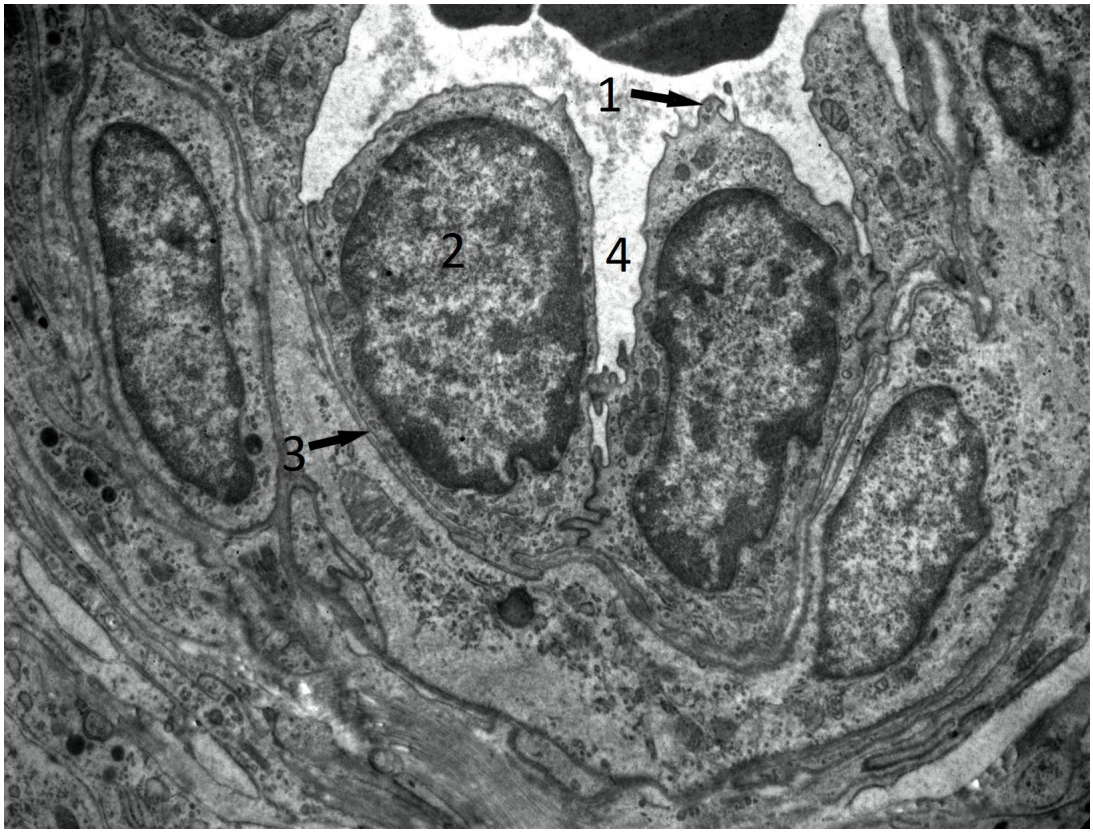

Fig. 7.- An arteriole of the carotid sinus wall of an albino rat following 4 weeks of MG consumption and 2 week-long withdrawal. Magnification 4000x. 1 – cytoplasmic protrusion; 2 – intact endotheliocyte nucleus; 3 – structured basal membrane; 4 – microvascular lumen.

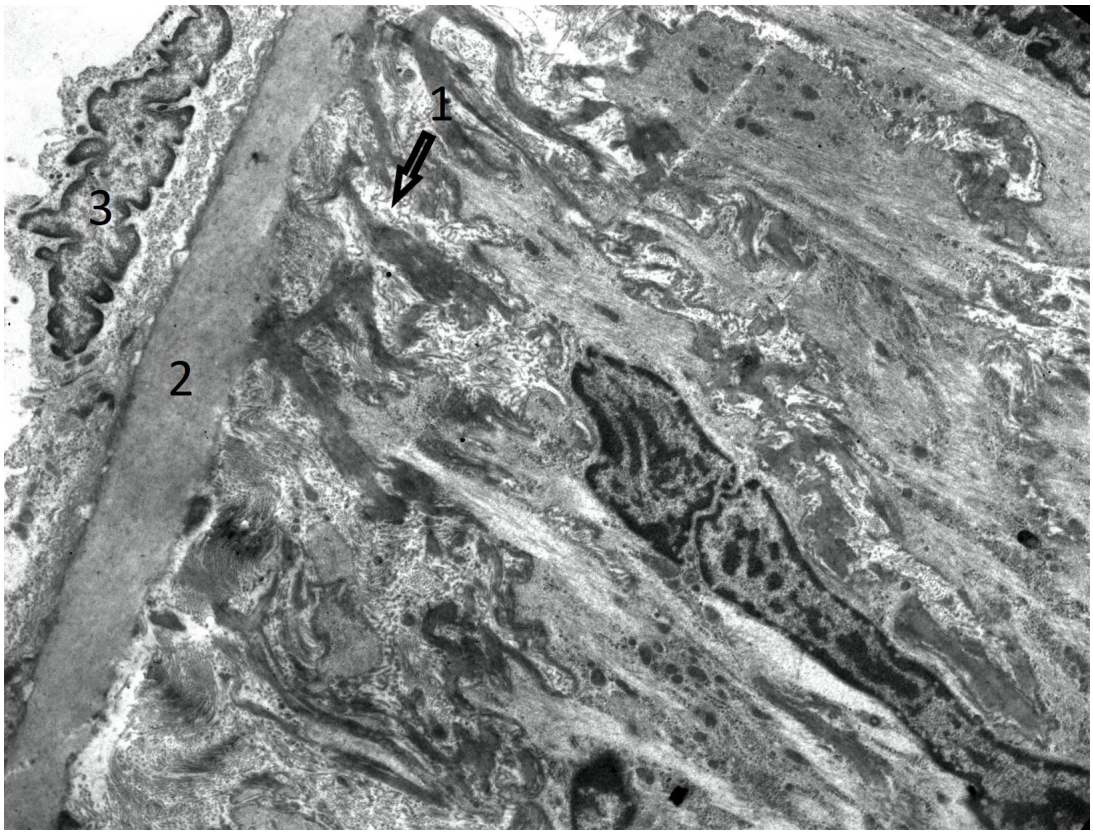

Fig. 8a.- A fragment of the carotid sinus wall of an albino rat after 8 weeks of MG oral consumption and 2 week-long withdrawal. Magnification 2000x. 1 – vacuolated dystrophy of a myocyte; 2 – deformed elastic membrane; 3– fragmented nucleus of a de-structured endotheliocyte.

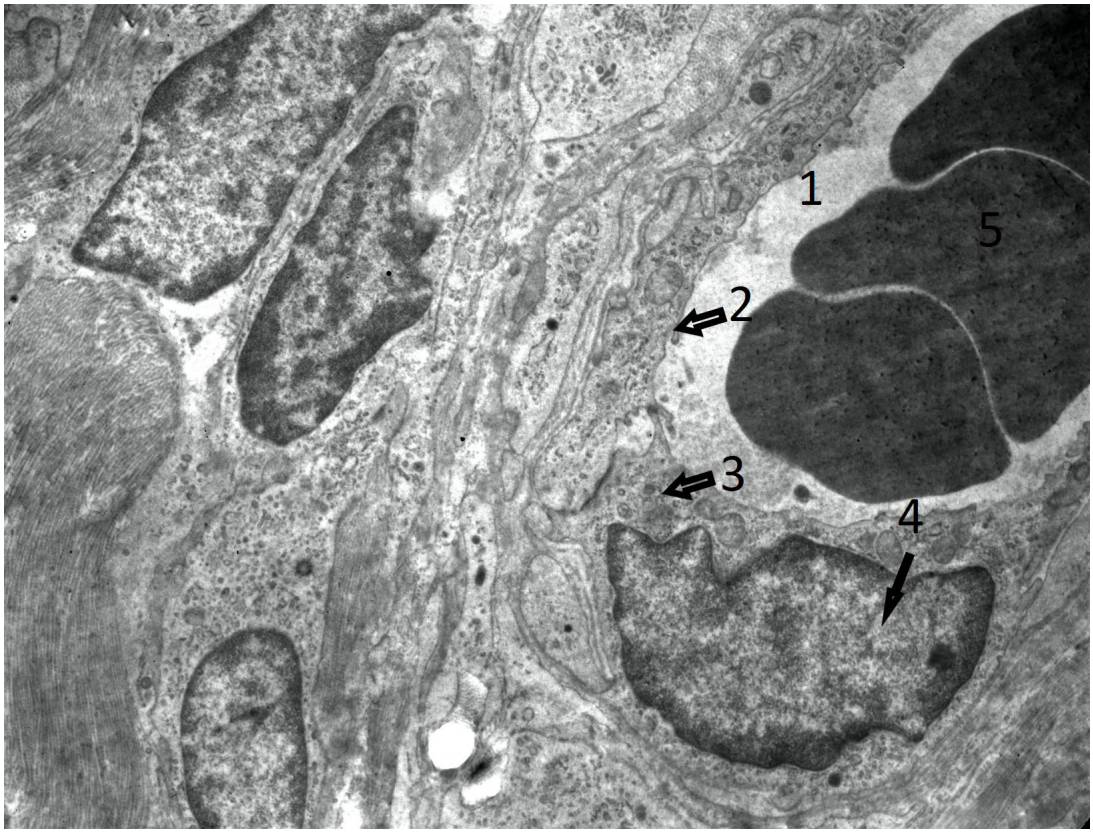

Fig. 8b.- A capillary of the carotid sinus wall of an albino rat of the control group. Magnification 3800x. 1 – lumen of the vessel; 2 – vascular wall; 3 – endotheliocyte; 4 – intact nucleus of the endotheliocyte; 5 – erythrocyte in the vascular lumen.

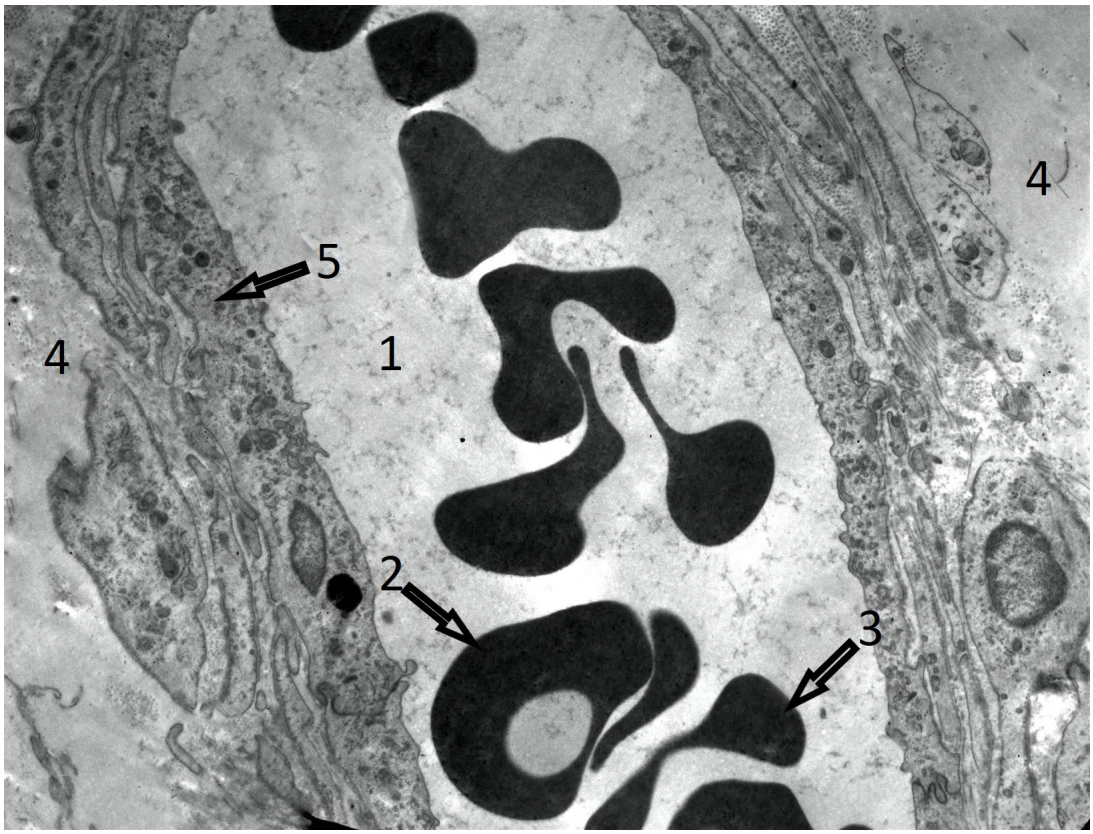

Fig. 9a.- A venule of the carotid sinus wall of an albino rat after 8 weeks of MG oral consumption and 2 week-long withdrawal. Magnification 3000x. 1 – dilated lumen of a venule in the carotid sinus wall; 2 – basket cells in the lumen of a venule; 3 – degmacyte in the lumen of a venule; 4 – perivascular edema; 5 – de-structured wall of a venule.

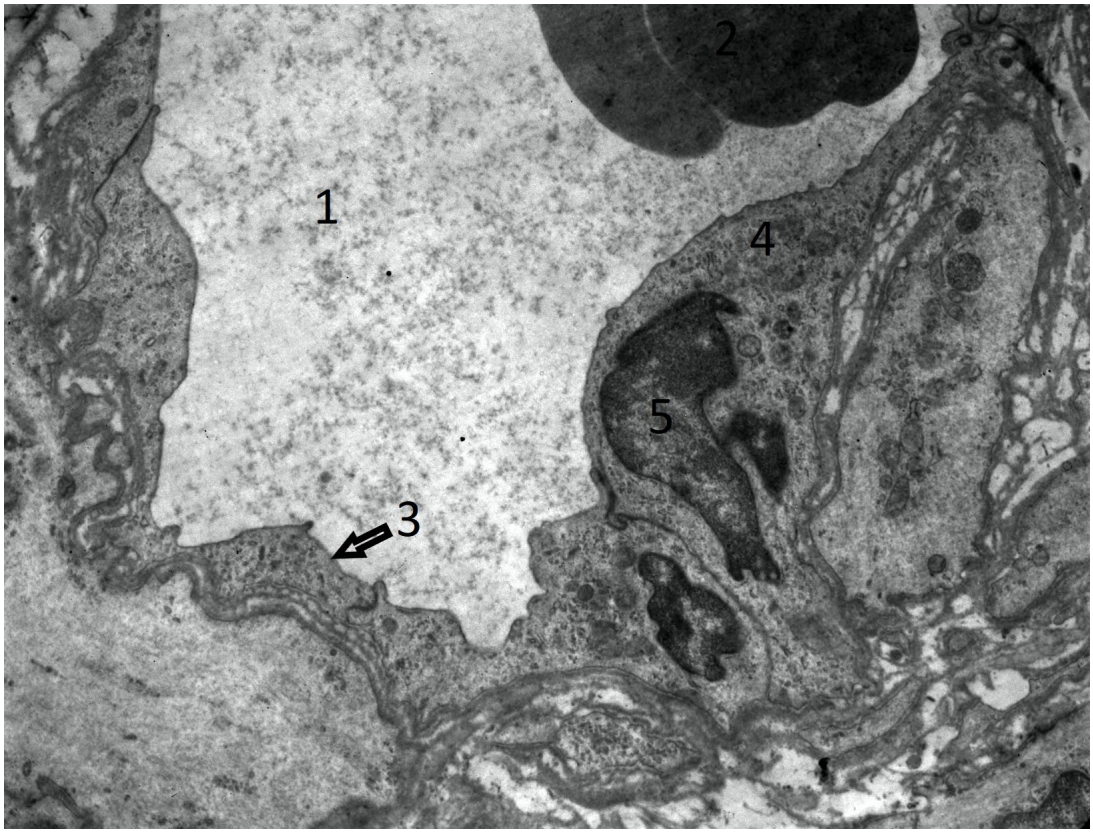

Fig. 9b.- A venule of the carotid sinus wall of an albino rat from the control group. Magnification 3800x. 1 – lumen of the venule; 2 – erythrocyte in the lumen; 3 – wall of the venule; 4 – endotheliocyte; 5 – intact nucleus of the endotheliocyte.

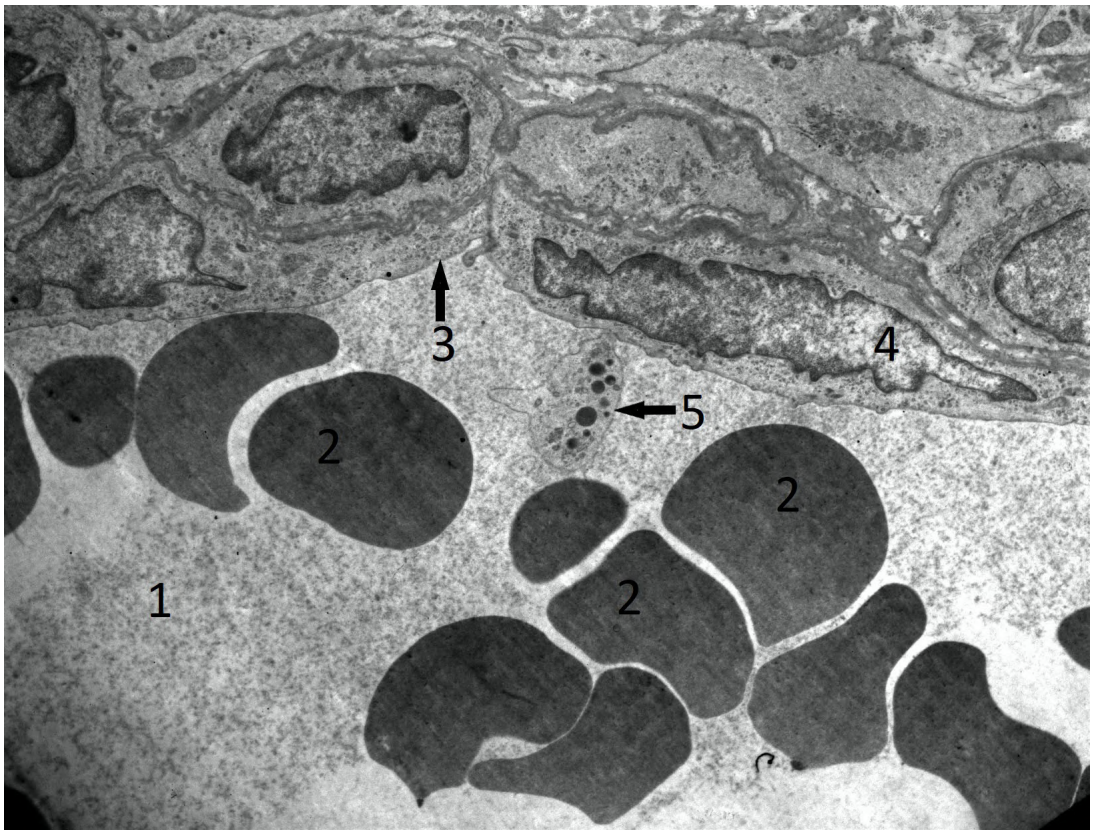

Fig. 9c.- A venule of the carotid sinus wall of an albino rat from the control group. Magnification 4000x. 1 – lumen of the venule; 2 – erythrocytes in the lumen; 3 – wall of the venule; 4 – endotheliocyte; 5 – platelet in the lumen.

DISCUSSION

Mechanisms of MG toxic action on humans and animals have been triggering interest in researches worldwide for quite some time (Umbuzeiro et al., 2017; Bevzo, 2017). During decades, MG has been allowed for consumption, considered relatively safe and widely used in many countries. At the same time, it was shown in numerous scientific studies that prolonged and systematic MG consumption may be associated with a number of pathological conditions, such as metabolic syndrome (Banerjee et al., 2021a, b), diabetes mellitus, dyslipidemia and obesity (Bautista et al., 2019), hypertension and other cardiovascular disorders (Malik, Sabahelkhier, 2019), neuroendocrine disturbances, depression and anxiety (Kumar et al., 2021; Kraal at al., 2020), reproductive and urinary disorders (Pongking at al., 2020), liver disease (Albrahim et al., 2018) and others. MG was also reported to cause increase in food intake (Onaolapo, 2019), which we also observed in our study. This fact might have contributed to the accumulation of excessive fat in the tissues surrounding the carotid sinus and within its wall in our study. A link between extracranial carotid pathology and covert brain infarctions has previously been established (Baradaran et al., 2022). Notably, large artery atherosclerosis has been also associated with cerebral small vessel disease (Ding et al., 2017). These considerations point towards possible pathogenetic implications of morphological changes of the carotid arteries, particularly the carotid sinus wall, in the context of cerebral circulation impairment with subsequent cerebrovascular disturbances and events. Moreover, in our study, impairment of endotheliocytes' nuclei was noted, which indicates MG's ability to cause nuclear damage, potentially leading to genotoxicity. Gene mutations can lead to development of different pathologies, including neurologic defects, metabolic disturbances and neoplasia that may manifest in the next generations (Syed Imam at al., 2019). Therefore, further research is needed to clarify the role of MG in cells apoptosis induction, as well as its possible ability to interfere with structural integrity of cellular genetic material. MG was shown to have a role in metabolic disturbances, namely increase in prostanoid synthesis, together with hypersensitivity to thromboxane A2 combined with potassium channels inhibition, and decrease in nitric oxide levels were shown to have the ability to lead to arterial hypertension in the setting of MG-induced obesity (Majewski at al., 2018). MG consumption combined with high-fat diet causes rise in nitric oxide levels and oxidative stress, hence increasing the affected area in myocardial infarction in experimental setting (Aghajani at al., 2017). Structural changes of myocytes of carotid sinus media observed by us were similar to the damage of cardiomyocytes described in the setting of ischemia and diabetes mellitus (Nadraga at al., 2020; Vlasiuk at al., 2018). Besides changes in the intima and media layers of the carotid sinus wall seen in our study, adventitia was also remarkable for structural changes, with microvasculature impairment and fatty deposits being the most notable ones. Our results are supported by a previous study of MG consumption effects on the aortic wall (Heil et al., 2020). Our research suggests that MG consumption in the experimental setting affects each layer of the vascular wall. This can potentially result in cerebral perfusion compromise due to impairment of the morphology of the carotid arteries.

In our study, some of the structural changes of the carotid sinus that occurred as a result of MG consumption and high food intake were reversible, following MG discontinuation and switching to standard diet, provided that this occurred early enough, suggesting that diet composition and food intake modifications can alter the unfavorable effects of MG consumption, especially at early stages.

The original results of our study are related to identification of specific morphological changes of the carotid sinus wall of albino rats under the influence of MG, and after its withdrawal at different stages of the experiment using light and electron microscopy.

Prospects for further development

Further investigation of possible ways of correction of micro- and ultra-structural changes of the carotid sinus wall in the setting of MG influence is a promising direction for research, opening pos-

sibilities of minimization of its unfavorable action and prevention of vascular disorders associated with structural damage of the carotid sinus wall and adjacent structures.

CONCLUSIONS

Eight week-long MG consumption causes pronounced micro- and ultrastructural changes of the carotid sinus wall in experimental albino rats.

Withdrawal of MG within 4 weeks of its consumption and switching the experimental animals to standard diet considerably improves the morphology of the carotid sinus wall.

Withdrawal of MG within 8 weeks of consumption does not result in restoration of micro- or ultra-structure of the carotid sinus wall.

ACKNOWLEDGEMENTS

We would like to express our gratitude to our colleagues from departments of Danylo Halitskiy Lviv National Medical University and Medical Faculty of Uzhhorod National University for their support and collaboration.

REFERENCES

ABDOU HM, HASSAN EH, ALY RG (2020) Monosodium glutamate (MSG): promoter of neurotoxicity, testicular impairment, inflammation and apoptosis in male rats. *Swed J BioSci Res,* 1(2): 78-90.

AGHAJANI M, IMANI A, FAGIHI M, MAHDAVI MRV, MAHBOUBI S, MORADI F, MOGHADDAM EK (2017) Does increased nitric oxide production and oxidative stress due to high fat diet affect cardiac function after myocardial infarction? *J Cell Mol Anesthesia*, 2: 3-8.

AIRAODION AI, OGBUAGU EO, OSEMWOWA EU, OGBUAGU U, ESONU CE, AGUNBIADE AP, OKEREKE D, OLORUNTOBA A (2019) Toxicological effect of MG in seasonings on human health. *Global J Nutrit Food Sci*, 1(5): 40-49.

ALBRAHIM T, BINOBEAD MA (2018) Roles of Moringa oleifera leaf extract in improving the impact of high dietary intake of MG-induced liver toxicity, oxidative stress, genotoxicity, DNA damage, and PCNA alterations in male rats. *Oxid Med Cell Longev*, 2018: 4501097.

BANERJEE A, MUKHERJEE S, MAJI BK (2021a) Efficacy of Coccinia grandis against MG induced hepato-cardiac anomalies by inhibiting NF-kB and caspase 3 mediated signaling in rat model. *Hum Exp Toxicol*, 40(11): 1825-1851.

BANERJEE A, MUKHERJEE S, MAJI BK (2021b) Worldwide flavor enhancer monosodium glutamate combined with high lipid diet provokes metabolic alterations and systemic anomalies: An overview. *Toxicol Rep,* 8: 938-961.

BARADARAN H, CULLETON S, STODDARD G, ALEXANDER MD, ROMERO JR, HADLEY JR, KIM SE, PARKER DL, MCNALLY JS (2023) Association between high-risk extracranial carotid plaque and covert brain infarctions and cerebral microbleeds. *Neuroradiology*, 65: 287-295.

BAUTISTA RJH, MAHMOUD AM, KONIGSBERG M, GUERRERO NELD (2019) Obesity: Pathophysiology, monosodium glutamate-induced model and anti-obesity medicinal plants. *Biomed Pharmacother,* 111: 503-516.

BEVZO VV (2016) Research of toxodynamic of MSG on the rats' body during its prolonged entering. *Clin Exp Pathol*, 15(2): 13-16.

BEVZO VV (2017) Superoxide, catalase and general antioxidant activity of blood and liver of rats based on action of MSG. *Ukrain J Med, Biol Sport Med Sci,* 1(3): 12-16.

CHAKRABORTY SP (2019) Patho-physiological and toxicological aspects of monosodium glutamate. *Toxicol Mech Meth,* 29(6): 389-396.

COUTINHO JM, DERKATCH S, POTVIN AR, TOMLINSON G, CASAUBON LK, SILVER FL, MANDELL DM (2017) Carotid artery web and ischemic stroke: A case-control study. *Neurology,* 88(1): 65-69. Erratum in: *Neurology*, 2017, 89(5): 521.

DING L, HONG Y, PENG B (2017) Association between large artery atherosclerosis and cerebral microbleeds: a systematic review and meta-analysis. *Stroke Vasc Neurol,* 2(1): 7-14.

EL MALIK A, SABAHELKHIER MK (2019) Changes in lipid profile and heart tissues of Wistar rats induces by using monosodium glutamate as food additive. *Int J Biochem Physiol*, 4(1): 141-147.

FUCHSBERGER T, YUSTE R, MARTINEZ-BELLVER S, BLANCO-GANDIA MC, TORRES-CUEVAS I, BLASCO-SERRA A, ARANGO R, MIÑARRO J, RODRÍGUEZ-ARIAS M, TERUEL-MARTI V, LLORET A, VIÑA J (2019) Oral monosodium glutamate administration causes early onset of Alzheimer's disease-like pathophysiology in APP/PS1 mice. *J Alzheimer's Dis*, 72(3): 957-975.

HARAPKO T, MATESHUK-VATSEBA L (2021) Effects of MSG on the lymph nodes of the albino rat: ultrastructural and morphometric studies. *Eur J Anat*, 25(1): 75-81.

HAZZAA SM, EL-ROGHY ES, ABD ELDAIM MA, ELGARAWANY GE (2020) MG induces cardiac toxicity via oxidative stress, fibrosis, and P53 proapoptotic protein expression in rats. *Environ Sci Pollut Res Int*, 27(16): 20014-20024.

HEIL EM, AL-BAZI W, AL-AAMELI MH (2020) The histological alteration of proximal part of aorta exposed to (MSG) and protective effect of a lipoic acid (ALA) in male rabbits. *Indian J Forensic Med Toxicol*, 14(3): 942-948.

KOLENCHENKO OO, FALALYEYEVA TM, FALALYEYEVA TV, KURIK OH (2017) Structural-functional changes in the colon wall under conditions of sodium glutamate usage. *Ukrain J Med Biol Sport Exp Med Morphol*, 5(7): 39-43.

KONOPELNIUK VV, PRYBYTKO IY, TSYRIUK IY, FALALYEYEVA TM (2016) Pathophysiology characteristics of the experimental model of obesity in female rats induced by neonatal administration of MG. *Sci Rise: Biol Sci*, 3(3): 14-18.

KRAAL AZ, ARWANITIS NR, JAEGER AP, ELLINGROD VL (2020) Could dietary glutamate play a role in psychiatric distress? *Neuropsychobiology*, 79(1): 13-19.

KUMAR P, KRAAL AZ, PRAWZIK AM, RINGOLD AE, ELLINGROD V (2021) Dietary glutamic acid, obesity, and depressive symptoms in patients with schizophrenia. *Front Psychiatry*, 11: 620097.

KYYAK YH, BARNETT OY, HALKEVYCH MP, LABINSKA OY, KYYAK HU, KYSIL OY (2019) Impact of risk factors of ischemic heart disease on the development of acute coronary syndrome, platelet ultrastructure, and aspirin resistance. *Wiad Lek*, 72(11.1): 2099-2103.

MAJEWSKI M, JURGONSKI A, FOTSCHKI B, JUSKIEWICZ J (2018) The toxic effects of MG (MSG) - the involvement of nitric oxide, prostanoids and potassium channels in the -reactivity of thoracic arteries in MSG-obese rats. *Toxicol Appl Pharmacol*, 359: 62-69.

MATESHUK-VATSEBA LR, HARAPKO TV, KYRYK HA, BLYSHAK NB, PRYMACHENKO VI, PIDVALNA UY, TA IN, VYNAKHIDNYKY; L'VIVS'KYY NATSIONAL'NYY MEDYCHNYY UNIVERSYTET IMENI DANYLA HALYTS'KOHO, PATENTOVLASNYK. (2020) Experimental model for

alimentary obesity induction by indirect influence of monosodium glutamate. *Utility patent of Ukraine* UA 144191 U G09B 23/28 (2006.01), G01N 33/50 (2006.01). №2020 02310, 17 https://sis.ukrpatent.org/en/search/detail/1451574/.

MONDAL M, SARKAR K, NATH PP, PAUL G (2018) MG suppresses the female reproductive function by impairing the functions of ovary and uterus in rat. *Environ Toxicol*, 33(2): 198-208.

MORTENSEN A, AGUILAR F, CREBELLI R, et al. EFSA Panel on Food Additives and Nutrient Sources added to Food (ANS) (2017) Re-evaluation of glutamic acid (E 620), sodium glutamate (E 621), potassium glutamate (E 622), alcium glutamate (E 623), ammonium glutamate (E 624) and magnesium glutamate (E 625) as food additives. *EFSA J*, 15(7): e04910. doi: 10.2903/j.efsa.2017.4910.

MURPHY SJX, WERRING DJ (2020) Stroke: causes and clinical features. *Medicine (Abingdon),* 48(9): 561-566.

NADRAGA KHI, STRUS AM, YASHCHENKO AD, LUTSYK OD (2020) Immunohistochemical investigation of rat cardiac muscle in experimental ischemia. *Acta Med Leopoliensia*, 26(1): 11-20.

NAGARGOJE M, GUPTA R (2020) Effect of sinus size and position on hemodynamics during pulsatile flow in a carotid artery bifurcation. *Computer Meth Programs Biomed,* 192: 105440.

ONAOLAPO AY, ODETUNDE AS, AKINTOLA MO, OGUNDEJI MO, AJAO A, OBELAWO AY, ONAOLAPO OJ (2019) Dietary composition modulates impact of food-added monosodium glutamate on behaviour, metabolic status and cerebral cortical morphology in mice. *Biomed Pharmacother,* 109: 417-428.

PONGKING T, HAONON O, DANGTAKOT R, ONSURATHUM S, JUSAKUL A, INTUYOD K, SANGKA A, ANUTRAKULCHAI S, CHA'ON U, PINLAOR S, PINLAOR P (2020) A combination of MG and high-fat and high-fructose diets increases the risk of kidney injury, gut dysbiosis and host-microbial co-metabolism. *PLoS One*, 15(4): e0231237.

SASAKI-HAMADA S, HOJYO Y, MIZUMOTO R, KOYAMA H, YANAGISAWA S, OKA JI (2021) Cognitive and hippocampal synaptic profiles in MG-induced obese mice. *Neurosci Res*, 170: 201-207.

SYED IMAM R, IMAM RABBANI S (2019) Genotoxicity of MG: a review on its causes, consequences and prevention. *Indian J Pharmaceut Educ Res*, 53(4): S510-517.

THONGSEPEE N, MARTVISET P, CHANTREE P, SORNCHUER P, SANGPAIROJ K, PRATHAPHAN P, RUANGTONG J, HIRANYACHATTADA S (2022) Daily consumption of monosodium glutamate pronounced hypertension and altered renal excretory function in normotensive and hypertensive rats. *Heliyon,* 8(10): e10972.

UMBUZEIRO GA, HERINGA M, ZEIGER E (2017) In vitro genotoxicity testing: significance and use in environmental monitoring. *Adv Biochem Eng Biotechnol*, 157: 59-80.

VIRANI S, et al. (American Heart Association Council on Epidemiology and Prevention Statistics Committee and Stroke Statistics Subcommittee) (2020) Heart disease and stroke statistics – 2020 update: a report from the American Heart Association. *Circulation*, 141: e139-e596.

VLASIUK TI, ZHURAKIVSKA OY (2018) Prospects for the use of exenatide in the correction of experimental diabetic cardiomyopathies. *Pharma Innovation J*, 7(9): 35-40.

Deep femoral artery branching by MDCT in a Turkish population and its potential clinical implications

Ali Keleş[1], Mehmet T. Yilmaz[2], Cengiz Kadiyoran[3], Duygu A. Saygin[2]

[1] Department of Anatomy, Karamanoglu Mehmetbey University, Karaman, Türkiye
[2] Department of Anatomy, Necmettin Erbakan University, Konya, Türkiye
[3] Department of Radiology, Necmettin Erbakan University, Konya, Türkiye

SUMMARY

The deep femoral artery and its branches are vital for the arterial circulation of the lower extremity. The aim of the current study is to obtain morphometric and morphological data on the deep femoral artery and its branches and to investigate their clinical importance in the Turkish population. Morphometric measurements of the deep femoral artery and femoral artery were performed. The diameters of the femoral artery and deep femoral artery were measured in the axial plane. Classification was made according to the size of these diameters. A morphological classification was obtained by examining the variations of the deep femoral artery branches.

The distance from the origin of the deep femoral artery to the midpoint of the inguinal ligament was 39.56 ± 8.52 mm, and the distances from the origin of the lateral circumflex femoral artery to the medial circumflex femoral artery were 17.15 ± 4.79 mm and 12.52 ± 4.58 mm, respectively. The study results show that there was a significant difference between genders in terms of the diameters measured. In the classification made by using the diameters, Type D (39%) had the highest rate, whereas Type C had the lowest rate (7.3%). According to the morphological classification, Type I (52.1%) was the most common in all individuals, and Type V and Type VII (2.3%) were the least common. Our study includes both morphometric and morphological information about the femoral artery and deep femoral artery of the Turkish population. We consider that the current study will be useful for cardiologists, interventional radiologists, orthopedists, and regional surgeons in clinical practice.

Key words: Femoral artery – Lateral circumflex femoral artery – Medial circumflex femoral artery – Classification – Computed tomography

INTRODUCTION

The external iliac artery continues as the femoral artery (FA) after the inguinal ligament (IL). The FA is the main artery responsible for supplying the lower extremity. The thickest branch of the FA is the deep femoral artery (DFA). Several variations can be seen in the morphology of the FA and its branches. The course and anatomical

Corresponding author:
Ali Keleş. Department of Anatomy, Karamanoglu Mehmetbey University, Karaman, Türkiye. Phone: +90 (0338) 226 25 20. E-mail: alikeles@kmu.edu.tr

Submitted: January 3, 2023. **Accepted:** February 21, 2023

https://doi.org/10.52083/XSAN1528

variations of the vessels of the lower extremities have attracted the attention of anatomists and surgeons for a long time (Prakash et al., 2010; Nasr et al., 2014; Manjappa and Prasanna, 2014; Rajani et al., 2015; Łabętowicz et al., 2019). The cause of these variations, which are based on the formation of unusual channels from the primary capillary plexuses, is usually embryological. Arterial patterns may occur as appropriate channels develop and others recede and disappear (Sanudo et al., 1993; Łabętowicz et al., 2019).

As treatment with endovascular techniques has increased, precise knowledge of vascular anatomy and its variations has become crucial. Due to its wide diameter, the FA is preferred as the primary access site by angiographers performing invasive cardiac and peripheral vascular procedures (Schnyder et al., 2001; Yu et al., 2020). Information about the anatomical variants of the FA and its branches is important for clinicians in procedures such as transluminal stenting, angioplasty and embolectomy in peripheral occlusive arterial diseases, evaluation of arterial status in trauma, imaging of vascular malignancies and identification of arterial diseases. Also, this information is valuable for orthopedists performing total hip replacements and trochanteric or intertrochanteric osteotomy (Łabętowicz et al., 2019; Sudarshana and Chaudhary, 2020).

The DFA, medial circumflex femoral artery (MCFA), and lateral circumflex femoral artery (LCFA) are used in vascular, orthopedic, plastic and reconstructive surgery (Choy et al., 2013; Tzouma et al., 2020). The LCFA and its branches are used for anterolateral thigh flaps, aortopopliteal bypass, coronary artery bypass graft, and extracranial-intracranial bypass surgeries. The MCFA may be exposed to iatrogenic injuries during hip joint surgery and flap plastic surgery, resulting in femoral head necrosis. Therefore, knowledge of variation about the length and origin of the DFA and its branches can help prevent complications during or after surgical procedures (Fukuda et al., 2005; Üzel et al., 2008; Tomaszewski et al., 2016; Vuksanović-Božarić et al., 2018; Tzouma et al., 2020).

In line with all this information, it is seen that both morphological and morphometric data of the FA and its branches are clinically very important. Therefore, in our study, the aims were to obtain data on the FA and to reveal the morphological and morphometric differences by gender and/or side.

MATERIAL AND METHODS

In this study, the files of 630 patients were retrospectively scanned: these patients had been admitted to the Department of Radiology in Necmettin Erbakan University, Meram Faculty of Medicine, between August 2008 and March 2021, and the data of 130 (70 male, 60 female) individuals were included in the study. The study was approved by the Institutional Ethics Committee. In the study, images obtained by a Multidetector Computed Tomography (MDCT) device (Sensation 64, Siemens, Erlangen, Germany) with the parameters of KV: 120, Effective MaS: 50-170, MAS: 86, Pitch 1.4, Rotation speed: 0.5 sec, Detector area: 1.2 mm, Slice thickness: 1.5 mm were used. The images obtained from MDCT were reconstructed and analyzed on a MacBook Air (13-inch, 2017) laptop computer running macOS Big Sur (Version 11.2.3) and using the OsiriX Lite (V. 12.01.1) software. Images were transferred from MDCT in DICOM format to a folder on the computer via an external disk. Then, the measurements were taken on axial and 3D images in the OsiriX Lite software. All measurements were made by the same person and the results were given in millimeters (mm). Poor image quality, lack of contrast material and arterial aneurysm were our exclusion criteria. In addition, double DFA was detected on the right side of a female individual, and that extremity was excluded from the study. Because if we had included both DFAs in both distance and diameters, we could have obtained erroneous results by not following our methodology. In our study, the mean age was found as 50.33 ± 20.90 years (18-88) in males and 60.17 ± 17.76 years (18-86) in females.

The distances between the origin of the DFA from the midpoint of the anterior superior iliac spine and the pubic tubercle (midpoint of the IL) (Fig. 1a), between the origin of the LCFA originating the DFA and the origin of the DFA (Fig. 1b) and between the origin of the MCFA originating the DFA and the origin of the DFA (Fig. 1c) were measured.

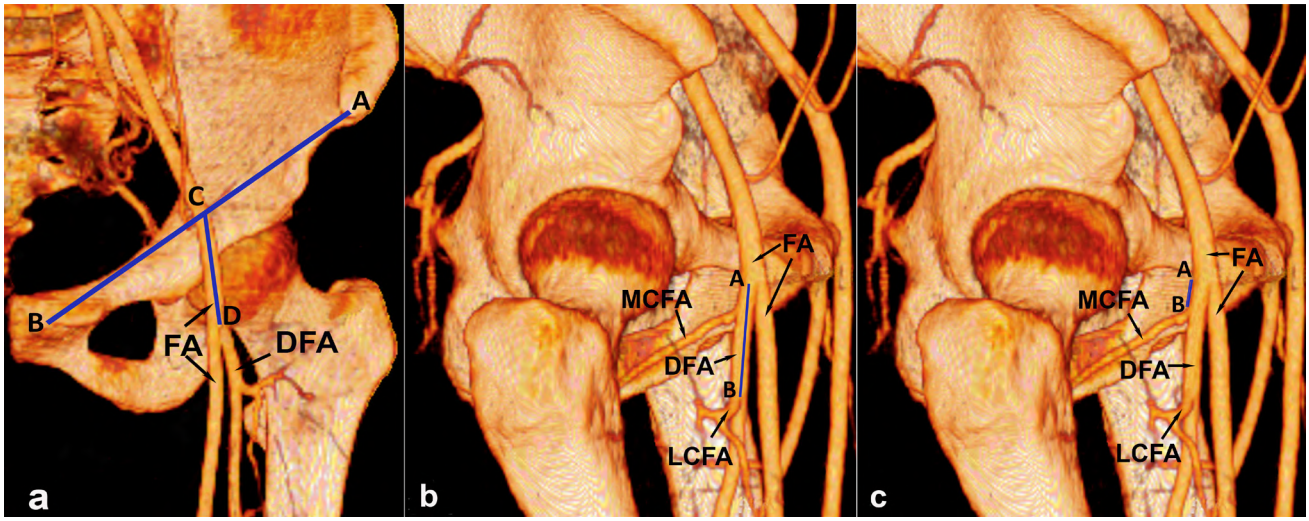

Fig. 1.- Three-dimensional volume-rendering CT reconstruction showing the length measurements: **a.** A left lower limb showing the distance between the origin of the DFA from the midpoint of the anterior superior iliac spine and the pubic tubercle (The distance between points C-D) (Observed from the anterior). **b.** A right lower limb showing the distance between the origin of the LCFA originating the DFA and the origin of the DFA (The distance between points A-B) (Observed from the lateral). **c.** A right lower limb showing the distance between the origin of the MCFA originating the DFA and the origin of the DFA (The distance between points A-B) (Observed from the lateral). (FA: Femoral artery, DFA: Deep femoral artery, MCFA: Medial circumflex femoral artery, LCFA: Lateral circumflex femoral artery).

The FA diameter at the level of the IL in the axial plane was noted (Fig. 2a). The FA diameters in the axial plane just before and after the separation of the DFA from the FA were measured (Figs. 2b,2c). The origin of the DFA in the axial plane was recorded.

Morphometric classification of femoral artery

In our study, the classification proposed by Kawashima et al., (2021) according to the size of the FA and DFA diameters and the presence or absence of an ectopic side branch (ESB) deviating from the FA was used. Morphometric types according to Kawashima et al., (2021) are as follows:

Type A: DFA diameter ≥ FA Diameter just after the separation of the DFA from the FA.

Type B: DFA diameter < FA Diameter just after the separation of the DFA from the FA and the presence of originating ESB before originating the DFA from the FA.

Type C: DFA diameter < FA Diameter just after the separation of the DFA from the FA and the presence of an ESB originate the FA bifurcation.

Type D: DFA diameter < FA Diameter just after the separation of the DFA from the FA and the absence of ESB.

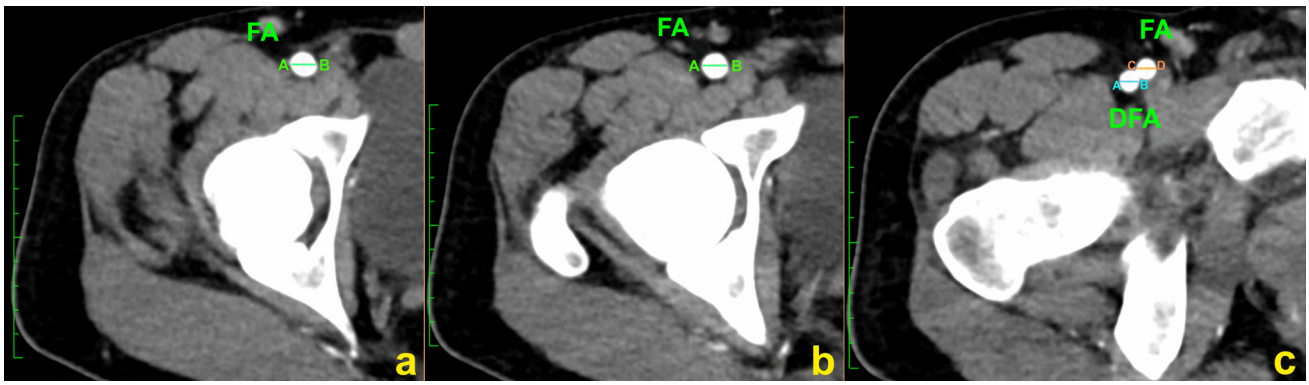

Fig. 2.- Showing the diameters in the axial plane: **a.** A right lower limb showing the diameter of the proximal FA (at the level of the IL). **b.** A right lower limb showing the diameter of the FA just before the separation of the DFA from the FA. **c.** A right lower limb showing the diameter of the DFA and the diameter of the FA just after the separation of the DFA from the FA. (IL: Inguinal ligament, FA: Femoral artery, DFA: Deep femoral artery, MCFA: Medial circumflex femoral artery, LCFA: Lateral circumflex femoral artery).

Morphological classification of femoral artery

In our study, a modified classification given below was obtained using Adachi's (1928) classification:

Type I: The DFA originates from the FA. The MCFA and LCFA originate separately from DFA.

Type II: The DFA originates from the FA. The MCFA originates from the FA, and the LCFA originates from the DFA.

Type III: The DFA originates from the FA. The LCFA originates from the FA, and the MCFA originates from the DFA.

Type IV: The DFA, MCFA, and LCFA originate from the FA separately.

Type V: The DFA and the descending branch of the LCFA originate from the FA separately. The MCFA and the ascending branch of the LCFA originate from the DFA.

Type VI: The DFA originates from the FA. The MCFA and LCFA originate from a common trunk originating from the FA.

Type VII: The DFA, MCFA and the descending branch of the LCFA originate from the FA separately. The ascending branch of the LCFA originates from the DFA.

Type VIII: The DFA and LCFA separately originate from the FA. There is no MCFA.

In our study, the side of origin from the FA of the DFA was also examined. DFAs originating from the posterolateral (P-L), posterior (P), lateral (Lat), posteromedial (P-M), medial (Med), and anterolateral (A-L) aspects of the FA were recorded. In addition, the artery from which the MCFA and LCFA originate (FA or DFA) was examined.

In our study, descriptive statistical analysis was performed with IBM SPSS Statistics 21.0. The independent-samples t-test was used to compare all measured values by gender, and the paired-samples t-test was employed to compare the individuals' right and left values.

RESULTS

The mean ± SD values of the measurement scores of all, male and female individuals in our study are given in Table 1 and Table 2. Although the data obtained from males were higher than those of females in terms of all measurement parameters, only the differences in diameters were significant between males and females (Table 2). Besides, there was no significant difference between the right and left side values (Table 1) ($p<0.05$).

Table 1. Total and gender and right-left values of length measurements (mm).

Measurements	Total		Male		Female		p	Right		Left		p
	N	Mean±SD	N	Mean±SD	N	Mean±SD		N	Mean±SD	N	Mean±SD	
Distance between the origin of the DFA from the midpoint of the IL	259	39,56 ± 8,52	140	40,13 ± 8,58	119	38,89 ± 8,44	0,245	129	39,58 ± 8,71	130	39,53 ± 8,37	0,960
Distance between the origin of the LCFA originating the DFA and the origin of the DFA	214	17,15 ± 4,79	84	17,55 ± 5,48	100	16,69 ± 3,86	0,188	107	17,01 ± 4,28	107	17,28 ± 5,28	0,684
Distance between the origin of the MCFA originating the DFA and the origin of the DFA	167	12,52 ± 4,58	140	12,85 ± 3,97	83	12,19 ± 5,13	0,350	79	12,65 ± 4,41	88	12,41 ± 4,75	0,732

FA: Femoral artery**, DFA:** Deep femoral artery**, IL:** Inguinal ligament**, N:** Number of samples measured, **SD:** Standart deviation, ($p<0,05$).

Table 2. Total and gender and right-left values of diameters (mm).

Measurements	Total		Male		Female		p	Right		Left		p
	N	Mean±SD	N	Mean±SD	N	Mean±SD		N	Mean±SD	N	Mean±SD	
FA Diameter (at the level of the IL)	259	7,78 ± 1,21	114	8,11 ± 1,04	119	7,04 ± 1,28	<0,001	129	7,78 ± 1,19	130	7,79 ± 1,22	0,972
FA Diameter (just before the separation of the DFA from the FA)	259	6,67 ± 1,26	140	7,07 ± 1,11	119	6,21 ± 1,27	<0,001	129	6,67 ± 1,21	130	6,68 ± 1,31	0,983
FA Diameter (just after the separation of the DFA from the FA)	259	5,48 ± 1,19	140	5,87 ± 1,08	119	5,01 ± 1,15	<0,001	129	5,45 ± 1,13	130	5,50 ± 1,26	0,757
DFA Diameter	259	5,18 ±1,31	140	5,46 ± 1,25	119	4,85 ± 1,31	<0,001	129	5,20 ± 1,28	130	5,16 ± 1,35	0,849

FA: Femoral artery, **DFA:** Deep femoral artery, **IL:** Inguinal ligament, **N:** Number of samples measured, **SD:** Standart deviation, (p<0,05).

In our study, four morphometric types were observed according to the classification suggested by Kawashima et al. (2021). Among these types, the most common one was Type D (39%). In type D, the diameter of the DFA was smaller than the diameter of the FA (below DFA), and there was no ESB. Type B (29%) was the second most common type, in which the diameter of the DFA was smaller than the diameter of the FA (below DFA), and there was ESB originating from the FA. In Type A (24.7%), the third most common type, the diameter of the DFA was larger than the diameter of the FA (below DFA). The least detected type was Type C (7.3%) in which, the diameter of the DFA was smaller than the diameter of the FA (below DFA), and there was ESB originating from the FA bifurcation (Table 3) (Figs. 3-6).

In addition, in this study, eight types were examined according to the morphological classification made according to Adachi (1928), but six types were found. Type VI was not observed in the study, because the MCFA and LCFA did not originate from a common trunk. Besides, since there were no individuals without MCFA in our study, we did not encounter Type VIII. Type I (52.1%) was the most common one among the types obtained in the morphological classification. In this type, the LCFA and MCFA originated from the DFA. Type II (29.8%) was the second most common type in which the MCFA originated from the FA, while the LCFA originated from the DFA. The third most common type was observed to be Type III (10.4%) in which, the LCFA originated from the FA, while the MCFA originated from the DFA. The incidence of Type IV was found to be 3.1%. In this type, the DFA, LCFA, and MCFA were separately originated from the FA. The least detected types were Type V (2.3%) and Type VII (2.3%). In Type V, the descending branch of the LCFA originated from the FA, while the ascending branch of the

Table 3. Total and gender and right-left values according to morphometric classification (%).

Study	Type	Male % (N)	Female % (N)	Right % (N)	Left % (N)	Total % (N)
Morphometric classification	Type A	21,4 (30)	28,6 (34)	24 (31)	25,4 (33)	24,7 (64)
	Type B	33,6 (47)	23,5 (28)	31,8 (41)	26,1 (34)	29 (75)
	Type C	7,9 (11)	6,7 (8)	6,2 (8)	8,5 (11)	7,3 (19)
	Type D	37,1 (52)	41,2 (49)	38 (49)	40 (52)	39 (101)

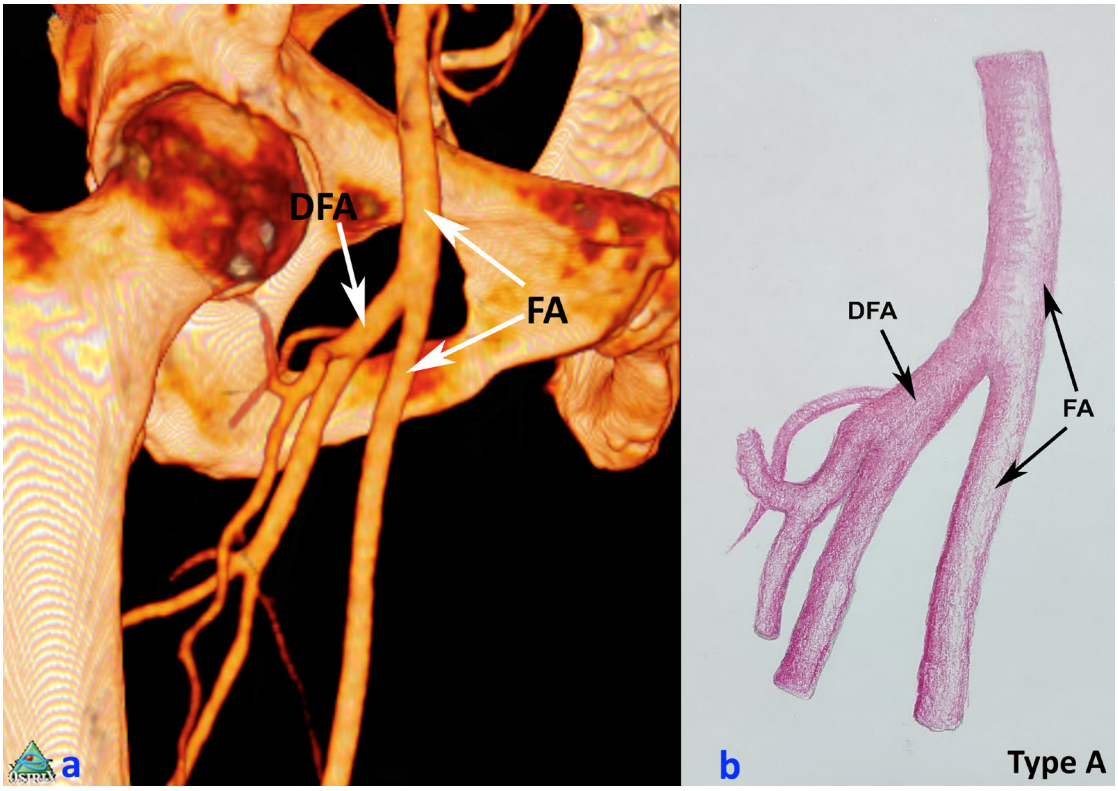

Fig. 3.- A right lower limb showing the image of Type A (Observed from the anterolateral). **a:** Three-dimensional volume-rendering CT reconstruction showing the image of Type A. **b:** The schema showing the image of Type A **(**DFA diameter ≥ diameter of FA just after the separation of DFA from FA) (FA: Femoral artery, DFA: Deep femoral artery).

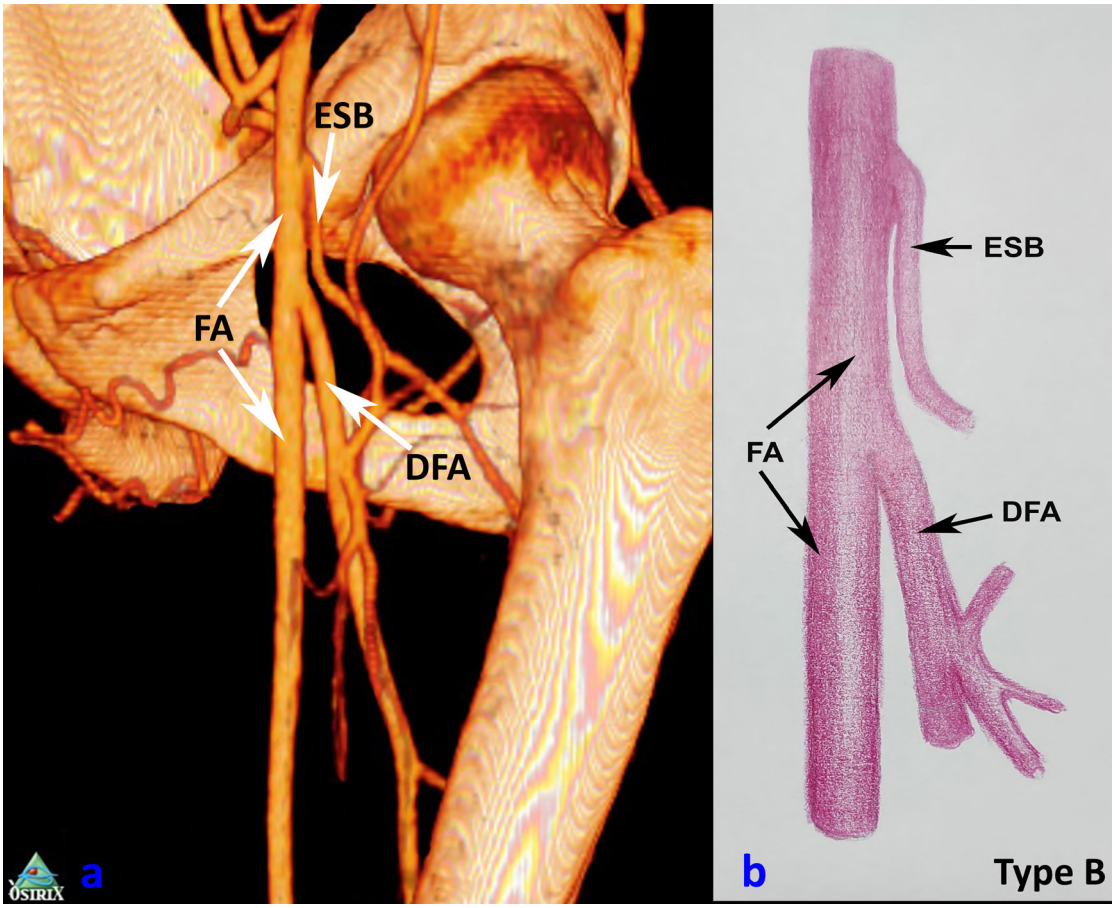

Fig. 4.- A left lower limb showing the image of Type B (Observed from the anterolateral). **a:** Three-dimensional volume-rendering CT reconstruction showing the image of Type B. **b:** The schema showing the image of Type B (DFA diameter < diameter of FA just after the separation of DFA from FA and presence of originating ESB before originating DFA from FA) (FA: Femoral artery, DFA: Deep femoral artery, ESB: Ectopic side branch).

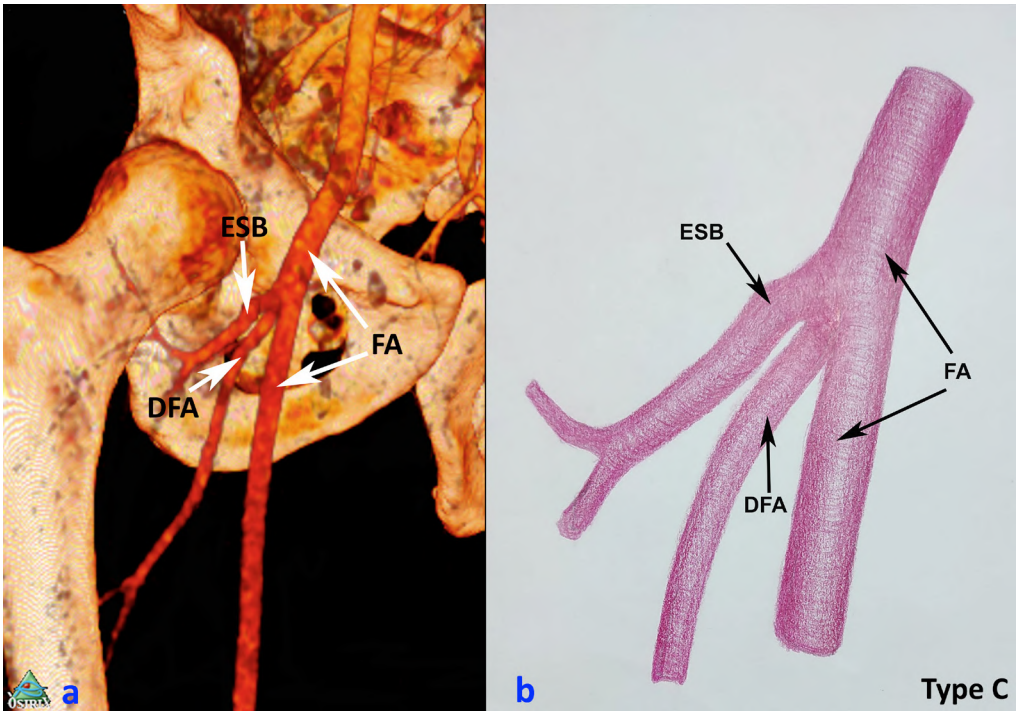

Fig. 5.- A right lower limb showing the image of Type C (Observed from the anterolateral). **a:** Three-dimensional volume-rendering CT reconstruction showing the image of Type C. **b:** The schema showing the image of Type C **(**DFA diameter < diameter of FA just after the separation of DFA from FA and presence of an ESB originating the FA bifurcation) (FA: Femoral artery, DFA: Deep femoral artery, ESB: Ectopic side branch).

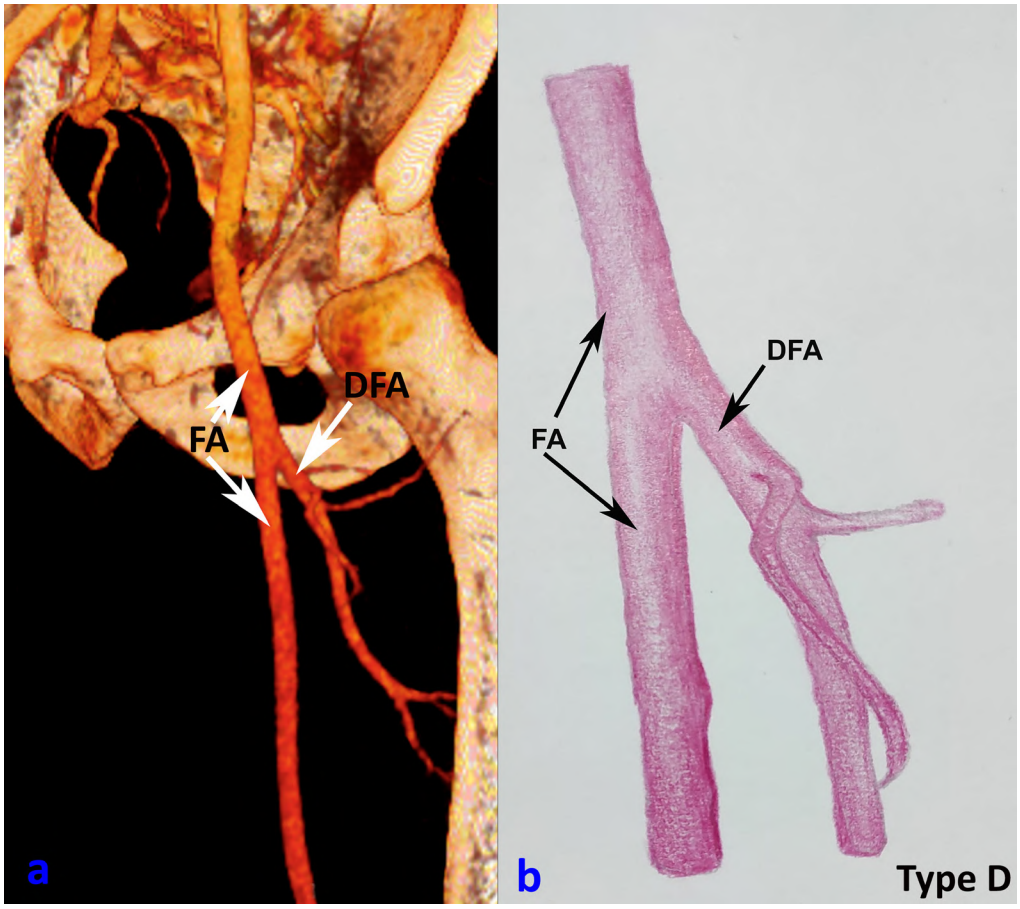

Fig. 6.- A left lower limb showing the image of Type D (Observed from the anterolateral). **a:** Three-dimensional volume-rendering CT reconstruction showing the image of Type D. **b:** The schema showing the image of Type D **(**DFA diameter < diameter of FA just after the separation of DFA from FA and absence of ESB) (FA: Femoral artery, DFA: Deep femoral artery, ESB: Ectopic side branch).

MCFA and LCFA originated from the DFA. In Type V, the descending branch of the LCFA and MCFA originated from the FA separately, while the ascending branch of the LCFA originated from the DFA (Table 4) (Figs. 7-12).

In all individuals, it was observed that the DFA branched from the FA the most from the posterolateral side (72.6%) and the least from the anterolateral side (0.4%) (Table 5). It was determined that 64.9% of the MCFA originated from the DFA, while 85.8% of the LCFA originated from the DFA (Table 6). In our study, it was observed that all LCFAs and MCFAs branching from the FA originated from under the inguinal ligament. In addition, circumflex arteries were not observed to originate from any artery other than the FA and DFA.

Table 4. Total and gender and right-left values according to morphological classification (%).

Study	Type	Male % (N)	Female % (N)	Right % (N)	Left % (N)	Total % (N)
Morphological classification	Type I	47,2 (66)	58 (69)	50,4 (65)	53,9 (70)	52,1 (135)
	Type II	33,5 (47)	25,2 (30)	32,6 (42)	26,9 (35)	29,8 (77)
	Type III	11,4 (16)	9,2 (11)	9,3 (12)	11,5 (15)	10,4 (27)
	Type IV	2,9 (4)	3,4 (4)	2,3 (3)	3,9 (5)	3,1 (8)
	Type V	1,4 (2)	3,4 (4)	2,3 (3)	2,3 (3)	2,3 (6)
	Type VI	0	0	0	0	0
	Type VII	3,6 (5)	0,8 (1)	3,1 (4)	1,5 (2)	2,3 (6)
	Type VIII	0	0	0	0	0

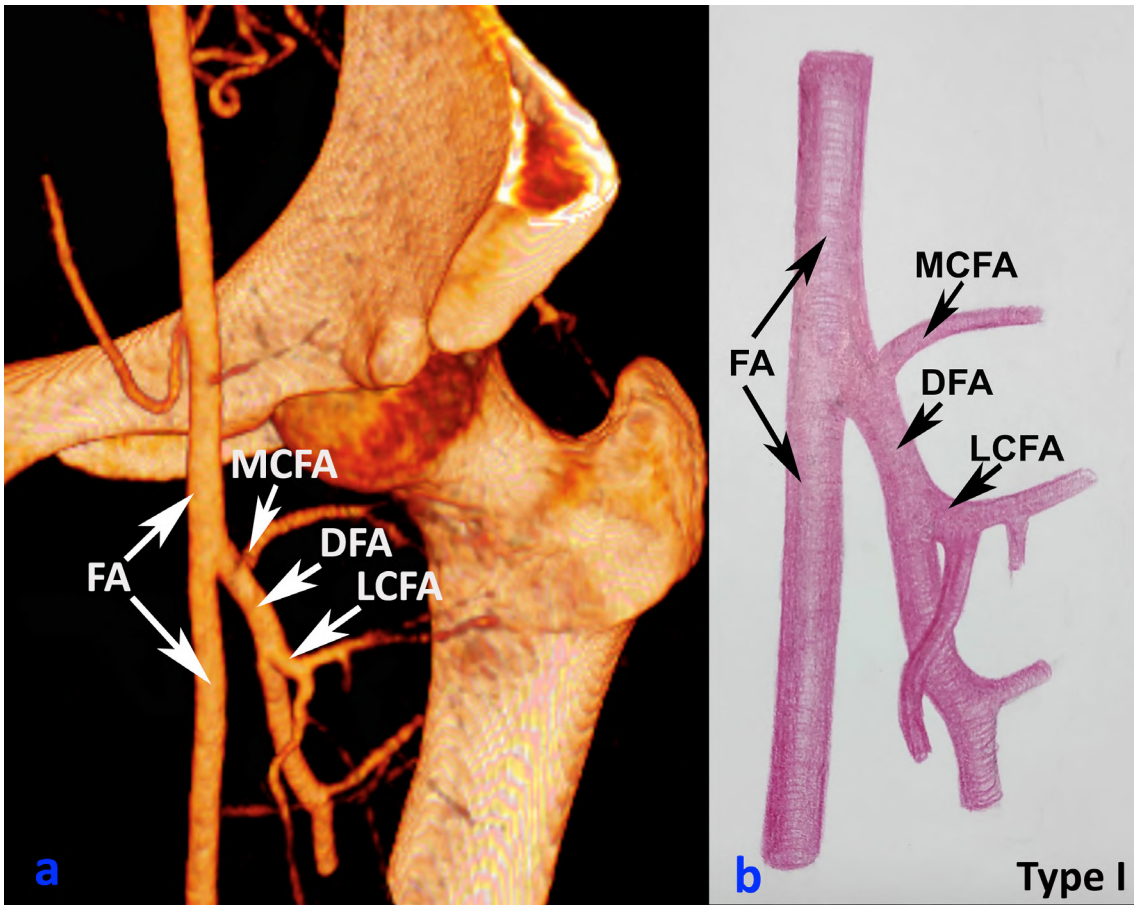

Fig. 7.- A left lower limb showing the image of Type I (Observed from the anterolateral). **a:** Three-dimensional volume-rendering CT reconstruction showing the image of Type I. **b:** The schema showing the image of Type I (MCFA and LCFA originate separately from DFA) (DFA: Deep femoral artery, MCFA: Medial circumflex femoral artery, LCFA: Lateral circumflex femoral artery).

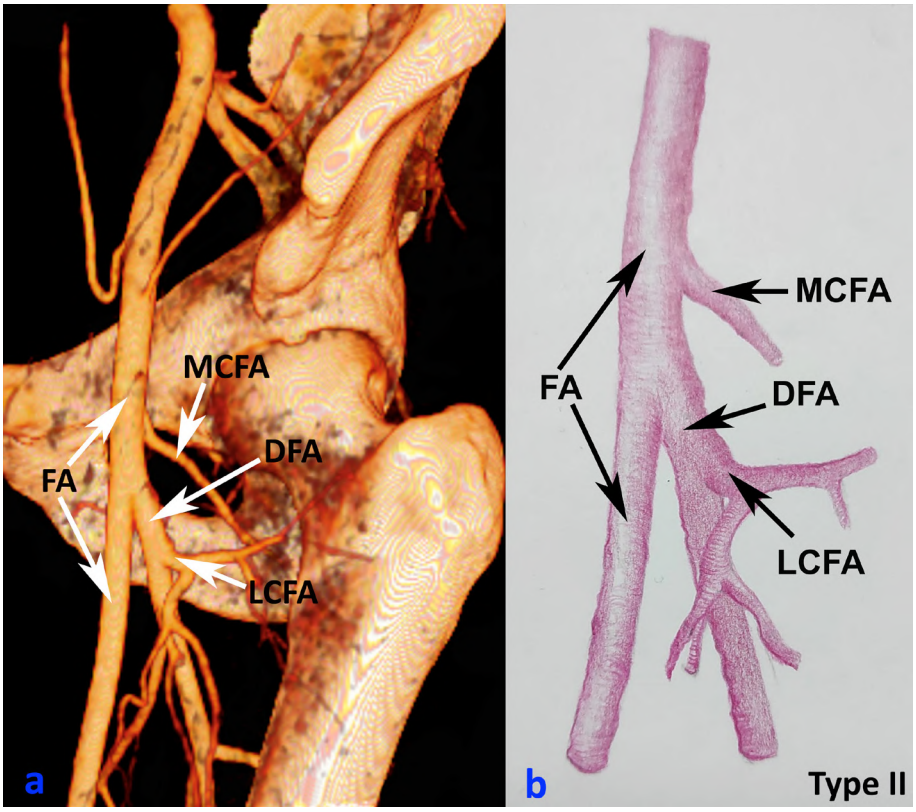

Fig. 8.- A left lower limb showing the image of Type II (Observed from the anterolateral). **a:** Three-dimensional volume-rendering CT reconstruction showing the image of Type II. **b:** The schema showing the image of Type II **(**MCFA originates from FA and LCFA originates from DFA) (FA: Femoral artery, DFA: Deep femoral artery, MCFA: Medial circumflex femoral artery, LCFA: Lateral circumflex femoral artery).

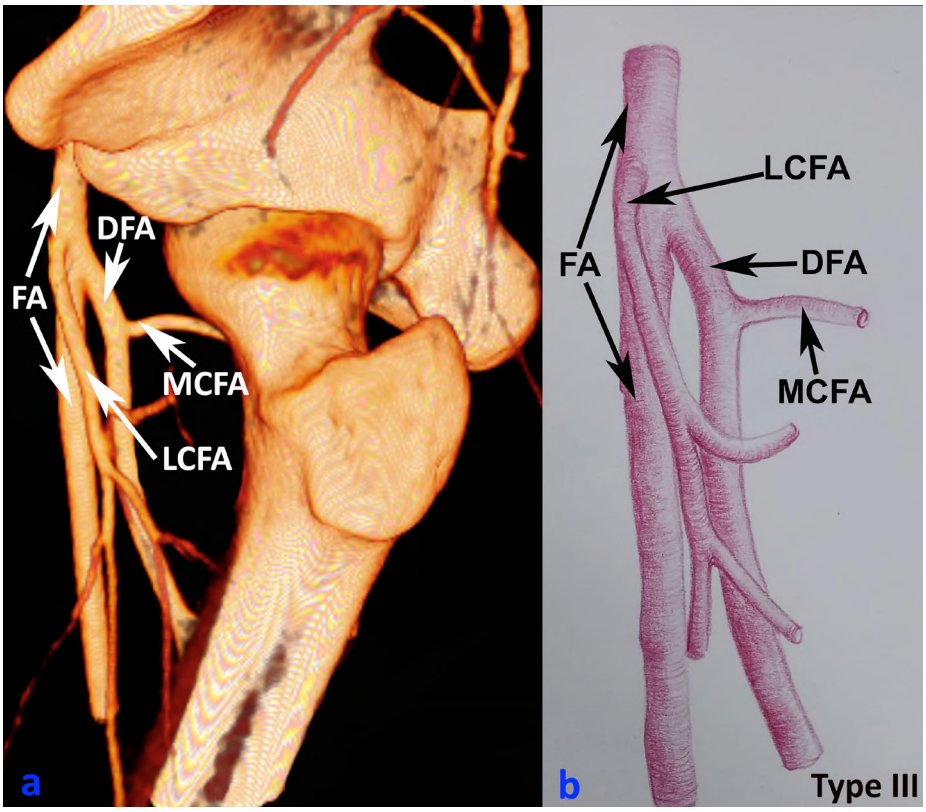

Fig. 9.- A left lower limb showing the image of Type III (Observed from the lateral). **a:** Three-dimensional volume-rendering CT reconstruction showing the image of Type III. **b:** The schema showing the image of Type III (LCFA originates from FA, MCFA originates from DFA) (FA: Femoral artery, DFA: Deep femoral artery, MCFA: Medial circumflex femoral artery, LCFA: Lateral circumflex femoral artery).

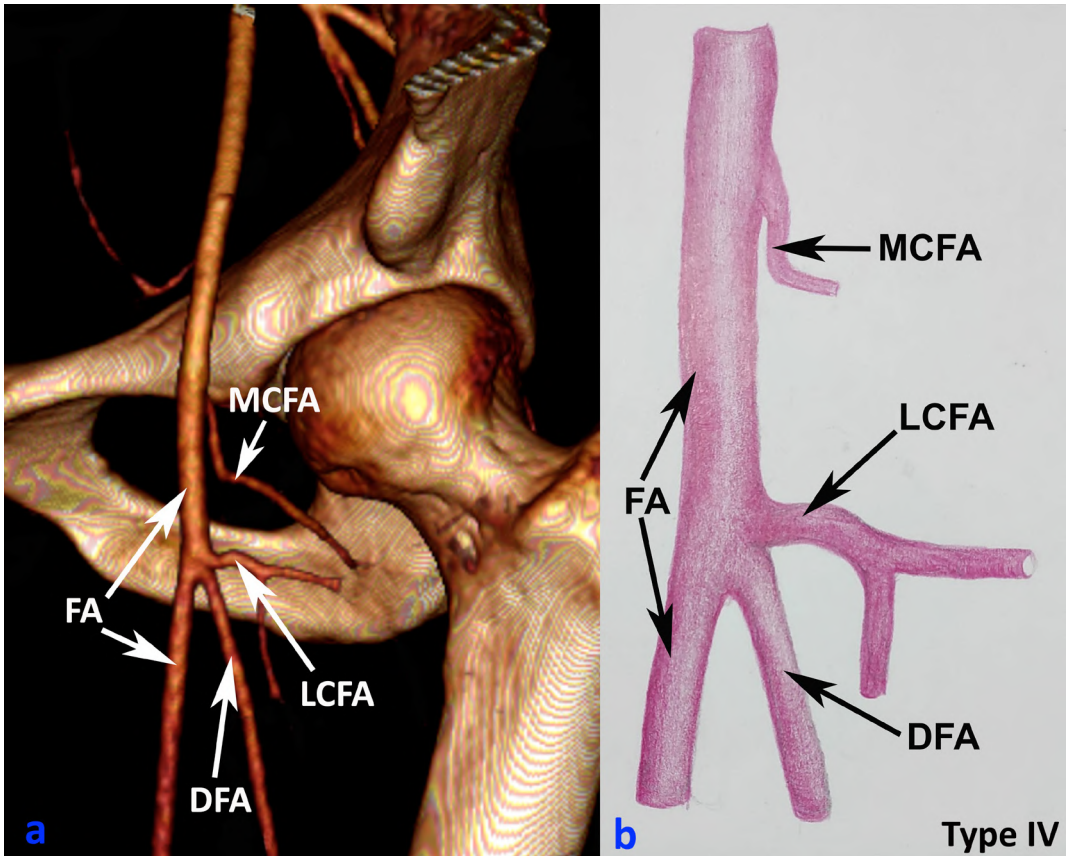

Fig. 10.- A left lower limb showing the image of Type IV (Observed from the anterolateral). **a:** Three-dimensional volume-rendering CT reconstruction showing the image of Type IV. **b:** The schema showing the image of Type IV **(**DFA, MCFA, and LCFA originate from FA separately) (FA: Femoral artery, DFA: Deep femoral artery, MCFA: Medial circumflex femoral artery, LCFA: Lateral circumflex femoral artery).

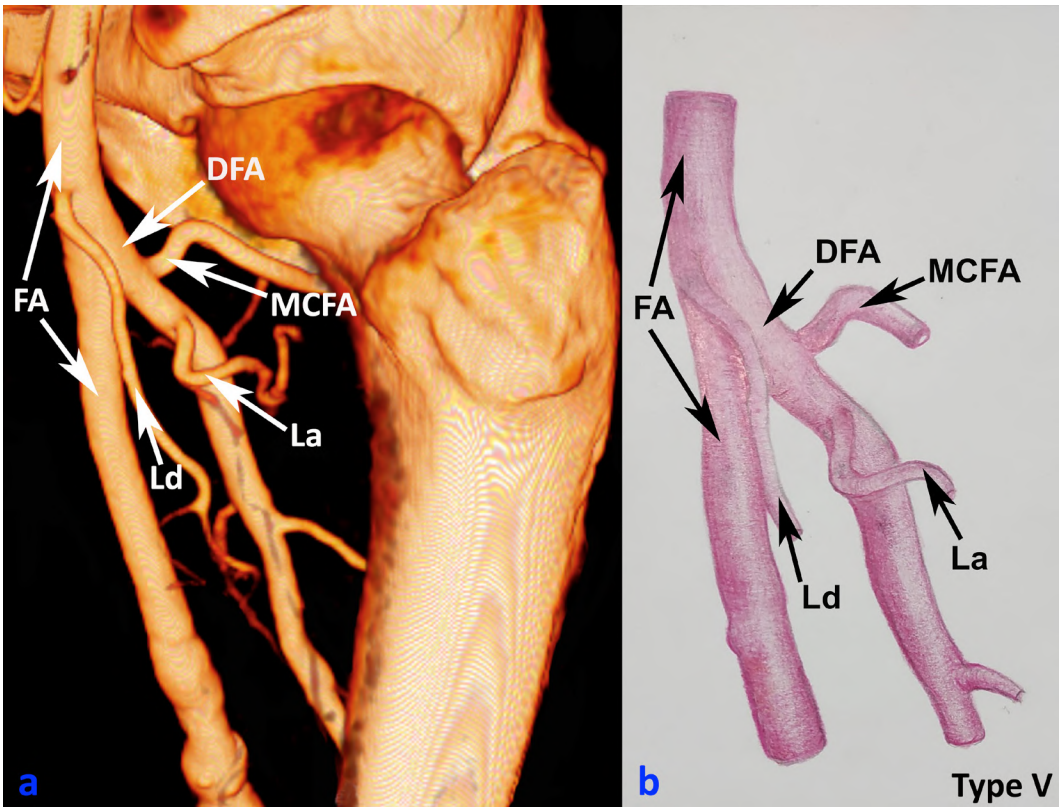

Fig. 11.- A left lower limb showing the image of Type V (Observed from the lateral). **a:** Three-dimensional volume-rendering CT reconstruction showing the image of Type V. **b:** The schema showing the image of Type V (DFA and the descending branch of LCFA originate from FA separately. MCFA and the ascending branch of LCFA originate from DFA) (FA: Femoral artery, DFA: Deep femoral artery, MCFA: Medial circumflex femoral artery, LCFA: Lateral circumflex femoral artery).

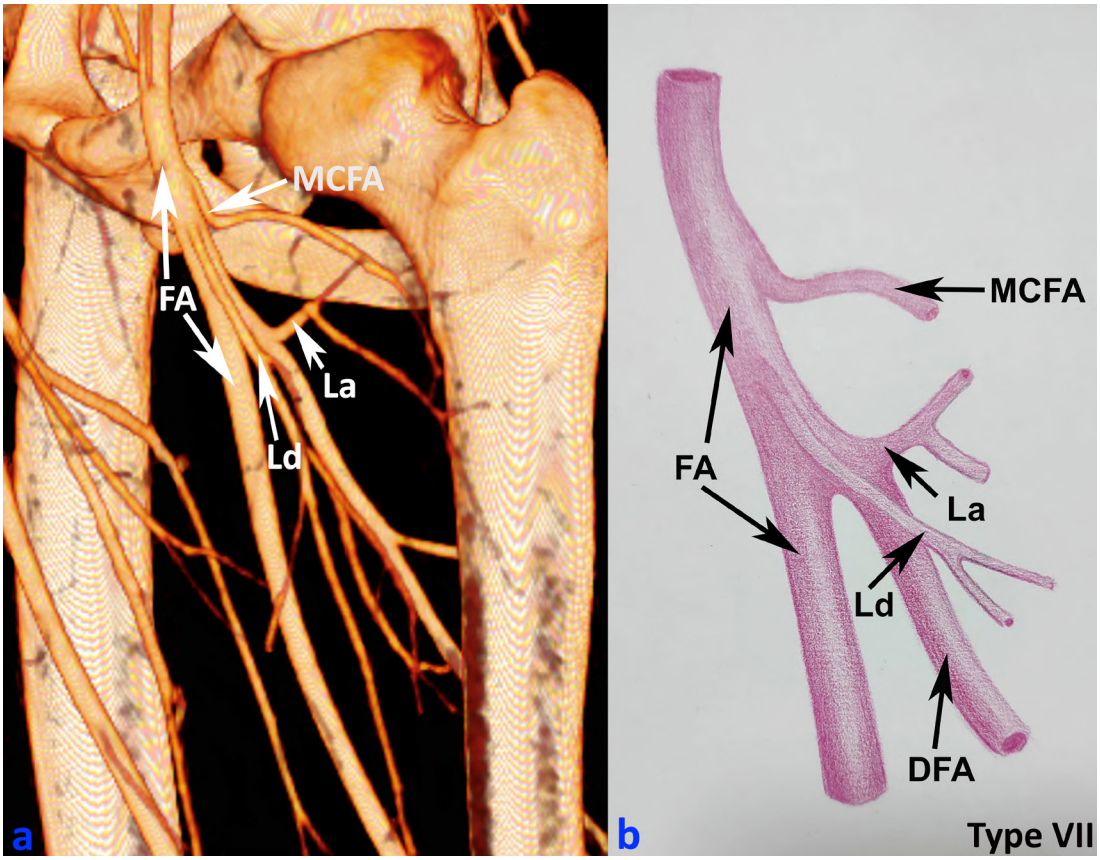

Fig. 12.- A left lower limb showing the image of Type VII (Observed from the anterolateral). **a:** Three-dimensional volume-rendering CT reconstruction showing the image of Type VII. **b:** The schema showing the image of Type VII **(**DFA, MCFA, and the descending branch of LCFA originate from FA separately. The ascending branch of LCFA leaves DFA) (FA: Femoral artery, DFA: Deep femoral artery, MCFA: Medial circumflex femoral artery, **LCFA:** Lateral circumflex femoral artery).

Table 5. Ratios of various positions where the DFA originates from the FA (%).

Position of DFA origin	Male % (N)	Female % (N)	Right % (N)	Left % (N)	Total % (N)
P-L	75,7 (106)	68,9 (82)	72 (93)	73,1 (95)	72,6 (188)
P	17,2 (24)	21 (25)	18,6 (24)	19,2 (25)	18,9 (49)
Lat	1,4 (2)	5,9 (7)	4,7 (6)	2,3 (3)	3,4 (9)
P-M	4,3 (6)	3,4 (4)	3,9 (5)	3,8 (5)	3,9 (10)
Med	0,7 (1)	0,8 (1)	0,8 (1)	0,8 (1)	0,8 (2)
A-L	0,7 (1)	0	0	0,8 (1)	0,4 (1)

N: Number of samples measured, **P-L:** Posterolateral, **P:** Posterior, **Lat:** Lateral, **P-M:** Posteromedial, **Med:** Medial, **A-L:** Antero-lateral.

Table 6. Findings on which artery originates MCFA and LCFA (%).

	Direct origins of the MCFA without of a common trunk		Direct origins of the LCFA without of a common trunk	
	FA	**DFA**	**FA**	**DFA**
Male	40	60	15	85
Female	29,4	70,6	13,2	86,8
Right	38	62	13,9	86,1
Left	32,3	67,7	14,4	85,6
Total	35,1	64,9	14,2	85,8

N: Number of samples measured, **FA:** Femoral artery, **DFA:** Deep femoral artery, **MCFA:** Medial circumflex femoral artery, **LCFA:** Lateral circumflex femoral artery.

DISCUSSION

The FA is the main artery supplying blood to the lower extremities. The DFA, on the other hand, is the most important branch of the FA and supplies the femur, hip joint and thigh muscles (Zlotorowicz et al., 2018). Comprehensive knowledge regarding the normal anatomy and variations of the origin and course of the DFA and its circumflex branches is of paramount importance during diagnostic vascular interventions and surgeries. In addition, detailed anatomy knowledge helps reduce the possibility of intraoperative secondary bleeding and postoperative complications (Dixit et al., 2011).

In a study conducted on cadavers, Manjappa and Prasanna (2014) observed that the lowest distance from the origin of the DFA to the midpoint of the IL (31.95 mm) was on the left side. As shown in Table 7, the mean distance from the origin of the DFA to the midpoint of the IL was determined to be 39.56 ± 8.52 mm in our study, which was very close to the result (39.55 mm) reported by Verma et al. (2016). The data of the Sri Lankan (Samarawickrama et al., 2009), Greek (Panagouli et al., 2011), Arabian (Nasr et al., 2014), and Polish (Łabętowicz et al., 2019) populations, which were shown in Table 7, were higher than those found in the current study. It was thought that this variability among the results might be due to racial differences.

The data for the Indian populations were observed to be both lower (Sabnis, 2013; Manjappa and Prasanna, 2014; Murthy et al., 2022) and higher (Sudarshana and Chaudhary, 2020; George and Santhakumary, 2021) than ours (Table 7). This can be explained by the use of different measurement methods. Vuksanović-Božarić et al. (2007) emphasized that the distance from the origin of the DFA to the midpoint of the IL should be known to prevent flap necrosis and to perform safe cardiac catheterizations in plastic and reconstructive surgery practices.

In our study, the distances between the origin of the LCFA originating from the DFA and the origin of the DFA and between the origin of the MCFA originating from the DFA and the origin of the DFA were measured, and the data obtained were compared with the results reported by other researchers (Table 7). The data for the British population (Vazquez et al., 2007) were found to be lower than ours. However, the data of the Arabian (Nasr et al., 2014) and Indian (Prakash et al., 2010) populations were observed to be higher than ours. We think that the reason for this variability may be due to racial differences and the use of different measurement methods. Knowing the original locations and distances of the DFA, MCFA, and LCFA allows the surgeon to identify the vascular pattern and avoid unexpected iatrogenic injuries before performing any invasive procedure (Nasr et al., 2014).

As listed in Table 8, both data of Sabnis (2013) and Chauhan et al. (2015) were larger than our data. This difference may be attributed to the different measurement methodologies employed. The external diameters of the arteries were measured in those studies, whereas the internal (lumen) diameters of the arteries were measured in our study. Kashyap and Kasote (2018) measured the lumen diameter of the FA in their study on cadavers. The results obtained by these researchers were similar to our data. Kawashima et al. (2021) performed diameter measurements with CT before the invasive procedure in the Japanese population in 2021. The comparison revealed that the results obtained in our study were lower than those of the Japanese population (Table 8). We think that this may be linked to racial differences. Kaur et al. (2019) emphasized the importance of knowledge of the mean diameter and location of the FA and its branches when performing clinical interventions in the femoral region and hip joint replacement. We are of the opinion that it would be more accurate to know the lumen diameters rather than external diameters in arterial interventional procedures.

Kawashima et al. (2021) analyzed CT images of 82 patients and classified the FA morphometrically and reported that they mostly detected Type A (55%). They also stated that during FA cannulation for minimally invasive cardiac surgery, the prolongation of cardiopulmonary bypass time and the presence of Type D are factors predisposing to the development of asymptomatic limb ischemia. In addition to the fact that Type D was the most

Table 7. Comparison of distance measurements related to DFA origin with other studies (mm).

Author	Country	KS	N	T R/L M/F	The distance between the origin of the DFA from the midpoint of the IL	The distance between the origin of the LCFA leaving the DFA and the origin of the DFA	The distance between the origin of the MCFA leaving the DFA and the origin of the DFA
Vazquez et al. (2007)	England	Ca	346	T		14,8	9
Samarawickrama et al. (2009)	Sri Lanka	Ca	26	T	50		
				R	55		
				L	45		
Prakash et al. (2010)	India	Ca	64	T		25	20
Panagouli et al. (2011)	Greece	Ca	123	R	48 ± 15,5		
				L	43 ± 15,4		
Sabnis (2013)	India	Ca	60	T	32		
Nasr et al. (2014)	Arabia	Ca	90	M	50,6 ± 1,3	21,3 ± 1,6	19, 1± 1,4
				F	48,8 ± 1,5	21,3 ± 1,8	18,9 ± 1,7
Manjappa and Prasanna (2014)	India	Ca	40	R	35,6		
				L	31,95		
Verma et al. (2016)	India	Ca	38	T	39,55		
				R	37,55		
				L	41,55		
Łabętowicz et al. (2019)	Poland	Ca	80	T	43,15		
Sudarshana and Chaudhary (2020)	India	Ca	50	T	41,1		
Mogale et al. (2021)	South Africa	Ca	90	T	38,9		
				R	44		
				L	36,8		
George and Santhakumary (2021)	India	Ca	60	T	52,2		
				R	56,4		
				L	48		
Murthy et al. (2022)	India	Ca	70	T	36 ± 1,3		
				R	35,8 ± 1,2		
				L	35,7 ± 1,3		
Our study	Türkiye	CT	259	T	39,56 ± 8,52	17,15 ± 4,79	12,52 ± 4,58
				R	39,58 ± 8,71	17,01 ± 4,28	12,65 ± 4,41
				L	39,53 ± 8,37	17,28 ± 5,28	12,41 ± 4,75
				M	40,13 ± 8,58	17,55 ± 5,48	12,85 ± 3,97
				F	38,89 ± 8,44	12,19 ± 5,13	16,69 ± 3,86

N: Number of samples measured, **KS:** Kind of study**, Ca:** cadaver, **MA:** Meta-analysis, **CT**: Computed Tomography, **T:** Total, **R:** Right, **L:** Left, **M:** Male, **F:** Female, **DFA:** Deep femoral artery, **MCFA:** Medial circumflex femoral artery, **LCFA:** Lateral circumflex femoral artery, **mm**: millimeter.

Table 8. Comparison of diameter lengths of FA and DFA with other studies (mm).

Author	T R/L M/F		Diameter of FA (at the level of the IL)	Diameter of FA (just before DFA leaves FA)	Diameter of FA (just after DFA leaves FA)	Diameter of DFA
Sabnis (2013)	T		10			6
Anjankar et al. (2014)	R					10,6
	L					10,9
Chauhan et al. (2015)	R					7,31 ± 0,21
	L					7,12 ± 0,32
	M					7,19 ± 0,23
	F					7,28 ± 0,32
Verma et al. (2016)	T					6,69
	R					6,88
	L					6,5
Kashyap and Kasote (2018)	M	R	7,46 ± 0,97			
		L	7,43 ± 0,93			
	F	R	6,33 ± 0,68			
		L	6,29 ± 0,69			
Łabętowicz et al. (2019)	M		12,11 ± 1,24	10,91±1,49	8,23 ±1,42	7,11 ± 1,31
	F		9,94 ±1,65	9,08 ±1,74	6,35±1,32	6,42 ± 1,39
Kawashima et al. (2021)	T		8,9 ± 1,5		6,4 ± 1,2	6,4 ± 1,3
	R		8,9 ± 1,5		6,5 ± 1,3	6,6 ± 1,2
	L		8,8 ± 1,4		6,3 ± 1,1	6,3 ± 1,3
Our study	T		7,78 ± 1,21	6,67 ± 1,26	5,48 ± 1,19	5,18 ±1,31
	R		7,78 ± 1,19	6,67 ± 1,21	5,45 ± 1,13	5,20 ± 1,28
	L		7,79 ± 1,22	6,68 ± 1,31	5,50 ± 1,26	5,16 ± 1,35
	M		8,11 ± 1,04	7,07 ± 1,11	5,87 ± 1,08	5,46 ± 1,25
	F		7,04 ± 1,28	6,21 ± 1,27	5,01 ± 1,15	4,85 ± 1,31

T: Total, **R:** Right, **L:** Left, **M:** Male, **F:** Female, **FA:** Femoral artery, **DFA:** Deep femoral artery, **IL:** Inguinal ligament, mm: millimeter.

common (39%) in our study, it is also noteworthy to mention that the rate of Type D (41.2%) was especially high in females. Considering the results obtained in the current study based on the classification of Kawashima et al. (2021), in the Turkish population, more attention should be paid to the risk of the development of lower extremity ischemia in patients (especially in females) with Type D who will undergo FA cannulation.

The morphological types obtained in our study are presented in Table 9 together with the classifications made by various researchers. As listed in Table 9, Type I was the most common type both in the literature and in our study. In addition, Type VI and Type VIII were not detected in our study. Troupis et al. (2013) emphasized the importance of knowing the branching pattern and anatomical variations of the FA according to both its origin and course, since a large number of procedures such as general surgery, orthopedic surgery, vascular surgery, plastic surgery, and invasive cardiology are performed in the femoral region.

In our study, the origin direction of the DFA from the FA was examined. As listed in Table 10, it has been reported in the literature that the DFA originates mostly from the posterolateral direction. It was also observed in our study that the DFA mostly originated from the posterolateral aspect of the FA (72.6%) in line with the literature.

The CT images examined in our study showed that the MCFA originated directly from the FA or DFA. As presented in Table 11, the literature

Table 9. Comparison of the obtained types with the corresponding types in other studies (%).

Author	T R/L M/F	Type I	Type II	Type III	Type IV	Type V	Type VI	Type VII	Type VIII
Adachi B (1928)	T	63,2	15	14,4	3,6	2,2	0,8	0,5	0,3
Massoud and Fletcher (1997)	T	81	6,4	2,8	5,9	0	0,7		
Vazquez et al. (2007)	T	78,8	15,95	4,55	0,5				
	R	82,11	12,84	5,04	0				
	L	75,9	19,09	4,09	0,9				
	M	75,6	18,53	4,87	0,97				
	F	81,97	13,73	4,29	0				
Łabętowicz et al. (2019)	T	40	15	16,25	3,75				
Vuksanović-Božarić et al. (2018)	T	66,7	10	5	5				
Zlotorowicz et al. (2018)	T	50	31	15	2		1		1
Tomaszewski et al. (2016)	T	64,6	32,2				0,4		0,4
Our study	T	52,1	29,8	10,4	3,1	2,3	0	2,3	0
	R	50,4	32,6	9,3	2,3	2,3	0	3,1	0
	L	53,9	26,9	11,5	3,9	2,3	0	1,5	0
	M	47,2	33,5	11,4	2,9	1,4	0	3,6	0
	F	58	25,2	9,3	3,4	3,4	0	0,8	0

T: Total, **R:** Right, **L:** Left, **M:** Male, **F:** Female.

Table 10. Comparison of various positions where the DFA originates from the FA with other studies (%).

Author	Country	KS	N	T R/L M/F	P-L (%)	P (%)	Lat (%)	P-M (%)	Med (%)	A-L (%)
Prakash et al. (2010)	India	Ca	64	T	50	46,9			3,1	
Nasr et al. (2014)	Arabia	Ca	90	M	42	24	20	14		
				F	42,5	27,5	20	10		
Manjappa and Prasanna (2014)	India	Ca	40	R	50	40	5			
				L	70	10	15	5		
Anjankar et al. (2014)	India	Ca	120	R	48,33	20	18,33	13,33		
				L	46,67	23,33	15	15		
Rajani et al. (2015)	India	Ca	66	T	53,03	10,61	18,17	13,63	3,03	1,51
Sudarshana and Chaudhary (2020)	India	Ca	50	T	64	12	22			2
George and Santhakumary (2021)	India	Ca	60	R	60	6,67	23,3	3,33	3,33	3,33
				L	66,7	6,67	20	3,33	3,33	0
Our Study	Türkiye	CT	259	T	72,6	18,9	3,4	3,9	0,8	0,4
				R	72	18,6	4,7	3,9	0,8	0
				L	73,1	19,2	2,3	3,8	0,8	0,8
				M	75,7	17,2	1,4	4,3	0,7	0,7
				F	68,9	21	5,9	3,4	0,8	0

N: Number of samples measured, **P-L:** Posterolateral, **P:** Posterior, **Lat:** Lateral, **P-M:** Posteromedial, **Med:** Medial, **A-L:** Anterolateral, **KS:** Kind of study**, Ca:** Cadaver, **MA:** Meta-analysis, **CT**: Computed Tomography, **T:** Total, **R:** Right, **L:** Left, **M:** Male, **F:** Female. (Rates for MCFAs that directly originate (without a common trunk) are compared)

Table 11. Comparison of arteries from which MCFA originates with other studies (%).

Author	Country	KS	N	T R/L M/F	From DFA (directly)	From FA (directly)
Massoud and Fletcher (1997)	USA	Ta	188	T	76	22
Vazquez et al. (2007)	England	Ca	438	T	83,4	16,4
Prakash et al. (2010)	India	Ca	64	T	67,2	32,8
Nasr et al. (2014)	Arabia	Ca	90	M	60	22
				F	57,5	27,5
Manjappa and Prasanna (2014)	India	Ca	40	R	40	50
				L	60	35
Anjankar et al. (2014)	India	Ca	120	R	65	20
				L	60	23,33
Al-Talalwah (2015)	Scotland	Ca	342	T	57	15,6
Ogeng'o et al. (2015)	Kenya	Ca	104	T	79,6	4,1
Tomaszewski et al. (2016)	World	MA	4351	T	64,6	33,2
Verma et al. 82016)	India	Ca	38	T	73,68	26,32
				R	66,67	33,33
				L	80	20
Vuksanović-Božarić et al. (2018)	Monte-negro	Ca	60	T	78,3	16,7
Zlotorowicz et al. 82018)	Poland	CT	100	T	65	34
Kaur et al. 2019)	India	Ca	40	R	85	15
				L	75	25
Łabętowicz et al. (2019)	Polonya	Ca	80	T	62,5	18,75
Our study	Türkiye	CT	259	T	64,9	35,1
				R	62	38
				L	67,7	32,3
				M	60	40
				F	70,6	29,4

N: Number of samples measured, **KS:** Kind of study**, Ta**: Transfemoral aortogram, **Ca:** Cadaver, **MA:** Meta-analysis, **CT**: Computed Tomography, **T:** Total, **R:** Right, **L:** Left, **M:** Male, **F:** Female, **FA**: Femoral artery, **DFA:** Deep femoral artery.
(Rates for LCFAs that directly originate (without a common trunk) are compared)

data similarly indicate that the MCFA directly originates from the FA or DFA. Manjappa and Prasanna (2014) stated that the right-side MCFA mostly originates from the FA, while all other researchers reported that it originates mostly from the DFA. In our study, it was found that the MCFA mostly originated from the DFA and the results of the current study show similarities with previous studies. Accurate anatomy knowledge of the MCFA is important to prevent femoral head necrosis and iatrogenic injuries to this artery during hip joint surgery and flap plastic surgery (Tomaszewski et al., 2016; Tzouma et al., 2020).

In the current study, it was detected that the LCFA originated directly from the FA or DFA. As listed in Table 12, the data obtained in previous studies reveal that the LCFA directly originates from the FA or DFA. Although most researchers have stated that the LCFA directly originates from the DFA, Kaur et al. (2019) reported that the right of the LCFA originates equally both from the

Table 12. Comparison of arteries from which LCFA originates with other studies (%).

Author	Country	KS	N	T R/L M/F	From DFA (directly)	From FA (directly)
Massoud and Fletcher (1997)	USA	Ta	188	T	80	19
Fukuda et al. (2005)	Japan	Fa	262	T	81,7	17,2
Vazquez et al. (2007)	England	Ka	438	T	94,8	5,02
Uzel et al. (2008)	Türkiye	Ka	110	T	77,3	20,9
Prakash et al. (2010)	India	Ka	64	T	81,25	18,75
Sinkeet et al. (2012)	Kenya	Ka	84	T	65,55	2,4
Sabnis (2013)	India	Ka	60	T	80	16,6
Nasr et al. (2014)	Arabia	Ka	90	M	74	12
				F	65	20
Manjappa and Prasanna (2014)	India	Ka	40	R	80	20
				L	70	25
Anjankar et al. (2014)	India	Ka	120	R	70	13,33
				L	66,67	15
Ogeng'o et al. (2015)	Kenya	Ka	104	T	66,7	33,5
Verma et al. (2016)	India	Ka	38	T	84,21	15,79
				R	77,77	22,23
				L	90	10
Vuksanović-Božarić et al. (2018)	Montenegro	Ka	60	T	83,3	8,4
Kaur et al. (2019)	India	Ka	40	R	50	50
				L	60	40
Łabętowicz et al. (2019)	Poland	Ka	80	T	78,75	21,25
Mogale et al. (2021)	South Africa	Ka	90	T	78,9	21,1
				R	82,2	17,8
				L	75,6	24,4
Our study	Türkiye	CT	247	T	85,8	14,2
				R	86,1	13,9
				L	85,6	14,4
				M	85	15
				F	86,8	13,2

N: Number of samples measured, **KS:** Kind of study**, Ta**: Transfemoral aortogram, **Fa:** Femoral angiography**, Ca:** Cadaver, **MA:** Meta-analysis, **CT**: Computed Tomography, **T:** Total, **R:** Right, **L:** Left, **M:** Male, **F:** Female, **FA**: Femoral artery, **DFA:** Deep femoral artery.

DFA and FA. In our study, it was observed that the LCFA mostly originated from the DFA (85.8%). It is important to have information about the anatomical variations of the LCFA and its branches, as they are used in aortopopliteal bypass, coronary artery bypass graft, extracranial-intracranial bypass surgeries, and anterolateral thigh flaps (Fukuda et al., 2005; Üzel et al., 2008; Olasińska-Wiśniewska et al., 2017).

Prakash et al. (2010), in their study on cadavers, reported that if the MCFA and LCFA originate directly from the FA, the level of separation of the DFA from the FA would be more distal. For this reason, they emphasized that these anatomical facts should be taken into account before planning different diagnostic and therapeutic interventions for the FA and its branches.

Our study has two limitations. The first is the small sample size included in the study. The second is that the study was conducted in a population in a limited region.

CONCLUSION

It is necessary to know the morphometric information of the FA and its branches, especially to perform intravenous applications more safely. Information about the branching model and vascular system of the FA and DFA is very important in terms of cardiology, radiology, general surgery, plastic surgery and orthopedic surgery. Our study includes morphological information, as well as morphometric information. Therefore, we believe that it will be of significant use to both clinicians and the literature in this regard.

REFERENCES

ADACHI B (1928) Das Arteriensystem der Japaner. Kaiserlich-Japanischen Universitat zu Kyoto, Kyoto.

AL-TALALWAH W (2015) The medial circumflex femoral artery origin variability and its radiological and surgical intervention significance. *Springerplus,* 4: 149.

ANJANKAR VP, PANSHEWDİKAR P, THAKRE G, MANE U, TEKALE V (2014) Morphological study on branching pattern of Femoral artery: A Cadaveric study. *Asian J Biomed Pharm*, 4(28): 34-38.

CHAUHAN PR, ADHVARYU MA, RATHWA AJ, CHAUHAN AP, CHAVDA S, RATHOD SP (2015) Study of profunda femoris artery of human cadavers in Rajkot city, India. *Int J Anat Res,* 3(1): 873-877.

CHOY KW, KOGILAVANI S, NORSHALIZAH M, RANI S, ASPALILAH A, HAMZI H, FARIHAH HS, DAS S (2013) Topographical anatomy of the profunda femoris artery and the femoral nerve: Normal and abnormal relationships. *Clin Ter,* 164(1): 17-19.

DIXIT D, KUBAVAT DM, RATHOD SP, PATEL MM, SINGEL TC (2011) A study of variations in the origin of profunda femoris artery and its circumflex branches. *Int J Biol Med Res,* 2(4): 1084-1089.

FUKUDA H, ASHIDA M, ISHII R, ABE S, IBUKURO K (2005) Anatomical variants of the lateral femoral circumflex artery: An angiographic study. *Surg Radiol Anat,* 27(3): 260-264.

GEORGE A, SANTHAKUMARY MT (2021) A cadaveric study on the variations of the profunda femoris artery in South India. *Asian J Med Sci,* 12(2): 86-90.

KASHYAP SD, KASOTE AP (2018) Study of variations in the origin of profunda femoris artery and internal diameter of femoral artery in human cadavers. *Indian J Anat,* 7(2): 129-137.

KAUR A, SHARMA A, KUMAR SHARMA M (2019) Variation in branching pattern of femoral artery. *Int J Anat Res,* 7: 6171-6177.

KAWASHIMA T, OKAMOTO K, WADA T, SHUTO T, UMENO T, MIYAMOTO S (2021) Femoral artery anatomy is a risk factor for limb ischemia in minimally invasive cardiac surgery. *Gen Thorac Cardiovasc Surg,* 69(2): 246-253.

ŁABĘTOWICZ P, OLEWNIK, PODGÓRSKI M, MAJOS M, STEFAŃCZYK L, TOPOL M, POLGUJ M (2019) A morphological study of the medial and lateral femoral circumflex arteries: A proposed new classification. *Folia Morphol (Warsz),* 78(4): 738-745.

MANJAPPA T, PRASANNA LC (2014) Anatomical variations of the profunda femoris artery and its branches—a cadaveric study in South Indian population. *Indian J Surg,* 76(4): 288-292.

MASSOUD TF, FLETCHER EWL (1997) Anatomical variants of the profunda femoris artery: an angiographic study. *Surg Radiol Anat,* 19(2): 99-103.

MOGALE N, OLORUNJU SAS, MATSHIDZA S, BRIERS N (2021) Anatomical variations in the origins of the lateral circumflex femoral arteries in a South African sample: A cadaver study. *Transl Res Anat,* 22: 100098.

MURTHY CK, MUBEEN KARNUL A, BHANU A (2022) Study on various patterns of profunda femoris artery and its branches. *Int J Acad Med Pharm,* 4(4): 264-269.

NASR AY, BADAWOUD MH, AL-HAYANI AA, HUSSEIN AM (2014) Origin of profunda femoris artery and its circumflex femoral branches: Anatomical variations and clinical significance. *Folia Morphol (Warsz*), 73(1): 58-67.

OGENG'O J, MISIANI M, WAISIKO B, OLABU BO, MARANGA E (2015) Variant branching of the common femoral artery in a black Kenyan population: trifurcation is common. *Anat J Africa,* 4(1): 528-533.

OLASIŃSKA-WIŚNIEWSKA A, GRYGIER M, LESIAK M, ARASZKIEWICZ A, TROJNARSKA O, KOMOSA A, MISTERSKI M, JEMIELITY M, PROCH M, GRAJEK S (2017) Femoral artery anatomy-tailored approach in transcatheter aortic valve implantation. *Postepy Kardiol Interwencyjnej,* 13(2): 150-156.

PANAGOULI E, LOLIS E, VENIERATOS D (2011) A morphometric study concerning the branching points of the main arteries in humans: Relationships and correlations. *Ann Anat,* 193(2): 86-99.

PRAKASH KJ, KUMAR BA, BETTY AJ, KUMAR YS, SINGH G (2010) Variations in the origins of the profunda femoris, medial and lateral femoral circumflex arteries: a cadaver study in the Indian population. *Rom J Morphol Embryol,* 51: 167-170.

RAJANI SJ, RAVAT MK, RAJANI JK, BHEDI AN (2015) Cadaveric study of profunda femoris artery with some unique variations. *J Clin Diagn Res,* 9(5): AC01-AC03.

SABNIS AS (2013) Anatomical variations of profunda femoris artery. *J Clin Res Letters,* 4(1): 54-56.

SAMARAWICKRAMA MB, NANAYAKKARA BG, WIMALAGU-NARATHNA KWR, NISHANTHA DG, WALAWAGE UB (2009) Branching pattern of the femoral artery at the femoral triangle: a cadaver study. *Galle Med J,* 14(1): 31-34.

SANUDO JR, ROIG M, RODRIGUEZ A, FERREIRA B, DOMENECH JM (1993) Rare origin of the obturator, inferior epigastric and medial circumflex femoral arteries from a common trunk. *J Anat,* 183: 161-163.

SCHNYDER G, SAWHNEY N, WHISENANT B, TSIMIKAS S, TURI ZG (2001) Original studies common femoral artery anatomy is influenced by demographics and comorbidity: implications for cardiac and peripheral invasive studies. *Catheter Cardiovasc Interv,* 53(3): 289-295.

SINKEET SR, OGENG'O JA, ELBUSAIDY H, OLABU BO, IRUNGU MW (2012) Variant origin of the lateral circumflex femoral artery in a black Kenyan population. *Folia Morphol (Warsz),* 71(1): 15-18.

SUDARSHANA S, CHAUDHARY AR (2020) A study of anatomical variations in the origin of profunda femoris artery in human cadavers. *Gal Int J Health Sci Res,* 5(4): 37-41.

TOMASZEWSKI KA, HENRY BM, VIKSE J, ROY J, PĘKALA PA, SVENSEN M, GUAY DL, SAGANIAK K, WALOCHA JA (2016) The origin of the medial circumflex femoral artery: A meta-analysis and proposal of a new classification system. *PeerJ,* 4: e1726.

TROUPIS T, MICHALINOS A, MARKOS L, SAMOLIS A, TSAKOTOS G, DIMITROULIS D, VENIERATOS D, SKANDALAKIS P (2013) "Trifurcation" of femoral artery. *Artery Res,* 7(2): 106-108.

TZOUMA G, KOPANAKIS NA, TSAKOTOS G, SKANDALAKIS PN, FILIPPOU D (2020) Anatomic variations of the deep femoral artery and its branches: clinical implications on anterolateral thigh harvesting. *Cureus,* 12(4): e7867.

UZEL M, TANYELI E, YILDIRIM M (2008) An anatomical study of the origins of the lateral circumflex femoral artery in the Turkish population. *Folia Morphol (Warsz*), 67(4): 226-230.

VAZQUEZ MT, MURILLO J, MARANILLO E, PARKIN A, SANUDO J (2007) Patterns of the circumflex femoral arteries revisited. *Clin Anat,* 20(2): 180-185.

VERMA RK, PANKAJ AK, RANI A, KUMAR N, RANI A (2016) Variations in the origin of profunda femoris and circumflex femoral arteries: A cadaveric study. *Indian J Clin Anat Physiol,* 3(4): 478-481.

VUKSANOVIĆ-BOŽARIĆ A, ABRAMOVIĆ M, VUČKOVIĆ L, GOLUBOVIĆ M, VUKČEVIĆ B, RADUNOVIĆ M (2018) Clinical significance of understanding lateral and medial circumflex femoral artery origin variability. *Anat Sci Int,* 93(4): 449-455.

VUKSANOVIĆ-BOŽARIĆ A, STEFANOVIĆ N, PAVLOVIĆ S, ĐURAŠKOVIĆ R, RANĐELOVIĆ J (2007) Analysis of deep femoral artery origin variances on fetal material. *Med Biol,* 14: 112-116.

YU SH, HWANG JH, KIM JH, PARK S, LEE KH, CHOI ST (2020) Duplication of superficial femoral artery: Imaging findings and literature review. *BMC Med Imaging,* 20(1): 99.

ZLOTOROWICZ M, CZUBAK-WRZOSEK M, WRZOSEK P, CZUBAK J (2018) The origin of the medial femoral circumflex artery, lateral femoral circumflex artery and obturator artery. *Surg Radiol Anat,* 40(5): 515-520.

Long-term supplementation with young coconut juice help prevent bone loss of orchidectomized rats by increasing connectivity density, percentage bone volume and osteoblast-/osteocyte-(ERα-/ERβ-) immunoreactive cells of the L5 vertebra and femur

Asma Asae[1], Albert M. Hutapea[2], Jirawat Saetan[1], Nisaudah Radenahmad[1]

[1] Division of Health and Applied Sciences, Faculty of Science, Prince of Songkla University, Hat Yai, Songkhla, Thailand

[2] Department of Pharmacy, Faculty of Science, Universitas Advent Indonesia Bandung, Indonesia

SUMMARY

Adult male rats were orchidectomized (ORX) and treated with 17β-estradiol or young coconut juice (YCJ) for ten weeks. Their femur and L5 vertebra were dissected, and the percentage of bone volume was measured using a Micro-CT scan. Immunohistochemistry was used to detect ERα and ERβ to determine if the osteoporotic protective effects of YCJ were due to the attachment of the YCJ active component(s) to estrogen receptors. It was found that both ERα and ERβ were found in osteocytes and osteoblasts, but not osteoclasts. Compared to normal rats, the percentage of bone volume and number of osteoblast- and osteocyte-reactive cells of both femur and L5 were significantly reduced in ORX rats. Those numbers in the ORX rats were restored to normal by injecting estradiol benzoate or by feeding YCJ to the rats, which was not dose-related. Significant correlations were detected between osteoblast-/osteocyte- (ERα-/ERβ)-reactive cells vs. serum E2 level. The optimal dose of this study was 10 mL/kg BW/day for ERα-of both osteoblasts and osteocytes and 40 mL/kg BW/day for ERβ-of both osteoblasts and osteocytes. The results suggest that YCJ may be as efficient as estradiol benzoate in attenuating osteoporosis, probably by being a selective estrogen receptor moderator.

Key words: *Cocos nucifera* L – *Arecaceae* – Micro-CT scan – Osteoblasts – Osteocytes – Osteoporosis

ABBREVIATIONS

CB	Calbindin
CIA	chemiluminescent immunoassay
E2	17β-estradiol

Corresponding author:
Dr. Nisaudah Radenahmad. Division of Health and Applied Sciences, Faculty of Science, Prince of Songkla University, Hat Yai, Songkhla, Thailand. E-mail: nisaudah.r@psu.ac.th

Submitted: March 10, 2022. **Accepted:** February 25, 2023

https://doi.org/10.52083/CJWJ5539

EB Estradiol benzoate
EDTA Ethylenediaminetetraacetic acid
ER Estrogen receptor
ERα Estrogen receptor-α
ERβ Estrogen receptor-β
GI Gastrointestinal
OPG Osteoprotegerin
ORX Orchidectomized
RANKL Receptor activator of nuclear factor κB ligand
SERM Selective estrogen receptor modulator
T Testosterone
VDR Vitamin D receptor
YCJ Young coconut juice

INTRODUCTION

Being one of the commonest human metabolic bone maladies, osteoporosis has been a growing health concern in both women and men (Sozen et al., 2017). Numerous studies reported that estrogens exert a vital role in human bone homeostasis (Noirrit-Esclassan et al., 2021). Bone loss in aging men is due to androgen deficiency (Shigehara et al., 2021). Several studies, however, reported the effect of estrogen in maintaining men's bone mass (Noirrit-Esclassan et al., 2021). Although testosterone, one of the androgenic hormones, can be converted to estrogen in peripheral tissue, its level is not as high as in women. Effective prevention of bone loss has been proven by estrogen replacement treatment. However, this therapy also causes gynecomastia (Chen et al., 2015), increasing the risk for benign prostate cancer and prostatic hyperplasia (Capogrosso et al., 2021). Therefore, a better choice than estrogens is the plant-derived nonsteroidal compounds phytoestrogens, with biological activities like estrogen, maybe. Various phytoestrogens inhibit bone loss with limited consequences on reproduction organ tissues that function as selective estrogen receptor modulators (SERMs) (Zhou et al., 2021). Recently, the discovery of SERMs has pointed to the fact that estrogenic substances that positively affect bone but do not affect the gonads and the mammary glands available. Our previous studies for the past ten years strongly indicated that YCJ could act as a kind of SERMs (Balit et al., 2018; Payanglee et al., 2021; Radenahmad et al., 2009, 2010, 2012, 2015; Suwanpal et al., 2011).

Our team has gradually accumulated preliminary studies to investigate the anti-osteoporotic effects of YCJ for many years. We first started with relevant cells involved with gastrointestinal (GI) functions in the GI tract (Radenahmad et al., 2014). Those studies indicated that the reduction of the GI argyrophil cells density might influence osteoporosis among orchidectomized (ORX) rats. In turn, this phenomenon would add to the motility, calcium absorption activities, hormone production, and secretion processes in the GI tract that is often evident in osteoporotic andropause and elderly patients. Diminishing absorption of calcium, and perhaps of other minerals in the GI tract in the ORX rats, may have caused osteoporosis that can be treated with exogenous estrogen, e.g., estradiol benzoate (EB) and phytoestrogen, or YCJ feeding (Yusuh et al., 2010). The study then moved to the next step, investigating cartilage and bone of temporomandibular joint of ORX rats. We found that YCJ with a high dose of YCJ at 100 mL/kg BW/day could increase the thickness of the cartilage and mandibular cancellous bone in cell layer ORX rats (Suwanpal et al., 2011; Yusuh et al., 2010). We found that ORX rats that were given a dose of 100 mL/kg BW/day YCJ produced an unfavorable glycogen deposition in the liver (Radenahmad et al., 2012, unpublished data). As an established model of osteoporosis, castrated rats (Blouin et al., 2008) develop substantial osteoporosis with a decrease to about 35% in bone mass (Mohamad et al., 2018; Chin and Ima-Nirwana, 2015). In addition, we have proven that YCJ at three lower doses (10, 20, and 40 mL/kg BW) had no feminizing nor adverse effects on male gonads (Balit et al., 2018). Therefore, in the present study, these three lower doses were used to investigate whether it effectively prevents osteoporosis without adverse effects in ORX rats.

Bone cell phytoestrogen therapy has been reported by many studies. Kim (2021) found that isoflavones are structurally similar to 17-β-estradiol and bind to estrogen α and β receptors (Kim, 2021). Domazetovic et al. (2020) reported that blueberry juice can prevent the inhibition of osteogenic differentiation and mineralization induced by oxidative stress and triggered by glutathione depletion using human osteoblast-like

SaOS-2 cells (Domazetovic et al., 2020). Icariside I and icariside II of *Epimedii Folium* were reported by Liu et al. (2017) as two active compounds that greatly enhanced cell proliferation and osteoblast development. Estrogen is crucial for male bone health, acting through ERα (Noirrit-Esclassan et al., 2021). Characteristically, phytoestrogens show affinity to α and β estrogen receptors, like 17β-estradiol (E2) (Domínguez-López et al., 2020; Rietjens et al., 2017), and these two estrogen receptors are found in both mice and human bones (Khalid and Krum, 2016). It was found that ERα of osteocytes has an essential function in male mice trabecular bone formation (Farman, 2019). Panche et al., (2016) reported that flavonoids found in most phytoestrogens possess wound-healing properties. Our previous studies showed that YCJ accelerated wound healing (Radenahmad et al., 2012; 2015). Therefore, YCJ was presumably considered as one of the flavonoid groups that could have anti-osteoporotic effects.

Altogether, the present study aimed to explore the functioning properties of YCJ (*Cocos nucifera*, L) in preventing bone loss in the femur and the L5 vertebra, a proper model of osteoporosis among ORX rats. This study used immunohistochemistry of estrogen receptor (ER) of both ERα and ERβ in osteoblasts and osteocytes to explore whether YCJ could act through these receptors. As an established method, the micro-CT is popularly used to quantify *in vivo* anti-osteoporotic agents (Effendy et al., 2013), and microradiographs of post-mortem undecalcified histological sections provide higher resolution. Thus, this study used a micro-CT scan to investigate microarchitectural changes of the bones in detail, i.e., number, length, width, and localization.

MATERIAL AND METHODS

YCJ preparation

Substantial volume of YCJ was obtained from Khlong Hoi Khong district, Hat Yai, Songkhla, Thailand, which was then processed to become powder. The YCJ powder was maintained at -30°C temperature until used. Solution of the powder was freshly prepared before being given to the rats. Our previous publication provides the complete preparation and administration of the YCJ (Radenahmad et al., 2006).

Animals

The study used 8-month-old, 250-300 g BW adult male Wistar rats obtained from Mahidol University (Salaya, Thailand). The animals were then maintained at our animal House laboratory facilities, given standard food pellets, housed in contamination-free room that was artificially lighted with a 12h dark/light cycle, with25 ± 1°C temperature, and 50 ± 5% humidity. All animals were given normal care complying with Animal Care and Use Committee of Prince of Songkla University and the National Institutes of Health guidelines (NIH publication 86-23 revised 1985). The research protocol was approved under license number 01/59.

Experimental design

At the end of a one-week acclimatization period, the animals were divided into seven groups, each consisting of ten rats, then treated for ten weeks. First group, the baseline control (NC) animals without any treatment, sacrificed on the first day of the experiment. This first group was used as an initial baseline value in determining skeletal tissue changes resulting from aging and surgery operations (Kalu, 1991). Second group, sham-operated rats (SC). Third group, orchidectomized rats (OC). Fourth group (OE), ORX rats injected estradiol benzoate intraperitoneally with a dose of (2.5 µg/kg BW/day) for three days per week, as in our previous studies (Radenahmad et al., 2009; 2012), Fifth, sixth and seventh groups each consisted of ORX rats with YCJ gavage dose of 10 (OJ10), 20 (OJ20), and 40 ml/kg BW/day (OJ40), respectively (Table 1a). The EB injection and the feeding with YCJ began a week after orchidectomy. SC and OC rats were forced-fed with reverse osmosis water, the injection vehicles. The feeding with YCJ was done once daily, a week after the orchidectomy. The rats were sacrificed at the end of the ten-week feeding and injection treatment. The L5 vertebral body and the femur were removed, fixated using neutral formalin (10%), then decalcified. This was then followed by paraffin sectioning and immunohistochemical staining processes (Radenahmad

Table 1. Animal grouping, antibodies, concentration, and manufacturer used for bone sections of each rat.

1a. Animal grouping (10 rats per group).

Groups	Treatments
NC	Normal (normal control)
SC	Sham-operated, received reverse-osmosis water (sham control)
OC	Orchidectomized, received reverse-osmosis water (orchidectomized control)
OE	Orchidectomized, and injected with estradiol benzoate (EB, 2.5 µg/kg BW) 3 days a week, for 10 wks
OJ10	Orchidectomized, received YCJ at 10 mL/kg BW/d for 10 wks
OJ20	Orchidectomized, received YCJ at 20mL/kg BW/d for 10 wks
OJ40	Orchidectomized, received YCJ at 40mL/kg BW/d for 10 wks

1b. Immunostaining for each rat bone sections.

Section No.	Staining
1-2	H & E staining, for histological orientation
3-4	Immunostaining for mouse anti-estrogen receptor α (aa-120-170) antibody (MAB447, Millipore, CA, USA)
5-6	Immunostaining for rabbit anti-estrogen receptor β antibody (PA1-310B, Thermo Fisher Scientific, IL, USA)
7-8	Immunostaining, omitting primary antibodies (negative control), one for each antibody

1c. Dilutions of each antibody.

	Antibodies	
Bones	ER-alpha	ER-beta
Femur	1:400	1:100
Lumbar (L5)	1:200	1:100

et al., 2009). Serum estradiol and testosterone was measured using the chemiluminescent immunoassay (CIA) technique (ECLIA, Modular E 170C, Estradiol II 03000079 122, Roche, Germany and ECLIA, Modular E 170C, testosterone 11776061 122, Roche, Germany, respectively). The CIA technique details have been explained in our previous publication (Radenahmad et al., 2009).

Bone decalcification

Muscles were removed as much as possible from the bones, then fixed in 10% neutral buffer formalin for seven days. All well-fixed specimens were decalcified with 10% EDTA (ethylenediaminetetraacetic acid) chelating agent twenty times their volume changed once a week for ten weeks. The endpoint of decalcification was adjusted by X-ray (the most accurate method).

Bone morphology assessment

The excised L5 and femur were thawed at room temperature for two hours before scanning process using the micro-computed tomography method (Scanco Medical, Bassersdorf, Switzerland), and evaluation using Scanco program (version 6.5-1, Scanco Medical). The optical microscope (Axioskop 40) was used to measure %bone volume with a digital video camera (NOPL-A662, Media Cybernetics, Silver Spring, MD, USA) and the imaging software (CellSense version 1.6, Germany). The Bone volume/total volume (BV/TV), bone mineral density (BMD), trabecular thickness (Tb.Th), trabecular separations (Tb.Sp), trabecular numbers (Tb.N.), and connectivity density (Conn.D) are the structural parameters measured. The collected data were compared between groups and different levels of vertebra or femur within the group.

1.1. Percentage prevention calculation

BMD values from micro-CT scan of the control and the experimental groups were calculated for % prevention using a formula as follows (Urasopon et al., 2007):

$$\% \text{ prevention} = \left(\frac{\text{average value of treatment groups - average value of the OC group x 100}}{\text{average value of the SC group - average value of the OC group}} \right)$$

1.2. Percentage change calculation

BMD values from micro-CT scan of the control and the experimental groups were calculated for % change using a formula as follows (Urasopon et al., 2007):

$$\% \text{ change} = \left(\frac{\text{average value of treatment groups- average value of the OC group x100}}{\text{average value of the OC group}} \right)$$

1.3. Percentage Bone volume (H&E staining)

Histomorphometric analysis was done on randomly five areas of three separate 60 µm trabecular bone areas. Analysis of the bone area (%) was done using the formula described by Parfitt et al. (1987) and Suwanpal et al. (2011):

$$\text{Bone volume (\%)} = \left(\frac{\text{area of trabeculae x100}}{\text{area of trabeculae+ marrow space}} \right)$$

Immunohistochemistry

Each block was sliced with microtome to eight 5 µm-thick sections, stained with Hematoxylin and Eosin (H&E), and prepared for ERα and ERβ antibody immunostaining (Table 1b and 1c). The glass slides were coated with a poly-L-lysine solution for immunostaining. The positive controls for ERα and ERβ immunostaining from normal female rats were done on the uterus and ovary sections, respectively. The whole preparation process was guided according to our method previously reported (Radenahmad et al., 2009; 2012). The details of all antibodies, concentrations, and manufacturers used for bone sections of each rat described in Table 1b and 1c.

Quantitative analysis of ERα and ERβ immunoreactive cells

The immunoreactive cells from the L5 vertebral body and the femur were counted using light microscopy (LM) at 40x magnification power. Using an image analysis system (Samba Technologies, Meylan, France), two double-blind observers analyzed ten random fields of each slide. The mean number of immunoreactive cells/mm^2 was obtained by averaging the three antibody readings in each section.

Statistical analysis

The calculations of the sample size used Altman's nomogram. The microscopic fields were randomized for selection using Excel version 5.0. Results were expressed as mean ± SEM. The confidence interval used was $p<0.05$. Shapiro-Wilk test was used to test the normal distribution, one-way ANOVA followed by the LSD test was performed using SPSS version 16.0 (SPSS, Inc., Chicago, IL, USA).

RESULTS

Body weight

After the ORX rats were treated with EB or YCJ for ten weeks, the body weight of the OE group on the day of termination was significantly lower than that on the day of onset (Table 2). Com-

Table 2. Body weight (g) (mean ± SEM) of the 7 groups of rats examined, NC = baseline normal control group, SC = sham-operated group, OC = orchidectomized rats, OE = orchidectomized rats + estradiol benzoate (EB), OJ10 = orchidectomized rats receiving YCJ 10 mL/kgBW, OJ20 = orchidectomized rats receiving YCJ 20 mL/kgBW, OJ40 = orchidectomized rats receiving YCJ 40 mL/kgBW. *p<0.05 comparison between the body weight at the commencement of the study and the day that the rats were terminated.

Groups BW	NC (n=10)	SC (n=10)	OC (n=10)	OE (n=10)	OJ10 (n=10)	OJ20 (n=10)	OJ40 (n=10)
BW Started	552.60 ± 32.69	540.70 ± 28.82	530.00 ± 27.33	571.70 ± 32.50	520.50 ± 22.14	504.70 ± 21.58	485.30 ± 21.06
BW finished	552.60 ± 32.69	528.20 ± 17.53	493.80 ± 17.69	489.30 ± 19.94 *	511.70 ± 21.12	485.10 ± 16.95	473.40 ± 15.04

pared between the initiation day and the last day of the experiment after force feeding with YCJ for 10 weeks, the body weight of all the 3 OJ groups (OJ10, OJ20 and OJ40) was lower, even though statistically significant was not exhibited.

Bone Parameters

Bone volume percentage. The results presented in Figs. 1A and 1B demonstrates 3D images of micro-CT measurements of the L5 vertebra and femur, respectively. Following orchidectomy (OC group), the percentage of bone volume (Figs. 2A, a-b) was significantly lower in L5 (Fig. 2A, a) but not in the femur (Fig 2A, b) compared with the control groups (NC and SC groups). That percentage of bone volume increased when the ORX rats were treated with EB (OE group) or YCJ treatments. With YCJ treatments (OJ10, OJ20, and OJ40 groups), the bone volume percentage increased but was not dose-related. The OJ20 was the best dose for both the L5 vertebra (Fig. 2A, a) and femur (Fig. 2A, b). Nevertheless, the bone vol-

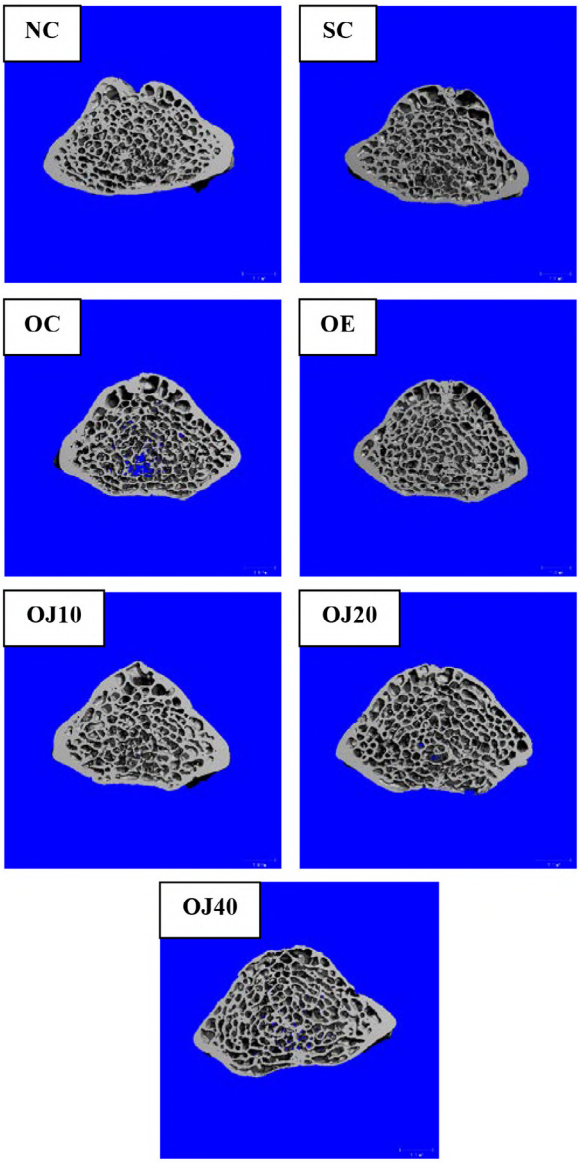

Fig. 1A.- The 3D image of micro-CT measurement of the vertebral body of 5th lumbar (L5). NC = baseline control group; SC = sham-operated group; OC = orchidectomized group; OE = orchidectomized rat receiving estradiol benzoate (EB) 2.5 µg/kgBW/day; OJ10 = orchidectomized rat receiving YCJ 10 mL/kgBW/day; OJ20 = orchidectomized rat receiving YCJ 20 mL/kgBW/day; OJ40 = orchidectomized rat receiving YCJ 40 mL/kgBW/day.

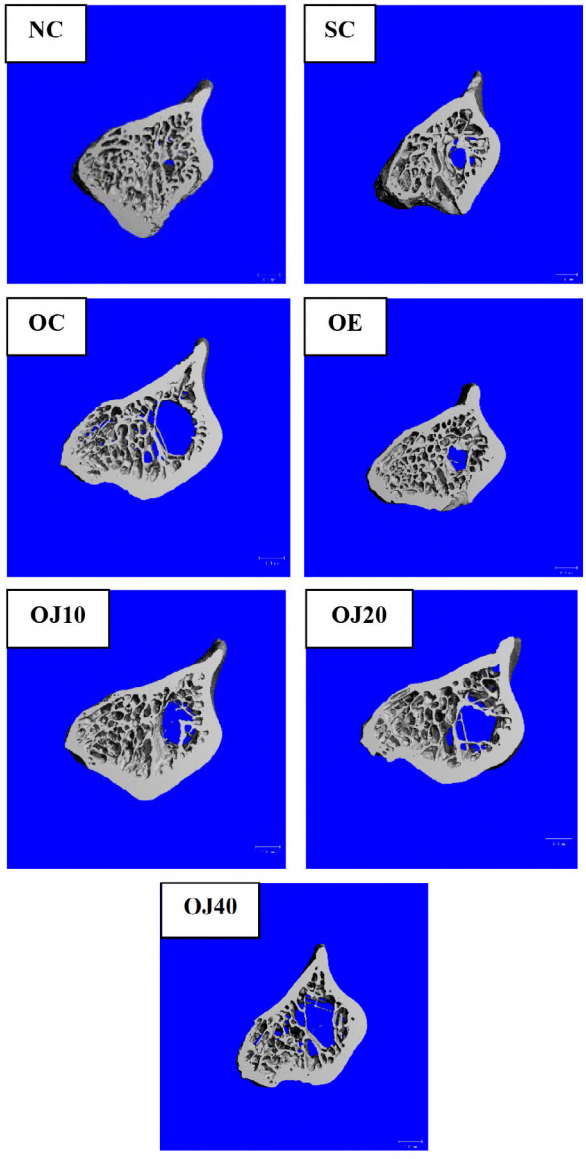

Fig. 1B.- The 3D image of micro-CT measurement of the left femur. NC = baseline control group; SC = sham-operated group; OC = orchidectomized group; OE = orchidectomized rat receiving estradiol benzoate (EB) 2.5 µg/kgBW/day; OJ10 = orchidectomized rat receiving YCJ 10 mL/kgBW/day; OJ20 = orchidectomized rat receiving YCJ 20 mL/kgBW/day; OJ40 = orchidectomized rat receiving YCJ 40 mL/kgBW/day.

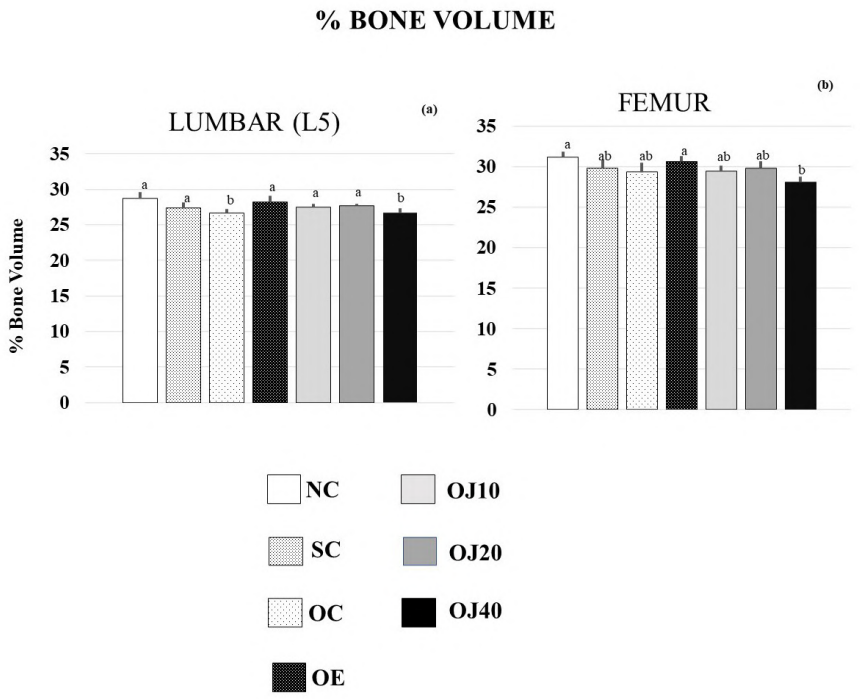

Fig. 2A.- The percentage of bone volume of the lumbar (L5) vertebra and the femur of 7 groups examined. Data expressed as mean ± SEM. Columns superscript with different letters are significantly different at $p < 0.05$. NC = baseline control group; SC = sham-operated group; OC = orchidectomized group; OE = orchidectomized rat receiving estradiol benzoate (EB) 2.5 µg/kgBW/day; OJ10 = orchidectomized rat receiving YCJ 10 mL/kgBW/day; OJ20 = orchidectomized rat receiving YCJ 20 mL/kgBW/day; OJ40 = orchidectomized rat receiving YCJ 40 mL/kgBW/day.

ume percentage of OJ10 and OJ20 groups in both the L5 vertebra and femur were not significantly different from each other (Figs. 2A, a-b). Among three doses of YCJ treatments, that of the OJ40 group was the lowest (Figs. 2A, a-b), even though in the femur, the significant difference was not detected when compared with the OJ10 and OJ20 groups (Fig. 2A, b).

Bone density connectivity. The micro-CT scan image of the femur indicated that Conn.D of the ORX group (OC group) was significantly less than the baseline group (NC group), while the ORX groups fed with YCJ were not different significantly from either the sham (SC) or baseline (NC) groups. BV/TV of the ORX groups fed with YCJ (OJ groups) was significantly less than the baseline group, but the difference was not significant from the ORX group (Fig. 2C, e). Other bone parameters of the OJ groups, e.g., BMD% prevention, BMD% change, Tb.Th., Tb.N., Tb.Sp. was not significantly different from the sham or ORX groups (Figs. 2C, c, d, f, g, and h). In contrast, all bone parameters in the micro-CT scans of the L5 of the OJ groups were not significantly different when compared to the control groups (Figs. 2B, a-h). Unexpectedly, the Conn.D of the L5 of the OJ40 group was higher than that of the NC, OC, OE, OJ10, and OJ20 groups. Interestingly, the Conn.D. of both OJ40 and the SC groups was not significantly different (Fig. 2B, b).

Estrogen Receptors

Fig. 3 demonstrates ERα-ir and ERβ-ir reactive cells of both femur and the L5 vertebra compared between the ORX+YCJ (OJ) groups and the control (SC, OC, and OE) groups. Reactivity of both ERα and ERβ were detected in osteocytes and osteoblasts in femur bone and L5 vertebrae *(*Fig. 3*)*.

ERα-ir cells. Fig 4A depicts the number of ERα-ir cells of osteoblasts and osteocytes of the L5 vertebra (Figs. 4A, a, b) and the femur (Figs. 4A, c, d). In the NC and SC groups, the reactive cells were observed at high frequency. Following orchidectomy (OC group), the numbers of ERα -ir cells significantly dropped, particularly osteoblasts of L5 (Fig. 4A, a). The values of ERα-osteoblasts (Figs.

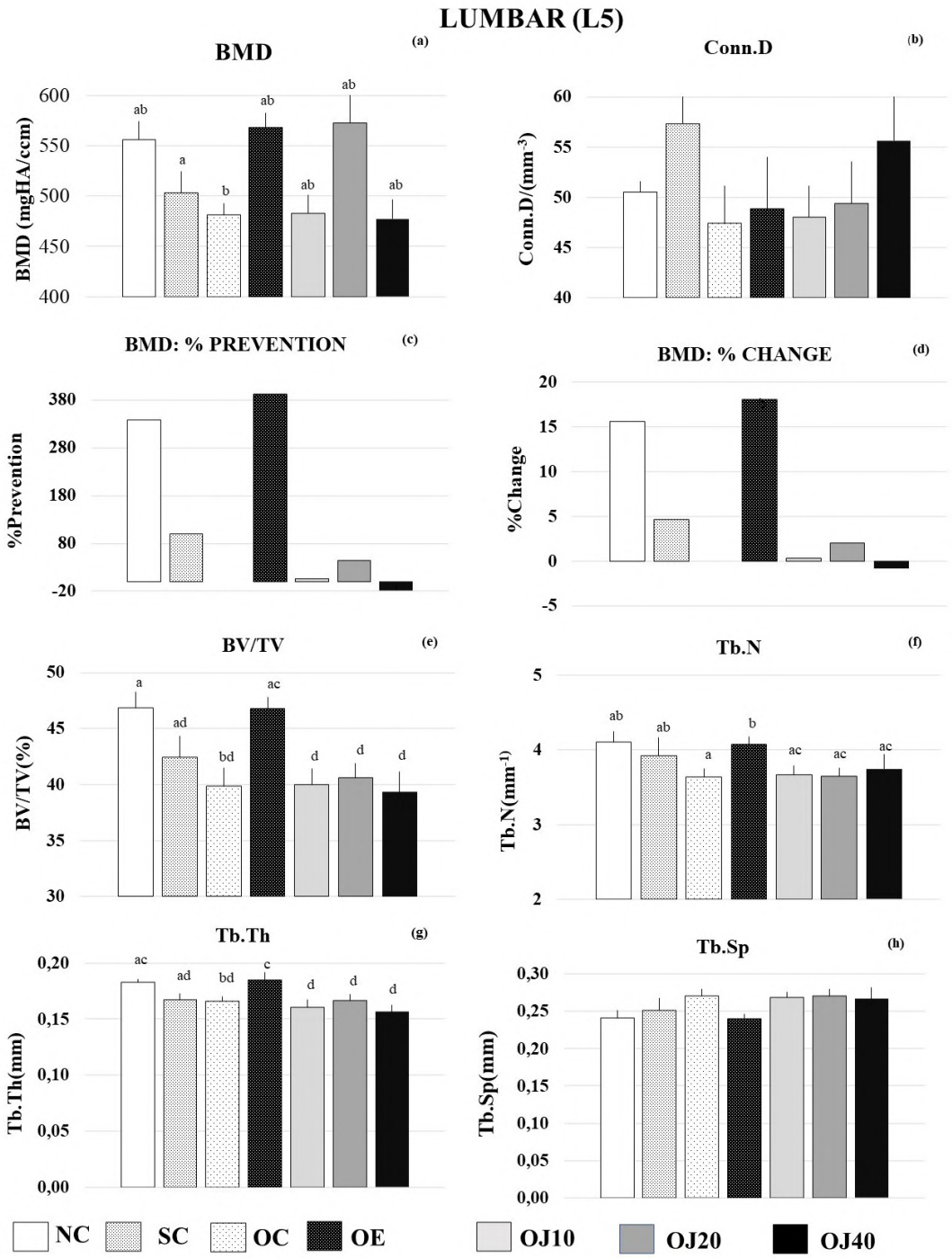

Fig. 2B.- The results of histomorphometric analyses of the 5th lumbar vertebra (L5). Data expressed as mean ± SEM. Columns superscript with different letters are significantly different at $p < 0.05$. BMD = bone mineral density; Conn.D = Connectivity density; BMD % Prevention = percentage prevention of the experimental/control groups; BMD % Change = percentage changes of the experimental/control groups; BV/TV = trabecular bone volume fraction; Tb.N = trabecular number; Tb.Th = trabecular thickness; Tb.Sp = trabecular separation of lumbar (L5).Data expressed as mean ± SEM. NC = baseline control group; SC = sham-operated group; OC = orchidectomized group; OE = orchidectomized rat receiving estradiol benzoate (EB) 2.5 µg/kgBW/day; OJ10 = orchidectomized rat receiving YCJ 10 mL/kgBW/day; OJ20 = orchidectomized rat receiving YCJ 20 mL/kgBW/day; OJ40 = orchidectomized rat receiving YCJ 40 mL/kgBW/day.

4A, a, c), but not of osteocytes (Figs. 4A, b, d), of both L5 and femur, significantly increased when the ORX rats were treated with EB (OE group). When ORX rats were treated with YCJ (OJ10, OJ20, and OJ40 groups), the numbers of the osteoblast- and osteocyte-reactive cells increased but were not dose-related (Figs. 4A, a-d). When compared to each other, the difference in the number of ERα–ir cells in all three OJ groups were not significant from each other. Similarly, the osteoblasts

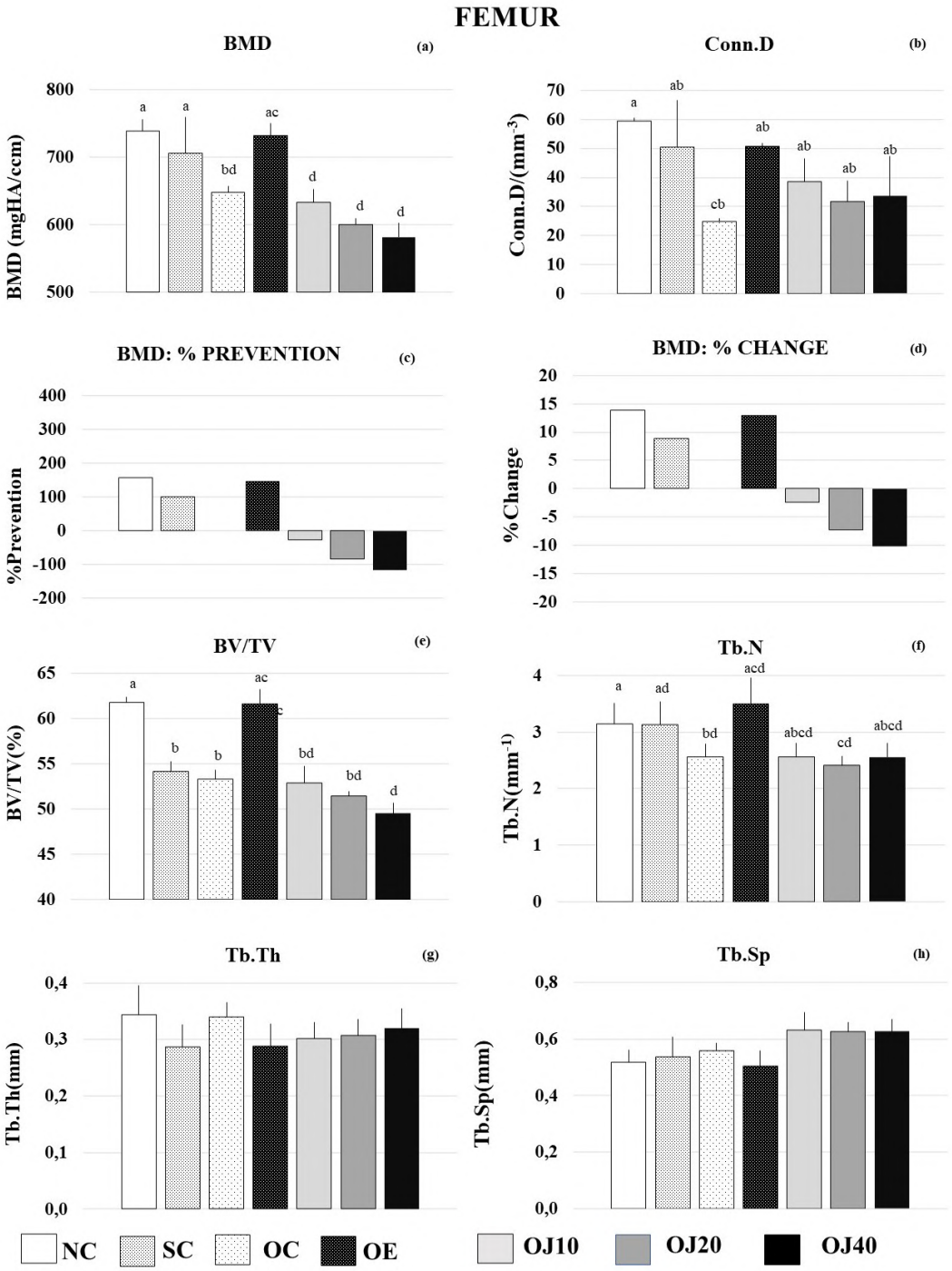

Fig. 2C.- The results of histomorphometric analyses of the femur. Data expressed as mean ± SEM. Columns superscript with different letters are significantly different at $p < 0.05$. BMD = bone mineral density; Conn.D = Connectivity density; BMD % Prevention = percentage prevention of the experimental/control groups; BMD % Change = percentage changes of the experimental/control groups; BV/TV = trabecular bone volume fraction; Tb.N = trabecular number; Tb.Th = trabecular thickness; Tb.Sp = trabecular separation of femur. Data expressed as mean ± SEM. NC = baseline control group; SC = sham-operated group; OC = orchidectomized group; OE = orchidectomized rat receiving estradiol benzoate (EB) 2.5 µg/kgBW/day; OJ10 = orchidectomized rat receiving YCJ 10 mL/kgBW/day; OJ20 = orchidectomized rat receiving YCJ 20 mL/kgBW/day; OJ40 = orchidectomized rat receiving YCJ 40 mL/kgBW/day.

and osteocytes in all these three OJ groups and the control (NC, SC, OC, and OE) groups were not significantly different (Figs. 4A, a-d).

ERβ-ir cells. Fig. 4B depicts the number of ERβ-ir cells of osteoblasts and osteocytes of the L5 vertebra and the femur. In the NC and SC groups, these reactive cells were observed at high frequency. Following orchidectomy (OC group), the number of ERβ–ir in osteoblasts of L5 (Fig. 4B, a) but not the femur (Fig. 4B, c) significantly decreased. That

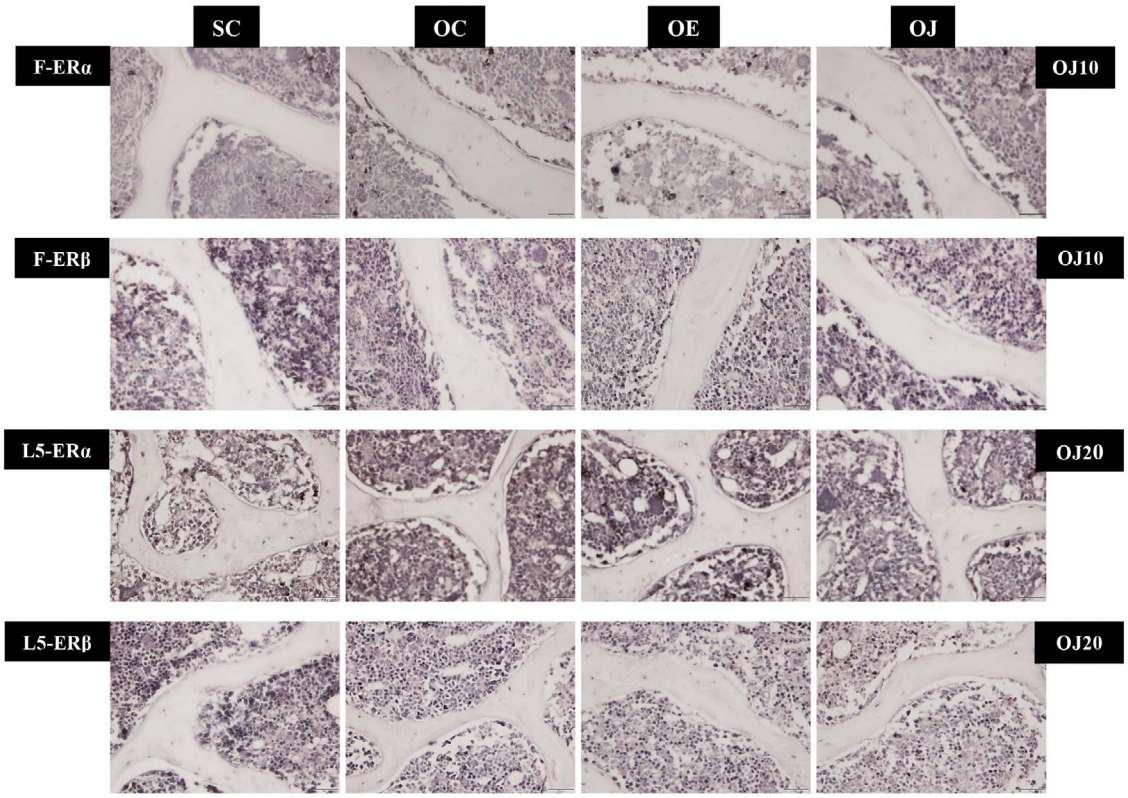

Fig. 3.- Immunohistochemical staining of ERα and ERβ cells of the femur (F-ERα and F-ERβ) and the lumbar vertebra (L5) (L-ERα and F-ERβ) at 40x magnification. Both ERα-ir and ERβ-ircells were detected on 2 kinds of bone cells: osteoblasts and osteocytes of both femur and lumbar (L5). SC = sham-operated group; OC = orchidectomized group; OE = orchidectomized rat receiving estradiol benzoate (EB) 2.5 µg/kgBW/day; OJ10 = orchidectomized rat receiving YCJ 10 mL/kgBW/day; OJ20 = orchidectomized rat receiving YCJ 20 mL/kgBW/day; Scale bar = 20 µm.

values increased when the ORX rats were treated with EB (OE group) (Fig. 4B, a-d). With YCJ treatments (OJ10, OJ20, and OJ40 groups), the numbers of the osteoblast- and osteocyte-reactive cells increased but not in a dose-related manner (Figs. 4B, b, c, d), except in osteoblasts of L5 (Fig. 4B, a). There was no significant difference in the number of ERβ–ir cells of the three OJ groups when compared to each other nor when compared with the control (NC, SC, OC, and OE) groups (Fig. 4B, a-d).

To find out if the numbers of ERα-, ERβ- osteoblasts and osteocytes correlated with serum E2 or serum testosterone (T), the number of ERα-, ERβ-cells were plotted against those of these serum sex hormone levels in the same animals, regardless of groups (Fig. 5, a-h).

DISCUSSION

The 3D reconstructions of the femur and L5 are presented in Figs. 1A and 1B. The Micro-CT scan image of the femur showed that the BMD of the OC group was less than the NC and SC groups, while those of the ORX groups given YCJ were not significantly different from the OC group. Comparison of other parameters of the femur e.g., BMD: % prevention and % change, Tb.N, Tb.Th, Tb.Sp of the YCJ and the controls (NC, SC, OE) groups showed no significant difference, except for the Conn.D and BV/TV parameters. The OC group showed significantly less Conn.D than the NC group, while the Conn.D of all YCJ treated groups showed no significant difference from the SC, NC or OE groups (Fig. 2C, b). These results agree with the results of the previous studies (Bouxsein et al., 2010; Kleerekoper et al., 1985; Parfitt, 1987) that trabecular bone Conn.D value is a better indicator of osteoporosis than bone density. The femur's BV/TV parameter of the OE group was significantly higher than that of the three OJ and the SC groups (Fig. 2C, e). This also agrees with Lindberg (2002), who found that the proximal tibia of seven-month-old ORX mice given 17β-estradiol benzoate 0.7 µg/day five days/week for three weeks has a significantly higher BV/TV value than that of the vehicle group. In addition, except for the

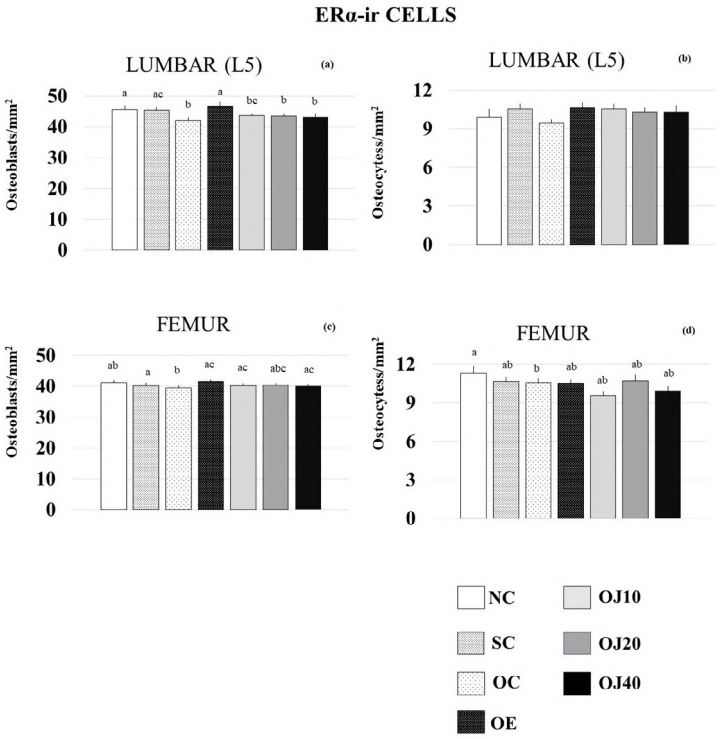

Fig. 4A.- The number of ERα-ir osteoblasts and osteocytes of the lumbar vertebra (L5) and the femur. Data expressed as mean ± SEM. Columns superscript with different letters are significantly different at $p < 0.05$. NC = baseline control group; SC = sham-operated group; OC = orchidectomized group; OE = orchidectomized rat receiving estradiol benzoate (EB) 2.5 µg/kgBW/day; OJ10 = orchidectomized rat receiving YCJ 10 mL/kgBW/day; OJ20 = orchidectomized rat receiving YCJ 20 mL/kgBW/day; OJ40 = orchidectomized rat receiving YCJ 40 mL/kgBW/day.

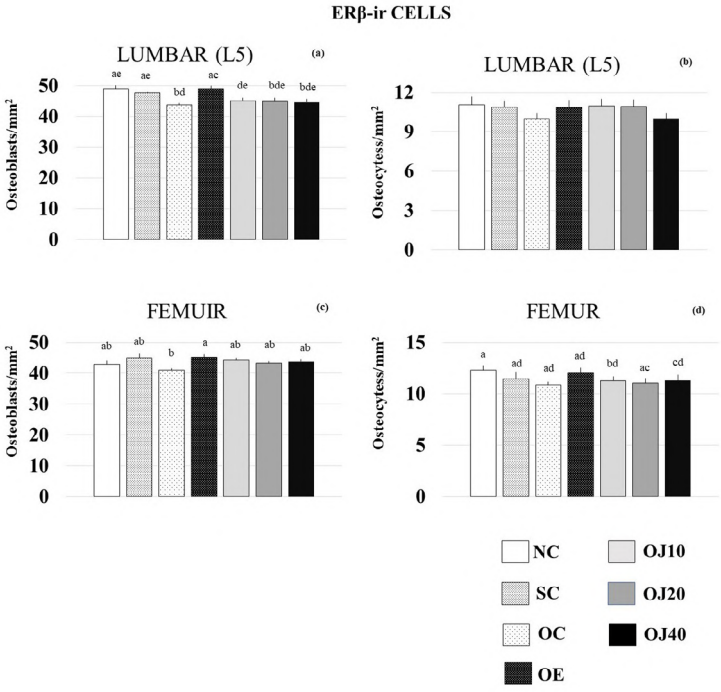

Fig. 4B.- The number of ERβ-ir osteoblasts and osteocytes of the lumbar vertebra(L5) and the femur. Data expressed as mean ± SEM. Columns superscript with different letters are significantly different at $p < 0.05$. NC = baseline control group; SC = sham-operated group; OC = orchidectomized group; OE = orchidectomized rat receiving estradiol benzoate (EB) 2.5 µg/kgBW/day; OJ10 = orchidectomized rat receiving YCJ 10 mL/kgBW/day; OJ20 = orchidectomized rat receiving YCJ 20 mL/kgBW/day; OJ40 = orchidectomized rat receiving YCJ 40 mL/kgBW/day.

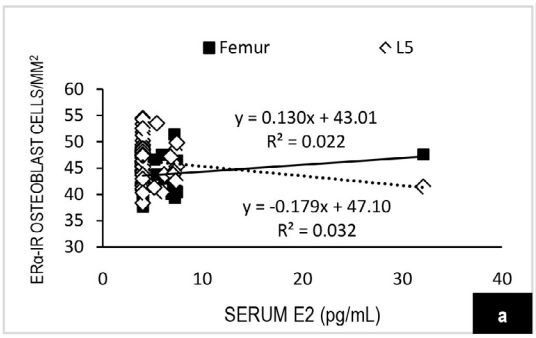

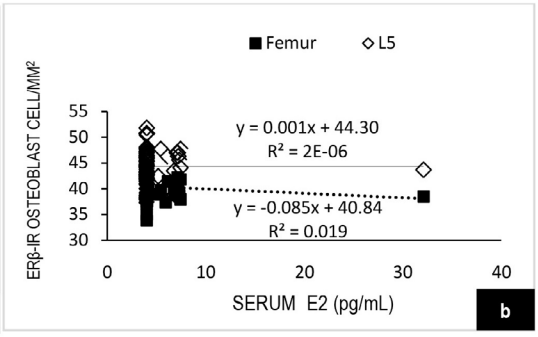

Femur (R^2 = 0.022, p-value = 0.22)

Lumbar (R^2 = 0.032, p-value = 0.14)

Femur (R^2 = 0.019, p-value = 0.26)

Lumbar (R^2 = 0.2^{-6}, p-value = 0.99)

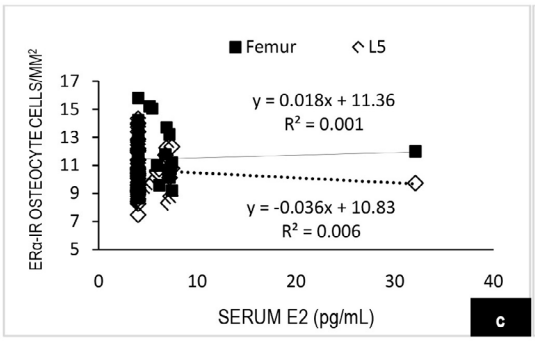

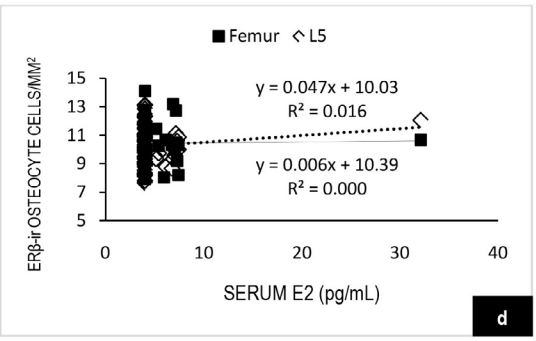

Femur (R^2 = 0.001, p-value = 0.99)

Lumbar (R^2 = 0.006, p-value = 0.51)

Femur (R^2 = 0.000, p-value = 0.89)

Lumbar (R^2 = 0.016, p-value = 0.30)

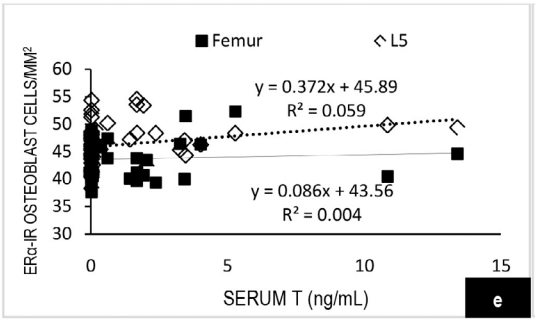

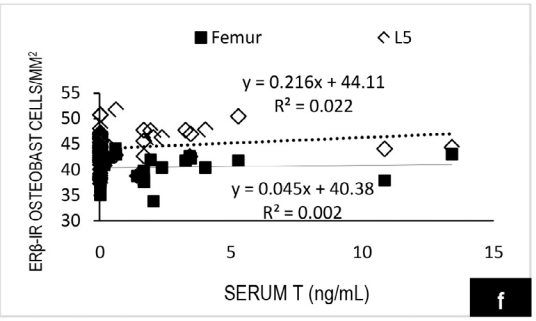

Femur (R^2 = 0.004, p-value = 0.60)

Lumbar (R^2 = 0.059, p-value = 0.05)

Femur (R^2 = 0.002, p-value = 0.69)

Lumbar (R^2 = 0.022, p-value = 0.22)

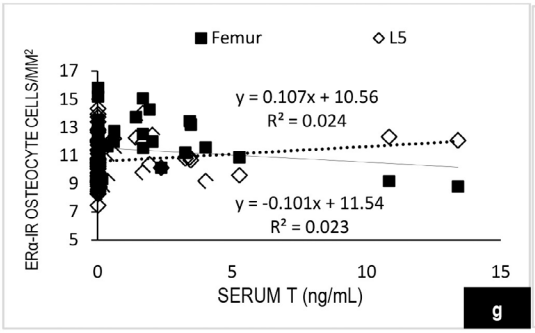

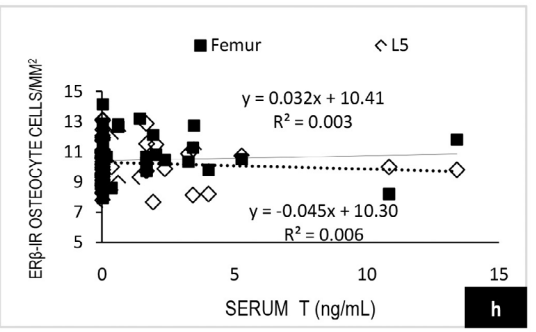

Femur (R^2 = 0.023, p-value = 0.22)

Lumbar (R^2 = 0.024, p-value = 0.20)

Femur (R^2 = 0.003, p-value = 0.63)

Lumbar (R^2 = 0.006, p-value = 0.52)

Fig. 5.- Plot of numbers of serum E2 level against ERα-ir osteoblast cells (a), ERβ-ir osteoblast cells (b), ERα-ir osteocyte cells (c), and ERβ-ir osteocyte cells (d); serum testosterone (T) level against ERα-ir osteoblast cells (e), ERβ-ir osteoblast cells (f), ERα-ir osteocyte cells (g), ERβ-ir osteocyte cells (h) from the same rats and from all animal groups.

OJ40 group, the percentage bone volume of ORX receiving YCJ, was not significantly different from all control (NC, SC, OE, and OC) groups. This result agrees with Ramli et al. (2012) that treated 10-12 months old Sprague Dawley rats *with Eurycoma longifolia* containing quassinoids phytoestrogen 90 mg/kg for six days. The treatment helped prevent bone density and volume loss at metaphysis of the distal femur of the ORX group, as shown by the insignificant difference in bone density from the sham group (Ramli et al., 2012).

In contrast, results from the Micro-CT scan of L5 indicated that there was no significant difference in all bone parameters, when the ORX groups given YCJ were compared with the control groups (Fig. 2B, a-h). Furthermore, femur % bone volume of OJ40 was significantly lower than that of the control (NC, SC, and OE) groups, but that of the OJ10 and OJ20 groups showed no significantly difference when compared with the same control groups. This indicated that YCJ is not a dose-related effect and is likely to have a SERM activity.

Several studies suggested that the Conn.D may be the parameter most affected by osteoporosis (Ramli et al., 2012). The present study demonstrated the ability of YCJ to help prevent volume loss of the femur by increasing its trabecular bone Conn.D, but not of the L5 vertebra. This is in agreement with Shaltiel et al. (2013), that reported estrogen deficiency triggering bone mass loss, causing osteoporosis by influencing vertebra less than femur and tibia. In addition, it was found that testosterone alone prevented the decline of the trabecular bone mass but not the cortical bone mass by dwindling osteoclastogenesis (Mohamad et al., 2016). Estrogen mediates androgen's bone-sparing effects only after its aromatization process. The gene expression and activity of aromatase have been indicated in male rodents and humans (Noirrit-Esclassan et al., 2021). Osteoporosis occurred in estrogen receptor-α knock-out and aromatase knock-out mice indicating that in bone, estrogen works through ERα (Noirrit-Esclassan et al., 2021). These previous studies support our current work. Furthermore, it was confirmed by immunohistochemistry study showing YCJ affecting cell number of ERα-osteoblasts in ORX+YCJ groups rather than ERα-osteocytes, and these results are obviously seen in femur rather than L5 (Fig. 4A, a-d). In contrast, either in femur or L5, immunoreactivity of ERβ-osteoblasts or osteocytes was not affected by YCJ treatments (Fig. 4B, a-d).

The regression correlation graphs (Fig. 5, a-h) between the numbers of ERα-osteoblasts and ERα-osteocytes with serum E2, or serum testosterone (T) indicated that the number of ERα-osteoblasts correlated with serum E2 and serum testosterone much more than ERα-osteocytes, and much more than ERβ-osteoblasts and osteocytes. Altogether, immunohistochemistry results and the regression correlation graphs confirmed that YCJ action was produced via ERα rather than ERβ and via osteoblasts rather than osteocytes. It is of interest to note that our result indicated that in bone tissue sections ERs staining occurred in cytoplasm and nucleus, consistent with ER mode of action, indicating the possibility of a non-genotropic pathway (Sonavane, 2022).

Estrogen plays a crucial part in male skeletal growth (Rochira et al., 2015). In this study, a dose of 2.5 µg/kg BW/day estradiol benzoate (EB) (OE group) that was intraperitoneally injected for three days a week preserved the trabecular bone. Even though some are not significantly different, the dose also countered ORX effects for all measured parameters, more than YCJ treatments. Previous studies showed that E2 is pro-osteoblastic that generate a net increase in bone-building process (Khalid and Krum, 2016), has an anti-apoptotic property in osteoblast, where ovariectomy prompts an increase in apoptosis of osteocyte and osteoblast (Rochira et al., 2015), and E2 also regulates the osteoblast anti-apoptotic protein Bcl2 (Komori, 2015; Pantschenko et al., 2005). Contrariwise, Kousteni et al. (2001) reported that E2 may inhibit dexamethasone, TNFα-induced apoptosis, or etoposide in osteoblasts. E2 also stimulates the transcription of alkaline phosphatase, a marker of osteoblast differentiation (Krum et al., 2008b). There are not many known direct targets of E2 in normal osteoblasts, and much less is reported on the targets of estrogen receptors, particularly ERβ (Farman, 2019; Khalid and Krum, 2016). Even at the physiological level of testosterone, low estrogen levels are associated with an in-

crease fracture risk in men. Therefore, although the mechanisms of osteoporotic fractures are multifactorial, estrogen deficiency plays crucial roles in the pathogenesis of osteoporosis in men and women (Khosla and Pacifici, 2021).

This study carried out immunohistochemical analyses to examine the part of estrogen receptors that facilitate osteogenic response to estrogen. The results revealed that osteoblasts and osteocytes expressed ERα and ERβ at significant quantities in the cancellous bone. These results agree with previous reports by (Khalid and Krum, 2016). These findings indicate a direct osteoblast ERα-dependent activation which contributes to bone formation induced by estrogen, was consistent with a report that estrogen has a direct action on osteoblasts in inhibiting their apoptosis (Rochira et al., 2015).

Several mechanisms contribute to the protective effects of E2 in bone. In the present study, speculatively, YCJ may induce osteoblast transcription of Fas Ligand (FasL) via ERα activation. FasL separates from the cell surface by MMP3, and this soluble FasL then stimulates osteoclast apoptosis (Garcia et al., 2013, Krum et al., 2008a). Another action is mediated by the suppression of osteoclasts involving the RANKL/(OPG) ratio regulation. Receptor activator of nuclear factor κB ligand (RANKL) is a crucial cytokine in osteoclast formation and differentiation processes, and in bone resorption activation and enhancement. Conversely, osteoprotegerin (OPG), a decoy receptor produced by osteoblastic lineage cells, counteracts RANKL thus, prevents bone loss. Therefore, the RANKL-OPG ratio is crucial for osteoclastogenesis. E2 has been indicated to escalate the transcription of OPG (Farman, 2019) and to influence RANKL positioning at the osteoblast surface (Martin et al., 2015). It was reported that in a human osteoblastic cell line, 17β-estradiol activates the ERα which in turn increases OPG mRNA levels and protein secretion (Jia et al., 2017). Windahl et al. (2013) found that in male mice osteocyte, ERα is essential for trabecular bone formation and therefore, trabecular bone volume. In the present study, however, it was found that YCJ affects the parameters tested with ERα-osteocytes were less than ERα-osteoblasts, either in femur or L5.

Our previous studies have shown that YCJ is likely to have acted as SERM. For example, flavonoids exist in most of the phytoestrogens with healing properties (Panche et al., 2016), and our previous studies found that YCJ accelerated wound healing (Radenahmad et al., 2012; 2015). Previous studies with the SERM and raloxifene prevented both postmenopausal and andropausal osteoporosis (Farman, 2019; Pankova and Tsvetkova, 2015; Zhou et al., 2021).

The results of body weights of rats in the same rat experiment groups were published by Balit et al. (2018). We found that after 10 weeks of ORX, the OE group's body weight on the day of termination was considerably lower than on the day of initiation (Table 2). These findings suggest that in the OE group, testosterone shortage after ORX and estrogen supplementation by injection with EB contributed to the weight loss. Pratchayasakul et al. (2011) reported that the body weight of both normal and high fat diet male mice treated with estrogen was considerably lower than the vehicle treatment group.

The body weight of all three OJ groups (OJ10, OJ20, and OJ40) was lower at the end of the experiment after force feeding with YCJ for 10 weeks compared with the onset albeit not statistically significant. YCJ might not influence the accumulation of fat in ORX rats, even though YCJ contains a high proportion of 44.9 percent glucose and 43.9 percent fructose (Santoso et al., 1995), these monosaccharides might have been converted to glycogen in the liver or fat in the body.

YCJ had no effects on male accessory organs, e.g., seminal vesicle, prostate gland, and have positive effects on serum cholesterol and mineral levels e.g., phosphorus, sodium, calcium, potassium, and magnesium; blood sugar, renal and liver function tests (Balit et al., 2018). Therefore, YCJ may also be a good selection for male osteoporosis therapy. In this study, however, YCJ mimicked the estrogen conserving effects but could not achieve the estrogenic level in all parameters. YCJ significantly preserved the microstructure of the osteoporotic bones, but this effect is not dose-related. It is interesting to see whether higher doses of YCJ would produce the same results as EB treatment.

YCJ contains various phytoestrogens, but has β-sitosterolis as its main component (58%). It also contains other sterols i.e., stigmastatrienol, stigmasterol, α-spinasterol, and fucosterol (Pungmatharith, 1988). As plant-derived estrogen, phytoestrogens possess different characteristics from estrogen but is like SERMs, having higher binding for ERβ (Pankova and Tsvetkova, 2015). The ERα is found predominantly in cortical bone, whereas ERβ in cancellous bone. In our study, preserving the effects of YCJ acts predominantly on ERα-osteoblasts. Therefore, the preventive effects for osteoporosis are not as straightforward as they should be. In addition, the lower doses (10, 20, 40 mL/kg BW) used in this study as well as in another study (Matsushita et al, 2017) using 15 mL/kg BW dose might account for the slight results compared with the apparent results of our previous studies at 100 mL/kg BW/day (Matsushita et al., 2017; Sayoh et al., 2008; Suwanpal et al., 2011). In bone, the function of ERβ in males is less than ERα, while in female ERβ controls ERα functions (Farman, 2019). Supplementation may prevent the periosteal apposition of cortical bone but not trabecular bone. Therefore, we speculate that YCJ supplementation reversed bone loss, possibly via ERα, not via ERβ, as speculated by Matsushita (2017). ERα is definitely the major core of estrogen osteoprotective actions, and ERβ is insufficient to compensate for ERα (Noirrit-Escalssan et al., 2021)

There have been many research works on molecular mechanisms of phytoestrogens in preventing osteoporosis. For example, Domazetovic et al. (2020) found that in humans, blueberry juice (BJ) protects osteoblast-like SaOS-2 cells from Runt-related transcription factor 2 and alkaline phosphatase as oxidative damage components associated with bone formation and remodeling. It did so by stimulating the expression a potential molecular target for anti-osteoporotic medicines, the sirtuin type 1 deacetylase. It has been suggested that blueberry polyphenols may be advantageous for bone regeneration because, TSP (total soluble polyphenols) quantitative studies revealed that BJ contains high bioavailability of anthocyanins having exceptional antioxidant properties (Domazetovic et al, 2020). Genistein, a type of isoflavone, enhances osteoprotegerin protein expression in bone-forming osteoblasts. This isoflavone facilitates osteoblastic differentiation and proliferation by inhibiting the transformation of a receptor activator of the nuclear factor-κB ligand (RANKL) into an osteoclast in bone marrow stem cells via the Wnt3a/beta-catenin signaling pathway (Hsiao et al., 2020; Kim, 2021; Yu et al., 2015). Astragalin (AG), also known as kaempferol-3-O-glucoside, enhances osteoblastic differentiation and bone formation through synergistic interactions that involve both BMP and MAPK pathways. BMP (bone morphogenetic protein) is a significant member of the TGF (transforming growth factor) family of proteins. MAPKs (mitogen-activated protein kinases) are a type of serine/threonine kinase that are involved in a variety of cellular processes include differentiation, proliferation, and inflammation (Liu et al. (2019). Whether YCJ action is the same as phytoestrogens' action mentioned above needs further verification in future studies. Further investigation is vital for a full comprehension on the impact of YCJ on osteogenic cells.

Since calcium is an essential mineral in bones, absorption of calcium in the intestine performs a significant part in calcium uptake into the body as facilitated by the essential function of vitamin D and by the work of calbindin, a calcium-binding protein (Wongdee et al., 2019). Our parallel work in the same rats with the same model and experimental design investigated CB, VDR, ERα and ERβ using immunohistochemistry techniques. We have found that exogenous estrogen (EB) and YCJ prevent osteoporosis by increasing CB-, VDR-, ERα- and ERβ-reactive cells in the gastrointestinal tract of orchidectomized rats (Hayeelateh et al., 2022). Therefore, estrogen/phytoestrogen-YCJ may influence calcium-binding protein, CB, and VDR cell production, resulting in bone calcium deposition by increasing ERα- and ERβ-reactive cell numbers, %bone volume, and other factors Micro-CT parameters in the femur and L5 vertebra as occurred in this study.

In summary, long-term YCJ consumption slightly improved indices of bone mass or bone histomorphometry in ORX rats, contending suggestion of the full benefits of YCJ for the prevention of os-

teoporosis in andropausal or aging men. Considering, however, the results of our previous studies (Suwanpal et al., 2011; Yusuh et al., 2010), YCJ may be beneficial in lessening bone loss in men at early andropause at a young age, which we hypothesize may delay the need and lessen the time duration of anti-apoptotic treatment as reported by Morii et al. (2015) and Matsushita et al. (2017) who worked on osteoporotic female rats.

CONCLUSION

YCJ had a noticeable effect and delayed the bone loss at trabecular structures associated with osteoporosis. Its effects, however, did not achieve the level of the estrogen-protective effect on the microfracture incidence, the basis of osteoporotic fractures. YCJ, nevertheless, may provide a potential male osteoporosis treatment, considering that the feminizing effects of estrogen do not counsel its use in males.

This study revealed that (1) EB injection at 2.5 µg/kg BW/day for three days per week is enough to restore all reactive cells as detected by anti-ERα- and anti-ERβ-ir antibodies and all parameters detected by Micro-CT scans. (2) YCJ treatment at various doses restored the declined numbers of ERα- and ERβ-ir cells caused by orchidectomy to normal in either L5 vertebra or femur. (3) Immunohistochemistry technique revealed that the effects of YCJ were comparable to EB treatment effects. In most cases, the optimal dose was 10 mL/kg BW/day for ERα- of both osteoblasts and osteocytes and 40 mL/kg BW/day for ERβ-of both osteoblasts and osteocytes. (4) YCJ action influenced via ERα rather than ERβ and osteoblasts rather than osteocytes. (5) Using Micro-CT scan, YCJ treatment, at the doses tested in this study, rebuilt the connectivity density and % bone volume of L5 vertebra and femur. These findings indicate that feeding YCJ might account for, at least in part, for a partial protective role of estrogen replacement in preventing or reducing the risk of osteoporosis in male rats.

ACKNOWLEDGEMENTS

Prince of Songkla University supported this study, grant no. SCI590730S. We thank technical support from the technicians of the Faculty of Dentistry, Prince of Songkla University.

REFERENCES

BALIT T, ASAE A, BOONYOUNG P, HIRANPHAN P, PANITYAKUL T, RADENAHMAD N (2018) Optimal dose and neuroprotective effects of prolonged treatment with young coconut juice in orchidectomized rats A preliminary study. *Songklanagarin J Sci Technol,* 404: 482-490.

BALIT T, ABDEL-WAHHAB AM, RADENAHMAD N (2019) Young coconut juice reduces histopathological changes associated with Alzheimer's disease through the modulation of estrogen receptors in orchidectomized rat brains. *J Aging Res*, 2019: 7416419.

BLOUIN S, LIBOUBAN H, MOREAU MF, CHAPPARD D (2008) Orchidectomy models of osteoporosis. *Osteoporosis: Methods Mol Biol*, 455: 125-134.

BOUXSEIN ML, BOYD SK, CHRISTIANSEN BA, GULDBERG RE, JEPSEN JK, MÜLLER R (2010) Guidelines for assessment of bone microstructure in rodents using Micro-computed tomography. *J Bone Miner Res,* 25(7): 1468-1486.

CAPOGROSSO P, SALONIA A, MONTORSI F (2021) Book chapter: Evaluation and nonsurgical management of benign prostatic hyperplasia. In: *Campbell-Walsh-Wein Urology*, 12nd ed. Elsevier, 145, 3343-3402.e11.

CHEN Z, WANG O, NIE M, ELISON K, ZHOU D, LI M, JIANG Y, XIA W, MENG X, CHEN S, XING X (2015) Aromatase deficiency in a Chinese adult man caused by novel compound heterozygous CYP19A1 mutations: Effects of estrogen replacement therapy on the bone, lipid, liver, and glucose metabolism. *Mol Cell Endocrinol,* 399: 32-42.

CHIN K-Y, IMA-NIRWANA S (2015) The effects of orchidectomy and supraphysiological testosterone administration on trabecular bone structure and gene expression in rats. *Aging Male,* 18(1): 60-66.

DOMAZETOVIC V, MARCUCI G, FALSETTI I, BILIA AR, VINCENZINI MT, BRANDI ML, IANTOMASI T (2020) Blueberry juice antioxidants protect osteogenic activity against oxidative stress and improve long-term activation of the mineralization process in human osteoblast-like SaOS-2 cells: involvement of SIRT1. *Antioxidants*, 9(2): 125.

DOMINGUEZ-LÓPEZ I, YAGO-ARAGÓN M, SALAS-HUETOS A, TRESSERRA-RIMBAU A, HURTADO-BARROSO S (2020) Effects of dietary phytoestrogens on hormones throughout a human lifespan: a review. *Nutrients,* 12: 2456.

EFFENDY NM, KHAMIS MF, SHUID AN (2013) Micro-CT assessments of potential anti-osteoporotic agents. *Curr Drug Targets,* 14(13): 1542-1551.

FARMAN H (2019) The role of estrogen receptor α in the regulation of bone mass. Department of Internal Medicine and Clinical Nutrition Institute of Medicine Sahlgrenska Academy, University of Gothenburg, Gothenburg, Sweden. ISBN 978-91-7833-251-9 (TRYCK).

GARCIA AJ, TOM C, GUEMES M, POLANCO G, MAYORGA ME, WEND K, MIRANDO-CARBONI GA, KRUM SA (2013) ER-alpha signaling regulates MMP3 expression to induce FasL cleavage and osteoclast apoptosis. *J Bone Miner Res,* 282: 283-290.

HAYEELATEH M, HUTAPEA AM**,** RADENAHMAD N (2022) Young coconut juice increased calbindin and vitamin D receptor cells via estrogen receptors in the gastrointestinal tract of male rats. *Eur J Anat*, 26(2): 199-216.

HSIAO YH, HO CT, PAN MH (2020) Bioavailability and health benefits of major isoflavone aglycones and their metabolites. *J Funct Foods,* 74: 104164.

JIA J, ZHOU H, ZENG X, FENG S (2017) Estrogen stimulates osteoprotegerin expression via the suppression of miR-145 expression in MG-63 cells. *Mol Med Rep,* 15: 1539-1546.

KALU DN (1991) The ovariectomized rat model of postmenopausal bone loss. *Bone Miner,* 15: 175-191.

KHALID AB, KRUM SA (2016) Estrogen receptors alpha and beta in bone. *Bone,* 187: 130-135.

KHOSLA S, PACIFICI R (2021) Estrogen deficiency and the pathogenesis of osteoporosis. In: *Marcus and Feldman's Osteoporosis (Fifth edition).* Vol. 1: 773-797.

KIM I-S (2021) Current perspectives on the beneficial effects of soybean isoflavones and their metabolites for humans. *Antioxidants*, *10*(7): 1064.

KLEEREKOPER M, VILLANUEVA AR, STANCIU J (1985) The role of three-dimensional trabecular microstructure in the pathogenesis of vertebral compression fractures. *Calci Tissue Int,* 376: 594-597.

KOMORI T (2015) Animal models for osteoporosis. *Eur J Pharmacol,* 759: 287-294.

KOUSTENI S, BELLIDO T, PLOTKIN LI, ÓBRIEN CA, BODENNER DL, HAN L, HAN K, DIGREGORIO GB, KATZENELLENBOGEN JA, KATZENELLENBOGEN BS, ROBERSON PK, WEINSTEIN RS, JILKA RL, MANOLAGAS SC (2001) Nongenotropic, sex-nonspecific signaling through the estrogen or androgen receptors: dissociation from transcriptional activity. *Cell,* 1045: 719-730.

KRUM SA, MIRANDO-CARBONI GA, HAUSCHKA PV, CARROLL JS, LANE TF, FREEDMAN LP, BROWN M (2008a) Estrogen protects bone by inducing Fas ligand in osteoblasts to regulate osteoclast survival. *Embo J,* 273: 535-545.

KRUM SA, MIRANDO-CARBONI GA, LUPIEN M, EECKHOUTE J, CARROLL JS, BROWN M (2008b) Unique ER {alpha} cistromes control cell type-specific gene regulation. *Mol Endocrinol,* 2211: 2393-2406.

LINDBERG MK, WEIHUA Z, ANDERSSON N, MOVERARE S, GAO H, VIDAL O, ERLANDSSON M, WINDAHL S, ANDERSSON G, LUBAHN DB, CARLSTEN H, DAHLMAN-WRIGHT K, GUSTAFSSON JA, OHLSSON C (2002) Estrogen receptors specify the effects of estrogen in ovariectomized mice. *J Endocrinol*, 174: 167-178.

LIU M, XU H, MA Y, CHENG J, HUA Z, HUANG G (2017) Osteoblasts proliferation and differentiation stimulating activities of the main components of *Epimedii folium*. *Pharmacogn Mag*, 13(49): 90-94.

MARTIN A, XIONG J, KOROMILA T, JI JS, CHANG S, SONG YS, MILLER JL, HAN CY, KOSTENUIK P, KRUM SA, CHIMGE NO, GABET Y, FRENKEL B (2015) Estrogens antagonize RUNX2-mediated osteoblast-driven osteoclastogenesis through regulating RANKL membrane association. *Bone,* 75: 96-104.

MATSUSHITA H, MINAMI A, KANAZAWA H, SUZUKI T, SUBHADHIRASAKUL S, WATANABE K, WAKATSUKI A (2017) Long-term supplementation with young coconut juice does not prevent bone loss but rather alleviates body weight gain in ovariectomized rats. *Biomed Rep*, 6: 585-591.

MOHAMAD N-V, SOELAIMAN I-N, CHIN K-Y (2016) A concise review of testosterone and bone health. *Clin Interv Aging,* 11: 1317-1324.

MOHAMAD N-V, ZULKEPLI MAAC, THESEIRA KM, ZULKIFLI N, SHAHROM NQ, RIDZUAN NAM, JAMIL NA, SOELAIMAN I-N, CHIN K-Y (2018) Establishing an animal model of secondary osteoporosis by using a gonadotropin-releasing hormone agonist. *Int J Med Sci,* 15(4): 300-308.

MORII Y, MATSUSHITA H, MINAMI A, KANAZAW H, SUZUKI, T, SUBHADHIRASAKUL S, WATANABE K, WAKATSUKI A (2015) Young coconut juice supplementation results in greater bone mass and bone formation indices in ovariectomized rats: A preliminary study. *Phytother Res,* 29: 1950-1995.

NOIRRIT-ESCLASSAN E, VALERA M-C, TREMOLLIERES F, ARNAL J-F, LENFANT F, FONTAIN C, VINEL A (2021) Critical role of estrogens on bone homeostasis in both male and female: From physiology to medical implications. *Int J Mol Sci,* 2021, 22(4): 1568.

PANCHE AN, DIWAN AD, CHANDRA SR (2016) Flavonoids: an overview. *J Nutr Sci,* 5(47): 1-15.

PANKOVA S, TSVETKOVA D (2015) Role of phytoestrogens in prevention of osteoporosis. *Int J Curr Pharm Res,* 7(2): 1-6.

PANTSCHENKO AG, ZHAN W, NAHOUNOU M, MCCARTHY MB, STOVER ML, LICHTLER AC, CLARK SH, GRONOWICZ GA (2005) Effects of osteoblast-targeted expression of BCL-2 in bone: differential response in male and female mice. *J Bone Miner Res,* 208: 1414-1429.

PARFITT AM (1987) Trabecular bone architecture in the pathogenesis and prevention of fracture. *Am J Med*, 821: 68-72.

PAYANGLEE K, HUTAPEA AM, RADENAHMAD N (2021) Young coconut juice prevents neuronal cell death via ChAT and NMDAR1 and estrogen receptors in the hippocampus and prefrontal cortex of ovariectomized rats. *Eur J Anat*, 254: 407-422.

PRATCHAYASAKUL W, CHATTIPAKORN N, CHATTIPAKORN SC (2011) Effects of estrogen in preventing neuronal insulin resistance in hippocampus of obese rats are different between genders. *Life Sci,* 89: 702-707.

PUNGHMATHARITH B (1988) Sex hormone-like substances in young coconut juice and their effects on uterine growth in rats. *Songklanagarin J Sci Technol,* 10: 221-226.

RADENAHMAD N, VONGVATCHARANON U, WITHYACHUMNARNKUL B, CONNO RJ (2006) Serum levels of 17β-estradiol in ovariectomized rats fed young-coconut juice and its effect on wound healing. *Songklanagarin J Sci Technol,* 285: 897-910.

RADENAHMAD N, SALEH F, SAWANGJAROEN K, RUNDORN W, WITHYACHUMNARNKUL B, CONNOR RJ (2009) Young coconut juice reduces histopathological changes in the brain that is induced by hormonal imbalance A possible implication to postmenopausal women. *Histol Histopathol: Cell Mol Biol,* 24(6): 667-674.

RADENAHMAD N, SALEH F, SAWANGJAROEN K, VONGVATCHARANON U, SUBHATHIRASAKUL P, RUNDORN W, WITHYACHUMNARNKUL B, CONNOR RJ (2010) Young coconut juice, a potential therapeutic agent that could significantly reverse some pathologies associated with Alzheimer's disease: novel findings. *Brit J Nutr*, 1055: 738-746.

RADENAHMAD N, SAYOH I, SALEH F, SAWANGJAROEN K, SUBHATHIRASAKUL P, BOONYOUNG P, RUNDORN W, MITRANUN W (2012) Young coconut juice can accelerate the healing process of cutaneous wounds. *BMC Compl Altern Med,* 12: 252.

RADENAHMAD N, BOONYOUNG P, KAMKAEW K, CHANCHULA K, KIRIRAT P (2014) Effects of young coconut juice on the number of argyrophil cells in the gastrointestinal tract of male rats Novel preliminary finding. *Songklanagarin J Sci Technol,* 366: 599-606.

RADENAHMAD N, SUWANSA-ARD S, SAYOH I (2015) Young coconut juice accelerated wound healing via downregulating macrophage migratory inhibitory factor MIF: Novel findings. *Songklanagarin J Sci Technol,* 374: 417-423.

RAMLI R, KHAMIS MF, SHUID N (2012) Bone micro-CT assessments in an orchidectomized rat model supplemented with *Eurycoma longifolia*. *Evid Based Complement Alternat Med,* 2012: 501858.

RIETJENS IMCM, LOUISSE J, BEEKMANN K (2017) The potential health effects of dietary phytoestrogens. *Br J Pharmacol,* 174(11): 1263-1280.

ROCHIRA V, KARA E, CARANI C (2015) The endocrine role of estrogens on human male skeleton. *Int J Endocrinol,* 2015, 15 pages, Article ID: 165215.

SANTOSO U, KUBO K, OTA T, TADOKORO T, MAEKAWA A (1995). Nutrient composition of *kopyor* coconuts (*Cocos nucifera* L.). *Food Chem,* 57: 299-304.

SAYOH I, RADENAHMAD N, KIRIRAT P, BOONYOUNG P, CHUNCHULA K, MITRANUN W (2008) Changes of argyrophil cells in gastrointestinal tract of ovariectomized rats fed with young coconut juice. *Malay J Microsc,* 4: 237-245.

SHALTIEL G, DAVID EB, MEIRONOE, WALTMAN E, SHECHTER A, AFLALO ED, STEPENSKY D, BERMAN A, MARTIN BR, WEAVER CM, SAGI A (2013) Bone loss prevention in ovariectomized rats using stable amorphous calcium carbonate. *Health,* 5: 18-29.

SHIGEHARA K, IZUMI K, KADONO Y, MIZOKAMI A (2021) Testosterone and bone health in men: A narrative review. *J Clin Med*, *10*(3): 530.

SONAVANE M (2022) Chapter 1: Classical and Non-Classical Estrogen Receptor Effects of Bisphenol A. In: *Bisphenol A: A Multi-modal Endocrine Disruptor*, pp 1-25.

SOZEN T, ÖZISIK L, BASAREAN NC (2017) An overview and management of osteoporosis. *Eur J Rheumatol*, 4(1): 46-56.

SUWANPAL P, RADENAHMAD N, YUSUH M, EKSOMTRAMATE M, RUANGSRI P, CHANTANASUKSILPA A (2011) Effects of young-coconut juice on increasing mandibular cancellous bone in orchidectomized rats: Preliminary novel findings. *Songklanagarin J Sci Technol,* 336: 617-623.

URASOPON N, HAMADA Y, ASAOKA K, CHERDSHEWASART W, MALAIVIJITNOND S (2007) *Pueraria Mirifica*, a phytoestrogen-rich herb, prevents bone loss in orchidectomized rats. *Maturitas*, 563: 322-331.

WINDAHL SH, BŐRJESSON AE, FARMAN HH, ENGDAHL C, MOVÉRARE-SKRTIC S, SJŐGREN K, LAGERQUIST MK, KINDBLOM JM, KOSKELA A, TUUKKANEN J, PAJEVIC PD, FENG JQ, DAHLMAN-WRIGHT K, ANTONSON P, GUSTAFSSON JÅ, OHLSSON C (2013) Estrogen receptor-α in osteocytes is important for trabecular bone formation in male mice. *Proc Natl Acad Sci USA*, 110(6): 2294-2299.

WONGDEE K, RODRAT M, TEERAPORNPUNTAKIT J, KRISHNAMARA N, CHAROENPHANDHU N (2019) Factors inhibiting intestinal calcium absorption: hormones and luminal factors that prevent excessive calcium uptake. *J Physiol Sci,* 69: 683-696.

YU F, LIU Z, TONG Z, ZHAO Z, LIANG H (2015) Soybean isoflavone treatment induces osteoblast differentiation and proliferation by regulating analysis of Wnt/beta-catenin pathway. *Gene,* 573: 273-277.

YUSUH M, PHOCHANUKOON N, RADENAHMAD N, EKSOMTRAMATE M, RUANGSRI P, CHANTANASUKSILPA A, REUNGCHAUMRATKUL A (2010) Changes of condyle cartilage in orchidectomized rats fed with young coconut juice: Novel preliminary findings. *Songklanagarin J Sci Technol,* 324: 333-339.

ZHOU L, WONG K-Y, YU W, POON CC-W, XIAO H, CHAN C-O, MOK DK-W, ZHANG Y, WONG M-S (2021) Selective estrogen receptor modulator-like activities of Herba epimedii extract and its interactions with Tamoxifen and Raloxifene in bone cells and tissues. *Front Pharmacol,* 11: 571598.

Examination of the cross-sectional area of the carpal tunnel on fetal cadavers

Mehtap Kondak[1], Merve Celep[2], Mehmet Haluk Uluutku[3]

[1] *Vocational School of Health Services, Avrasya University, Trabzon, Turkey*
[2] *Department of Anatomy, Health Sciences Institute, Karadeniz Technical University, Trabzon, Turkey*
[3] *Department of Anatomy, Faculty of Medicine, Uşak University, Uşak, Turkey*

SUMMARY

This study aimed to determine the anatomical features of the carpal tunnel (CT) in fetal cadavers and understand the role of etiology in the development of carpal tunnel syndrome (CTS). Seventy hand-wrist regions (35 right, 35 left) of 35 fetal cadavers (24 females; 11 males) that were not exposed to environmental factors and handedness were examined. The contents and cross-sectional area (CSA) of the CT were measured using ImageJ©. The CSA consisting of the flexor tendons and median nerve (MN) in the CT were calculated as a percentage. The results showed that the area covered by the MN and flexor tendons in the CT was significantly smaller in female fetuses ($P<0.05$). There was no significant difference in other ratios between male and female fetuses ($P>0.05$). There was no significant difference in the ratios regarding the CT and contents between the right and left-hand sides ($P>0.05$). It was concluded that the difference in CT anatomy may help explain the variations in the prevalence of CTS among genders. The lack of a difference between the right- and left-hand sides supports the theory that repetitive hand activities, hand dominance, and functional factors play a key role in the development of CTS by causing morphological changes in the CT, MN, and flexor tendons. In our opinion, the examination of CTs that have not been exposed to any environmental effects may provide guidance in understanding the effect of anatomical and morphometric features on the etiology of CTS.

Key words: Carpal tunnel syndrome – Hand – Median nerve – Mononeuropathy – Wrist

INTRODUCTION

The carpal tunnel (CT) is an osteofibrous tunnel which is located between the transverse carpal ligament and the carpal bones. Ten structures pass through the CT. These structures are the median nerve (MN), four tendons of the flexor digitorum superficialis (FDS), four tendons of the flexor digitorum profundus (FDP) and the tendon of the flexor pollicis longus (FPL) (Chammas et al., 2014; Rotman and Donovan, 2002). Carpal tunnel syndrome (CTS) develops due to the compression of the MN under the transverse carpal ligament while passing through the CT (Kim et al., 2013). The etiology of CTS is essentially idiopathic. It

Corresponding author:
Mehtap Kondak (MSc). Vocational School of Health Services, Avrasya University, Trabzon, Turkey. Contact address: Yalıncak District, Rize Street, No: 125/1, 61030, Ortahisar/Trabzon. Phone: +90 462 334 0550. E-mail: mehtap.kondak@avrasya.edu.tr - Orcid No: 0000-0001-9736-0640

Submitted: August 10, 2022. **Accepted:** February 25, 2023

https://doi.org/10.52083/BZOK4444

is also associated with abnormalities in the CT structures (carpal bone deformities, subluxation, distal radius fractures, wrist arthrosis, inflammatory arthritis, acromegaly, etc.). Other factors in the etiology are gender (female), obesity, diabetes mellitus, infection, vibration tools, burns, and hemophilia (Chammas et al., 2014; Newington et al., 2016).

The best-known parameters regarding CT morphometry relate to the cross-sectional area (CSA) of the CT and its contents. It has been shown that morphological changes in the CSA of the CT associated with overuse, profoundly affect the dominant hand (Dec and Zyluck, 2018; Lakshminarayanan et al., 2020; Newington et al., 2016). However, only a few studies have compared CT anatomy and morphometry by hand side. Earlier research has investigated the relationship between CT morphometry and gender. It has been reported that the CSA of the CT and its contents are smaller in women when compared to men (Bower et al., 2006; Pacek et al., 2010; Peterson et al., 2013).

When literature is examined, it can be seen that only a few studies have investigated the CT region in fetal cadavers. Some researchers have focused on the anatomy of the CT in adult cadavers. Adults are more likely to develop CTS as a result of morphological changes that occur in the CT, MN, and FTs due to exposure of environmental factors and overuse of the dominant hand (Bland, 2005; Loh et al., 2019; Marquardt et al., 2016). In the present study, the anatomy of the CT was examined more objectively, because it focused on fetal cadavers that were not exposed to environmental risk factors and handedness. The aim of this study was to determine the anatomical features of CT in fetal cadavers and clarify the role of CT anatomy in the development of CTS. Furthermore, it was planned to establish a basis for future studies by investigating the structure of the CT in the fetal period.

MATERIALS AND METHODS

The sample group consisted of 35 fetal cadavers (24 females; 11 males). The ages of the sample group were determined using the foot length method (Mercer et al., 1987), and it was determined that the fetal cadavers had an intrauterine age of 21.2 to 39.2 weeks. The cadavers were examined in the Anatomy Department of Karadeniz Technical University. The study was approved by a local ethics committee (Protocol number: 2018/72, Decision date: May 25, 2018) and was conducted in accordance with the ethical principles outlined by the Declaration of Helsinki. All cadavers had been embalmed in 10% formaldehyde solution. The upper extremities of the cadavers had no external pathology or anomaly. Gender was identified based on the external morphology of gonads. The cadavers were grouped according to their gender. Each cadaver was assigned a number.

The palmar faces of the wrist and hand were dissected using classical anatomical dissection methods. A consensus was reached on the dissection protocol. The same researcher performed all the dissection and subsequent procedures. All dissections were performed under a surgical microscope (Kaps [SOM]® 62, Asslar, Wetzlar, Germany). After removing the skin and subcutaneous adipose tissue, the transverse carpal ligament forming the roof of the CT was identified.

Following the dissection process, the wrists were cut proximal to the distal wrist fold and separated from the forearm. The hand samples were frozen at -18 °C. The proximal and distal borders of the transverse carpal ligament were determined by the insertions of the transverse fibers at the trapezium, hamate, scaphoid and pisiform. A single section, perpendicular to the CT short axis was obtained with a guillotine mechanism from the determined level. In each hand specimen, a single cut was made concerning a line parallel and equidistant from the proximal and distal borders of the transverse carpal ligament. Thus, all samples were equivalent (Fig. 1). All exposed sections were photographed at a 90° angle to the center of the CT. The images were recorded as the right and left-hand sides for each fetal cadaver.

The images were analyzed using ImageJ©, an image analysis program developed by US NIH Image. The program is Java-based, open-source, enables free ImageJ© software edits and analyzes images and measures area, distance, and angles. It can read many image formats, such as TIFF, GIF, JPEG, and DICOM (Schneider et al., 2012). The im-

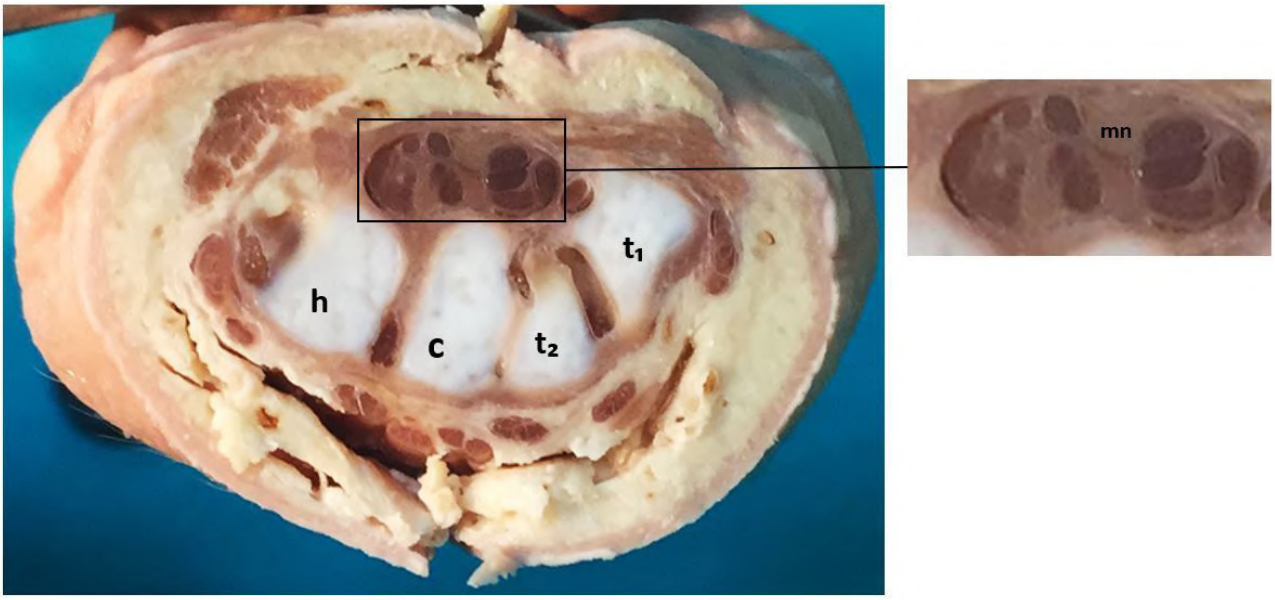

Fig. 1.- Transverse section of the carpal tunnel in a 38.4-week-old male fetus (t_1: trapezium, t_2: trapezoid, c: capitate, h: hamate, mn: median nerve).

ages used in this study were in JPEG format. All measurements were repeated three times by the same researcher.

The arithmetic mean was calculated and recorded as right and left-hand sides for each fetal cadaver.

First, the "Polygon Selection" tool was used to determine the boundaries of CT and MN. Second, the cross-sectional areas of CT and MN were calculated using the "Measure" tool (Fig. 2, Fig. 3).

The areas covered by the tendons were determined using the "Threshold" method to measure the CSAs of the flexor tendons. Calculations were made using the "Measure" tool. Thus, the CSAs of the FPL, FDS, and FDP tendons, and the total flexor tendons were determined (Fig. 4).

Fig. 2.- Determining the borders and measuring the CSA of the carpal tunnel by ImageJ.

Fig. 3.- Determining the borders and measuring the CSA of the median nerve by ImageJ.

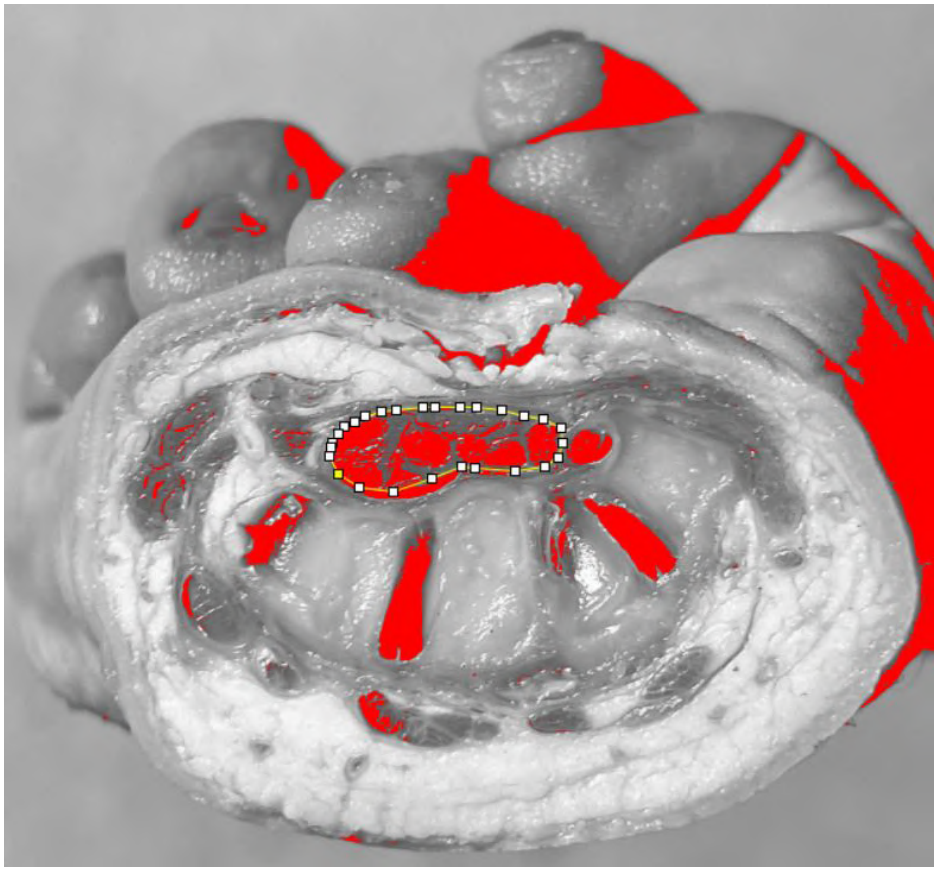

Fig. 4.- Determining and measuring the CSA covered by the all flexor tendons with ImageJ.

The height of the tunnel (CTH) was measured as the maximum length between the dorsal boundary of the transverse carpal ligament and the volar boundary of the capitate bone. The distance between these two points was calculated using the "Measure" tool. The maximum distance between the medial and lateral borders of the tunnel was calculated using the "Measure" tool to obtain the width of the tunnel (CTW).

Ratio calculations were made regarding the CSAs of the CT, MN, and flexor tendons. Thus, the percentage value of the area covered by the nerve and flexor tendons in the tunnel was obtained.

The ratio of the area covered by the MN in the CT (MN/CT) was calculated as follows:

$$MN / CT = CSA_{MN} / CSA_{CT} \times 100$$

The following equation was used to determine the ratio of the area covered by the FPL tendon (FPL/CT), FDS and FDP tendons (FDS.FDP/CT), and all flexor tendons (TFT/CT) in the CT:

$$TFT / CT = CSA_{FT} / CSA_{CT} \times 100$$

The ratio of the total area covered by the MN and all flexor tendons in the carpal tunnel (MN.TFT/CT) was calculated as follows:

$$MN.TFT / CT = MN / CT + TFT / CT$$

The ratio of the empty area outside the CT content (EA/CT) was calculated as follows:

$$EA / CT = 100 - MN.TFT / CT$$

The following equation was used to calculate the CT ratio (CTR):

$$CTR = CTH / CTW$$

The data were analyzed using the Statistical Package for Social Sciences (SPSS 23.0, IBM, Armonk, NY, United States of America) at a significance level of 0.05. Mean and standard deviation (SD) values were used for numerical variables. The Shapiro Wilk test was used for normality testing. The results showed that the data were normally distributed. The data were analyzed using a student's t-test.

RESULTS

This study examined 70 hand-wrist regions (35 right and 35 left) of 35 fetal cadavers. The ratios of the CSAs of the CT, MN and flexor tendons were calculated. The data were compared based on hand side and gender.

Table 1. Comparison of mean intrauterine ages by gender.

Gender		Intrauterine age (week)		
	n	**Min**	**Max**	**Mean±SD**
Female	24	21.2	39.2	27.68±4.59
Male	11	22.7	38.4	28.83±4.88
Total	35	21.2	39.2	28.04±4.64

Table 2. Comparison of ratio calculations by gender.

Ratio	Right Side (Mean±SD)			Left Side (Mean±SD)		
	Female (n=24)	**Male (n=11)**	**p**	**F (n=24)**	**M (n=11)**	**p**
MN/CT	7.401±1.775	8.100±1.938	0.301	7.470±1.756	7.500±1.759	0.963
FPL/CT	5.600±1.474	6.148±9.205	0.281	5.417±1.727	6.098±1.492	0.268
FDS.FDP/CT	37.761±6.558	42.627±9.205	0.082	39.030±6.315	39.196±7.673	0.946
TFT/CT	43.361±6.779	48.754±8.757	0.055	44.451±6.262	45.296±8.720	0.746
NM.TFT/CT	50.762±7.557	56.855±8.482	**0.041***	52.461±7.471	53.451±9.509	0.741
EA/CT	49.237±7.557	43.145±8.481	**0.041***	47.517±7.503	47.414±9.332	0.972
CTR	0.392±0.074	0.372±0.063	0.440	0.419±0.083	0.412±0.097	0.838

CT Carpal tunnel, *CSA* Cross-sectional area, *MN* Median nerve, *FDS* Flexor digitorum superficialis muscle, *FDP* Flexor digitorum profundus muscle, *FPL* Flexor pollicis longus muscle, *TFT* Total flexor tendons, *MN/CT* The proportional value of the CSA covered by the median nerve in the carpal tunnel FPL/CT: The proportional value of the CSA covered by the FPL tendon in the carpal tunnel, FDS.*FDP/CT* The proportional value of the CSA covered by the FDS and FDP tendons in the carpal tunnel, *TFT/CT* The proportional value of the total area covered by all flexor tendons in the carpal tunnel, *NM.TFT/CT* The proportional value of the total area covered by the carpal tunnel contents, *EA/CT* The proportional value of the empty area outside the carpal tunnel contents, *CTR* Carpal tunnel ratio. *p<0.05

There was no difference between intrauterine ages according to gender (p> 0.05) (Table 1). Male fetal cadavers had a significantly higher right MN.TFT/CT ratio than their female counterparts (p<0.05). Female fetal cadavers had a significantly higher right EA/CT ratio than their male counterparts (p<0.05). There was no significant difference in the other parameters between male and female fetal cadavers (p>0.05) (Table 2).

There were no significant differences in the ratios regarding the CT and its content between the right and left-hand sides (p>0.05) (Table 3).

DISCUSSION

Research shows that the CSA is an important morphological factor due to the area allocated to the contents of the carpal tunnel (Michelsen and Posner, 2002; Mitchell et al., 2009). It has been shown that the CSAs of the MN and flexor tendons (FTs) are greater larger in people with CTS and that the CSA of the CT, MN, and FTs is are associated with the compression of the MN in the tunnel (Lee et al., 2005; Li et al., 2011; Monagle et al., 1999). In this study the cross-sectional areas of the CT and its contents were measured. The cross-sectional areas covered by the flexor tendons and MN in the CT were calculated as a percentage. The data were compared according to hand side and gender.

Research shows that women are more likely to develop CTS due to smaller hand dimensions and CTs, hormonal factors, and pregnancy (Ablove and Ablove, 2009; Becker et al., 2002; Sassi and Giddins, 2016). Peterson et al. (2013) found that

Table 3. Comparison of ratio calculations by right and left-hand sides.

Ratio	Right Side (n=35)	Left Side (n=35)	
	Mean±SD	**Mean±SD**	**p**
MN/CT	7.621±1.829	7.479±1.731	0.740
FPL/CT	5.772±1.376	5.631±1.666	0.701
FDS.FDP/CT	39.290±7.698	39.082±6.665	0.904
TFT/CT	45.056±7.752	44.717±7.003	0.848
NM.TFT/CT	52.677±8.248	52.772±8.035	0.961
EA/CT	47.322±8.247	47.485±7.981	0.933
CTR	0.386±0.071	0.417±0.087	0.111

CT Carpal tunnel, *CSA* Cross-sectional area, *MN* Median nerve, *FDS* Flexor digitorum superficialis muscle, *FDP* Flexor digitorum profundus muscle, *FPL* Flexor pollicis longus muscle, *TFT* Total flexor tendons, *MN/CT* The proportional value of the CSA covered by the median nerve in the carpal tunnel FPL/CT: The proportional value of the CSA covered by the FPL tendon in the carpal tunnel, *FDS.FDP/CT* The proportional value of the CSA covered by the FDS and FDP tendons in the carpal tunnel, *TFT/CT* The proportional value of the total area covered by all flexor tendons in the carpal tunnel, *NM.TFT/CT* The proportional value of the total area covered by the carpal t

female cadavers had smaller CSA of the CT than male cadavers, whereas the latter had smaller CTR than the former. Lakshminarayanan et al. (2019) reported that the height of the carpal arch, and the CSA of the CT were smaller in women at both distal and proximal levels. They concluded that women had a smaller CTR distally, but there were no differences in CTR between men and women proximally. Pacek et al. (2010) examined fresh-frozen hand samples and determined that females had narrower and smaller CTs than their male counterparts. Bower et al. (2006) examined the CSAs of the CT and its contents in healthy individuals. They reported that compared to females, both the CT and its contents were larger in males. However, they found that there was no difference in the ratios between content and tunnel size. Our results showed that the area covered by the structures forming the contents of the CT (MN.TFT/CT) was significantly smaller in female fetuses than in male fetuses ($p<0.05$) (Table 2). This difference in the CT anatomy of fetal cadavers may help explain the variations in the prevalence of CTS among genders.

Zambelis et al. (2010) argue that hand dominance affects the risk for developing CTS and state that right-hand-dominant patients are five times as likely to develop CTS in their right hands, while left-hand-dominant patients are thirteen times as likely to develop CTS in their left hands. Furthermore, Thomsen et al. (2008) showed that CTS had a higher prevalence in the dominant hand. Cobb et al. (1997) calculated the ratio of the volume of the contents of the CT to the volume of the carpal tunnel. They found that this rate was higher in CTS. In another study examining CT and its content, it was seen that the CSA of the CT was not significantly different in individuals with CTS and healthy individuals. However, it was observed that the area covered by the content in the carpal tunnel increased in CTS patients (Oge et al., 2012). Tagliafico and Martinoli (2013) compared the CSA of the MN according to hand side in healthy individuals. They found that there were no differences in CSA of the MN between dominant and non-dominant hands. Asghar et al. (2022) reported that the CSA of the MN in healthy adults was not different according to hand side and hand dominance. Our results showed that the CSAs of the CT and its contents did not differ significantly between the right and left- hand sides ($p>0.05$) (Table 3). Although carpal tunnel syndrome is rarely seen in children, there is no fetal-period evidence that explains the presence of CTS in the dominant hand in adulthood. Druzhinin et al. (2019) examined the CSA of the MN in children. They found that there was no statistically significant difference between right and left sides. In another study measuring the CSA of the MN in children, it was reported that the CSA of the MN increased with age, but no comparison was made according to the hand side. (Cartwright et al., 2012). Given that intrauterine handedness does not affect the morphology of the tunnel, the present study examined the structure of the CT by eliminating the hand dominance fac-

tor. The lack of difference between the right and left-hand sides supports the theory that repetitive hand activities, hand dominance, and functional factors play a key role in the development of CTS by causing morphological changes in the CT, MN, and flexor tendons (Lakshminarayanan et al., 2020; Newington et al., 2016). The present study examined the morphometry of CT in the wrists of fetal cadavers, in relation to CTS which is associated with overuse in adulthood. In our opinion, the examination of CTs that have not been exposed to any environmental effects may provide guidance in understanding the effect of anatomical and morphometric features on the etiology of CTS.

ACKNOWLEDGEMENTS

The authors sincerely thank those who donated their bodies to science so that anatomical research and teaching could be performed. Results from such research can potentially increase scientific knowledge and can improve patient care. Therefore, these donors and their families deserve our highest respect.

REFERENCES

ABLOVE RH, ABLOVE TS (2009) Prevalence of carpal tunnel syndrome in pregnant women. *WMJ*, 108(4): 194-196.

ASGHAR A, NAAZ S, ANSARI S, KUMAR A, SINGH V (2022) The cross-sectional morphology of media nerve in carpal tunnel of healthy, adult population: A systematic review and meta-analysis. *Morphologie,* 107(356): 99-115.

BECKER J, NORA DB, GOMES I, STRINGARI FF, SEITENSUS R, PANOSSO JS, EHLERS JAC (2002) An evaluation of gender, obesity, age and diabetes mellitus as risk factors for carpal tunnel syndrome. *Clin Neurophysiol*, 113(9): 1429-1434.

BLAND JDP (2005) Carpal tunnel syndrome. *Curr Opin Neurol,* 15: 581-585.

BOWER JA, STANISZ GJ, KEIR PJ (2006) An MRI evaluation of carpal tunnel dimensions in healthy wrists: Implications for carpal tunnel syndrome. *Clin Biomech,* 21(8): 816-825.

CARTWRIGHT MS, MAYANS DR, GILLSON NA, GRIFFIN LP, WALKER FO (2012) Nerve cross-sectional area in extremes age. *Muscle Nerve,* 47(6): 890-893.

CHAMMAS M, BORETTO J, BURMANN LM, RAMOS RM, NETO DSFC, SILVA JB (2014) Carpal tunnel syndrome- Part I (anatomy, physiology, etiology and diagnosis). *Rev Bras Ortop,* 49(5): 429-436.

COBB TK, BOND JR, COONEY WP, METCALFF BJ (1997) Assessment of the ratio of carpal contents to carpal tunnel volume in patients with carpal tunnel syndrome: A preliminary report. *J Hand Surg Am,* 22(4): 635-639.

DRUZHININ D, NAUMOVA E, NIKITIN S (2019) Nerve ultrasound normal values in children and young adults. *Muscle Nerve,* 60(6): 757-761.

DEC P, ZYLUK A (2018) Bilateral carpal tunnel syndrome- A review. *Neurol Neurochir Pol*, 52(1): 79-83.

KIM HS, JOO SH, CHO HK, KIM YW (2013) Comparison of proximal and distal cross-sectional areas of the median nerve, carpal tunnel, and nerve/tunnel index in subjects with carpal tunnel syndrome. *Arch Phys Med Rehabil,* 94(11): 2151-2156.

LAKSHMINARAYANAN K, SHAH R, LI ZM (2019) Genders-related differences in carpal arch morphology. *PLoS One,* 14(5): e0217425.

LAKSHMINARAYANAN K, SHAH R, LI ZM (2020) Morphological and positional changes of the carpal arch and median nerve associated with wrist deviations. *Clin Biomech,* 71: 133-138.

LEE CH, KIM TK, YOON ES, DHONG ES (2005) Postoperative morphologic analysis of carpal tunnel syndrome using high-resolution ultrasonography. *Ann Plast Surg,* 54(2): 143-146.

LI ZM, MASTERS TL, MONDELLO TA (2011). Area and shape changes of the carpal tunnel in response to tunnel pressure. *J Orthop Res,* 29(12): 1951-1956.

LOH PY, YEOH WL, MURAKI S (2019) An overview of hand postures and aging on morphological changes of the median nerve. *J Physiol Anthropol,* 38(1): 9.

MARQUARDT TL, EVANS PJ, SEITZ WH, LI ZM (2016) Carpal arch and median nerve changes during radioulnar wrist compression in carpal tunnel syndrome patients. *J Orthop Res*, 34(7): 1234-1240.

MERCER BM, SKLAR S, SHARIATMADAR A, GILLIESON MS, D'ALTON ME (1987) Fetal foot length as a predictor of gestatioanal age. *Am J Obstet Gynecol,* 156(2): 350-355.

MICHELSEN H, POSNER MA (2002) Medical history of carpal tunnel syndrome. *Hand Clin,* 18(2): 257-268.

MITCHELL R, CHESNEY A, SEAL S, MCKNIGHT L, THOMA A (2009) Anatomical variations of the carpal tunnel structures. *Can J Plast Surg,* 17(3): e3-7.

MONAGLE K, DAI GU, CHU A, BURNHAM RS, SNYDER RE (1999) Quantitative MR imaging of carpal tunnel syndrome. *Am J Roentgenol,* 172(6):1581-1586.

NEWINGTON L, HARRIS EC, WALKER-BONE K (2016) Carpal tunnel syndrome and work. *Best Pract Res Clin Rheumatol,* 29(3): 440-453.

OGE HK, ACU B, GUCER T, YANIK T, SALVARLI S, MURAT MM (2012) Quantitative MRI analysis of idiopathic carpal tunnel syndrome. *Turk Neurosurg,* 22(6): 763-768.

PACEK CA, TANG J, GOITZ RJ, KAUFMANN RA, LI ZM (2010) Morphological analysis of the carpal tunnel. *Hand,* 5(1): 77-81.

PADUA L, CORACI D, ERRA C, PAZZAGLIA C, PAOLASSO I, LORETI C, CALIANDRO P, HOBSON-WEBB LD (2016) Carpal tunnel syndrome: clinical features, diagnosis, and management. *Lancet Neurol,* 15(12): 1273-1284.

PETERSON CA, WACKER CA, PHELAN TL, BLUME MK, TUCKER RP (2013) Anatomical differences in the shape of the male and female carpal tunnels. *J Women´s Health Physical Therapy,* 37(3): 108-112.

ROTMAN MB, DONOVAN JP (2002) Practical anatomy of the carpal tunnel. *Hand Clin*, 18(2): 219-230.

SASSI SA, GIDDINS G (2016) Gender differences in carpal tunnel relative cross-sectional area: A possible causative factor in idiopathic carpal tunnel syndrome. *J Hand Surg Eur Vol,* 41(6): 638-642.

SCHNEIDER CA, RASBAND WS, ELICEIRI KW (2012) NIH Image to ImageJ: 25 years of image analysis. *Nat Methods,* 9(7): 671-675.

TAGLIAFICO A, MARTINOLI C (2013) Reliability of side-to-side sonographic cross-sectional area measurements of upper extremity nerves in healthy volunteers. *J Ultrasound Med,* 32(3): 457-462.

THOMSEN JF, GERR F, ATROSHI I (2008) Carpal tunnel syndrome and the use of computer mouse and keyboard: A systematic review. *BMC Musculoskelet Disord,* 9: 134-143.

ZAMBELIS T, TSIVGOULIS G, KARANDREAS N (2010) Carpal tunnel syndrome: Associations between risk factors and laterality. *Eur Neurol,* 63(1): 43-47.

Lawsonia inermis and para-phenylenediamine exerts an insidious effect on the epidermal, renal, and hepatic tissue with repeated application: a histological and morphometrical study

Samuel E. Jen[1], Maimuna A. Adam[1], Sani H. Garba[1], Martha Orendu O. Attah[1,2], Nathan I. Dibal[1]

[1] *Department of Human Anatomy, Faculty of Basic Medical Sciences, University of Maiduguri, Borno State, Nigeria*
[2] *Faculty of Medicine, Cyprus International University, Nicosia, Cyprus*

SUMMARY

Ground leaves of *Lawsonia inermis* (LI) made into a paste has been used from the Bronze Age as cosmetic application. Para-Phenylenediamine (PPD) is an organic compound that is added to LI to increase its aesthetic appearance and longevity. Addition of PPD increases the possibility of allergic contact dermatitis from LI tattoo combinations, and may be absorbed through the skin, affecting body organs. The current study was conducted to determine the effect of this mixture on the histology of skin, liver and kidney tissue. Thirty albino rats were grouped into five groups. The treatment protocol included a control group (I), application of LI paste alone for a period of two weeks (II), and four weeks (III), and a combination of LI and PPD for two weeks (IV), and four weeks (V). All rats in each group had an area on the lumbar region shaved and marked, and the paste was applied to this region. The rats were sacrificed after the experimental period and the tissues of interest removed for further histological and morphometric analysis.

Application of LI alone caused no observable histological changes, however, in combination with PPD, LI caused thinning of the epidermis, reduction in the quantity of collagen fibers in the dermis, distorted the arrangement of hepatocytes, caused infiltration of inflammatory cells into the liver tissue and distortion in the arrangement of renal tubular epithelial cells. The longer the exposure to LI and PPD, the more alteration to the normal histology of tissues.

Key words: Lawsonia inermis – Renal – Dye – Henna – Epidermis – Hepatic

INTRODUCTION

Lawsonia inermis L. (LI) is a shrub from the family *Lythraceae,* also known with the following names: henna tree, Inai, hina, mignonette tree and Egyptian privet. It is used as a dye for coloring the epi-

Corresponding author:
Dr Martha Orendu Oche Attah. Department of Human Anatomy, Faculty of Basic Medical Sciences, University of Maiduguri, Borno State, Nigeria. Phone: +2348038135715. E-mail: marthaorendua@unimaid.edu.ng – Orcid no.: 0000-0002-3954-9186

Submitted: December 16, 2022. **Accepted:** February 25, 2023

https://doi.org/10.52083/HYKA4571

dermis of the hands, feet, hair, and fingernails, as well as fabrics—silk, wool, and leather (Ezzat et al., 2021). LI is one of the most important medicinal plants in use because of its medicinal and cosmetic properties. The plant has been present and used for several decades as drug, cosmetic and preservative in many cultures and tribes across the globe especially India and Africa (Ezzat et al., 2021; Aremu and Oridupa, 2022).

LI has been found to contain carbohydrates, phenolic, flavonoids, saponins, proteins, alkaloids, terpenoids, quinones, coumarins, xanthones, fat, resin and tannins (Aremu and Oridupa, 2022; Al-Snafi, 2019). Many phytochemicals including alkaloids, naphthoquinone derivatives, phenolics and flavonoids have been isolated from different components of LI. Pharmacological studies of the plant show that LI possesses antifungal (Rahmoun et al., 2013), antibacterial (Habbal et al., 2013), antiparasitic, molluscicidal, antioxidant, hepatoprotective, central nervous, analgesic, anti-inflammatory (Manuja et al., 2021), antipyretic, burn and wound healing, immunomodulatory, antiurolithiatic, antidiabetic, hypolipidemic, antiulcer, it is used as an antidiarrhoeal agent, diuretic, has been used as anticancer and has many other pharmacological effects (Aremu and Oridupa, 2022; Al-Snafi, 2019; Badoni et al., 2014). The antioxidant and anti-inflammatory properties of LI has been attributed to its phenolic and flavonoid contents (Rahmoun et al., 2013).

LI has been nominated in African alternate therapy and ayurvedic medicine as a purgative, abortifacient agent and astringent (Badoni et al., 2014). LI has also been reportedly used for some pharmacologic potentials, including its usage as pain reliever, anti-diabetic, hepatoprotective, immune booster, antioxidant, anticancer, anti-inflammatory and inhibitory action against several microbes (fungal, viral, trypanosome and plasmodium) (Al-Snafi, 2019; Manuja et al., 2021; Badoni et al., 2014; Khantamat et al., 2021). Biologically, it is also beneficial in the management of hair and scalp issues as well as in eye syndromes and hair loss (Ezzat et al., 2021).

The use of LI has been depicted in literary pieces and artwork indicating that LI has always played an important atomistic role in the everyday activities of many ancient cultures, supplying psychological and medicinal benefits, as well as being used for personal ornamentation and decoration (Habbal et al., 2013; Manuja et al., 2021). Although LI was historically applied to the hands and feet to protect against fungal pathogens and to hair to combat lice and dandruff, other traditional uses soon included the treatment of liver and digestive disorders, reduction of tissue loss in leprous individuals, and conditions like diabetic foot disorders and ulcers (Badoni et al., 2014). As indicated above, as many as 70 phenolic compounds were distilled and separated from various parts of the plant. Naphthaquinones, which include the dyeing component lawsone, have been connected to many of its pharmacological activities (Badoni et al., 2014; Khantamat et al., 2021).

The paste, decoction or infusion made from the leaves of LI has been used from the Bronze Age to dye skin, hairs and fingernails, especially at the times of festivals as a cosmetic application (Pradhan, 2012). In recent times, henna paste has been used for body art paintings and designs in many western countries. Henna application for cosmetic purposes is customary in the culture of Northern Nigeria, especially during celebratory occasions like weddings, naming ceremonies and religious festivals. Despite such widespread use in dyeing and body art painting, there has been many concerns about the use of the dye in combination with other substances, which makes the dye more pronounced with exposure to air. Para-phenylenediamine is one of such substances used in the manner described above.

Para-Phenylenediamine (PPD) is an organic compound, which appears as a white to purple crystalline solidified matter that turns purple-to-black color when exposed to air. When mixed with an oxidizer (typically hydrogen peroxide) and applied, it penetrates shafts of hair and changes into an oxidized form whose molecules are too large to 'escape', thus creating long-lasting color very effectively. There is no better chemical for the job.

On the flip side, is is highly allergenic, and potentially dangerous to those who have developed a sensitivity to it. There are 'milder' chemicals similar to PPD (other phenylenediamines or tol-

uenediamines), which are a little less allergenic, but these are not quite as effective. It is also toxic by skin absorption, inhalation or ingestion, and used for production of aramid fiber, antioxidants, as a laboratory reagent, in photographic developing, and as a dye for hair and furs (National Center for Biotechnology Information, 2022). Very often, PPD is added to LI paste to make the color appear darker and to speed up the dyeing process (Kang and Lee, 2006).

The addition of PPD to LI, which is a common practice, may produce a more aesthetic appearance, but it may also increase the risk of allergic contact dermatitis from LI tattoo combinations, and a number of cases have been reported (Kang and Lee, 2006; Calogiuri et al., 2010; Uzuner et al., 2009; Turan et al., 2003). Given the increasing popularity with use of IL for cosmetic purposes among teenagers and older individuals, coupled with dearth of information of the effect of these substances on the tissues of interest, this study was undertaken to determine the effect of this mixture on the histology of the skin, as well as the liver and kidney tissue.

The ensuring information obtained will serve as information on the effect of the paste on these tissues over a period of time.

MATERIALS AND METHODS

Collection and identification of plant

The leaves of LI and PPD were obtained from the central (Monday) market, Maiduguri Borno State, Nigeria. The plant was identified and authenticated by a Taxonomist at the Department of Biological Sciences, Faculty of Sciences, University of Maiduguri, Borno state, Nigeria. The leaves were identified and authenticated by a taxonomist from the Department of Biological Science. The plant sample was deposited at the herbarium of the Department of Human Anatomy with a voucher number UM/HAH/2021/006.

Preparation of plant extract

The powdered extract of the plant was obtained by shade-drying the leaves of LI, and then mechanically pulverizing the dried leaves to obtain the powdered product. This was then sieved by passing through a fine sifter to remove the larger particles. The fine powder was then weighed and collected into a dry container, and refrigerated prior to use.

Experimental animals and animal husbandry

Thirty (30) male albino rats weighing between 91 and 160 g were purchased from the Department of Human Physiology, University of Maiduguri for the experimental study. They were 4-to-5 months old at the period of the experimental study. The animals were kept in the animal house for a period of one week to acclimatize.

Their accommodation was well ventilated, and room temperature was maintained according to laboratory guidelines (20-26^{o}C/68-78.8^{o}F); the cages were kept in hygienic conditions and under a natural light (13 hours) and dark (11 hours) schedule. The rats were fed with standard rat chow and water *ad libitum*.

Experimental design

The thirty (30) male Wistar albino rats were assigned into five groups with six (6) animals each, using the block method to ensure an average weight of 135 g across each group.

Group I: Control group; nothing was applied to the skin of rats. Group II: 100 mg LI paste was applied once weekly for two weeks. Group III: 100 mg LI paste was applied once weekly for four weeks. Group IV: 100 mg LI paste + PPD was applied once weekly for two weeks. Group V: 100 mg LI paste + PPD was applied once weekly for four weeks.

Experimental procedure

All the rats in each group had an area on the lumbar region of the back shaved to expose the skin in this region. This was done using a pair of scissors to remove the surface hair. The hair that was not removed was cleared using shaving cream (Veet, Reckitt, Canada). This was removed by cleaning the surface of the shaved region repeatedly with alcohol solution to remove the residue shaving cream and also to sterilize the skin over this region. The shaved skin was closely observed for a period of two days to examine for inflammation

or rashes which would indicate a reaction to the shaving cream. None of these were observed on any of the shaved skin. The exposed skin was then marked to obtain a region with an area of 2x4 cm^2. This area was marked for application of the powdered extract as determined by the experimental design. Topical application of the extract was repeated every 7 days for rats in groups II and IV for two weeks, and every 7 days for 4 weeks for rats in groups III and V.

Animal sacrifice

The animals were humanely sacrificed after two weeks and four weeks respectively, by administrating ketamine hydrochloride injection (0.1 mg/kg) as anesthesia. This was given as an intramuscular injection on the left thigh of the rats in all groups. The shaved skin over the marked region to which the extract was applied was carefully dissected out by separating the epidermis from the subcutaneous tissue. A median incision along the abdomen of the rats provided access to the liver and the kidney tissue, which were quickly dissected, fixed and histologically processed for further observation to determine the effect of the extract on these tissues.

Tissue preparation

The skin, liver and kidney tissues were fixed for 24 hours to prevent autolysis and putrefaction. Thereafter, the tissues were trimmed and conveyed through a series of solvents as per schedule for dehydration, clearing and paraffin infiltration. The tissues underwent normal histological procedures, which included dehydration in ascending grades of alcohol (50, 70, 80, 95 and 100%), clearing using pure xylene, followed by impregnation in molten paraffin wax, and sectioning with a rotatory microtome. 5 µm sections were obtained and fixed on a clean albumenized surface of the slide of glass for Haematoxylin and Eosin staining.

Morphological studies and histological observation

The micrographs of the liver, kidney and skin tissues were observed under the microscope and areas of interest were measured using morphometric methods described by Attah et al., (2022). Images from the histological sections were produced using an Amscope light microscope (MB-JX-ISCOPE, Los Angeles, USA), to which a digital camera was attached (M500, X64, version 3.7). The images were photographed at using a magnification of X100 and X200. An ocular micrometer was previously standardized, and was also used to measure areas of interest in the histological slides for morphometric analyses also based on established methods described by Omar (2018; Zaki, (2015), and Attah et al., (2019). Morphometric analysis was performed using the computerized image analysis system, ImageJ 1.53a (Wayne Rasband, National Institutes of Health, USA).

The micrometer was used to calibrate the ImageJ application to establish the unit of measurement in micrometers (µm) instead of pixels. The micrometer used was the same objective and pixel resolution as that of the micrograph being examined.

The skin tissue was examined, and parts of the epidermis measured by using the free hand tool of imageJ application to determine the length of the various strata. Strata granulosum and basale were measured as a single unit, as they were not distinguishable in the micrograph. Stratum corneum and granulosa were measured as the distances form where the skin tissue originated to where each strata terminated. In the liver tissue, the width of the hepatocytes and sinusoidal spaces were measured for rats in each group. Each length was represented in µm.

Data from the above measurements were statistically analyzed using GraphPad Prism 8 software by using One-way Analysis of Variance (ANOVA) and expressed as mean ± SEM and percentage followed by Tukey Multiple Comparisons Test. $p<0.05$ was considered to be statistically significant.

Ethical considerations

The current research study was conducted in accordance with the University of Maiduguri Research and Ethical Committee guidelines, the ARRIVE guidelines (reporting of in vivo experiment), and the National Institutes of Health (NIH) guide for the CARE and use of laboratory animals (NIH Publications No. 8023, revised 1978). It was ap-

proved by the Ethical Committee of the Department of Human Anatomy, University of Maiduguri, on 21st March, 2021 with code number UM/HA/UGP 19.20-007.

RESULTS

The layers of the epidermis were individually measured starting with stratum corneum. The strata were found to be thickest in group I, with a mean length of 16.5 µm, which was statistically thicker when compared to other groups. The group with the thinnest stratum corneum was group V, with a mean thickness of 2.5 µm (Fig. 1). The length of stratum granulosum in all groups was significantly thicker in rats in group III, which had a mean thickness of 3.8 µm compared to the other groups. The mean thinnest stratum granulosum was also found in the rats in group V (0.7 µm) (Fig. 2).

Stratum spinosum and basale were measured together in all groups, as these strata were not distinguishable in all groups. Rats in group III had the thickest of these combined layers (14.5 µm), and this value was statistically significant when compared to the other groups (Fig. 3). The thinnest strata basale and spinosum were found in rats in group V (2.7 µm).

The hepatic sinusoids were widest in livers of rats in group II and this value was statistically significant when compared to the width of sinusoids in group V (Fig. 4). The thickness of the hepatocytes in all group was not significantly significant, however, the hepatocytes of the rats in group II showed the greatest thickness (6.7 µm) whereas the thickness in group IV was 5.4 µm (Fig. 5).

The skin in the control group showed the typical features present in skin tissue with the basal layer resting on the dermis, composed of simple columnar epithelium with their numerous nuclei, which appeared basophilic with prominent nucleoli. Stratum spinosum was eosinophilic and the cells were not easy to distinguish. Their nuclei were lighter in color compared to the nuclei found in stratum basale. Stratum granulosum was thick and compact across the skin tissue and stratum corneum was observed as sheets of tissue that sloughed from the surface of the skin. The dermis of the rats in this group was composed of numerous robust collagen fibers within which blood vessels could be observed (Fig. 6A).

The cells in stratum basale were not as prominent as observed in group I, and stratum spinosum consisted of cells with round and clear nuclei, and some cells had one or more nucleoli. The cytoplasm of the keratinocytes in this layer were eosinophilic. Stratum granulosum was broader and more distributed when compared to the strata in group I. Stratum corneum was sparse and the dermis had less robust collagen fibers (Fig. 6B).

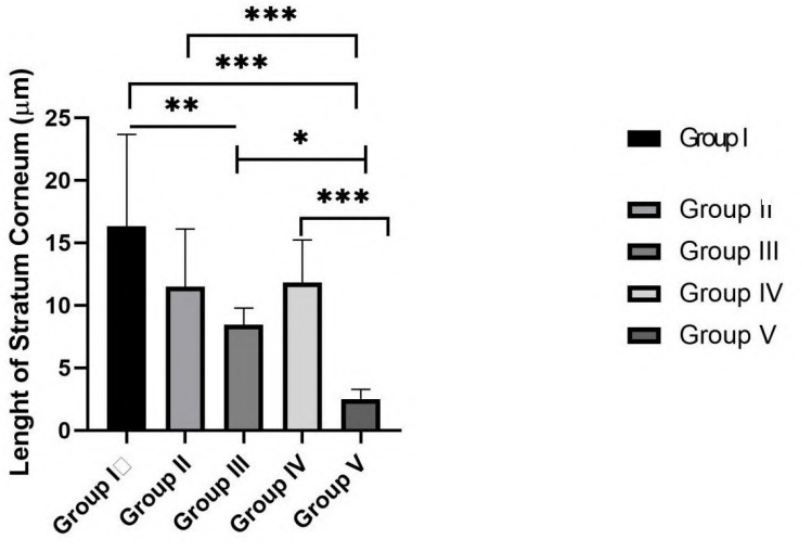

Fig. 1.- Length of stratum corneum in all groups (* - p<0.05, **p<0.01, ***-p<0.001, µm - micrometers, n=6, N=30).

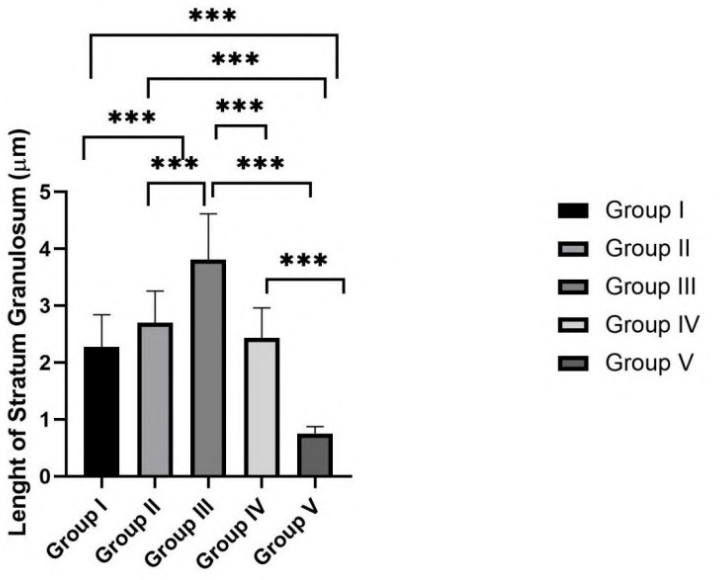

Fig. 2.- Length of stratum granulosum in all groups (* - p<0.05, **p<0.01, ***-p<0.001, µm - micrometers, n=6, N=30).

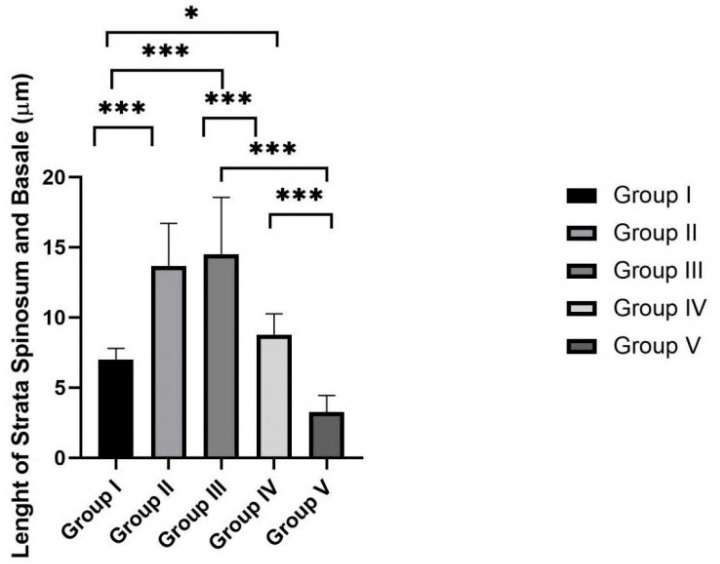

Fig. 3.- Length of strata spinosum and basale (* - p<0.05, **p<0.01, ***-p<0.001, µm - micrometers, n=6, N=30).

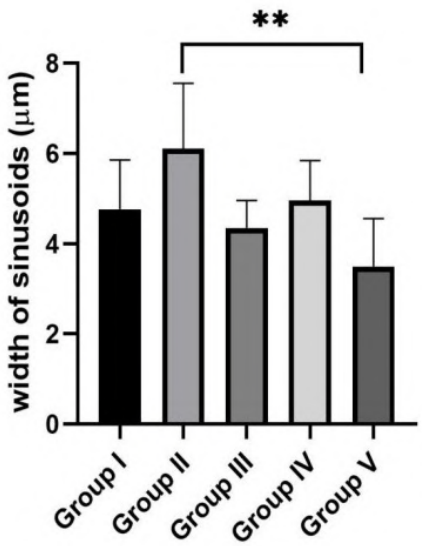

Fig. 4.- Width of sinusoids in all groups (* - p<0.05, **p<0.01, ***-p<0.001, µm - micrometers, n=6, N=30).

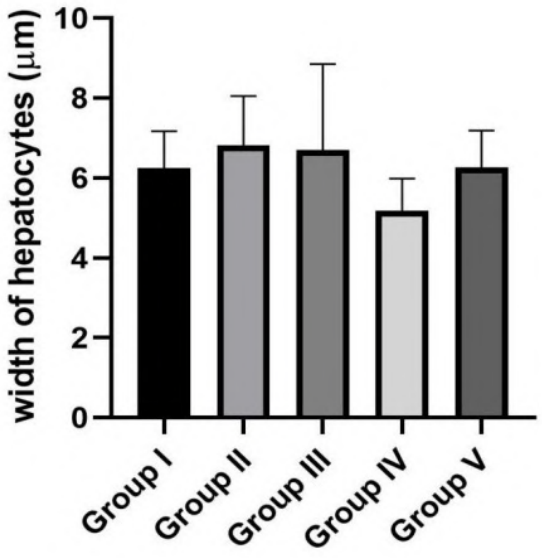

Fig. 5.- Width of hepatocytes in all groups (* - p<0.05, **p<0.01, ***-p<0.001, µm - micrometers, n=6, N=30).

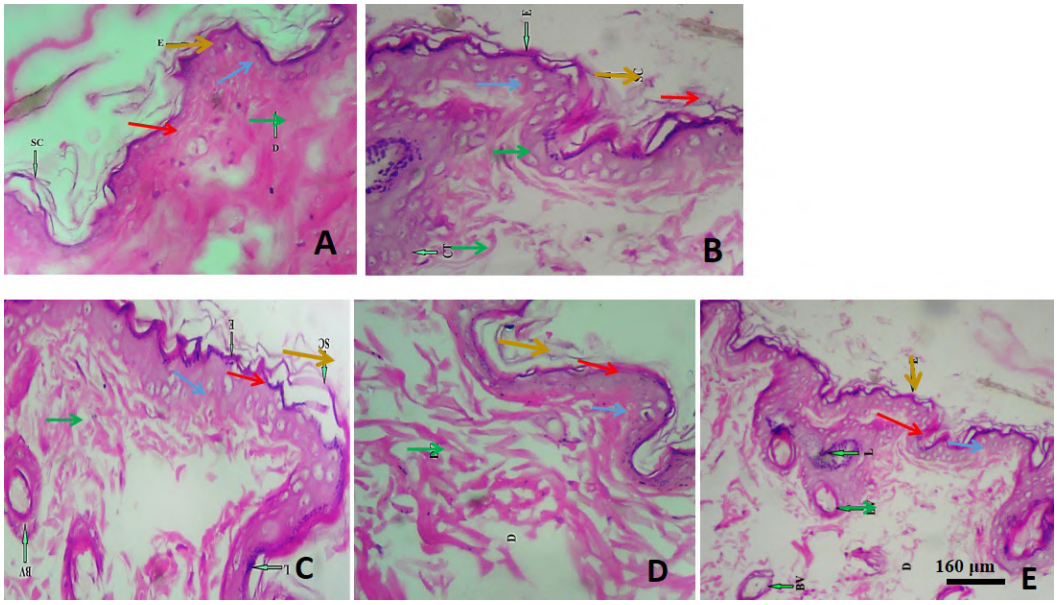

Fig. 6.- A-E: skin of the rats in the experimental groups (I-V) showing the epidermal layers and dermis: Stratum corneum SC (yellow arrow) which is mostly eroded in groups IV and V. Stratum granulosum (red arrow) is unaltered in all groups and stratum spinosum (blue arrow) was thinnest in group V. The dermis D (green arrow) in all experimental groups had blood vessels and collagen fibers. BV - blood vessel. H & E staining. Magnification = x200; Scale bar A-E = 160 µm.

The skin of the rats in group III showed similar appearance with rats in group II. However, stratum basale appeared sparser, stratum granulosum was more compact and continuous, and stratum corneum was relatively thicker. The blood vessels were more abundant in the dermis, and collagen fibers were sparsely arranged (Fig. 6C). Figure 6D represents the skin in rats in group IV, showing very thin strata spinosa and basale with very few keratinocytes present in these layers. Stratum granulosum was continuous over the surface of the skin, and stratum corneum was equally sparse. The dermis showed collagen fiber bundles which were loosely arranged.

The micrograph representing the skin of rats in group V showed a thinner epithelium with little defined stratum basale. Stratum spinosum was easier to distinguish and the keratinocyte nuclei

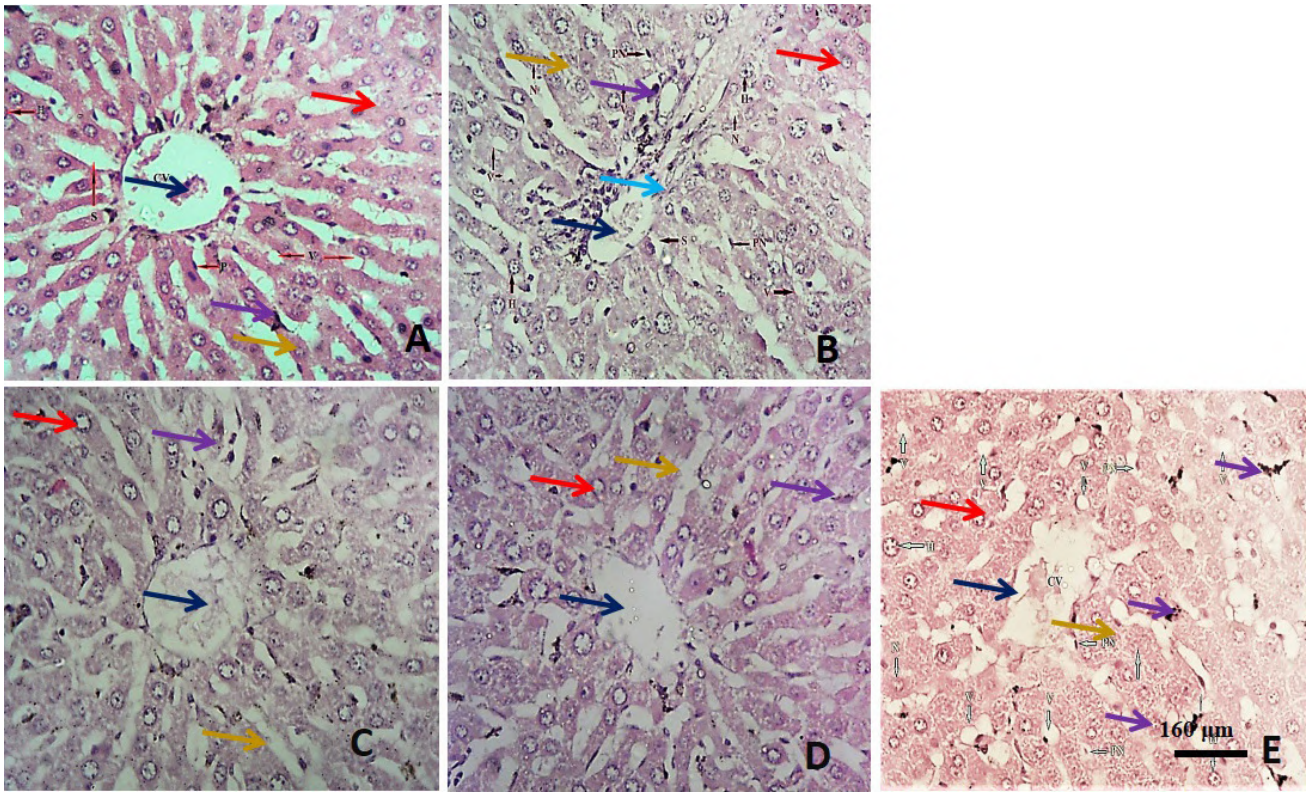

Fig. 7.- A-E: micrographs of the liver in groups I-V showing the central vein (navy arrow) surrounded by flat endothelial cells, the hepatocytes (red arrow) form columnar cords that radiate towards the central vein. This arrangement is more disorganized in group V. Sinusoids (yellow arrow) are found between the columnar cords. Kupffer cells (purple arrow) were more abundant in group IV and an aggregation of lymphocytes were found in the space surrounding the central vein in group II. H & E staining. Magnification = x200; Scale bar A-E = 160 µm.

were more clearly defined by their round and clear nuclei. Stratum granulosum was continuous and stratum corneum was barely observed. Numerous blood vessels were however found in the dermis, and very few collagen fibers were loosely arranged in the dermis (Fig. 6E).

Figures 7A-E show the liver tissue in all groups. Figure 7A showed the liver tissue in group I. The hepatocytes radiated towards the central vein separated by sinusoids. The cells had eosinophilic cytoplasm and prominent dark-staining, centrally located nuclei with 2-4 nucleoli (Fig. 7A). The liver tissue of rats in group II showed an aggregation of lymphoid/inflammatory cells around the central vein and pericentral regions, and several Kupffer cells located in the sinusoidal spaces. Lymphocytes are distinguished from the hepatocytes using H & E stains by observing their deep staining, prominent nucleus and a relatively small amount of agranular and poorly stained basophilic cytoplasm. These cells are easily differentiated from the histological appearance of hepatocytes, which are polygonal cells with abundant granular eosinophilic cytoplasm, centrally placed round/ovoid nuclei, and prominent nucleoli. The hepatocytes are also arranged in plates that are a single cell thick.

The hepatocytes were wider when compared to that in the rats in group I (Fig. 7B). The liver of rats in groups III and IV had identical histological structures with radiating hepatocytes and several ameboid-shaped Kupffer cells, which were easily identified by their ovoid, indented and/lobulated nuclei, and inflammatory cells found in the sinusoidal spaces attached to the sinusoidal endothelial cells (Figs. 7C and D). Figure 6E shows the liver tissue in group V. The hepatocytes appeared disorganized and the cytoplasm was granular in appearance, and the sinusoids appeared narrow and closely spaced compared to the other groups as was also observed in Fig. 4. The width of the sinusoid in groups II and VII appeared slightly wider when compared to the rats in groups III and V, who were exposed to the extract for a longer period of time.

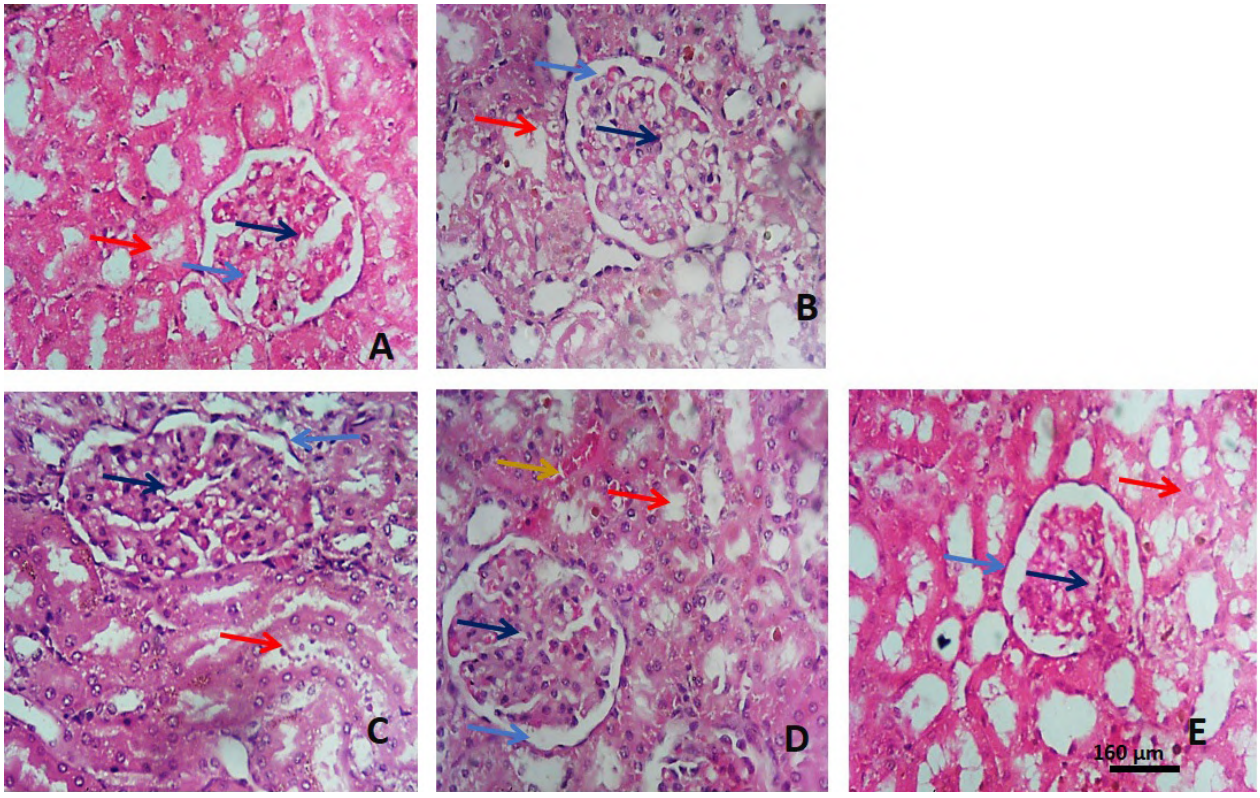

Fig. 8.- A-E: kidney tissue in groups I-V. The glomerulus in all groups were surrounded by Bowman's space and membrane (blue arrow). The renal tubules (red arrow) were dilated and distended in group V when compared to the other groups. There was a little interstitial bleeding (mustard arrow) in the renal parenchyma in group VI. H & E staining. Magnification = x200; Scale bar A-E = 160 µm.

Figures 8 A-E show the kidney tissue in all groups. Figure 8A shows the normal renal architecture showing the glomerulus surrounded by Bowman's capsule and space. The renal tubules contained simple cuboidal cells, and these had clear luminal spaces (Fig. 8A). The kidney tissue in groups II was similar to that found in the control group and the renal tissue showed similar histological arrangement (Fig. 8B). The kidney tissue in group III has dilated renal tubules (Fig. 8C), and in group IV there was some interstitial bleeding found in the renal parenchyma (Fig. 8D). The renal histology in group V showed slightly dilated renal tubules, which showed slight distortion in the arrangement of tubular lining cells (Fig. 8E).

DISCUSSION

Henna (LI) has been used aesthetically and as a medicament for more than 9,000 years, as documented by archaeological and anthropological evidence. These records indicate that henna traditions originated from early times in the Mediterranean, Nubia, Libya, Tunisia, Arabia, Assyria, Mesopotamia, Persia, and India (Othman et al., 2020).

A paste made of LI leaves is usually used for coloring the skin, hair and fingernails for cosmetic purposes. Henna body art is presently popular as adornment for weddings and other celebrations in India, South Asia, the Middle East and Africa (Aremu and Oridupa, 2022; Othman et al., 2020). The traditional use of LI as a natural dye seems not to exert toxic effects and appears biosecure (Khantamat et al., 2021). However, many times, the dye is mixed with PPD before use, and even though allergy to natural henna is not usual, the addition of PPD to the natural henna increases the risk of allergic contact dermatitis (Othman et al., 2020; Al-Suwaidi and Ahmed, 2010).

Hair removal in the current study was achieved by chemical methods by using creams also called depilatories, which are cosmetic preparations used to remove hair from the skin. They work by breaking down the sulphur bonds in the hair's keratin that are sensitive to strong alkaline and

deoxidation agents. The active ingredient for deoxidizing the sulphur bonds is a salt of thioglycolic acid (Tsai et al., 2021). Chemical depilation generally does not destroy the dermal papilla, and hair is able to grow back afterwards, because relatively small amounts of chemicals are used (Pohl et al, 2013). In the current study, the depilatory cream did not appear to affect the dermis and epidermis, as the cream was applied to the surface of the skin in all groups and the control group showed no adverse effect and the histological structures appeared intact.

Effect of LI paste on the histology of the skin

The use of LI paste in the current experimental study presented very little changes on the skin tissue when used alone. The strata of the skin showed similar appearance with the control group when only henna was used, and this is in agreement with many studies previously conducted (Aremu and Oridupa, 2022; Al-Snafi, 2019; Othman et al., 2020; Al-Suwaidi and Ahmed, 2010). However, the skin tissue that was treated with LI and PT showed a change in the skin architecture, as the thickness of the epidermal layer and quantity of collagen in the dermis was reduced in group V. In the current experimental study, no signs of allergy were observed with the use of LI and PPD over a period of time. Other researchers have reported allergic reactions on the skin following the use of LI and PPD (Kang and Lee, 2006; Calogiuri et al., 2010; Uzuner et al., 2009; Turan et al., 2003).

The effect of LI on the histology of the liver

There is adequate literature available to support the fact that substances applied to the epidermis can be easily absorbed through blood vessels in the dermis, which consequently affects other organs in the body, including the liver and kidney tissue (Feldmann and Maibachk, 1970; Franz, 1978). The liver tissue in the group treated with LI and PPD showed disorganization of the hepatic tissue. This result is similar to studies carried out by Eissa et al. (2021), and Lee et al. (2015), where it is discovered that PPD induced allergic activity and increased the probability of tumors in the kidney, liver, thyroid gland and urinary bladder, although its effect on dermal papilla cells remained to be clarified. PPD was also found to induce several cytotoxic effects through modification of miRNA expression levels (Lee et al., 2015).

The effect of LI on the histology of the kidney

The kidney tissue showed slight distortion of the arrangement of renal tubular cuboidal epithelium in the group that was exposed to LI and PPD for a period of 4 weeks. This agrees with studies carried out by Eissa et al. (2021), Lee et al. (2015), and Devecioğlu et al. (2001), which found that kidney parts of the PPD-poisoned victims had regions exhibiting extreme tubular necrosis. In addition, there were cellular ghosts that had lost cellular information and sloughed into the luminal cavity, which was not observed in the same study. In addition, Ibrahim et al. (2006) demonstrated a distortion of the lobular structure of the kidney, accompanied with the thickening of the Bowman capsule of the kidney.

In the current study, the period of exposure to LI and PPD was proportional to the alteration of tissue, as most changes to skin, hepatic and renal tissue were observed in rats in group V. This also agrees with research carried out by Eissa et al. (2021), who determined that, with time, more absorption through the skin occurs, and PPD appeared in the urine samples of subjects exposed to PPD and LI, and the quantities found were directly proportional to the period of use and dermal exposure, which led to noticeable effects in the morphology and number of blood cells and extended to renal and liver functions.

CONCLUSION

In the current study, LI and PPD were applied topically to the skin over a period of time to determine its effect on the epidermal, dermal, renal, and hepatic tissues. LI was first applied alone before a mixture of LI and PPD were applied. At the end of the experimental period, the authors determined that application of LI alone did not cause a lot of changes to the histological architecture of the organs listed. However, in combination with PPD, LI caused a thinning of the epidermis, and reduction in the quantity of collagen fibers in the dermis. It also caused distortion in the arrangement of hepatocytes and caused infiltration

of inflammatory cells in the liver tissue, as well as distortion in the arrangement of renal tubular epithelial cells. More study is recommended to test the effect of the combination of LI and PPD on these tissues over a longer period of time and on other tissues. Also, serum markers of liver function and urinalysis should be tested to observe the effect of the extract on the function of the kidney and liver. Other staining techniques aside from H and E should be performed to confirm an increase in collagen fibre and immune cell infiltration.

ACKNOWLEDGEMENTS

The authors acknowledge the administrative contributions of Dr. J.V. Zirahei, Dr. H.B. Ishaya, Dr. L.P. Mshelia, Dr. M.S. Chiroma, Dr. N.I. Dibal and all staff of the Department of Human Anatomy, University of Maiduguri for emotional and moral support. Profound gratitude goes to the Staff of the Histology Laboratory, University of Maiduguri for their support and help.

AUTHOR'S CONTRIBUTIONS

Conceptualization: SEJ, MAA, SHG and MOOA, Acquisition and design: SEJ, MAA, and SHG, Methodology: SEJ, MAA, SHG and MOOA, Administrative support/Supervision: SHG and MOOA Provision of study materials: SEJ, MAA, and SHG Data collection and assembly: SEJ, MAA, SHG and MOOA Data analysis and interpretation: SEJ, MAA, SHG and MOOA Funding Acquisition: SEJ, MAA, SHG and MOOA Writing: Review and Editing: SEJ, MAA, SHG and MOOA Final approval of manuscript: SEJ, MAA, SHG and MOOA.

REFERENCES

AL-SNAFI A (2019) A review on *Lawsonia Inermis*: a potential medicinal plant. *Int J Curr Pharmaceut Res,* 11: 1-13.

AL-SUWAIDI A, AHMED H (2010) Determination of para-phenylenediamine (PPD) in henna in the United Arab Emirates. *Int J Environ Res Public Health,* 7(4): 1681-1693.

AREMU A, ORIDUPA A (2022) Lawsonia inermis Linn; review of plant with both industrial and medicinal properties. *Media Kedokteran Hewan,* 33: 105-130.

ATTAH MO, JACKS TW, GARBA SH, ISHAYA HB (2019) Histological and morphometric assessment of cutaneous wound healing in streptozotocin-induced diabetic rats treated with n-hexane extract of Leptadenia hastata. *J Exp Clin Anat,* 18: 19-29.

ATTAH MOO, JACKS TW, GARBA SH (2022) A potential treatment strategy for the treatment of diabetic kidney disease in streptozotocin-induced diabetic rats: *Leptadenia Hastata* extract. *Iran J Toxicol,* 16(3): 175-184.

BADONI SR, SEMWAL DK, COMBRINCK S, CARTWRIGHT-JONES C, VILJOEN A (2014) Lawsonia inermis L. (henna): ethnobotanical, phytochemical and pharmacological aspects. *J Ethnopharmacol,* 155(1): 80-103.

CALOGIURI G, FOTI C, BONAMONTE D, NETTIS E, MURATORE L, ANGELINI G (2010) Allergic reactions to henna-based temporary tattoos and their components. *Immunopharmacol Immunotoxicol,* 32(4): 700-704.

DEVECIOĞLU C, KATAR S, DOĞRU O, TAŞ MA (2001) Henna-induced hemolytic anemia and acute renal failure. *Turk J Pediatr.* 43(1): 65-66.

EISSA UB, KHOGALI F, MOHAMED EE, OSMAN EE, ELMAHI OM, WAGGIALLAH HA (2021) The potential effect of Henna (Stone Dye) extract paraphenylenediamine on human blood cells, live rand renal function. *J Pharmaceut Res Int,* 33(60B): 192-200.

EZZAT SM, EL BISHBISHY MH, EL KERSH DM, ZAYED A, SALEM MA, SALAMA MM (2021) Preparation of phytopharmaceuticals for the management of disorders. Academic Press, pp 129-168.

FELDMANN RJ, MAIBACH HI (1970) Absorption of some organic compounds through the skin in man. *J Invest Dermatol,* 54(5): 399-404.

FRANZ TJ (1978) The finite dose technique as a valid in vitro model for the study of percutaneous absorption in man. *Curr Probl Dermatol,* 7: 58-68.

HABBAL O, HASSON SS, EL-HAG AH, AL-MAHROOQI Z, AL-HASHMI N, AL-BIMANI Z, AL-BALUSHI MS, AL-JABRI AA (2011) Antibacterial activity of Lawsonia inermis Linn (Henna) against Pseudomonas aeruginosa. *Asian Pac J Trop Biomed,* 1(3): 173-176.

IBRAHIM AB, AFIFI HA, ABASS WH, HAMOUDASY, GAWISH ES (2006) Fatal PPD hair dye intoxication among autopsy cases referred to Medico logical Department from some Upper Egypt Governorates (Doctoral dissertation, MSC Thesis).

KANG IJ, LEE MH (2006) Quantification of para-phenylenediamine and heavy metals in henna dye. *Contact Dermatitis*, 55(1): 26-29.

KHANTAMAT O, DUKAEW N, KARINCHAI J, CHEWONARIN T, PITCHAKARN P, TEMVIRIYANUKUL P (2021) Safety and bioactivity assessment of aqueous extract of Thai Henna (Lawsonia inermis Linn.) leaf. *J Toxicol Environ Health A,* 84(7): 298-312.

LEE OK, CHA HJ, LEE MJ, LIM KM, JUNG JW, AHN KJ, AN IS, AN S, BAE S (2015) Implication of microRNA regulation in para-phenylenediamine-induced cell death and senescence in normal human hair dermal papilla cells. *Mol Med Rep,* 12(1): 921-936.

MANUJA A, RATHORE N, CHOUDHARY S, KUMAR B (2021) Phytochemical screening, cytotoxicity and anti-inflammatory activities of the leaf extracts from Lawsonia inermis of Indian origin to explore their potential for medicinal uses. *Med Chem,* 17(6): 576-586.

NATIONAL CENTER FOR BIOTECHNOLOGY INFORMATION (2022) PubChem Compound Summary for CID 7814, p-Phenylenediamine. Retrieved July 21, 2022, from https://pubchem.ncbi.nlm.nih.gov/compound/p-Phenylenediamine.

OMAR SM (2010) Effect of chromium picolinate on histological skin alterations of streptozotocin diabetic rats, a light and electron microscopic study. *Egypt J Histol,* 33(1): 178-191.

OTHMAN MR, AHMAD K, OTHMAN R, AWANG K, YUSOFF Z (2020) Use of Henna in the Malay World: from traditional uses to scientific approaches. T ibb Nabawi on Nature-Based Products, University of Malaya Press, Kuala Lumpur, pp 99-114.

POHL S, VARCO J, WALLACE P, WOLFRAM LJ (2013) Hair preparations. In: Othmer K (ed). *Kirk-Othmer chemical technology of cosmetics*. 5th ed. John Wiley & Sons, Hoboken (NJ), pp 85-122.

PRADHAN R, DANDAWATE P, VYAS A, PADHYE S, BIERSACK B, SCHOBERT R, AHMAD A, SARKAR FH (2012) From body art to anticancer activities: perspectives on medicinal properties of henna. *Curr Drug Targets,* 13(14): 1777-1798.

RAHMOUN N, BOUCHERIT-OTMANI Z, BOUCHERIT K, BENABDALLAH M, CHOUKCHOU-BRAHAM N (2013) Antifungal activity of the Algerian Lawsonia inermis (henna). *Pharm Biol*, 51(1): 131-135.

TSAI PF, CHOU FP, YU TS, LEE HJ, CHIU CT (2021) Depilatory creams increase the number of hair follicles, and dermal fibroblasts expressing

interleukin-6, tumor necrosis factor-α, and tumor necrosis factor-β in mouse skin. *Korean J Physiol Pharmacol*, 25(6): 497-506.

TURAN H, OKUR M, KAYA E, GUN E, ALIAGAOGLU C (2013) Allergic contact dermatitis to para-phenylenediamine in a tattoo: a case report. *Cutan Ocul Toxicol,* 32(2): 185-187.

UZUNER N, OLMEZ D, BABAYIGIT A, VAYVADA O (2009) Contact dermatitis with henna tattoo. *Indian Pediatr,* 46(5): 423-424.

ZAKI SM (2015) Characteristics of the skin of the female albino rats in different ages: Histological, morphometric and electron microscopic study. *J Cytol Histol,* S3: 4.

Measuring low formaldehyde exposure values in the dissection hall after embalming human body donors with ethanol-based fixation methods

Anke Schnapper-Isl[1], Frank Klose[2], Andreas Schmiedl[1]

[1] *Institute of Functional and Applied Anatomy, Hannover Medical School, Hannover, Germany*
[2] *TÜV Nord Umweltschutz GmbH & Co. KG, Hannover, Germany*

SUMMARY

The dissection course plays a central role in teaching anatomy and body donors are also needed in clinical-anatomical courses. In order to reduce formaldehyde exposure of students, participants and staff during these courses, we employed fixation solutions with low formaldehyde content. In this study, we present two ethanol-based protocols, and elucidate their suitability for the dissection process and compliance with occupational exposure limits for formaldehyde and other hazardous substances.

Body donors were fixed according to an ethanol-based fixation protocol for the dissection course or an ethanol-glycerin-based fixation protocol for specialist training courses. The quality of fixation was determined during the dissection process. Exposure to hazardous substances (formaldehyde, ethanol, 2-phenoxyethanol) was measured in a regular dissection course setting at different locations (room-related and person-related measurements), and exposure indices were calculated.

The quality of fixation of both methods was good and fulfilled all requirements of the student dissection course and the specialist training courses, respectively. Exposure to all hazardous substances remained well below the exposure limits. Room-related air concentration measurements were 0.073/0.058 mg/m³ (2016/2017) for formaldehyde and 65/107 mg/m³ (2016/2017) for ethanol. Person-related measurements amounted to 0.107-0.229 mg/m³ for formaldehyde and 268-388 mg/m³ for ethanol. Room-related and person-related concentrations of 2-phenoxyethanol remained below the detection limit.

The ethanol-based embalming protocols presented here offer a good alternative for the different applications. The protocols are discussed regarding current regulations and further measures to reduce formaldehyde exposure.

Key words: Ethanol – Formaldehyde – Embalming – Dissection course – Occupational exposure

Corresponding author:
Anke Schnapper-Isl. Institute of Functional and Applied Anatomy, Hannover Medical School, Carl-Neuberg-Str. 1, 30625 Hannover, Germany. Phone: +49 511 532 2989. E-mail: Schnapper.Anke@mh-hannover.de

Submitted: January 23, 2023. **Accepted:** March 3, 2023

https://doi.org/10.52083/CYOJ3969

INTRODUCTION

Teaching anatomy to medical students is based on a combination of theoretical and practical lessons to which the dissection course is central (Gunderman and Wilson, 2005; Rizzolo and Stewart, 2006; Korf et al., 2008; Böckers et al., 2010; Ochs et al., 2012; Vorstenbosch et al., 2013; Schmiedl, 2017; Bogomolova et al., 2020). Learning from a body teaches the complete intricacy of reality, which has a much higher level of complexity than models, whether digital or physical (Ochs et al., 2012). So it is not surprising that the majority of final-year medical students asked at the end of their curriculum about the relevance of gross anatomy classified the dissection course with integrated clinical problems as an important prerequisite and basis for their clinical courses and are interested in additional specialized dissection courses (Pabst, 1993). Also, the relevance of gross anatomy in respect to everyday work was ranked second of all medical subjects by physicians asked some years after graduation at their specialist examination (Pabst and Rothkötter, 1997).

In addition to the classical dissection course for undergraduate medical students, dissection of specific body regions is also conducted in postgraduate education and medical specialist training (Grechenig et al., 1999; Schwarz et al., 2002; Feigl et al., 2007; Schmiedl, 2017; Wedel et al., 2019; Shichinohe et al., 2022; Suzuki et al., 2022).

The dissection course relies on donors who bequeath their body to a specific anatomical institute. This bequest must be made personally in written form during the donor's lifetime (informed consent). After death, the bodies are fixed and conserved chemically to allow storage and preparation for long periods and to preclude infection risks (Brenner, 2014). At Hannover Medical School, ethanol-based fixation techniques have been used since its foundation in 1965, and were chosen as an alternative to formalin-based fixation in order to reduce occupational health hazards for employees and students (Pabst, 1987). Since then, ethanol-based fixation techniques have evolved continuously.

Occupational exposure to formaldehyde has received renewed attention due to a reassessment of its carcinogenicity. In its 2012 review on human carcinogens, the International Agency for Research on Cancer (IARC) saw sufficient evidence that formaldehyde causes cancer of the nasopharynx and leukemia in humans, and thus graded formaldehyde as a group-1 carcinogen (IARC, 2012). Based on the United Nations' Globally Harmonized System of Classification and Labelling of Chemicals (GHS) classification, the carcinogenicity of formaldehyde was subsequently graded as category 1B by the European Union (EU), resulting in a reduction of European occupational exposure limits to air concentrations of 0.37 mg/m³ (0.3 ppm) (Commisssion Regulation (EU) 605/2014, 2014; United Nations, 2021). Likewise, legal regulations or recommendations were also adapted in other countries. Current occupational exposure limits for long-term/time-weighted average of exposure vary between countries, and range from 0.12 to 2.5 mg/m³ (0.1-2.0 ppm). Additionally, many countries have imposed short-term and/or ceiling limits. All values are listed in Table 1.

Reduction or replacement of formaldehyde in fixatives requires alternative chemicals, which could also incorporate health hazards. Apart from formaldehyde, our fixatives contain ethanol, 2-phenoxyethanol and thymol, which are regulated as hazardous chemicals in the EU and other countries (Regulation (EC) 1272/2008, 2008; Commission Regulation (EU) 2018/669, 2018; Commission Delegated Regulation (EU) 2021/849, 2021). The main hazard associated with ethanol is flammability. Further hazards of the four substances include several acute hazards, which are listed in Table 2.

The aim of this study was to present two different ethanol-based fixation methods used at our institute for the dissection course or for clinical anatomy courses, and to assess occupational exposure to hazardous substances in a regular dissection course setting.

MATERIALS AND METHODS

Body donors

All body donors voluntarily bequeathed their body during lifetime and after informed consent for medical education and research to the Insti-

Table 1. International occupational exposure limits for formaldehyde, ethanol and 2-phenoxyethanol [mg/m³].

	Formaldehyde			Ethanol		2-Phenoxyethanol	
	Long- term/ TWA[1]	Short- term[2]	Ceiling[3]	Long- term/ TWA[1]	Short- term[2]	Long- term/ TWA[1]	Short- term[2]
Europe							
EU[4]	0.37 (0.15-0.37)	0.74 (0.5-0.74)	–	1900 (260-1900)	1900 (1520-9500)	– (5.7 to –)	– (5.7 to –)
Switzerland	0.37	0.74	–	960	1920	110	110
UK	2.5	2.5	–	1920	–	–	–
Asia							
Japan	0.12	0.18[5]	0.24[5]	–	–	–	–
Singapore	–	0.37	–	1880	–	–	–
South Korea	0.37	–	–	–	–	–	–
Australia/Ozeania							
Australia	1.2 (0.36[6])	2.5 (0.72[6])	–	1880	–	–	–
New Zealand	0.37	0.74	–	1880	–	–	–
America							
Canada[7]	0.9 to –	1.23 to –	1.85 to –	1880 to –	1900 to –	141 to –	–
Mexico	–	0.37	–	1900	–	–	–
USA[8]	0.93 (0.02[9])	2.47 (0.12[9])	–	1900	–	–	–

Occupational exposure limits according to national regulations and legal requirements
– A legal limit has not been imposed
[1] Long-term: General exposure limit during a working shift. It may be exceeded for short time periods. Or: TWA: Limit of time weighted average of exposures during a working shift
[2] Exposure limit for short time periods, defined by most countries as a 15 min interval
[3] Concentration should not be exceeded at any time
[4] National exposure limits can vary between countries: Listed is the limit valid in most EU countries and () range of national exposure limits
[5] Recommended by the Japan Society for Occupational Health (JSOH)
[6] Recommended by the National Industrial Chemicals Notification and Assessment Scheme (NICNAS)
[7] Exposure limits vary between Provinces
[8] Some states have different exposure limits
[9] Recommended by The National Institute for Occupational Safety and Health (NIOSH)

tute of Functional and Applied Anatomy, Hannover Medical School, where the study was performed. The authors state that every effort was made to follow all local and international ethical guidelines and laws that pertain to the use of human cadaveric donors in anatomical research (Iwanaga et al., 2022). Due to logistic reasons, most body donors come from the region of Hannover. Before conservation started, an additional second post-mortem examination by a coroner was carried out.

Ethanol-based standard fixation

Our standard fixation protocol was applied to bodies to be used in our student dissection courses. Conservation started preferably within 24 h after death of the body donor by perfusion fixation via the femoral artery. On average, 15 l of standard fixative (Table 3) were infused slowly (over several hours) at a low-pressure gradient (max. 100 kPa (1 bar)). The exact volume infused varied with the size of the body donor (approx. 0.18 l/kg body weight) and also depended on the vessel quality of the corpse (visual control of arrival of fixative in all body regions). Additionally, if necessary, fixation solution was applied s.c. and i.m. in body regions like, e.g., subcutaneous tissue of the neck, which are sometimes not reached well by perfusion.

Subsequently, perfusion-fixed bodies were immersed in 70% ethanol for additional external fixation of skin and subcutaneous tissue and storage. The storage period lasted for at least 6-12 months

Table 2. Hazard statements for formaldehyde, ethanol, 2-phenoxyethanol and thymol according to CLP regulation (Commission Delegated Regulation (EU) 2021/849, 2021; Commission Regulation (EU) 2018/669, 2018; Commisssion Regulation (EU) 605/2014, 2014; Regulation (EC) 1272/2008, 2008) and Safety Data Sheets (Carl Roth GmbH 2021a, b, 2022).

Hazard statement	Formaldehyde	Ethanol	2-Phenoxy-ethanol	Thymol
H255: Flammable liquid 2		x		
H301: Acute toxicity 3 (oral)	x			
H302: Acute toxicity 4 (oral)			x	x
H311: Acute toxicity 3 (dermal)	x			
H314: Skin corrosion 1B	x			x
H317: Skin sensitisation 1	x			
H318: Eye damage 1	x		x	
H319: Eye irritation 2		x		
H331: Acute toxicity 3 (inhalation)	x			
H335: STOT SE1 3 (respiratory tract irritation)	x		x	
H341: Mutagenicity 2	x			
H350: Carcinogenicity 1B	x			
H370: STOT SE1 1	x			
H411: Aquatic chronic 2				x

[1] Specific target organ toxicity, single exposure

Table 3. Composition of fixation solution for standard fixation and soft fixation.

	Standard fixation		Soft fixation	
	Volume	Effective concentration[1]	Volume	Effective concentration
Ethanol (99%)	8750 ml	86.63%	5000 ml	43,61%
Formalin (Formaldehyde 37.5%)	750 ml	2.83%	125 ml	0,41%
2-Phenoxyethanol	250 ml	2.50%	125 ml	1,10%
Glycerin (85%)	250 ml	2.13%	4250 ml	31,83%
Thymol solution	–	–	100 ml	0,88%
Nitrite curing salt	–	–	100 g/1750 ml aqua dest.	0,88%

[1] Effective concentration: water free concentration of chemical substance

during which the ethanol concentration of the storage solution was tested regularly. During the dissection course, the bodies were sprayed regularly with 20% ethanol when uncovered to prevent drying out. After the end of the course, the corpses were covered with a cloth, which was sprayed with an ethanol/thymol solution and a plastic cover to prevent evaporation.

Ethanol-glycerin-based soft fixation

Bodies conserved by soft fixation were used in our specialist training courses. These include courses for hip surgery and hip joint injection, courses for shoulder, hip and knee joint prosthesis surgery, courses for implantation of hand and foot endoprostheses, flap surgery courses, pelvic floor courses, and courses for implantation of left ventricular assist systems. Donated bodies were

perfusion-fixed using fixation solution for soft fixation. The concentration of formaldehyde has been further reduced from 1% to 0.41% (Table 3) compared to previous years to increase the flexibility of the corpses. The perfusion process was similar to standard fixation; perfusion volume averaged 12-15 l. For subsequent storage, the bodies were immersed in 30% ethanol. Storage time was on average about 6 months. It could vary between 4 weeks and 1.5 years, depending on the time schedule and frequency of our specialist training courses.

Evaluation of conservation quality

Throughout the dissection course, feedback of students participating in the dissection courses during the last 10 years was obtained orally regarding the visibility and haptic properties of anatomical structures, dissectability and handling. For ethanol-glycerin-based soft fixation used in specialist training courses, oral feedback was obtained from participants and external instructors. For both fixation methods, visual appearance of donated bodies was documented photographically. Haptic properties were determined descriptively by palpation.

Exposure measurements

Exposure measurements were taken during the regular dissection course for medical students. All students were working with body donors fixed with Hannover standard fixation. The dissection course is held in two dissection halls (area 220 m^2, air volume 840 m^3, each), which are ventilated and air conditioned (supply air: 6800 m^3/h, extract air: 6900 m^3/h, air exchange rate 8x, negative pressure ventilation; per dissection hall). Room temperature (set point: 17°C) and relative humidity were recorded during exposure measurements. Incoming air was delivered via 15 ducts located in the ceiling, and for exit air 4 suction ducts were located close to the floor. Table suction devices were not installed. Twelve bodies were placed in each dissection hall on stainless steel tables. Six bodies were dissected simultaneously while the other 6 remained covered. Covered and uncovered tables were arranged alternately, with always one covered table in between. Thus, the distance between uncovered tables amounted to 5 m and 3.5 m in longitudinal and transverse direction, respectively. Minimum diagonal distance between corners of uncovered tables was 2 m. Alternately 2 groups of 6 students worked on one body in a time-staggered manner. The students sprayed the bodies with ethanol solution (20%) regularly during the dissection course. Outside course hours, the bodies were covered and remained in the dissection hall.

Measurements of exposure to hazardous substances were conducted according to EU and German legal regulations (DIN EN 689, 1995; Regulation (EC) 1272/2008, 2008; Commisssion Regulation (EU) 605/2014, 2014; DIN EN 482, 2015; TRGS 900, 2015; TRGS 402, 2016; Chemikaliengesetz, 2021; Gefahrstoffverordnung, 2021; Arbeitsschutzgesetz, 2022) They included exposure measurements regarding formaldehyde, ethanol and 2-phenoxyethanol.

Sampling was performed during regular course hours by an accredited laboratory (TÜV Nord Umweltschutz GmbH, Hannover, Germany) on two days (18.2.2016 and 6.2.2017), and included room-related and person-related samples (TÜV NORD Umweltschutz Gmbh & Co. KG, 2016, 2017). Room-related samples were obtained in a central position in the dissection hall. Person-related samples were collected from one person (18.2.2016)/two persons (6.2.2017) directly involved in the preparation process and at inspiration height. These person-related samples were taken as long-term-exposure samples to determine mean exposure levels during the course (collection period 102-122 min). Sample collection started at the beginning of the course, including uncovering of body donors. Additionally, short-term-exposure samples were obtained from the two persons (2017) in maximum-exposure situations (collection period 15 min) (TÜV NORD Umweltschutz Gmbh & Co. KG, 2017). The sampling device (Personal Air Sampler, Type SKC 224PCEX8, ANALYT-MTC GmbH, Müllheim, Germany) comprised a pump sucking a defined air volume through substance-specific sample carriers (formaldehyde: 2,4-dinitrophenylhydrazin cartridge (Waters Sep-Pak Cartridge Type XPoSure Aldehyde Sampler); 2-phenoxyethanol and

ethanol: activated carbon tube (Type B, SKC Anasorb CSV) (TÜV NORD Umweltschutz Gmbh & Co. KG, 2016, 2017)).

The samples were analyzed by accredited laboratories. Formaldehyde analysis was performed by TÜV NORD Umweltschutz GmbH (Hamburg, Germany), using high pressure liquid chromatography (HPLC; LaChrom Ultra, VWR, Darmstadt, Germany). 2-phenoxyethanol and ethanol analysis was performed by ANECO Institut für Umweltschutz GmbH&Co. (Mönchengladbach, Germany), using capillary gas chromatography and a flame ionization detector (Capillary-GC-FID) (TÜV NORD Umweltschutz Gmbh & Co. KG, 2016, 2017).

Based on room air concentrations and occupational exposure limits according to TRGS 900, exposure indices were calculated according to TRGS 402 (TRGS, 900, 2015; TRGS 402, 2016). A substance index (I_i) was determined for formaldehyde, 2-phenoxythanol and ethanol, added to yield a total exposure index (BI) and time weighted to calculate the shift exposure index (I_M). Finally, hazards and safety precautions were evaluated according to TRGS 402 (TÜV NORD Umweltschutz Gmbh & Co. KG, 2017).

RESULTS

Conservation quality

Ethanol-based standard fixation was employed for donor bodies intended to be used in the dissection course. The condition of the corpses can be seen in Fig. 1. Muscles and internal organs were moderately decolored, although they retained enough color contrast for tissue differentiation. Shape and size of internal organs were not altered significantly. Tissues and organs of embalmed bodies were firm but not hard or brittle. The bodies remained in good condition during the whole dissection course (October to June). Mold infestation and tissue decompensation did not occur. Student feedback revealed that they could discern and dissect anatomical structures well, and that they were satisfied with the conservation quality.

Ethanol-glycerin-based soft fixation was performed in bodies used for specialist training courses. Figure 2 shows the conservation quality of bodies subjected to soft fixation. Organ and tissue colours were quite vivid, and exposed structures could be differentiated well. Participants and instructors of specialist training courses found it particularly helpful that extremities and trunk were flexible and most internal organs were quite soft. Thus, tissues and organs gave a realistic impression for the conduction of clinical procedures.

Exposure measurements

Ventilation and air conditioning kept the room temperature and the relative humidity at low comfortable levels during the dissection course (room temperature 18.7-20.5°C, relative humidity 30-32%, air pressure 1016 hPa).

Room related exposure measurements:

In a central position of the dissection hall a formaldehyde concentration of 0.073 and 0.058 mg/m³ was measured in 2016 and 2017, respectively. The concentration amounted to 19.7% and 15.7% of the occupational exposure limit in 2016/2017 (substance index 0.197 and 0.157; Table 4). Air concentration of ethanol was 65 and 107 mg/m³, i.e., 6.8% and 11.1% of the exposure limit in 2016 and 2017, respectively (Table 4). The exposure to 2-phenoxyethanol was below the detection threshold. The sum of all measured air concentrations resulted in a total exposure index of 0.27 in both years.

Person-related measurements:

Person-related long-term values, i.e., mean air concentrations at inspiration height directly above the corpses, were approximately twice as high as the room related values for formaldehyde and ethanol (Table 4). Air concentrations of 2-phenoxyethanol were still below the detection limit. All concentrations remained well below the exposure limit (I_i and BI < 1) (Table 4). Additionally, short-term exposure measurements were conducted for the two persons in 2017 (Table 4) when opening the abdominal cavity. This was regarded as the maximum exposure situation, not only of the course day but of the whole dissection course. From long-term and short-term exposure indices a time-weighted shift exposure index (I_M) was determined, which amounted to 0.35 for both per-

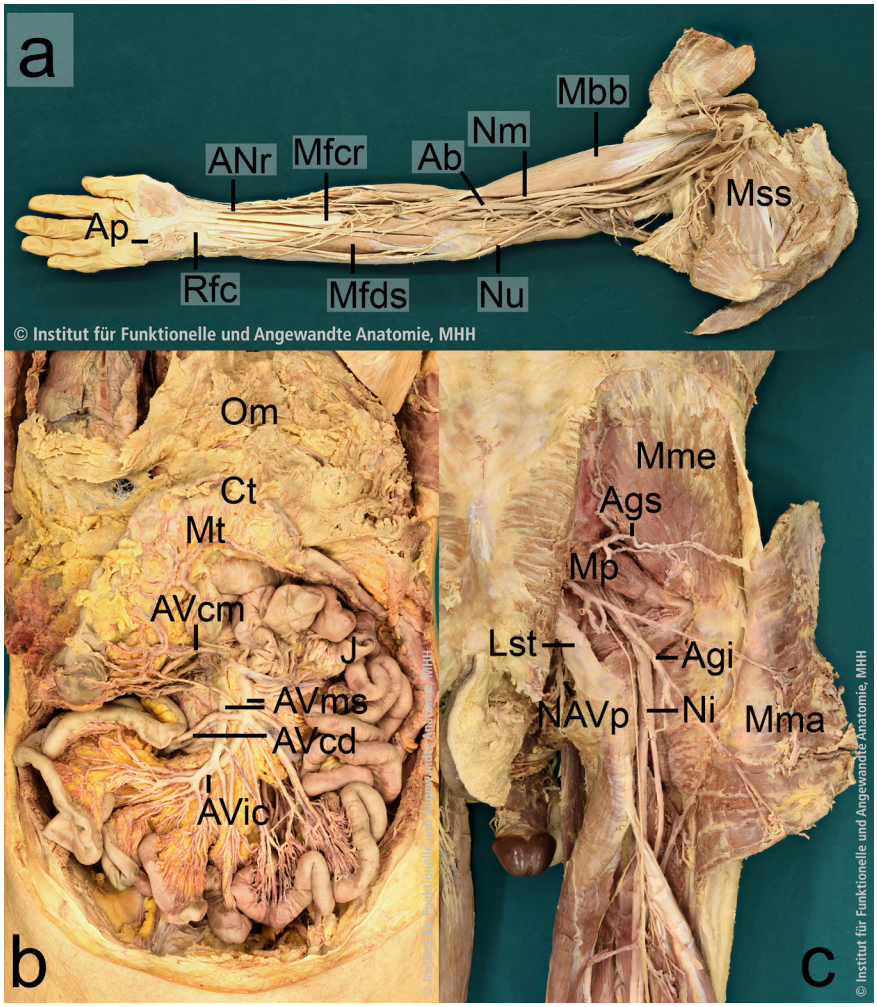

Fig. 1.- Ethanol-based standard fixation. Fixation quality was very good. Structures could be dissected easily and were well conserved. **a:** Right upper extremity. Mss Musculus (M.) subscapularis, Mbb M. biceps brachii, M. flexor carpi radialis, Mfds M. flexor digitorum superficialis, Rfc Retinaculum flexorium carpi, Ap Aponeurosis palmaris, Nm Nervus (N.) medianus, Nu N. ulnaris, Ab Arteria (a.) brachialis, ANr A. radialis and N. radialis ramus superficialis. **b:** Abdominal cavity opened and greater omentum flapped cranially. Om Omentum majus, Ct Colon transversum, Mt Mesocolon transversum, AVms A. and V. mesenterica superior, AVic A. and V. ileocolica, AVcd A. and V. colica dextra, AVcm A. and V. colica media. **c:** Right gluteal region. Mma M. gluteus maximus, Mme M. gluteus medius, Mp M. piriformis, Lst Ligamentum sacrotuberale, Ags A. glutea superior, Agi A. glutea inferior, Ni N. ischiadicus, NAVp N. pudendus, A. and A. pudenda interna.

Table 4. Air concentrations, substance indices, total exposure indices and shift exposure indices.

Location	Time interval	Formaldehyde		Ethanol		2-Phenoxyethanol		BI	I_M
		C_F [mg/m³]	I_F	C_E [mg/m³]	I_E	C_P [mg/m³]	I_P		
18.2.2016									
Room	Long- term	0.073	0.197	65	0.068	<0.238	<0.005	0.27	
Person	Long- term	0.229	0.619	268	0.279	<0.268	<0.005	0.90	0.45
6.2.2017									
Room	Long- term	0.058	0.157	107	0.111	<0.365*	<0.003	0.27	
Person 1	Long- term	0.118	0.319	278	0.290	<0.376*	<0.003	0.61	0.35
Person 1	Short- term	0.405	1.090	862	0.898	<2.760*	<0.025		
Person 2	Long- term	0.107	0.289	388	0.404	<0.336*	<0.003	0.70	0.35
Person 2	Short- term	0.135	0.365	352	0.367	<2.550*	<0.023		

Indices were determined according to TRGS 402 and TRGS 900 (TRGS 900 2015; TRGS 402 2016). According to TRGS 402, BI was not determined for short-term measurements. C Air concentration, I Substance index for formaldehyde (F), 2-phenoxyethanol (P) and ethanol (E), BI Total exposure index, IM Shift exposure index, * Detection limit with respect to sampling time and flow rate.

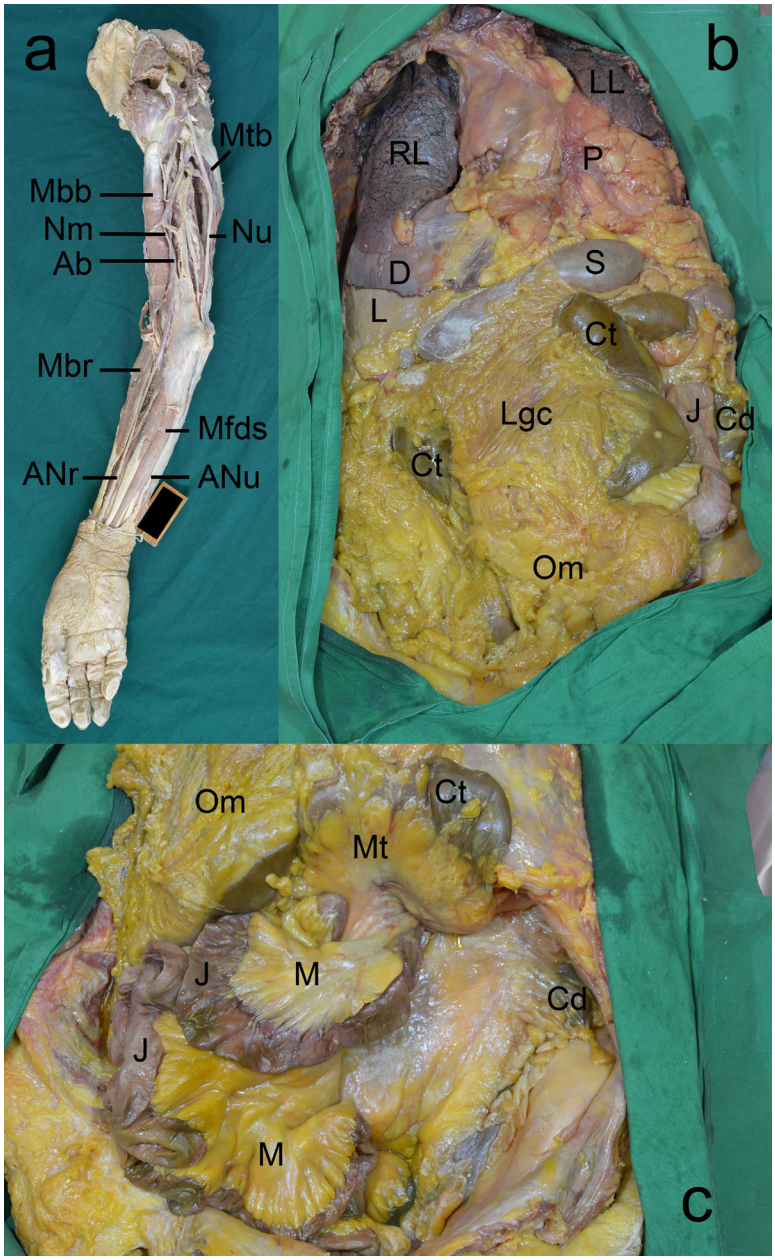

Fig. 2.- Ethanol-glycerin-based soft fixation. **a:** Right upper extremity; **b:** Thoracic and abdominal cavity opened; **c:** Abdominal cavity opened and greater omentum flapped cranially. Fixation quality is good. Organ and tissue colors were quite vivid and exposed structures could be differentiated well.

Mbb Musculus (M.) biceps brachii, Mtb M. triceps brachii, Mbr M. brachiioradialis, Mfds, M. flexor digitorum superficialis, Ab Arteria (A.) brachialis, Nm nervus (N.) medianus, Nu N. ulnaris, ANr A. radialis and N. radialis ramus superficialis, ANu A. and N. ulnaris, RL right lung, LL left lung, P Pericardium, D diaphragm, L liver, S stomach, J Jejunum, Ct Colon transversum, Cd Colon descendens, Lgc Ligamentum gastrocolicum, Om Omentum majus, M Mesenterium, Mt Mesocolon transversum.

sons in 2017. I_M was 0.45 in 2016. For both years, the final evaluation according to TRGS 402 was "Safety precautions are sufficient".

DISCUSSION

Using donated bodies in dissection courses requires fixation and conservation to inactivate possible pathogens and to provide sufficient tissue stability for storage and course times (Brenner, 2014; Balta et al., 2015; Schmiedl, 2017; Waschke et al., 2019).

Anatomical requirements for a fixative comprise fast and homogeneous diffusion through tissue, protein denaturation to prevent autolysis, rapid inhibition of bacterial and non-bacterial degradation processes, fast inactivation of pathogenic microorganisms and structural solidification of

tissues and organs as close to their natural state as possible. However, tissues should not become too rigid and organic tissue components should not be dissolved. Long preservation stability is favorable, as well as a contribution to depersonalization of the body donor by a modest change of complexion and haptic properties (Coleman and Kogan, 1998; Brenner, 2014; Schmiedl, 2017).

The main components of classical fixation solutions contribute to these requirements (Tables 5 and 6). In particular, formaldehyde is a constituent of almost all conservation solutions for donated bodies to be used in dissection courses due to its strong bactericidal, fungicidal and antiviral properties, as well as for its excellent tissue-fixation qualities (Brenner, 2014). The final concentration in fixatives usually varies between 3 and 10% (Waschke et al., 2019). However, health hazards and subsequent legislation continue to restrict utilization of formaldehyde (see below). Alternative fixation protocols with reduction or replacement of formaldehyde must meet the above demands while involving less health hazards.

Fixation techniques

Ethanol-based standard fixation for student dissection courses:

Our protocol used an arterial perfusion solution (Table 3) based on ethanol (86.6%) and containing formaldehyde (2.8%), 2-phenoxyethanol (2.5%) and glycerin (2.1%) as additional components, followed by immersion fixation in 70% ethanol and resulted in a good fixation quality as described in the result chapter. During intraarterial application the fixation solution diffused through tissue over several hours depending on vessel quality and condition of the corpse, i.e., fast enough to stop degradation processes successfully. The volume of fixation solution that can be infused varied with regard to body size but also vessel quality. Application of high volumes improved fixation quality. Subsequent immersion fixation in 70% ethanol postfixed skin and subcutaneous tissue. A storage time of at least 6-12 months assured reliable inactivation of possible pathogenic microorganisms, including a sufficient safety margin (Lischka et al., 1979).

In order to reduce formaldehyde exposure, several anatomical institutes have decreased the formaldehyde concentration of their arterial perfusion solutions to 1.6-4% during the recent past (Rissler and Hauke, 2021). Classical formaldehyde-based fixation (4-8%) yielded specimens with long-lasting stability for dissection, good tissue fixation and antimicrobial effectivity, but tissues became hard and discolored (Hayashi et al., 2016). A reduction of formaldehyde concentration may result not only in reduced health hazards, but also in improved specimen suitability for dissection courses. Requirements for student dissection courses differ to some extent from those for clin-

Table 5. Air concentrations, substance indices, total exposure indices and shift exposure indices.

Location	Time interval	Formaldehyde		Ethanol		2-Phenoxyethanol		BI	I_M
		C_F [mg/m³]	I_F	C_E [mg/m³]	I_E	C_P [mg/m³]	I_P		
18.2.2016									
Room	Long term	0.073	0.197	65	0.068	<0.238	<0.005	0.27	
Person	Long term	0.229	0.619	268	0.279	<0.268	<0.005	0.90	0.45
6.2.2017									
Room	Long term	0.058	0.157	107	0.111	<0.365*	<0.003	0.27	
Person 1	Long term	0.118	0.319	278	0.290	<0.376*	<0.003	0.61	0.35
Person 1	Short term	0.405	1.090	862	0.898	<2.760*	<0.025		
Person 2	Long term	0.107	0.289	388	0.404	<0.336*	<0.003	0.70	0.35
Person 2	Short term	0.135	0.365	352	0.367	<2.550*	<0.023		

Indices were determined according to TRGS 402 and TRGS 900 (TRGS 900 2015; TRGS 402 2016). According to TRGS 402, BI was not determined for short term measurements. C Air concentration, I Substance index for formaldehyde (F), 2-phenoxyethanol (P) and ethanol (E), BI Total exposure index, IM Shift exposure index, * Detection limit with respect to sampling time and flow rate.

Table 6. Main components of fixatives and their characteristics.

Chemical agent	Main characteristics
Formaldehyde	strongly bactericidal, fungicidal, insecticidal, antiviral, reversible crosslinking of proteins, very good tissue fixation
Ethanol	bactericidal, fungicidal, antiviral, protein coagulation
Phenol	bacteriostatic, bactericidal, fungicidal, denaturation of proteins
Phenoxyethanol	bactericidal
Glycerin	hydrophilic (moisturizing, emollient, softening agent)

From: Lischka et al., 1979; Lowe and Southern, 1994; Block, 2001; McDonnell, 2007; Koller et al., 2012; Brenner, 2014; Robert Koch-Institut, 2017; Schmiedl, 2017.

ical-anatomical courses. In particular, long-term usability is of importance. In this regard, antibacterial, antifungal, antiviral and anti-insecticidal properties of fixation and storage must be considered, and may limit reduction of formaldehyde concentration much below 2%, or even formaldehyde-free solutions (Waschke et al., 2019).

Using a formaldehyde-free nitrite pickling salt-ethanol-glycol solution for veterinary specimens (dog), tissue and organ consistency, and color remained invivo-like. But conservation of the abdominal organs was only sufficient when the abdominal cavity was opened, and thus the abdominal organs were post-fixed by immersion in the identical storage solution, and storage required cooling (Janczyk et al., 2011).

Ethanol-glycerin-based soft fixation for specialist training courses:

Apart from adverse health effects, formalin-based fixation also has some further disadvantages for specialist training courses, e.g., rigidity of the body, reduced joint flexibility, tissue decoloration, and change in the haptic properties of tissue. This has resulted in the introduction of several alternative conservation protocols, specifically designed for clinical-anatomical courses. They include Thiel solution, ethanol-glycerin-formaldehyde solution, Imperial College London soft preservation solution and saturated saline and nitrite pickling salt solution (Thiel, 1992; Coleman and Kogan, 1998; Thiel, 2002; Hayashi et al., 2016; Balta et al., 2019; Wedel et al., 2019; Shichinohe et al., 2022; Shirai et al., 2022; Suzuki et al., 2022). Also unfixed, thawed, fresh-frozen bodies are used (Hayashi et al., 2016; Shichinohe et al., 2022; Suzuki et al., 2022).

To meet the specific demands of our specialist training courses, an ethanol-glycerin-based soft fixation protocol was devised (Table 3). In contrast with the standard protocol, the soft fixation solution contained less formaldehyde (effective concentration 0.41%), ethanol (43.6%) and 2-phenoxyethanol (1.1%), but more glycerin (31.8%). Addition of thymol and nitrite curing salt provided sufficient conservation properties to the solution. High amounts of glycerin resulted in a softer consistency. The bodies retained sufficient flexibility, and internal organs were less rigid than after our standard fixation. The consistency was suitable to allow realistic procedures in training of surgical intervention techniques, as needed in our specialist training courses. On the other hand, the infection risk inherent in thawed, fresh-frozen corpses was reduced, but not eliminated (Hayashi et al. 2016; Schmiedl 2017). After perfusion with the ethanol-glycerin-based soft fixation solution, the bodies were stored in 30% ethanol, since higher ethanol concentrations (e.g., 70%) resulted in progressive tissue hardening not compatible with soft fixation purposes. Maximum storage times are about 1.5 years; after longer periods, the conservation quality declines.

Wedel et al. (2019) devised an ethanol-glycerol-lysoformin (70%-30%-0.3%) solution for laparoscopic gynecological surgery training, which comes closest to our solution with regard to glycerin content. The authors stated that they could obtain similar results, as with fresh-frozen or Thiel fixed body donors (Wedel et al., 2019). Thiel

fixation and its modifications produced a highly in vivo-like appearance of the fixed bodies and their organs at a macroscopic level, which included coloring, haptic and joint flexibility (Thiel, 1992; Thiel, 2002; Hayashi et al., 2016). However, some of the components are toxic or harmful (Janczyk et al., 2011). Yet another alternative is conservation with saturated saline solution (Coleman and Kogan, 1998; Hayashi et al., 2016). The formaldehyde content was slightly higher compared to our protocol, and the saturated saline solution contained phenol, one other critical chemical, which, however, might be replaced. The authors stated that bodies fixed by this method had a natural color, and that consistency was between Thiel and formalin-fixed specimens and imaging (ultrasound, x-ray), and that histological quality were good (Coleman and Kogan, 1998; Hayashi et al., 2016).

Health hazards of fixatives and exposure limits

Within the EU, occupational exposure to hazardous substances is regulated at EU level (Regulation (EC) 1272/2008, 2008; Commisssion Regulation (EU) 605/2014, 2014; Commission Regulation (EU) 2018/669, 2018; Commission Delegated Regulation (EU) 2021/849, 2021). Subsequent translation into national law is executed in Germany through a cascade of acts, ordinances and technical regulations (DIN EN 689, 1995; DIN EN 482, 2015; TRGS 900, 2015; TRGS 402, 2016; Chemikaliengesetz, 2021; Gefahrstoffverordnung, 2021; Arbeitsschutzgesetz, 2022). Specifically, TRGS 900 assigns occupational exposure limit values. Likewise, occupational exposure to hazardous substances is regulated in many other countries in Europe, Asia, Australia/Oceania and America (NORMA Oficial Mexicana NOM-010-STPS-2014, 2014; Industrial Safety and Health Act, 2018; Safe Work Australia, 2019; Ontario Regulation 833, 2019; Control of Substances Hazardous to Health Regulations 2002, 2020; Health and Safety Executive, 2020; Ministry of Employment and Labor Notice No. 2020-48, 2020; Occupational Safety and Health Act, 2020; Alberta Regulation 191/2021, 2021; Suva, 2021; Hygieniska gränsvärden, 2021; Industrial Chemicals Act, 2021; BEK nr 1054, 2022; Part 1910 - Occupational Safety and Health Standards, 2022; Regulation S-2.1 r.13, 2022; Sociaal Economische Raad, 2022; Workplace Safety and Health Act 2006, 2022; Worksafe, 2022)

Our standard fixation solution contains three chemical agents that are considered hazardous: formaldehyde, ethanol and 2-phenoxyethanol. The soft fixation solution additionally contains thymol as a regulated chemical (Regulation (EC) 1272/2008, 2008; Commission Regulation (EU) 2018/669, 2018; Chemikaliengesetz, 2021; Commission Delegated Regulation (EU) 2021/849, 2021; Gefahrstoffverordnung, 2021). Health hazards associated with those four substances are summarized in Table 2. To determine the health hazards of a fixation solution, all of its components have to be taken into account. If there is no reliable evidence to the contrary, risks of mixtures of chemical substances are assumed to be additive in many countries (TRGS 402, 2016; Ministy of Employment and Labor Notice No. 2020-48, 2020; Hygieniska gränsvärden, 2021; The Japan Society of Occupational Health, 2021; BEK nr 1054, 2022; Part 1910 - Occupational Safety and Health Standards, 2022).

Among the chemicals in our solutions, both number and severity of adverse health effects associated with formaldehyde clearly rank first. This applies in particular to the hazards mutagenicity and carcinogenicity, which are only found in formaldehyde. Carcinogenicity of formaldehyde in humans has long been suspected (Pabst, 1987), but in 2012 the IARC saw sufficient evidence of carcinogenicity in humans to reclassify formaldehyde from group 2A (probably carcinogenic to humans) to group 1 (carcinogenic to humans) (IARC, 2012). “Sufficient evidence of carcinogenicity in humans” means that a causal association between exposure to the agent and human cancer has been established (IARC, 2019). According to the body of evidence, the IARC concluded that formaldehyde causes nasopharyngeal cancer and leukemia in humans. Furthermore, the IARC Working Group reported a positive association between formaldehyde exposure and sinonasal cancer in humans, sufficient evidence for carcinogenicity of formaldehyde in experimental animals, and mechanistic evidence of cancer induction by formaldehyde *in vitro* and *in vivo* in

humans and experimental animals (IARC, 2012). The IARC, a research agency under the auspices of the World Health Organization (WHO), evaluates the carcinogenic risks of numerous agents, classifying substances on the strength of evidence for carcinogenicity (IARC, 2019). It does not quantify the amount of risk increase due to exposure or threshold levels. IARC classifications are solely based on scientific grounds and have no direct consequences for using the chemical in a specific country or setting.

However, subsequent legislative bodies in several countries adapted their hazard categorization and exposure limits for formaldehyde. In 2014, the EU adapted the hazard category from cat. 2 (suspected human carcinogen) to cat. 1B ("presumed to have carcinogenic potential for humans, classification is largely based on animal evidence"), but did not go as far as to classify formaldehyde as a cat. 1A carcinogen ("known to have carcinogenic potential in humans, classification is largely based on human evidence") (Regulation (EC) 1272/2008, 2008; Commisssion Regulation (EU) 605/2014, 2014).

Besides the strength of evidence for carcinogenicity, EU CLP categorization takes into account additional considerations, including, e.g., the level of concern for human carcinogenicity (Regulation (EC) 1272/2008, 2008). As a legislative body, the EU classification directly and indirectly (through national legislation) regulates usage, safety measures and occupational exposure limits, and thus it is relevant for individual institutions (Regulation (EC) 1272/2008, 2008; TRGS 900, 2015). All countries screened (Table 1) have imposed occupational exposure limits for formaldehyde. However, permissible concentration levels vary substantially among countries. Presently, the strictest legal regulations are found in Japan, with an exposure limit of 0.12 mg/m³, which is only one third of the EU exposure limit (0.37 mg/m³; both values for long-term/time weighted average) (Industrial Safety and Health Act, 2018; Directive 2004/37/EC, 2022). Even much lower is the recommendation of the American National Institute for Occupational Safety and Health of 0.02 mg/m³ (The National Institute for Occupational Safety and Health, 2022). Should a level like that become a legal standard, it would be very difficult to continue with fixation solutions containing formaldehyde.

The main hazard of ethanol is its physical property of high flammability. Its flash point is at 12°C. Ethanol vapors form explosive mixtures with air at concentrations between 2.5 and 13.5 vol% (Carl Roth GmbH, 2022). Since ethanol-based fixation, and in particular storage of whole bodies, requires large volumes of concentrated ethanol solutions, precautions regarding fire and explosion protection are necessary. These include sufficient ventilation and precautions against electrostatic discharge (Carl Roth GmbH, 2022) in all relevant rooms, but in particular in the mortuary. To ensure vapor concentrations remaining safely below the lower explosion limit, measurements of ethanol vapor concentrations and alarms signaling ventilation failure are expedient and intact good quality electric installations and leak-tight cuvettes should be standard. The legal requirements might vary according to local regulations.

Further health hazards of the four regulated chemical agents of our fixatives include several forms of acute toxicity, organ damage and/or irritation; further skin sensitization for formaldehyde and environmental toxicity for thymol (Table 2). In contrast to formaldehyde, not even all of the screened countries have long-term/TWA limits for ethanol, and only few assigned short-term values. To date, occupational exposure limits for 2-phenoxyethanol exist only in some EU countries, Switzerland and some Canadian provinces, and they vary greatly.

Exposure measurements

To evaluate occupational exposure in a regular dissection course setting, exposure measurements were conducted during normal dissection course hours. Exposure during the dissection course can vary, depending on the precise dissection situation. In particular, opening the body cavities is likely to result in greater exposure due to evaporation of fixation fluid which has accumulated inside the cavities and the exposure of large surface areas of organs and tissues saturated with fixative. Therefore, short-term exposure measurements were made on the opening of the

body cavities (15 min) and long-term exposure measurements were obtained on the same course day, i.e., working on corpses with newly opened body cavities.

Occupational exposure to hazardous substances is regulated at several levels. Firstly, limits of air concentrations [mg/m³] are imposed for each substance, and measured exposure is related to these limits (C_i, I_i) (TRGS 900, 2015; TRGS 402, 2016). Secondly, if exposure to a mixture of hazardous substances occurs during a working shift, hazards are considered additive; thus a total exposure index (BI) is determined, which must not exceed 1 (TRGS 402, 2016). Finally, time periods with varying exposure during a working shift are computed in a time-weighted manner, resulting in a shift exposure index (I_M) (TÜV NORD Umweltschutz Gmbh & Co. KG, 2017). Comparable procedures for calculating a time-weighted average of exposures and/or considering exposure to multiple substances exist also in other countries (Ministry of Employment and Labor Notice No. 2020-48, 2020; Grenzwerteverordnung, 2021; Hygieniska gränsvärden, 2021; Suva, 2021; The Japan Society of Occupational Health, 2021; BEK nr 1054, 2022; Part 1910 - Occupational Safety and Health Standards, 2022; Worksafe, 2022).

Both room-related and person-related (long-term) exposure measurements remained well below the limits for all three regulated substances of our fixation solution, i.e., $I_i \leq 1$ (Table 4). Also, BI and I_M remained below the limits (≤ 1). Exposure limits may be exceeded for short time periods by a substance-specific exceedance factor, which was two for all of our substances, and thus all short-term exposure limits were met (TRGS 900, 2015). Exposure measurements and deducted indices are the bases for the final evaluation according to TRGS 402, which relates to sufficiency of safety precautions (TRGS 402, 2016). For our dissection course situation, the final evaluation was “Safety precautions are sufficient” (TÜV NORD Umweltschutz Gmbh & Co. KG, 2017).

Looking in particular at formaldehyde exposure, room-related measurements were 0.073 mg/m³ (2016) and 0.058 mg/m³ (2017), person-related (long-term) measurements amounted to 0.229 (2016), 0.118 and 0.107 mg/m³ (2017). The occupational exposure limit of formaldehyde has been 0.37 mg/m³ since 2015, and has remained unchanged since then (TRGS 900, 2015, 2022). Thullner et al. (Thullner et al., 2015) conducted exposure measurements at five anatomical institutes using different fixation protocols and with different course settings. They found air concentrations of formaldehyde varying between 0.16-0.79 mg/m³ for room related and 0.41-1.14 mg/m³ for person-related measurements. As in our course situation, person-related measurements were higher than room related measurements (average approx. x2). Formaldehyde air concentrations after our standard fixation were lower than those determined by Thullner et al. (2015). This is probably mainly due to a low formaldehyde concentration in our standard fixation solution and storage of fixated body donors in 70% ethanol without formaldehyde addition, leading to a diffusion of formaldehyde into the alcohol solution. Formaldehyde concentration and/or absolute formaldehyde content in fixation and storage solution constitute the primary determinant for the magnitude of formaldehyde evaporation from the body donors during the dissection course (Thullner et al., 2015; Waschke et al., 2019). It may be easier to reduce or completely omit formaldehyde in preservation/storage solution than in fixation solution. In a survey, 8 of 23 anatomical institutes stated that they use formaldehyde-free storage solutions, and most of them abandoned the formaldehyde component recently (Rissler and Hauke, 2021). In order to reduce formaldehyde exposure, Waschke et al. (2019) recommended considering the protocols for perfusion fixation, storage and body humidification during the dissection course separately, and reducing the amount of formaldehyde in all phases of the embalming and dissection process. Additionally, some institutes have successfully applied neutralizing chemicals, e.g., monoethanolamine and urea solution, to decrease formaldehyde evaporation from the corpses (Coskey and Gest, 2015; Kawata et al., 2019; Otsuka et al., 2022).

Further, technical and structural measures can reduce exposure very effectively. These include basic constructional aspects of the dissection hall (e.g. size and height in relation to the number of

corpses), ventilation (e.g. room vs./plus single table extraction systems, air vent skirting, air flow, air extraction volumes) and temperature regulation (e.g. air conditioning/cooling/heating, illumination) (Thullner et al., 2015; Waschke et al., 2019). At our facility, size and height of the dissection halls are quite large, and an effective ventilation and air conditioning system is installed, allowing high air extraction volumes at low room temperature even in summer. Therefore, single table suction devices are not necessary.

Additional recommendations for exposure reduction are, e.g., small number of donated bodies per room, exclusion of very overweight body donations from the dissection course, uncovering of bodies prior to course start, small number of students per dissection table, and reduction of thermal loads in the room (Thullner et al., 2015; Waschke et al., 2019).

Limitations of the study

Exposure measurements were undertaken on two days, which were chosen as days with maximum exposure situations, since it was our intention to find out if we could conduct the course safely with the present precautions. To map the complete exposure situation during a whole dissection course longitudinally, it would be necessary to perform more measurements throughout the course year and during different dissection situations. Additionally, air concentrations in relationship with fixed bodies of different size and body condition would be interesting to monitor. Our present study focused on occupational exposure of teaching staff and students during the dissection course. Future studies focusing on technical staff should be carried out to measure exposure in the fixation laboratory, in the storage hall and during preparatory works for the dissection course. Exposure during specialist training courses is lower compared to the dissection course, because of the lower concentrations of formaldehyde, ethanol and 2-phenoxyethanol in our soft fixation solution, of a smaller number of corpses in the room – and often only selected body parts are used. Nevertheless, it would be interesting to establish measurements for different clinical anatomy courses.

CONCLUSION

The two different ethanol-based fixation protocols presented here offer suitable alternatives for student dissection courses and specialist training courses, respectively. Fixative properties of the solutions were sufficient for long-term usability during the dissection course (ethanol-based standard protocol) or the specific demands of the specialist training courses (ethanol-glycerin-based soft fixation). Dissectability of the bodies was good with respect to the requirements of student and specialist training courses, respectively. Exposure to formaldehyde and other hazardous substances in the dissection course was compatible with current legislation and health protection requirements.

ACKNOWLEDGEMENTS

The authors gratefully acknowledge the excellent technical assistance of S. Malinjoud, C. Grindley, A. Buchhorn and W. Kohne (Institute of Functional and Applied Anatomy, Hannover Medical School, Hannover, Germany) for preparation of fixation solutions, fixation of body donors and technical support for dissection courses as well as clinical-anatomical courses. We also thank C. Dorka and R. Kreimann (TÜV Nord Umweltschutz GmbH & Co. KG, Hannover, Germany) and G. Küpper (ANECO Institut für Umweltschutz GmbH, Mönchengladbach, Germany) for carrying out the chemical analyses as well as S. Fryk (Institute of Functional and Applied Anatomy, Hannover Medical School, Hannover, Germany) for reading the English manuscript.

The authors sincerely thank those who donated their bodies to science so that anatomical research could be performed. Results from such research can potentially increase mankind's overall knowledge and can improve patient care. Therefore, these donors and their families deserve our highest respect.

REFERENCES

ALBERTA REGULATION 191/2021 (2021) Occupational Health and Safety Code. [Online]. [Accessed: 23 August 2022]. Available from: https://www.alberta.ca/occupational-health-and-safety-code-and-explanation-guide.aspx.

ARBEITSSCHUTZGESETZ (2022) Act on the Implementation of Measures of Occupational Safety and Health to Encourage Improvements in the Safety and Health Protection of Workers at Work (Arbeitsschutzgesetz, ArbSchG) of 7 August 1996 (Federal Gazette I p. 1246), as last amended by Article 1 of the Competence Adjustment Ordinance of 16 September 2022 (Federal Gazette I p. 1454). [Online]. [Accessed: 24 October 2022]. Available from: https://www.gesetze-im-internet.de/arbschg.

BALTA J, CRONIN M, CRYAN J, O'MAHONY S (2015) Human preservation techniques in anatomy: A 21st century medical education perspective. *Clin Anat,* 28: 725-734.

BALTA JY, TWOMEY M, MOLONEY F, DUGGAN O, MURPHY KP, O'CONNOR OJ, CRONIN M, CRYAN, JF, MAHER MM, O'MAHONY SM (2019) A comparison of embalming fluids on the structures and properties of tissue in human cadavers. *Anat Histol Embryol*, 48: 64-73.

BEK NR 1054 (2022) Bekendtgørelse om grænseværdier for stoffer og materialer (kemiske agenser) i arbejdsmiljøet nr. 1054 of 28/06/2022 (Beskæftigelsesmin., Arbejdstilsynet, j.nr. 20225000297). [Online]. [Accessed: 24 August 2022]. Available from: https://www.retsinformation.dk/eli/lta/2022/1054.

BÖCKERS A, JERG-BRETZKE L, LAMP C, BRINKMANN A, TRAUE HC, BÖCKERS TM (2010) The gross anatomy course: an analysis of its importance. *Anat Sci Educ*, 3: 3-11.

BOGOMOLOVA K, HIERCK BP, VAN DER HAGE JA, HOVIUS SER (2020) Anatomy dissection course improves the initially lower levels of visual-spatial abilities of medical undergraduates. *Anat Sci Educ*, 13: 333-342.

BRENNER E (2014) Human body preservation - old and new techniques. *J Anat*, 224: 316-344.

CARL ROTH GMBH (2022) Sicherheitsdatenblatt gemäß Verordnung (EG) Nr. 1907/2006 (REACH) - Ethanol ≥99,8%. [Online]. [Accessed: 24 October 2022]. Available from: https://www.carlroth.com.

CHEMIKALIENGESETZ (2021) Gesetz zum Schutz vor gefährlichen Stoffen (Chemikaliengesetz - ChemG) of 28 August 2013 (Federal Law Gazette I p. 3498, 3991), as last amended by Article 115 of the Competence Adjustment Ordinance of 10 August 2021 (Federal Law Gazette I p. 3436). [Online]. [Accessed: 24 October 2022]. Available from: https://www.gesetze-im-internet.de/chemg.

COLEMAN R, KOGAN I (1998) An improved low-formaldehyde embalming fluid to preserve cadavers for anatomy teaching. *J Anat*, 192: 443-446.

COMMISSION DELEGATED REGULATION (EU) 2021/849 (2021) Commission Delegated Regulation (EU) 2021/849 of 11 March 2021 amending, for the purposes of its adaptation to technical and scientific progress, Part 3 of Annex VI to Regulation (EC) No 1272/2008 of the European Parliament and of the Council on classification, labelling and packaging of substances and mixtures. OJ L 188, 28.5.2021, p. 27–43. [Online]. [Accessed: 24 October 2022]. Available from: https://eur-lex.europa.eu.

COMMISSSION REGULATION (EU) 605/2014 (2014) Commission Regulation (EU) No 605/2014 amending, for the purposes of introducing hazard and precautionary statements in the Croatian language and its adaptation to technical and scientific progress, Regulation (EC) No 1272/2008 of the European Parliament and of the Council on classification, labelling and packaging of substances and mixtures. OJ L 167, 6.6.2014, p. 36-49. [Online]. [Accessed: 24 October 2022]. Available from: https://eur-lex.europa.eu.

COMMISSION REGULATION (EU) 2018/669 (2018) Commission Regulation (EU) 2018/669 of 16 April 2018 amending, for the purposes of its adaptation to technical and scientific progress, Regulation (EC) No 1272/2008 of the European Parliament and of the Council on classification, labelling and packaging of substances and mixtures. OJ L 115, 4.5.2018, p. 1. [Online]. [Accessed: 24 October 2022]. Available from: https://eur-lex.europa.eu.

CONTROL OF SUBSTANCES HAZARDOUS TO HEALTH REGULATIONS 2002 (2020) Control of Substances Hazardous to Health Regulations 2002 2020: Control of Substances Hazardous to Health Regulations 2002 No. 2677 as last amended of 31 December 2020. [Online]. [Accessed: 20 October 2022]. Available from: https://www.legislation.gov.uk/uksi/2002/2677/.

COSKEY A, GEST TR (2015) Effectiveness of various methods of formaldehyde neutralization using monoethanolamine. *Clin Anat*, 28: 449-454.

DIN EN 689 (1995) DIN EN 689 Workplace atmospheres - Guidance for the assessment of exposure by inhalation to chemical agents for comparison with limit values and measurement strategy. Beuth Verlag GmbH, Berlin.

DIN EN 482 (2015) DIN EN 482 Workplace exposure - General requirements for the performance of procedures for the measurement of chemical agents. Beuth Verlag GmbH, Berlin.

DIRECTIVE 2004/37/EC (2022) Directive 2004/37/EC of the European Parliament and of the Council of 29 April 2004 (OJ L 158, 30.4.2004, p. 50) as last amended by Directive 2022/431 of 9 March 2022 (OJ L 88, 16.3.2022, p. 1). [Online]. [Accessed: 24 August 2022]. Available from: https://eur-lex.europa.eu.

FEIGL G, ANDERHUBER F, SCHWARZ G, DORN C, FASEL JHD, LIKAR R (2007) Trainingsmethode für Regionalanästhesisten. Evaluierung und Vergleich. *Anaesthesist*, 56: 437-443.

GEFAHRSTOFFVERORDNUNG (2021) Verordnung zum Schutz vor Gefahrstoffen (Gefahrstoffverordnung - GefStoffV). Gefahrstoffverordnung of 26 November 2010 (Federal Law Gazette I p. 1643, 1644), as last amended by Article 2 of the Competence Adjustment Ordinance of 21 July 2021 (Federal Law Gazette I p. 3115). [Online]. [Accessed: 24 October 2022]. Available from: https://www.gesetze-im-internet.de/gefstoffv_2010/.

GRECHENIG W, FELLINGER M, FANKHAUSER F, WEIGLEIN AH (1999) The Graz learning and training model for arthroscopic surgery. *Surg Radiol Anat*, 21: 347-350.

GRENZWERTEVERORDNUNG (2021) Verordnung des Bundesministers für Arbeit über Grenzwerte für Arbeitsstoffe sowie über krebserzeugende und fortpflanzungsgefährdende (reproduktionstoxische) Arbeitsstoffe (Grenzwerteverordnung 2021 – GKV) of 27 July 2001 (Federal Law Gazette II Nr. 253/2001) as last amended by Änderung der Grenzwerteverordnung 2020 und der Verordnung biologische Arbeitsstoffe of 09 April 2021 (Federal Law Gazette Nr. 156/2021). [Online]. [Accessed: 18 August 2022]. Available from: https://www.ris.bka.gv.at.

GUNDERMAN RB, WILSON PK (2005) Viewpoint: exploring the human interior: the roles of cadaver dissection and radiologic imaging in teaching anatomy. *Acad Med*, 80: 745-749.

HAYASHI S, NAITO M, KAWATA S, QU N, HATAYAMA N, HIRAI S, ITOH M (2016) History and future of human cadaver preservation for surgical training: from formalin to saturated salt solution method. *Anat Sci Int*, 91: 1-7.

HEALTH AND SAFETY EXECUTIVE (2020) EH40/2005 Workplace exposure limits. TSO, Norwich. [Online]. [Accessed: 20 October 2022]. Available from: https://books.hse.gov.uk.

HYGIENISKA GRÄNSVÄRDEN (2021) Hygieniska gränsvärden Arbetsmiljöverkets föreskrifter och allmänna råd om hygieniska gränsvärden of 13 February 2018 (AFS 2018:1) as last amended of 22 September 2021. [Online]. [Accessed: 18 August 2022]. Available from: https://www.av.se/arbetsmiljoarbete-och-inspektioner/publikationer/foreskrifter/hygieniska-gransvarden-afs-20181-foreskrifter/.

IARC (2012) Chemical Agents and Related Occupations. IARC Monographs on the Evaluation of Carcinogenic Risks to Humans, Volume 100F. International agency for research on cancer, Lyon. ISBN-13 (PDF) 978-92-832-0138-0 [Online]. [Accessed: 24 October 2022]. Available from: https://monographs.iarc.who.int.

IARC (2019) Preamble to the IARC monographs (amended January 2019). International agency for research on cancer, Lyon. [Online]. [Accessed: 24 October 2022]. Available from: https://monographs.iarc.who.int/cards_page/preamble-monographs/.

INDUSTRIAL CHEMICALS ACT (2021) Industrial Chemicals Act Act. No. 12 of 2019 as last amended by Industrial Chemicals Legislation Amendment Act of 01 September 2021 (Federal Register of Legislation). [Online]. [Accessed: 20 October 2022]. Available from: https://www.legislation.gov.au.

INDUSTRIAL SAFETY AND HEALTH ACT (2018) Industrial Safety and Health Act (ISHA) (Act No. 57 of 8 June 1972) as last amended by Act No. 71 of 2018 [Online]. [Accessed: 20 October 2022]. Available from: https://www.japaneselawtranslation.go.jp/en/laws/view/3440#je_toc.

IWANAGA J, SINGH V, TAKEDA S, OGENG'O J, KIM HJ, MORYŚ J, RAVI KS, RIBATTI D, TRAINOR PA, SAÑUDO JR, APAYDIN N, SHARMA A, SMITH HF, WALOCHA JA, HEGAZY AMS, DUPARC F, PAULSEN F, DEL SOL M, ADDS P, LOURYAN S, FAZAN VPS, BODDETI RK, TUBBS RS (2022) Standardized statement for the ethical use of human cadaveric tissues in anatomy research papers: Recommendations from Anatomical Journal Editors-in-Chief. *Clin Anat*, 35: 526-528.

JANCZYK P, WEIGNER J, LUEBKE-BECKER A, KAESSMEYER S, PLENDL J (2011) Nitrite pickling salt as an alternative to formaldehyde for embalming in veterinary anatomy--A study based on histo- and microbiological analyses. *Ann Anat*, 193: 71-75.

KAWATA S, MARUTANI E, HIRAI S, HATAYAMA N, OMOTEHARA T, NAGAHORI K, LI Z, MIYASO H, PIEROH P, NAITO M, ITOH M (2019) Spraying urea solution reduces formaldehyde levels during gross anatomy courses. *Anat Sci Int*, 94: 209-215.

KORF HW, WICHT H, SNIPES RL, TIMMERMANS, JP, PAULSEN F, RUNE G, BAUMGART-VOGT E (2008) The dissection course - necessary and indispensable for teaching anatomy to medical students. *Ann Anat*, 190: 16-22.

LISCHKA MF, WEWALKA G, STANEK G, KRAMMER EB (1979) Vergleichsuntersuchungen der Desinfektionswirkung verschiedener Konservierungslösungen für Anatomieleichen. *Anat Anz*, 146: 295-306.

MINISTY OF EMPLOYMENT AND LABOR NOTICE NO. 2020-48 (2020) Exposure criteria for chemicals and physical factors. [Online]. [Accessed: 22 August 2022]. Available from: https://www.moel.go.kr/skin/doc.html?fn=2020011415460202ae79b648784733aac25448f202f783.hwp&rs=/viewer/BBS/2020/.

NORMA OFICIAL MEXICANA NOM-010-STPS-2014 (2014) NORMA Oficial Mexicana NOM-010-STPS-2014 (Diario Oficial de la Federación). [Online]. [Accessed: 23 August 2022]. Available from: https://www.gob.mx/cms/uploads/attachment/file/680155/NOM-010-STPS-2014.pdf.

OCCUPATIONAL SAFETY AND HEALTH ACT (2020) Occupational Safety and Health Act as last amended of 9 June 2020. [Online]. [Accessed: 24 October 2022]. Available from: https://www.law.go.kr/

OCHS M, MÜHLFELD C, SCHMIEDL A (2012) Präparierkurs: Grundlage ärztlichen Handelns. *Dtsch Arztebl,* 109: A2126-A2127.

ONTARIO REGULATION 833 (2019) Occupational Health and Safety Act, R.R.O. 1990, Reg. 833, Control of Exposure to Biological or Chemical Agents. [Online]. [Accessed: 23 August 2022]. Available from: https://www.ontario.ca/laws/regulation/900833.

OTSUKA S, KAWATA S, NANIZAWA E, HATAYAMA N, HAYASHI S, ITOH M, HIRAI S, NAITO M (2022) Efficacy of urea solution reperfusion to a formalin-embalmed cadaver for surgical skills training. *Anat Sci Int*, 97: 264272.

PABST R (1987) Exposure to formaldehyde in anatomy: an occupational health hazard? *Anat Rec*, 219: 109-112.

PABST R (1993) Gross anatomy: An outdated subject or an essential part of a modern medical curriculum? *Anat Rec*, 237: 431-433.

PABST R, ROTHKÖTTER HJ (1997) Retrospective evaluation of undergraduate medical education by doctors at the end of their residency time in hospitals: Consequences for the anatomical curriculum. *Anat Rec*, 249: 431-434.

PART 1910 - OCCUPATIONAL SAFETY AND HEALTH STANDARDS (2022) Occupational Safety and Health Standards. Standard number 1910. United States Department for Labor - Occupational Safety and Health Association (OSHA). [Online]. [Accessed: 23 August 2022]. Available from: https://www.osha.gov/laws-regs/regulations/standardnumber/1910.

REGULATION (EC) 1272/2008 (2008) Regulation (EC) No 1272/2008 of the European Parliament and of the Council of 16 December 2008 on classification, labelling and packaging of substances and mixtures, amending and repealing Directives 67/548/EEC and 1999/45/EC, and amending Regulation (EC) No 1907/2006. [Online]. [Accessed: 24 October 2022]. Available from: https://eur-lex.europa.eu.

REGULATION S-2.1 R.13 (2022) Chapter S-2.1, r.13 Regulation respecting occupational health and safety last updated to 1 March 2022 (Québec Official Publisher). [Online]. [Accessed: 23 August 2022]. Available from: https://www.legisquebec.gouv.qc.ca/en/document/cr/S-2.1, r. 13.

RISSLER J, HAUKE A (2021) Ergebnisse der Fragebogenerhebung „Maßnahmen der Reduzierung der inhalativen Exposition gegenüber Formaldehyd in Anatomien". Institut für Arbeitsschutz der Deutschen Gesetzlichen Unfallversicherung (IFA), Sankt Augustin.

RIZZOLO LJ, STEWART WB (2006) Should we continue teaching anatomy by dissection when ...? *Anat Rec B New Anat*, 289: 215-218.

SAFE WORK AUSTRALIA (2019) Workplace Exposure Standards for Airborne Contaminants. [Online]. [Accessed: 22 August 2022]. Available from: http://hcis.safeworkaustralia.gov.au/.

SCHMIEDL A (2017) Leichenöffnung und Leichenkonservierung aus anatomischer Sicht. In: Duttge G, Viebahn C (eds.). *Würde und Selbstbestimmung über den Tod hinaus.* Universitätsverlag Göttingen, Göttingen, pp 73-88.

SCHWARZ G, FEIGL G, KLEINERT R. DORN C, LITSCHER G, SANDNER-KIESLING A (2002) Pneumatic pulse simulation ofr teaching peripheral plexus blocks in cadavers. *Anesth Analg,* 95: 1817-1828.

SHICHINOHE T, DATE H, HIRANO S, KOBAYASHI E, IZAWA Y, SHIRAKAWA Y, HIRAMATSU M, MASE M, TANEICHI H, YAGINUMA H, FUJIMOTO T, TSURUMOTO T, WATANABE M, KURITA H, HATO N, KATO T, KANAYAMA H, SUZUKI T, YAMAGUCHI K, TAKEDA Y (2022) Usage of cadavers in surgical training and research in Japan over the past decade. *Anat Sci Int,* 97: 241-250.

SHIRAI T, HAYASHI S, MATSUMURA H, KAWATA S, NAGAHORI K, MIYAWAKI M, IDA Y, ITOH M (2022) Training on skin flap elevation in hand surgery using cadavers embalmed by the saturated salt solution method: effectiveness and usefulness. *Anat Sci Int*, 97: 283-289.

SOCIAAL ECONOMISCHE RAAD (2022) Wettelijke grenswaarde. [Online]. [Accessed: 18 August 2022]. Available from: https://www.ser.nl/nl/thema/arbeidsomstandigheden/Grenswaarden-gevaarlijke-stoffen/Grenswaarden.

SUVA (2021) Grenzwerte am Arbeitsplatz - Aktuelle MAK- und BAT-Werte. [Online]. [Accessed: 18 August 2022]. Available from: www.suva.ch/1903.d.

SUZUKI T, SUZUKI-NARITA M, KUBOTA K, MORI C (2022) Updates on cadaver surgical training in Japan: a systematic facility at Chiba University. *Anat Sci Int*, 97: 251-263.

THE JAPAN SOCIETY OF OCCUPATIONAL HEALTH (2021) Recommendation of occupational exposure limits (2021–2022). *Env Occup Heal Pract*, 3: 1-34.

THE NATIONAL INSTITUTE FOR OCCUPATIONAL SAFETY AND HEALTH (2022) Occupational Health Guidelines for Chemical Hazards - Formaldehyde. [Online]. [Accessed: 23 August 2022]. Available from: https://www.cdc.gov/niosh/docs/81-123/pdfs/0293.pdf?id=10.26616/NIOSHPUB81123.

THIEL W (1992) Die Konservierung ganzer Leichen in natürlichen Farben. *Ann Anat*, 174: 185-195.

THIEL W (2002) Ergänzung für die Konservierung ganzer Leichen nach W. Thiel. *Ann Anat*, 184: 267-269.

THULLNER I, STOCKMANN R, HOHENBERGER L (2015) Formaldehyd in der vorklinischen medizinischen Ausbildung (Anatomie). *Gefahrstoffe - Reinhaltung der Luft*, 75: 219-228.

TRGS 900 (2015) Technische Regeln für Gefahrstoffe TRGS 900 „Arbeitsplatzgrenzwerte". BArBl Issue 1/2006 pp. 41-55, as last amended by GMBl 2015, pp. 139 [No. 7] of 02.02.2015. [Online]. [Accessed: 24 June 2021]. Available from: https://www.gmbl-online.de/.

TRGS 402 (2016) Technische Regeln für Gefahrstoffe; Ermitteln und Beurteilen der Gefährdungen bei Tätigkeiten mit Gefahrstoffen: Inhalative Exposition; TRGS 402. GMBl 2010 pp. 231-253 of 25.2.2010 [No. 12], as last amended by GMBl 2016 pp. 843-846 of 21.10.2016 [No. 43]. [Online]. [Accessed: 24 October 2022]. Available from: https://www.baua.de.

TRGS 900 (2022) Technische Regeln für Gefahrstoffe TRGS 900 „Arbeitsplatzgrenzwerte". BArBl Issue 1/2006 pp. 41-55, as last amended by GMBl 2022, pp. 469 [No. 20-21] of 23.06.2022. [Online]. [Accessed: 24 October 2022]. Available from: www.baua.de.

TÜV NORD UMWELTSCHUTZ GMBH & CO. KG (2016) Bericht über Messungen von Gefahrstoffen in der Luft am Arbeitsplatz in mehreren Bereichen im Institut für Funktionelle und Angewandte Anatomie der Medizinischen Hochschule Hannover.

TÜV NORD UMWELTSCHUTZ GMBH & CO. KG (2017) Bericht über Messungen von Gefahrstoffen in der Luft am Arbeitsplatz im Bereich eines Präpariersaales im Institut für Funtionelle und Angewandte Anatomie der Medizinischen Hochschule Hannover.

UNITED NATIONS (2021) Globally Harmonized System of Classification and Labelling of Chemicals (GHS) Rev. 9, 9th edn. United Nations.

VORSTENBOSCH MA, KLAASSEN TP, DONDERS AR, KOOLOOS JG, BOLHUIS SM, LAAN RF (2013) Learning anatomy enhances spatial ability. *Anat Sci Educ*, 6: 257-262.

WASCHKE J, BERGMANN M, BRÄUER L, BRENNER E, BUCHHORN A, DEUTSCH A, DOKTER M, EGU DT, ERGÜN S, FASSNACHT U, FIETZ D, GUNDLACH S, HEERMANN S, HIRT B, KUGELMANN D, MÜLLER-GERBL M, NEISS W, NIMTSCHKE U, PLENDL J, PRETTERKLIEBER M, REDIES C, SCAAL M, SCHMIDT MHH, SCHMIEDL A, SCHNITTLER HJ, SCHOMERUS C, SEBESTÉNY T, SPITTAU B, STEINIGER B, TSCHERNIG T, UNVERZAGT A, VIEBAHN C, VOIGT E, WEIGNER J, WEYERS I, WINKELMANN A, WINKLER M, PAULSEN F (2019) Recommendations of the working group of the Anatomische Gesellschaft on reduction of formaldehyde exposure in anatomical curricula and institutes. *Ann Anat*, 221: 179-185.

WEDEL T, ACKERMANN J, HAGEDORN H, METTLER L, MAASS N, ALKATOUT I (2019) Educational training in laparoscopic gynecological surgery based on ethanol-glycerol-lysoformin-preserved body donors. *Ann Anat*, 221: 157-164.

WORKPLACE SAFETY AND HEALTH ACT 2006 (2022) Workplace Safety and Health Act (Chapter 354A, Section 65), Workplace Safety and Health (General Provisions) Regulations of 01 March 2006 (Singapore Statutes Online) as last amended by S26/2022 of 13 January 2022 (Singapore Statutes Online). [Online]. [Accessed: 22 August 2022]. Available from: https://sso.agc.gov.sg/Act/WSHA2006.

WORKSAFE (2022) Workplace exposure standards and biological exposure indices. [Online]. [Accessed: 23 August 2022]. Available from: https://www.worksafe.govt.nz/topic-and-industry/monitoring/workplace-exposure-standards-and-biological-exposure-indices/.

Congenital cervical teratoma – an amalgamation of embryology with clinical findings

Fariha Sabeen

Mahatma Gandhi Memorial Medical College, Jamshedpur, Jharkhand, India

SUMMARY

Teratoma means "A malformed body part of a monster" in Greek. A cervical teratoma is a very rare congenital tumor in the neck. These tumors tend to be large, disfiguring masses – partly solid and partly fluid. They make it impossible for a newborn to breathe upon birth. Knowledge of basic embryology of the brachial apparatus is necessary to understand neck malformations and congenital abnormalities. Here, a recent observation of this exceptional case is described. A pregnant woman, gravida 2, presented with pain abdomen in the 37th week of gestation. A male, living baby was delivered by caesarean section. A well-defined mass was present in the anterior neck region. A diagnosis of giant congenital cervical teratoma with airway compromise was made. The baby was intubated but could not survive. The objective of this study is the significance of a thorough knowledge of anatomy and embryology to prevent any late diagnosis or misdiagnosis. This report aims to create awareness about embryological development of a fetus to enhance the clinical recognition of this rare disorder, to highlight their occurrence in our locale, and to reiterate the associated management challenges in resource-limited settings. The present case highlights the importance of regular antenatal checkups, with timely ultrasounds, so that such congenital defects can be diagnosed prenatally and their management can be planned accordingly.

Key words: Teratoma – Neck – Embryology – Fetus – Brachial cleft – Congenital anomaly

INTRODUCTION

Congenital cervical teratomas are extremely rare germ cell tumors of the neck, composed of tissues derived from at least two of the three embryonic germ layers, but foreign to the anatomic site of occurrence (Benhoummad et al., 2021). These tumors are benign but may lead to serious consequences. Congenital cervical teratomas of the neck region compress the structures in the neck region and make breathing difficult for the baby (Benhoummad et al., 2021). Teratoma of the head and neck are interesting because of their obscure origin, unpredictable behavior and often dramatic clinical presentation. Teratomas are embryological neoplasms that arise when totipotent germ cells give rise to more or less organoid masses in which tissues are derived from all the three blastomeric layers (ectoderm, endoderm and meso-

Corresponding author:
Dr Fariha Sabeen, Master of Surgery (MS) Anatomy. Mahatma Gandhi Memorial Medical College, Jamshedpur, Jharkhand, India. E-mail: dfariha@gmail.com

Submitted: December 27, 2022. **Accepted:** February 4, 2023

https://doi.org/10.52083/DHMY7841

derm) (Alharbi et al., 2017). Cervical teratomas are rare benign tumors consisting of 3% of all teratomas and occur one in every 20,000-40,000 live births (Mohammed et al., 2021). These neoplasms are asymmetrical with both cystic and solid areas.

Knowledge of basic embryology of the brachial apparatus helps to understand neck malformations and congenital abnormalities. During the third week of development, the flat trilaminar embryo undergoes a series of complex folds that result in the formation of a cylindrical embryo. During this time, the laterally placed clefts, known as branchial clefts appear. These clefts are due to flexion folds of the fetus within the amniotic cavity. The basic tissues of development within the head and neck (ectoderm, endoderm, mesoderm, neuroepithelium) become organized into the pharyngeal apparatus, also known as the branchial apparatus, which is the forerunner of the head and neck structures.

Cervical teratomas often occur on the anterolateral surface of the neck, extending midline from the thyroid gland, as far as 12 cm in their longest axis; hence, unsuspected obstructive fetal giant neck masses often prove fatal, because of an inability to secure the airway and ventilate the baby upon delivery, which leads to hypoxia and acidosis (Mohammed et al., 2021).

Current evidence suggests that most teratomas are due to abnormal differentiation of fetal germ cells that arise from the fetal yolk sac. Normal migration of these germ cells may cause gonadal tumors, while abnormal migration produces extra gonadal tumors. Chromosomal abnormalities that have been reported are trisomy 13, ring X chromosome mosaicism with inactive ring X

Fig. 1.- A male baby with congenital cervical teratoma.

chromosome, gene mutation or abnormalities in early embryonic development (Mohammed et al., 2021). The etiology can be also aberrant fertilization, abnormal meiotic division, or even asexual development of an unfertilized ovum (Azam et al., 2021). Giant neck masses can obstruct the airway and cause serious ill effects, which are not compatible with life after delivery.

CASE REPORT

A pregnant woman of gravida 2, aged 28 years, presented with severe pain abdomen in the 37th week of gestation. On examination, the abdomen was over-distended, with fundal height of 40 weeks. As she came from a rural background, there was no history of any previous ultrasounds. There was history of a previous abortion. An ultrasound examination was done immediately. Her ultrasound report revealed a single, viable, cephalic fetus with a cystic and solid mass in the neck region. The length and breadth of the neck mass were 9.2 cm and 6.9 cm respectively. Both solid and cystic portions containing blood vessels were present. Moderate polyhydramnios was detected. No other congenital abnormality was detected. The parents were counseled about the outcomes, their consent was received and a decision was taken to proceed further with the EXIT (Extra Uterine Intrapartum Treatment) procedure.

A multidisciplinary team was formed which included anaesthetic, obstetricians, pediatric surgeon and a radiologist. A male, living baby weighing 1.8 Kg was delivered by caesarean section. A well-defined, predominantly solid lesion was present in the anterior neck region (Fig. 1). The baby was apneic, centrally cyanosed with a heart rate (HR) of 50 beats per minute. Apgar scores were 1 and 2 at 1 and 2 minutes. A diagnosis of giant congenital cervical teratoma with airway compromise was made. The baby was shifted to NICU (Neonatal Intensive Care Unit) and intubated immediately with much difficulty. The mass was irregularly-shaped with visible superficial vessels and spread to the lower half of face, including the mandible and both temporomandibular joints. A Cervicofacial Computerised Tomography (CT) scan was planned to enquire about any infiltrations, but unfortunately, he only survived for a few hours and then died. The parents were referred for Genetic Counseling.

DISCUSSION

Perinatal mortality is very high in cases of cervical teratoma. A large cervical teratoma usually causes airway obstruction, and any delay in treatment can cause 80% to 100% mortality (Azam et al., 2021). A congenital cervical teratoma is difficult to diagnose in utero, because of the similarities with other fetal neck masses such as cystic hygroma., branchial cyst, hemangioma or lymphangioma (Azam et al., 2021). To prevent such misdiagnosis, thorough knowledge of anatomy and embryology is crucial. Embryologically, brachial cleft cysts are developed by incomplete involution of brachial cleft structures; hence, they are present more posterior and lateral in position. Similarly, cystic hygroma, lymphangioma and hemangioma are also present laterally. On the other hand, cervical teratomas are usually found in mid-line structures such as anterior neck region, pineal body and supra-sellar space (Uchiyama et al., 1995).

CONCLUSION

The present case study is a compelling amalgamation of knowledge of embryology with radiology, obstetrics and pediatrics. Although rare, cervical teratomas can be diagnosed in utero. This particular case study highlights the importance of antenatal checkups along with anatomical anomaly scan. The importance of a skilled multidisciplinary team with complete understanding of the anatomical relations of the neoplasm is also emphasized. To ensure a successful management, careful planning and coordination is the key. The majority of these tumors are benign and cured by complete resection of the mass during neonatal period (Peiro et al., 2016). The author recommends a comprehensive prenatal evaluation including conventional ultrasounds, doppler, and echocardiography along with anatomical anomaly scan to be made compulsory before 20 weeks of gestation. Antenatal counseling helps the parents to better understand the natural history, fetal intervention and perinatal management[6]. Late diagnosis, lack of pre-plan-

ning and ignorance can lead to both physical and mental turmoil. Counseling, serial imaging, and well-planned deliveries with EXIT procedure are the mainstay of management (Mohammed et al., 2021; Azam et al., 2021; Uchiyama et al., 1995). Favorable prognosis depends on prenatal diagnosis by radiological examinations and proper management.

ACKNOWLEDGEMENTS

The author would like to express thanks to the Department of Obstetrics and Gynecology. The author also owes a big thank you to colleagues at the Department of Pediatrics for their great help whenever needed.

REFERENCES

ALHARBI ST, ALSAADI AS, YOSUPH AU, ABDULHAMEED FD, ARKOUBI MM (2017) Diagnostic imaging and surgical management of congenital cervical teratoma. *J Taibah Univ Med Sci,* 13(1): 83-86.

AZAM H, HANIF MA, KHAN MI, MASOOD A, HASHMI MU (2021) Cervical cystic teratoma: unusual cause of airway obstruction in the pediatric population. *Cureus,* 13(10): e19166.

BENHOUMMAD O, CHEHBOUNI M, ROCHDI Y, RAJI A (2021) Congenital cervical teratoma: about a case. *Eur J Med Health Sci*, 3(3): 35-38.

MOHAMMED SDE, SALAHELDIEN R, AHMED B (2021) Fetus diagnosed with cervical teratoma delivered by EXIT procedure (Extra Uterine Intrapartum Treatment). *MedCrave Online J Women's Health*, 10(4): 105-107.

PEIRO JL, SBRAGIA L, SCORLETTI F, LIM FY, SHAABAN A (2016) Management of fetal teratomas. *Pediatr Surg Int,* 32(7): 635-647.

UCHIYAMA M, IWAFUCHI M, NAITOH S, MATSUDA Y, NAITOH N, YAGI M, HOSHI E, NONOMURA N (1995) A huge immature cervical teratoma in a newborn: report of a case. *Surg Today,* 25(8): 737-740.

The clinical and operative impact of the hexafurcation of the celiac trunk - Report of an extremely rare case

Athina Anagnou[1], Alexandra Pentheroudaki[2], Evangelos Lolis[1]

[1] First Department of Surgery, General Hospital of Chania 'Saint Georgios', Greece

[2] Intensive Care Unit, General Hospital of Chania 'Saint Georgios', Greece

SUMMARY

The celiac trunk is a main splanchnic artery that supplies the intra-abdominal organs of the upper gastrointestinal system. Anatomic variations of the celiac trunk are encountered in 10% of the population, but can pose challenges to many surgical and interventional procedures. We present here a case of hexafurcation of the celiac trunk discovered preoperatively after image staging for gastric cancer. The branches of the celiac trunk were: left and right inferior phrenic artery, arc of Buhler along with the common pattern of common hepatic, left gastric and splenic artery. The highlight of the case is the rarity of this specific pattern, which is seen in less than 1% of the population, and also the presence of an anastomotic path, the arc of Bühler, as a branch of the celiac trunk. It is evident that the variations of the celiac trunk play a major role in operations of the upper abdomen, radiological interventional procedures and other uncommon cases. Thus, the surgeon must be aware of these variations and their frequency to avoid complications. Also, any physician should report any variation discovered, accidentally or not, to help the literature to be updated.

Key words: Computed tomography – Arc of Bühler – Inferior phrenic arteries variations – Celiac trunk variations – Celiac trunk hexafurcation

INTRODUCTION

The celiac artery, most commonly known as celiac trunk (CT), is one of the main branches of the abdominal aorta, which originates at the level of T12. It is surgically significant as a main splanchnic artery; thus, it has been studied thoroughly (Lipshutz, 1917; Adachi, 1928; Panagouli et al., 2013; Santos et al., 2018; Whitley et al., 2020). The common branching pattern of the celiac artery is the tripus Halleri, which is comprised of the common hepatic, the left gastric and the splenic artery (Panagouli et al., 2013). Anatomical variations of the celiac trunk include variants of the tripod (total absence, bifurcation), aberrant branches (more than three branches of CT), and a common origin with the superior mesenteric artery (celiacomesenteric trunk), or together with the inferior mesenteric artery (celiaco-bimesenteric trunk) (Adachi, 1928; Panagouli et al., 2013). Herein, we present an extremely rare case of hexafurcation of

Corresponding author:
Athina Anagnou. First Department of Surgery, 5th Floor, General Hospital of Chania 'Saint Georgios', Chania-73100 Greece. Mobile: +306937224147. E-mail: athinanagnou@gmail.com

Submitted: January 25, 2023. **Accepted:** February 25, 2023

https://doi.org/10.52083/VQME8067

the CT, where two parietal branches of the abdominal aorta derived from the CT and also an arch of Buhler (AOB), which is a significant anastomotic pathway, was detected.

CASE REPORT

An 82 years-old male patient was diagnosed with a distal (antrum) gastric cancer. He had a computed tomography (C/T) of the abdomen as part of the staging procedure. The C/T scan revealed a celiac trunk with six branches: common hepatic artery, left gastric artery, splenic artery, left and right inferior phrenic arteries and arc of Bühler (Figs. 1-4). The patient underwent an open subtotal gastrectomy with D2 lymph node dissection and a Roux-en-Y reconstruction. The left gastric artery was ligated for oncologic purposes during lymph node dissection. However, the aberrant branches of the CT were recognized and preserved. There was no intraoperative complication.

His postoperative period was uneventful.

COMMENTS

The variations of the CT are encountered in approximately 10% of the population according to the latest systematic reviews (Panagouli et al., 2013; Whitley et al., 2020). Many different classification systems of the configuration and branching patterns of the CT have been reported, the one by Adachi (1928) being the most frequently used. However, it seems that no existing system covers all the variations discovered, and there is an ongoing effort to create a universal classification of CT variations (Panagouli et al., 2013). In previous century, many large cadaveric studies established the common human vascular anatomy and started to mention variations unknown until then, despite the wide range of the percentages of these variations (Bühler, 1904; Tandler, 1904; Lipshutz, 1917; Adachi, 1928). Nowadays, the study method of the variations has shifted from cadaveric studies to studies via the multi-detector computed tomography (MDCT). Notwithstanding that a few studies comparing these two methods exist, it seems that MDCT has allowed for much larg-

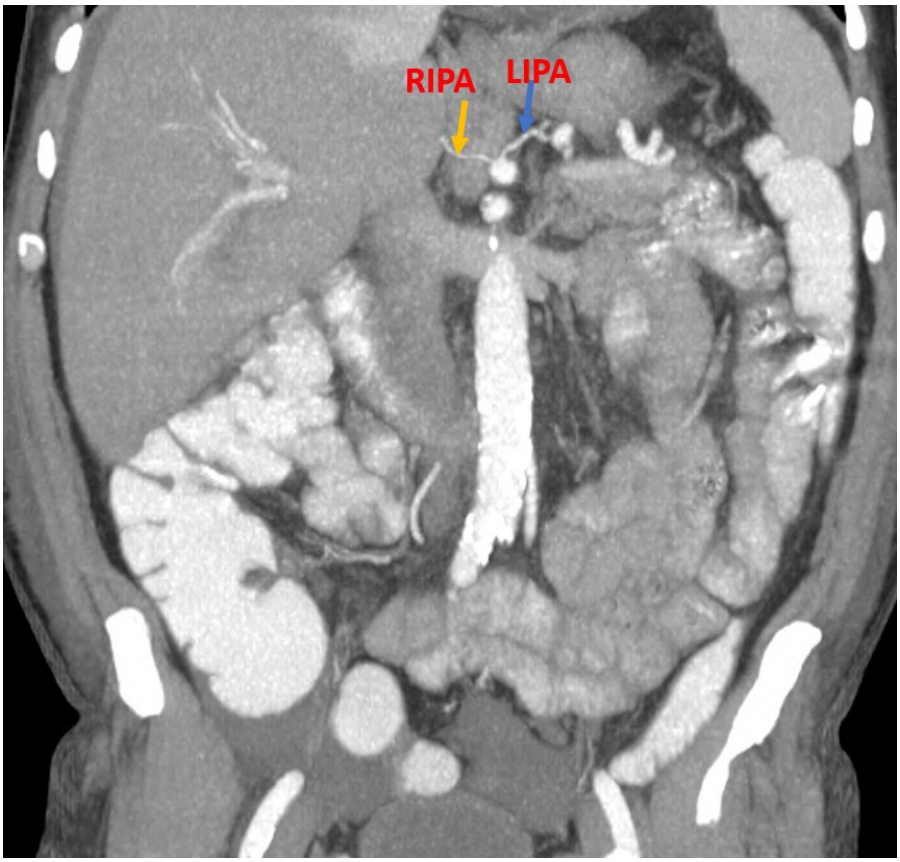

Fig. 1.- MDCT coronal view showing the right inferior phrenic artery (RIPA) (yellow arrow) and the left inferior phrenic artery (LIPA) (blue arrow) arise from the celiac trunk.

er study populations in fewer time and perhaps more accurate percentages, with the downside of the omission of variations beyond MDCT's image quality and the selection bias of the computer tomography's study (Marco-Clement et al., 2016; Whitley et al., 2020).

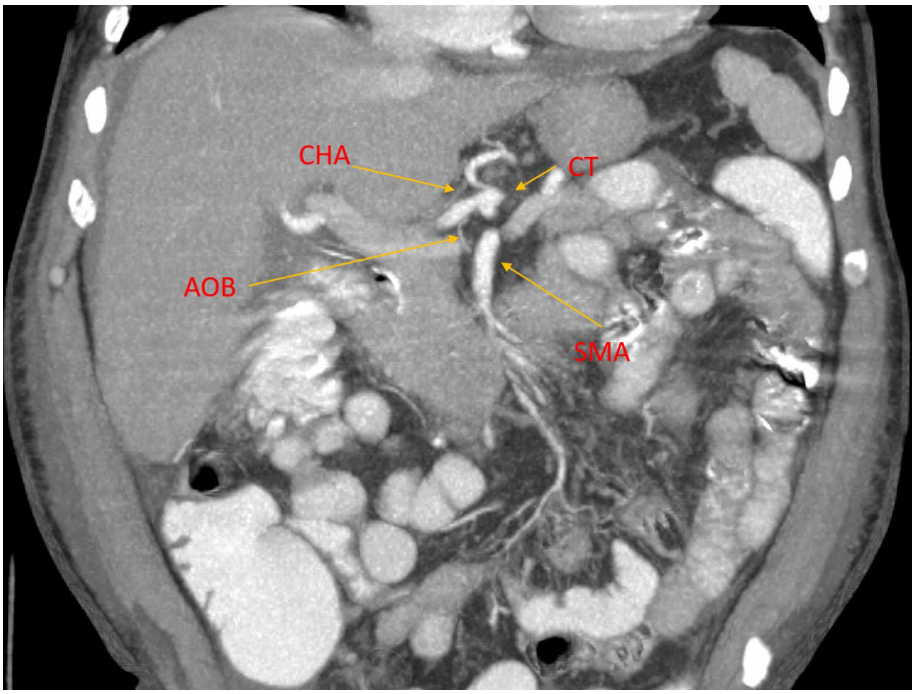

Fig. 2.- MDCT coronal view showing the arc of Bühler (AOB) derived from the celiac trunk (CT) and its anatomical correlations with the common hepatic artery (CHA) and the superior mesenteric artery (SMA).

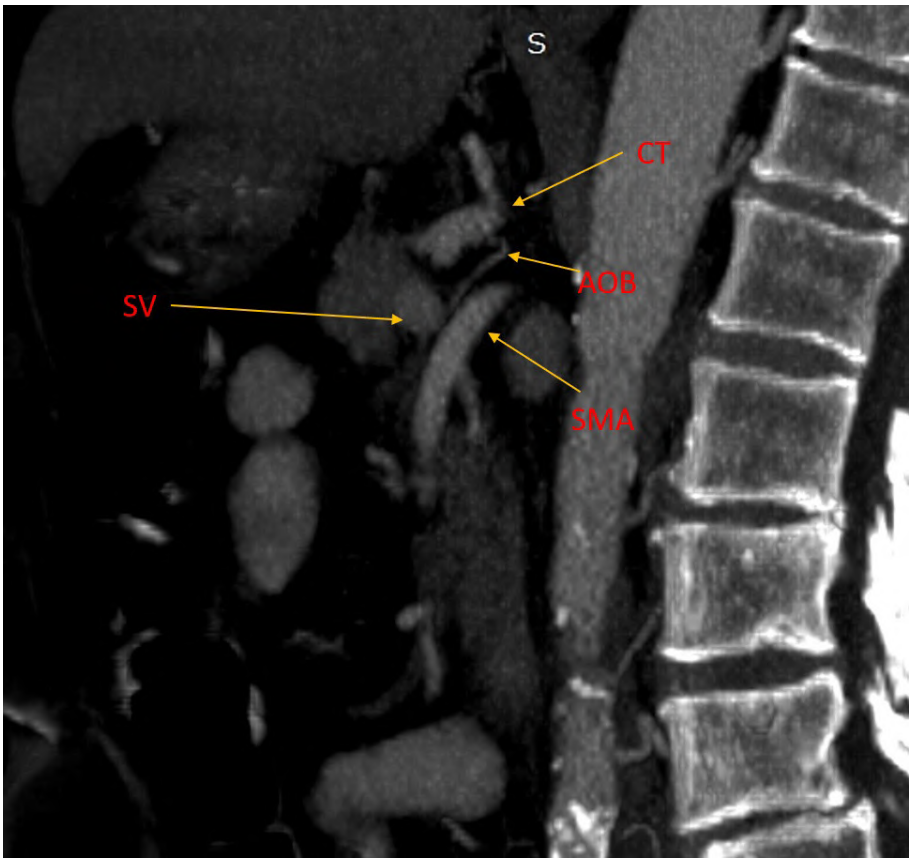

Fig. 3.- MDCT sagittal view showing the arc of Bühler (AOB) with its correlation with the splenic vein (SV). SMA: superior mesenteric artery.

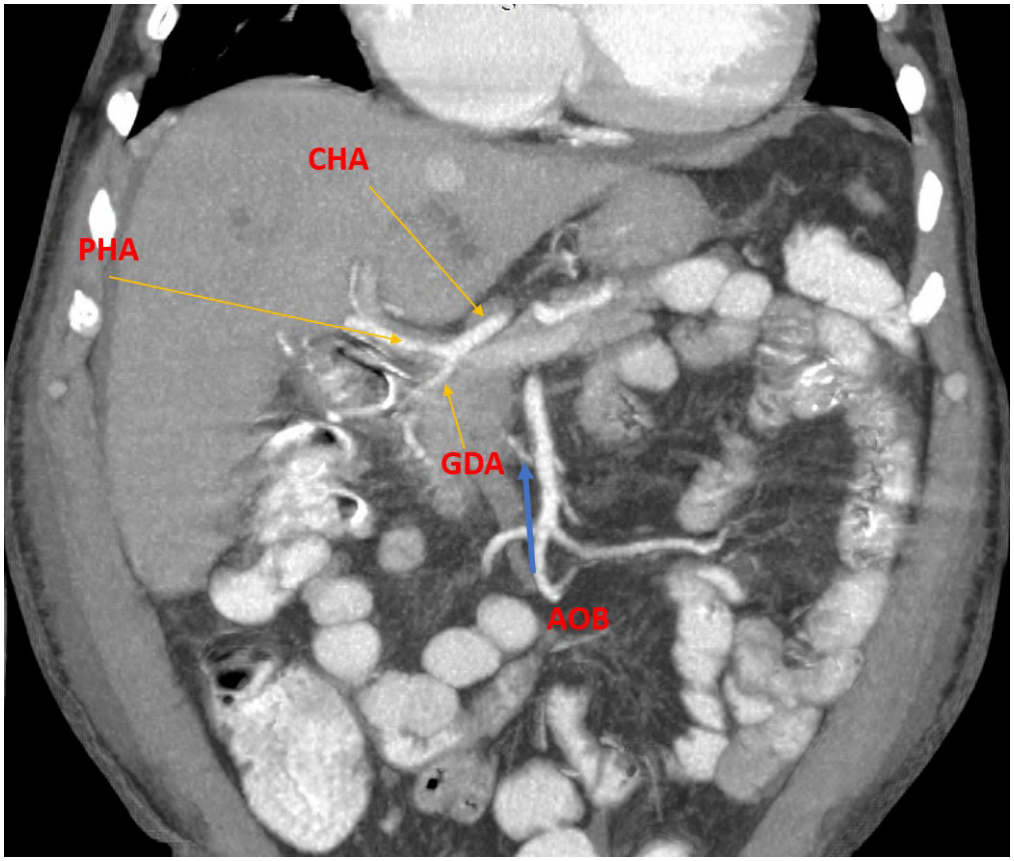

Fig. 4.- MDCT coronal view showing the arc of Bühler (AOB) (blue arrow) with its correlations with the common hepatic artery (CHA), the proper hepatic (PHA) and the gastroduodenal artery (GDA).

The anatomical variations of the CT include an incomplete celiac trunk (missing one of the branches of the tripod, following different patterns), the absence of the tripod, additional branches and a common trunk with other major arteries such as the superior mesenteric artery and the inferior mesenteric artery (Panagouli et al., 2013).

Additional branches of the celiac trunk may be parietal and visceral. The parietal branches include the inferior phrenic arteries (Lipshutz, 1917; Adachi, 1928; Whitley et al., 2020). The inferior phrenic artery may arise as a common trunk, the common inferior phrenic artery (CIPA), or as two individual arteries, the right and left inferior phrenic arteries (RIPA and IPA) (Whitley et al., 2021). They mainly supply the diaphragm, but may also contribute to the arterial supply of the esophagus, stomach, spleen, suprarenal glands, liver, inferior vena cava and adjacent structures (Whitley et al., 2020). The CIPA, according to the latest systematic reviews, is present in approximately 25-29% and most commonly originated from the aorta (57%) (Whitley et al., 2021). Two individual phrenic arteries are seen in about 70-75% of the cases. The origin of the RIPA is primarily the aorta (50%) and the CT (35%), and secondarily the right renal artery and the left gastric, whereas the origin of the LIPA is the aorta and the celiac trunk (appr. 46% each) (Marco-Clement et al., 2016). The concurrent origin of RIPA and LIPA from the celiac trunk is seen in 14%.

The variation of the inferior phrenic arteries can play a major role in some cases of an upper gastrointestinal bleeding due to its contribution to the arterial supply to the esophagogastric junction (Whitley et al., 2021). Also, these arteries could be the cause of extra-bronchial massive hemoptysis, and the lack of awareness could lead to rebleeding after bronchial embolization (Yoon et al., 2002). Also, this may be of great clinical significance in cases of transcatheter arterial chemoembolization (TACE) for inoperable hepatic malignancy (HCC), as the inferior phrenic arteries could be among the tumor-feeding arteries and thus should be embolized for palliative reasons (Whitley et al., 2021).

The arc of Bühler is a rare variation, which was first described from Buhler in 1904 (Buhler, 1904). It anastomoses the CT with the superior mesenteric artery and is encountered in less than 3% of the population, although its exact incidence is still unknown (Saad et al., 2005; Michalinos et al., 2018). The usual anastomoses between the celiac trunk (CT) and the superior mesenteric artery (SMA) are via pancreaticoduodenal arcades and dorsal pancreatic artery (Michalinos et al., 2018). The arc of Bühler (AOB) is an alternative arterial connection of these major arteries, and two major theories have been used to explain its origin. The Mac Kay arc theory suggested that in a 5 mm embryo the distribution of aorta branches is metameric, with each metamere giving rise to 3 pairs of branches, uniting in an arch: the posterior (vertebroparietal), the lateral (genitourinary) arch and the anterior (visceral) arch. During embryonic development variant processes such as fusion and obliteration of branches and development of the digestive tube result in the adult's common anatomy (celiac trunk, superior and inferior mesenteric arteries) (Saad et al., 2005; Douard et al., 2006; Michalinos et al., 2018). The Tandler's longitudinal anastomosis theory, first described by Tandler (1904), is generally used to explain the most of the celiac-mesenteric an intermesenteric anastomoses between splanchnic branches (Lipshutz, 1917; Michalinos et al., 2018). So, AOB is usually thought to be an embryonic remnant due to the failure of regression of the ventral anastomosis between the anlages of the celiac trunk and the superior mesenteric artery (Saad et al., 2005; Douard et al., 2006; Michalinos et al., 2018).

The arc of Bühler is of significant clinical importance as it forms a collateral pathway for arterial perfusion in case of mesenteric or liver ischemia and could be a life-saving variation (Michalinos et al., 2018). Especially, during pancreatic oncologic operations where the ligation of the gastroduodenal artery is mandatory, the presence of the arc acts as an alternative arterial supply to the liver especially if celiac stenosis coexists (McNulty et al., 2001; Manta et al., 2022b; Schumacher et al., 2022). Liver transplantation could also benefit from this arc in the presence of stenosis in the major splanchnic arteries (Incarbone et al., 2021). Also, even mesenteric ischemia due to an aortic dissection could be prevented due to the presence of the Arc of Bühler (Schizas et al., 2020). This arc, augmenting the anastomotic channels between the two arteries, is a positive predictor of adequate blood supply to organs (McNulty et al., 2001; Saad et al., 2005; Douard et al., 2006; Michalinos et al., 2018; Schizas et al., 2020). In interventional radiology it can provide direct access to SMA through the CT and vice versa for diagnostic and even therapeutic reasons (Michalinos et al., 2018).

The clinical significance of the hexafurcation of the CT is evident, during liver, pancreatic, esophagogastric surgery, liver transplantations, organ procurements for transplantation such as liver, pancreas, small bowel or multivisceral ones, lymph node dissection for oncological procedures and vascular surgery (abdominal aortic aneurysm, or even aortic dissection) (McNulty et al., 2001; Saad et al., 2005; Douard et al., 2006; Michalinos et al., 2018; Schizas et al., 2020; Manta et al., 2022b; Schumacher et al., 2022). These variations could complicate the aforementioned procedures with bleeding because of inadvertent injury if the surgical team is not aware of them. Moreover, the effort to avoid any injury to them, may prolong any surgical procedure. In addition, these variations could pose a challenge during the angiographic evaluation of a gastrointestinal bleeding or hemoptysis and the embolism of a tumor or a bleeding lesion (Michalinos et al., 2018).

The importance of this case report relies on the fact that the hexafurcation of the celiac trunk is a rare variant. According to the latest literature, the six-branch pattern of celiac trunk is seen in less than 1% (Panagouli et al., 2013; Manta et al., 2022a). Moreover, this case has a specific clinical impact as, additionally to the two inferior phrenic arteries, the sixth branch of the celiac trunk is not a splanchnic branch but an anastomotic path. The celiac trunk and the superior mesenteric artery have regularly anastomotic channels, but the uniqueness of this case is found in the direct connection of these large arteries with the arc of Bühler. To the best of our knowledge, this specific pattern has been reported only once before in literature with the arc of Bühler inserting into the

first jejunal artery, and not into the trunk of the superior mesenteric artery as we have mentioned here (Manta et al., 2022a).

Despite the well-established importance of AOB, there is still no mention of it in the current textbooks of anatomy (McNulty et al., 2001). Furthermore, the embryological hypothesis has not been proved yet (Michalinos et al., 2018). Surgeons and radiologists around the world have not concluded a commonly agreed system of classification of vascular variations (Panagouli et al., 2013). Pre-operative staging even for the most obscure areas of upper abdomen such as pancreas does not universally include MDCT angiography for establishment of vascular pattern. So, there is still work to be done and this case underline this fact.

CONCLUSION

It is obvious that the variations of the celiac trunk have an important clinical impact especially on the operative approach of the upper abdomen, and the surgeon should be aware of them. Thus, it is crucial to establish a pre-operative investigation which may include evaluation of the celiac trunk, in order to map out a better intra-operative plan. It is important and extremely useful to report any new variants discovered, accidentally or not, because the knowledge of CT branching pattern could improve the therapeutic results for a wide range of surgical and radiological, abdominal and vascular procedures.

AUTHORS' CONTRIBUTION

A Anagnou: Manuscript elaboration, data analysis, literature search and documentation. A. Pentheroudaki: Data management and collection. E. Lolis: Original idea, manuscript editing and critical review. All the authors read and approved the final manuscript.

REFERENCES

ADACHI B (1928) Das Arteriensystem der Japaner, Band II. Verlag der Kaiserlich-Japanischen Universitat zu Kyoto and Maruzen Publishing Co, Kyoto, pp 18-65.

BÜHLER A (1904) Über eine Anastomose zwischen den Stammen der Art. coeliaca und der Art. mesenterica superior. *Morph Jahrb*, 32: 185-188.

DOUARD R, CHEVALLIER JM, DELMAS V, CUGNENC PH (2006) Clinical interest of digestive arterial trunk anastomoses. *Surg Radiol Anat*, 28(3): 219-227.

INCARBONE N, DE CARLIS R, CENTONZE L, LAUTERIO A, DE CARLIS L (2021) Discovery of a rare variant of the arc of Bühler during liver procurement. *Exp Clin Transplant*, 19(12): 1345-1347.

LIPSHUTZ B (1917) A composite study of the coeliac axis artery. *Ann Surg*, 65(2): 159-169.

MANTA BA, RUSU MC, JIANU AM, ILIE AC (2022a) Hexafurcated coeliac trunks, trifurcated common hepatic artery, and a new variant of the arc of Bühler. *Folia Morphol (Warsz),* 81(2): 365-371.

MANTA BA, RUSU IR, RUSU MC (2022b) An arc of Bühler variant. *Morphologie,* 106(353): 136-140.

MARCO-CLEMENT I, MARTINEZ-BARCO A, AHUMADA N, SIMON C, VALDERRAMA JM, SANUDO J, ARRAZOLA J (2016) Anatomical variations of the celiac trunk: cadaveric and radiological study. *Surg Radiol Anat*, 38: 501-510.

MCNULTY JG, HICKEY N, KHOSA F, O'BRIEN P, O'CALLAGHAN JP (2001) Surgical and radiological significance of variants of Bühler's anastomotic artery: a report of three cases. *Surg Radiol Anat,* 23(4): 277-280.

MICHALINOS A, SCHIZAS D, NTOURAKIS D, FILIPPOU D, TROUPIS T (2019) Arc of Bühler: the surgical significance of a rare anatomical variation. *Surg Radiol Anat,* 41: 575-581.

PANAGOULI E, VENIERATOS D, LOLIS E, SKANDALAKIS P (2013) Variations in the anatomy of the celiac trunk: A systematic review and clinical implications. *Ann Anat,* 195(6): 501-511.

SAAD WE, DAVIES MG, SAHLER L, LEE D, PATEL N, KITANOSONO T, SASSON T, WALDMAN D (2005) Arc of Buhler: Incidence and diameter in asymptomatic individuals. *Vasc Endovascular Surg*, 39(4): 347-349.

SANTOS PVD, BARBOSA ABM, TARGINO VA, SILVA NA, SILVA YCM, BARBOSA F, OLIVEIRA ASB, ASSIS TO (2018) Anatomical variations of the celiac trunk: a systematic review. *Arq Bras Cir Dig,* 31(4): e1403.

SCHIZAS N, VASILIOS P, NIKI L, ARGYRIOU EO, THEODOROS K, ARGIRIOU M (2020) Arc of Buhler: A lifesaving anatomic variation. A case report. *J Vasc Bras,* 19: 20200045.

SCHUMACHER L, ALBRECHT HC, GRETSCHEL S (2022) A significant vascular variant in oncologic pancreaticoduodenectomy: the arc of Buhler. *Surg Case Rep,* 8(37).

TANDLER A (1904) Uber die Varietaten der Arteria coeliaca und deren Entwicklung. *Anat Hefte*, 25: 472-500.

WHITLEY A, OLIVERIUS M, KOCIÁN P, HAVLŮJ L, GÜRLICH R, KACHLÍK D (2020) Variations of the celiac trunk investigated by multidetector computed tomography: Systematic review and meta-analysis with clinical correlations. *Clin Anat*, 303(8): 1249-1262.

WHITLEY A, KŘEČEK J, KACHLÍK D (2021) The inferior phrenic arteries: A systematic review and meta-analysis. *Ann Anat*, 235: 151679.

YOON W, KIM JK, KIM YH, CHUNG TW, KANG HK (2002) Bronchial and nonbronchial systemic artery embolization for life-threatening hemoptysis: a comprehensive review. *Radiographics,* 22(6): 1395-1409.

Analysis of the use of human remains as teaching materials in higher education: examining differing opinions between population subgroups

Georgina A. Goodison [1,2], Christopher Aris [1,2]

[1] *Department of Archaeology, University of Sheffield, UK*
[2] *School of Chemical and Physical Sciences, Keele University, UK*

SUMMARY

Human components have been used as teaching resources for centuries. This study aimed to investigate the ethics and practicality surrounding this resource by analysing the opinions of students and professionals with exposure to human remains. Three questions were posed relating to the use of synthetic cadavers, the use of replicated bones, and the overall opinion regarding the ethics of using human material in teaching. These questions were disseminated through a survey aimed at students and professionals working with/studying using human remains in the UK, with 477 respondents. Kruskal-Wallis, Jonckheere Terpstra and Mann-Whitney U tests were used to identify any differences within the participants according to age and gender. Overall, all groups lent towards supporting the use of human remains in teaching. However, significant differences were noted between gender groupings and age categories, in particular between the 21-40 and 61+ age categories regarding the use of cadavers in teaching, and between male and female groups regarding the use of synthetic cadavers and replica bone. Even though multiple differences were noted, there was a consensus that use of human remains in teaching is ethical. The differences related to the degree to which materials should be used across different fields, with medical students and professionals believing that they should have sole access to real materials, whilst both archaeology and heritage professionals and non-professionals believed that all subjects should have access if it will help with students' education.

Key words: Anatomy – Bone – Body Donors – Ethics – Human Remains – Pedagogy

INTRODUCTION

The use of human remains used as a pedagogical aid is not a recent concept, with the earliest documentation dating to 5,000 years ago (Loukas et al., 2011). With human remains once belonging to the living, they hold a clear "significance within all human societies" (Mays, 2010). It has been fur-

Corresponding author:
Georgina Goodison. Lennard-Jones School of Chemical and Physical Sciences, Lennard-Jones Building, Keele University, Staffordshire ST5 5BG, UK. E-mail: g.goodison@keele.ac.uk

Submitted: January 10, 2023. **Accepted:** February 16, 2023

https://doi.org/10.52083/EWHY1593

ther stated that "British attitudes to dead bodies are ambivalent, contradictory and volatile" (Parker Pearson, 2003), whereas people are more able to detach themselves from the sight of skeletons, perhaps forgetting they were living people (Swain, 2002; Parker Pearson, 2003). This could lead to skeletal remains being viewed as components rather than an individual's remains, whilst fleshed bodies are easier to regard as human and are less likely to be seen as a series of components, and so, pedagogical aids. This potentially creates a divide in opinion on the use of human remains as learning resources between the public and those who interact with the dead on a daily basis. Even though attitudes vary towards different forms of human remains, their utility in teaching is clear.

While a pedagogical analysis has clear value, ethics must also be considered. In the present day, many countries have legislation for the care and treatment of human remains, including the United States, New Zealand, Australia and the United Kingdom (Gazi, 2014). It is worth noting that, although the United Kingdom still has a large Christian population, it is now a multi-faith environment, and unlike other countries, it is no longer deemed to have a "native" population (Coates, 2021). Whilst other countries have specific laws relating to the handling and display of the remains of native peoples – such as the Native American Graves Protection and Repatriation Act in the United States (White and Folkens, 2005; NAGPRA, 2021) – no such laws exist in the United Kingdom. However, the Honouring the Ancient Dead organisation introduced an initiative to protect remains determined to be from ancient British and non-Christian cultures (HAD, 2021). It also seeks to promote ethical and respectful interaction with human remains of any age. This national, as well as global, move towards more legislative support of ethical practice when handling human remains highlights the need for a review of where ethical opinion lies within the British community of those working with such remains.

The history of human remains as teaching materials

The study of human anatomy was first undertaken in the 3rd century BC in Alexandria, but was only permitted briefly under the Ptolemaic pharaohs (Standring, 2016). It was later, in Renaissance Italy, that the study of human anatomy, and thus dissection, became more widely acceptable (Papa and Vaccarezza, 2013). Legalised in the United Kingdom in the 16th century to continue on the same footing as European counterparts, the Barber-Surgeon Act of 1540 allowed for the bodies of four criminals to be given to medical schools for dissection each year (Thomas, 2006). However, with the introduction of more institutions, there was a greater demand for cadavers; thus, in 1752 the Murder Act was passed, stating that executed murderers could be used for public dissection (Cain, 2017; Tarlow and Battell Lowman, 2018). Again, there was an increased requirement for bodies leading to body-snatchers, or Resurrectionists, removing freshly interred corpses and selling them to anatomy schools (Cain, 2017). One famous case is that of Burke and Hare in Edinburgh, who murdered 16 people in order to profit from the sale of their bodies (Mitchell et al., 2011; Tarlow and Battell Lowman, 2018). This led to the introduction of the Anatomy Act in 1832, which allowed the bodies of unclaimed individuals to be anatomised, thus increasing the number of cadavers received legally by anatomy theatres. Moving into the late 20th century, this practice – although not abolished – was superseded by donation programmes, where individuals can choose to donate their bodies for teaching after death.

During the late 1990s, it was revealed that several hospitals in the United Kingdom had removed and retained tissue without consent (HTA 2021). Known as the Alder Hey Affair (Bauchner and Vinci, 2001), this instance led to the introduction of the Human Tissue Act in 2004, which oversees the regulation and storage of human tissues of individuals who have died within the last century (HTA, 2020), and the subsequent introduction of the Human Tissue Authority in 2005, which regulates the guidelines for the removal, storage and use of human tissue (HTA, 2021). The last public dissection in the United Kingdom succumbed to much scrutiny because of this. In 2002, Dr Gunther von Hagens, the creator of the Body Worlds exhibition, which uses plastinated human remains (von Hagens, 2014; Jones, 2016),

sold tickets for a public dissection undertaken in an abandoned building in London (MacDonald, 2005; Cain, 2017). This dissection, which was also televised, proved extremely controversial as, like his later exhibition, it appeared to be more of a performance piece than an educational event (MacDonald, 2005). This brings to the fore the ethics of both using and storing human remains. The clear progression of both public and professional opinion of the use of human remains in university teaching, and wider educational engagement, highlights the need for a direct analysis of where the opinion of related practitioners lies in regard to teaching with different forms of human remains.

Ethics Policies

Following on from the Human Tissue Act, the Department for Culture, Media and Sport published a generalised set of guidelines for human remains in museum collections within England, Wales, and Northern Ireland (DCMS, 2004) and provided detailed information concerning storage and display. Information is also provided on acquisition, conservation and deaccession should it be necessary (Jenkins, 2008). Within this document, the DCMS also encouraged institutions to think about and compile their own guidelines pertaining to the storage and display of human remains (DCMS, 2004; LaPorte, 2014). This has been undertaken by numerous institutions (i.e. Lohman and Goodnow, 2006; Wellcome Collection, 2018; British Museum, 2021). Even though the DCMS guidelines touch on the "use, access and education" purposes of human remains, the section is rather short, and mainly relates to the prospect of visitors handling remains whilst in a museum (DCMS, 2004). However, teaching institutions – universities and medical schools – tend to have their own ethics policies. In any instance where students have access to human remains, they must first become acquainted with the ethics policies of the institution that they belong to. This highlights the potential need for a more universal stance on ethics and, as a result, ethical policies – this itself requiring research into what is considered ethical by those currently learning from and/or working with human remains.

Dissection

Until recently, dissection was the primary method for studying human anatomy, with the addition of textbooks and photographs (Trelease, 2016). Only in the last thirty years have advances in technology and variations in teaching allowed for a different approach to studying anatomy. Multiple surveys have considered the use of dissection in teaching. Many of these studies broach the subject of whether cadavers, henceforth referred to as donor bodies, are necessary within teaching programmes when there are alternatives available, such as body painting, 3D printing (McMenamin et al., 2018), medical imaging and three-dimensional simulation (Trelease, 2016). In one study, as documented by Papa and Vaccarezza (2013), first- and second-year London medical students were asked whether they believed practical dissection classes aided in their knowledge and understanding of anatomy. Seventy-five percent of the 174 students surveyed stated that dissection was the "single most useful method of learning anatomy". Another study, undertaken over a twelve-month period at the University of Sheffield, interviewed thirteen students as part of a qualitative review, two of which were postgraduates from the Department of Archaeology (Burr et al., 2019). The overall conclusion was that the students gained a "unique and valuable learning experience", which enhanced their understanding of anatomy (Burr et al., 2019).

Although most studies relate to the use of donor bodies purely as teaching materials for medical and biomedical subjects, the consensus is that dissection is the best way for learning human anatomy, but that it should be also accompanied by other methods, including 3D models, software, and atlases (Davis et al., 2013). Students themselves have noted a better anatomical understanding through hands-on learning (Papa and Vaccarezza, 2013); in which case, as long as students are able to have an interactive experience, it could be possible to substitute a real human body for a replica composed of synthetic materials. However, it should be noted that these studies have been universally from within medical or biomedical schools, with a lack of analyses regarding wider fields that commonly teach using human

remains, including bioarchaeology and forensic anthropology.

Human Bones

Unlike complete human bodies, human skeletal remains are widely used outside of medical and biomedical subjects (i.e. archaeology and anthropology), and act as a useful reference for teaching (Hillier and Bell, 2007). Remains held on display and in storage have come up against scrutiny within recent years, due to the Human Tissue Act and the related changes in public opinion. Even though museums have on occasion surveyed the public, since the guidelines from the DCMS were published in 2005 there have been a greater number of surveys focused on human remains. A survey undertaken at the Museum of London in 2007 determined that 53% of respondents expected to see remains on display, and that, in total, 92% of respondents approved of human remains being displayed within collections (Roberts, 2009). Another survey, conducted at the Manchester Museum in 2008, showed that 91% of the 375 respondents were in favour of the display of human remains (Sayer, 2010). Further to this, a study undertaken by the English Heritage in 2009 determined that 87% of respondents felt that the display of human remains helped them to "understand how people have lived in the past" (English Heritage, 2009). These results suggest that the majority of museum goers are happy to view humans remains and for them to be held within collections.

It has been suggested that, instead of displaying human remains, alternative methods could be employed, such as using photographs or replica bones (Levitt, 2016). However, these surveys and alternative ideas relate to storage and display within museum collections (i.e., Bonney, Bekvalac & Phillips 2020; MDU, 2021), not to the use of human bones as a hands-on teaching material. Unlike engagement studies undertaken on dissection as mentioned above, there is less published material for skeletal engagement. In both cases, it is important that opinions be sought not solely from the students or professionals involved in the handling of material, but also by the general public in order to gain a larger picture of what is and is not considered ethical. Also worthy of note is the use of archaeological remains in teaching collections. With a donor system now in place, it could be possible for certain teaching units to replace archaeological skeletal material with donor skeletal material, for which consent has been given. However, this relies on other factors such as whether universities have medical teaching units to gain access to donor bones, and the licensing to hold them.

Aims of this Study

These studies mentioned previously have clear utility for helping develop anatomical education, but suffer from relatively small sample sizes. A larger study, and one which also considers the opinions of graduates now working in the field, alongside those of the public, would further this work. The research presented here thus aims to determine whether there are any differences in opinion regarding the type of remains used for teaching according to the type of remains and conditions of education. Moreover, in review we aim to place in a pedagogical analysis at the forefront of any analyses so that the conclusion may eventually advise on the development of teaching with, and thereby the handling of, human remains within a higher education setting.

MATERIALS AND METHODS

Survey Compilation and Distribution

For this study, a series of questions regarding the use of human remains as teaching materials was compiled into a survey, which was subsequently granted ethical approval by the University of Sheffield ethics board. The survey questions began with individual specific categories, including age, gender, and profession. These questions were necessary to set the demographic parameters of the respondents and had predetermined answer categories: for example, age was set within 20-year stages; <20, 21-40, 41-60 and 61+ to support subsequent statistical analyses. For this study, the responses to four specific questions, one yes/no question, and three graded questions, were analysed.

The first of these questions was a split-second decision about whether the use of human re-

mains as teaching materials is ethical, answered as yes or no. The graded questions were graded on a five-point Likert scale answering system: 1 – least strongly, 2 – less strongly, 3 – neither agree nor disagree, 4 – strongly, 5 – most strongly. The first graded question was whether it is acceptable for a range of subjects to use dissection as a resource, or if it should only be used by medical and biomedical students. This range of subjects, henceforth referred to as relevant subjects, comprises any discipline which may provide additional teaching regarding human anatomy, for example archaeology and forensics. The second question asked if synthetic bodies, such as those made from plastics and animal components, should be used for all non-medical and biomedical subjects. The third graded question asked whether replicated bones should be used for teaching instead of real human bones. The full list of survey questions can be found in the supplementary material.

The completed questions were uploaded and formatted within Google Forms, chosen because of its security and encryption software, in order to comply with GDPR requirements and ethical standards. The survey was then distributed through various professional platforms, including social media, relevant organisational email listings, and similarly relevant online forums. Distribution was also encouraged by professionals on said platforms to disseminate further, for example by the British Association for Biological Anthropology and Osteological Anthropology, the Sheffield Medical Teaching Unit and the British Archaeological Jobs Resource. Archaeological forums and university emailing lists allowed for a professional and student base, whilst social media was also used to target a non-professional audience. The survey was initially distributed in May 2020 with no official deadline set. Most responses came within the first two weeks, but the link was left live until early July of the same year, when data processing began. A comments section was added to the survey following requests from a number of correspondents on one social media group, which allowed additional participants to provide reasoning(s) as to why they had given some of their answers.

Statistical Analysis

Kruskal-Wallis (with pairwise comparisons) and Jonckheere-Terpstra tests were run to test differences between age groups and trends across ages respectively. Mann-Whitney U tests were conducted to test for differences between male and female groups. Non-parametric tests were selected due to the variation in sample sizes and to strengthen the project's statistical analyses. To limit any errors incurred by running multiple tests, Dunn-Bonferroni corrections were applied to adjust all p-values. Statistical analyses were run using SPSS v.26.

Demographic breakdown of respondents

In total, 477 people took part in the survey. A full breakdown of respondents can be seen in Table 1, outlining profession, gender, and age.

RESULTS

Variation between genders

Table 2 gives the results of the Mann-Whitney U tests between the male and female respondents. The results show a trend regarding the mean values provided for males and females, and also for the questions asked. Female respondents opted for lower scores in the scaled answers on average than males, with the mean value provided in each category for females being consistently lower than that for males (between 0.20 and 0.33 difference across the three questions). Interestingly, the order in which the questions were presented in the survey seems to be their order of importance regarding the scaled answers provided, with the use of donor bodies for all subjects scoring a higher mean value, whilst the use of bone casts instead of real bones has the lowest mean value.

When addressing whether donor bodies should only be used for medical and biomedical students, the Mann-Whitney U test determined that there was no statistical significance between the responses of male and female genders (seen in Table 2). However, statistical significances were noted for the two further questions. A p-value of 0.03 was obtained for the question of whether synthetic bodies should be used for non-medical/

Table 1. Demographic breakdown of respondents, showing gender, age, and profession.

Career			Gender				Total
			Male	Female	Gender Fluid	Prefer not to say	
Student	Age	<20	3	14	2		19
		21-40	18	73	7		98
		41-60	1	14	1		16
		61+	1	1			2
	Total		23	102	10		135
Arch/Heritage Professional	Age	21-40	10	81	2	1	94
		41-60	12	23	1		36
		61+	4	2			6
		Prefer not to say		1			1
	Total		26	107	3	1	137
Med/Bio Professional	Age	21-40	3	12			15
		41-60	1	6			7
		61+	2	3	1		6
	Total		6	21	1		28
Non- professional	Age	21-40	10	40	1		51
		41-60	21	38			59
		61+	26	39		1	66
		Prefer not to say		1			1
	Total		57	118	1	1	177
Total	Age	<20	3	14	2		19
		21-40	41	206	10	1	258
		41-60	35	81	2		118
		61+	33	45	1	1	80
		Prefer not to say		2			2
	Total		112	348	15	2	477

biomedical teaching, determining a difference of opinion between male and female respondents. Similarly, a significant p-value of 0.01 was obtained for the use of real bones versus casts. The mean value obtained for male respondents was 2.42 and 2.16 respectively to the two questions, whilst that for females was 2.14 and 1.83 respectively. These outcomes show a significantly higher score in the male group, but with groups on average giving scores supportive of the use of bone casts and synthetic bodies.

Variation between age groups

Table 3 displays the results of the Kruskal-Wallis and Jonckheere-Terpstra tests undertaken between age categories. Kruskal-Wallis and post-hoc tests were then run to determine if any statistical significances were noted between age categories. Interestingly, they seem to have the opposite result, with a statistical significance noted for the first question (the use of donor bodies for only medical/biomedical teaching), but not for the further two questions. The Kruskal-Wallis determined a p-value of 0.01 for the use of donor bodies for medical/biomedical versus non-medical/biomedical teaching. Associated pairwise analysis showed that specifically the 41-60 and 61+ age categories were significantly different (p=0.04). In addition, the results of the Jonckheere Terpstra test (p=0.01) allude to a significant trend towards increased scores to the use of donor bodies question with age. All mean scores, however, suggested positive responses to the three questions.

Table 2. Results of the Mann-Whitney U test comparing responses between male and female genders. P-values have been adjusted according to Dunn-Bonferroni corrections. Significant results are marked in bold. Note: Gender Fluid data was not included in the statistical analysis due to the differences in sample size compared to male and female groups, but was considered important and is thus reported in the table.

Question	Gender	N	Mean	SD	Mann-Whitney U sig.
Donor bodies for medical/biomedical vs non- medical/ biomedical teaching					.19
	Male	112	2.50	1.36	
	Female	348	2.30	1.33	
	GenderFluid	15	2.40	1.40	
Synthetic bodies for non- medical/biomedical teaching					.03
	Male	112	2.42	1.16	
	Female	348	2.14	1.05	
	GenderFluid	15	2.20	1.26	
Bone casts instead of real bones					.01
	Male	112	2.16	1.18	
	Female	348	1.83	1.01	
	Gender Fluid	15	2.40	1.54	

Table 3. Results of the Kruskal-Wallis test comparing responses between ages, with pairwise analysis between age group and Jonckheere Terpstra tests for significant Kruskal-Wallis tests. P-values have been adjusted according to Dunn-Bonferroni corrections. Significant results are marked in bold. Note: Gender Fluid data was not included in the statistical analysis due to the differences in sample size compared to male and female groups but was considered important and is thus reported in the table.

Question	Age Category	N	Mean	SD	Kruskal- Wallis sig.	21-40	41-60	61+	Jonckheere Terpstra sig.
Donor bodies for medical/ biomedical vs non-medical/biomedical teaching	<20	19	2.73	1.40	.01	.71	1.00	1.00	.01
	21-40	258	2.16	1.24			.55	.04	
	41-60	118	2.48	1.41				1.00	
	61+	80	2.68	1.43					
Synthetic bodies for non-medical/biomedical teaching	<20	19	2.52	1.17	.38				
	21-40	258	2.15	1.08					
	41-60	118	2.24	1.10					
	61+	80	2.30	1.08					
Bone casts instead of real bones	<20	19	2.36	1.01	.11				
	21-40	258	1.86	1.07					
	41-60	118	2.00	1.10					
	61+	80	1.85	1.05					

DISCUSSION

While several statistically significant differences were identified between select groups, there was an overwhelming majority of responses showing participants that believed that the use of teaching with human remains is both practical and ethical. Moreover, these differences at no point alluded to one group being against the use of human remains as pedagogical aids. Instead, the results rather showed that some groups were simply more conservative in terms of which groups should be taught using human remains, but within the context that human remains should be used.

The statistical results were supported and enhanced by the addition of respondents' comments, several of whom provided useful insights into the profession of the individual, and their personal experiences. In some cases, respondents have given reasoning for why specific answers

were chosen and outline their personal thoughts and feelings regarding the subjects of ethics and consent. These provide a valuable context to the more quantitative statistical results.

Is the use of human remains ethical as a teaching material?

Analysis of both the survey data and respondent comments point to a consensus among participants that it is ethical to use human remains as teaching materials, with 89.7% of participants (428/477) giving a "Yes" response. This has been also confirmed by analysis of the Likert scale questions (supplementary material – Tables A, B, and C), which opt for the use of donor bodies in education rather than replications. Even though limited access to donor bodies and replicated materials have been suggested for use outside of the medical and biomedical teaching spheres (discussed in detail later), it seems that the majority of respondents would prefer for everyone to have access to actual human remains in order to obtain a better understanding of anatomy, regardless of specialisation as seen by the mean values documented in Tables 2 and 3.

Overall, the most frequently raised point was of consent (mentioned by 43 individuals). Most respondents appear to approve of the use of donor bodies for teaching, whether for medical and biomedical students or for a broader subject base, because donors consented to give their body as a teaching material. The same, however, cannot be said of archaeological remains. Even though in most cases provenance and a general history of skeletal remains might be known, there is no knowledge of how individuals would have felt knowing their final resting place was no longer so. On this topic, Respondent 306 points out that many skeletons are excavated from funerary contexts, backed up by Respondent 390, who states that people in the past "went to their death with a reasonable expectation of remaining undisturbed". For many individuals in the past, it seems highly unlikely that they could ever imagine themselves being used to educate students. In this context, it is interesting that so many respondents supported the use of archaeological bone to be used in teaching.

As a counter-argument to this, allowing students to handle human remains, in both the form of donor bodies and as skeletal remains, provides them with the opportunity to learn about the ethics of what they are doing and ensures that they understand how to show respect to remains. As stated by Ghosh (2017), "as fellow human beings it is our responsibility to reciprocate the anatomical gift with respect, compassion, care and dignity". This is regardless of how human remains are used, whether they are complete donor bodies, prosections or skeletal material, they were still once living, breathing individuals and so must be treated with the utmost care and respect. Respondent 176 noted that using real bones allowed her to remember that they were once part of a living human – a feeling that might be lost with the use of casts. The best way to promote the respect of people who lived before us is to use them and learn from them, in as ethical and respectful a way as possible.

Use of cadavers for only medical and biomedical teaching

The results of the statistical analyses show no statistical significance between male and female groups; however, differences have been noted between certain age categories. In particular, significant differences were noted between 21-40 and 61+ age categories, along with increases in mean response scores with the increasing age groups analysed. This highlights a differing opinion between ages on the usage of donor bodies for the purposes of medical and biomedical versus non-medical and biomedical teaching.

Alongside the statistical significances, it is of value to note that over half the data – 57.4% – lies in categories 1 (least strongly – all relevant subjects should have access to cadavers) and 2 (less strongly), whilst only 21.8% of the data lies in categories 4 (strongly) and 5 (most strongly – donor bodies should only be used to teach medical and biomedical students). This can be seen broken down by gender in a crosstabulation in the supplementary material (Table A). The answers given by respondents could stem from the issue of consent, with 19 respondents agreeing that, if individuals have consented to dissection after death, it is ethical

Supplementary Material

Table A. A breakdown of scaled answers for the use of cadavers for biomedical vs non-biomedical teaching against gender.

		Use of cadavers for only medical and biomedical teaching					Total
		1.00	2.00	3.00	4.00	5.00	
Sex	Male	39	17	29	15	12	112
	Female	139	66	69	45	29	348
	Gender Fluid	3	9	0	0	3	15
	Prefer not to say	1	0	1	0	0	2
Total		182	92	99	60	44	477

Table B. A breakdown of scaled answers for the use of synthetic cadavers for non-biomedical teaching against gender.

		Use of synthetic cadavers for non-medical or biomedical teaching					Total
		1.00	2.00	3.00	4.00	5.00	
Sex	Male	32	23	40	11	6	112
	Female	134	62	125	21	6	348
	Gender Fluid	5	6	1	2	1	15
	Prefer not to say	0	0	2	0	0	2
Total		171	91	168	34	13	477

Table C. A breakdown of scaled answers for the use of replica human bones instead of real ones against gender.

		Use of replica bone instead of real human bones					Total
		1.00	2.00	3.00	4.00	5.00	
Sex	Male	47	19	31	11	4	112
	Female	186	57	84	18	3	348
	Gender Fluid	5	6	0	1	3	15
	Prefer not to say	2	0	0	0	0	2
Total		240	82	115	30	10	477

for any relevant subject to use them. Yet this is not an overall opinion, and alongside the statistical results two respondents specifically commented that donor bodies should only be used by medical and biomedical students. Respondent 152 believed that it is primarily medical and biomedical students who should have access to donor bodies, although within the context of their use in different subjects, they would not "be against their use if it adds value to the course". This was seconded by Respondent 291, who believed that donor bodies should be "prioritised for medical teaching", but had access through their own archaeological course and said that it had aided in their education and understanding.

Overall, with a mean value of 2.35 for the combined dataset, there is a general acceptance for all relevant subjects having access to dissection as a resource, rather than solely medical and biomedical subjects. There are a few counter-arguments, stating that donor bodies should be prioritised, but, on the whole, the respondents of this study appear to be of agreement that any relevant subject which would benefit from the use of dissection should have access to the resource.

Synthetic bodies for non-medical and biomedical teaching

The results of the statistical analyses revealed that the male group to have significantly higher mean response scores than the female group, but with no additional significances discovered between age categories. Again, the majority of data collected – 54.9% – was held in categories 1 (least strongly – all relevant subjects should have access to real donor bodies) and 2 (less strongly), whilst only 9.8% of the data was allocated as categories 4 (strongly) and 5 (most strongly – anyone not studying medical or biomedical subjects should use synthetic bodies). The mean score for male respondents was calculated at 2.42, for gender fluid at 2.20 and for females 2.14. The results of the statistical analysis show that, although males agree that access should be provided to real donor bodies, female respondents were more inclined towards this. Further information can be seen broken down by gender in a crosstabulation in the supplementary material (Table B).

There were also notable comments on this question from respondents. For example, Respondent 85 suggested that synthetic bodies would be highly useful for teaching if there was no access to real donor bodies, whilst Respondent 83 said they should be considered as an option, but if people had chosen to donate their bodies for teaching, their wishes should be adhered to. Perhaps this could suggest a compromise: if institutions have sufficient access to donor bodies for a variety of subjects, then this facility should be used, but if not, there is now an alternative. This can be seen in a study undertaken in 2019 using a SynDaver model (Richardson et al., 2021), which introduced a synthetic body into an anatomy module. Even though this experiment did not test whether students learnt more from a synthetic body than a real one, it concluded that students who had access to a synthetic body gained more skills than those who had no access, showing this as an invaluable teaching resource. This in part concurs with the results of this project and respondent comments, most notably the potential for using synthetic resources where donor bodies are unavailable.

However, all individuals are anatomically different and so may present different traits during dissection, including blood vessels in irregular places and additional growths (Mazhar et al., 2014): traits such as these could be easily missed if using a standard synthetic body. Also, the textures and densities of real human remains cannot be fully replicated in synthetic models. A study undertaken at a university in Poland asked students if they would prefer to use real donor bodies, synthetic bodies, or a combination of both. Over 70% of students opted for real donor bodies due to variance and degradation of the living body, seeing how it changes over time, whilst only 21.8% would rather have a replication in order to see how anatomy should look if it was without flaw (Wilk et al., 2020).

Although not asked to participants, there is a clear issue with the synthetic body relating to purchasing cost. The starting price of SynDaver organs is reasonable: for example, a synthetic spleen costs $139 (SynDaver, 2021), but a high-end, full body can cost around $350,000 (Hansman, 2015). However, synthetic bodies like these conversely have a relatively low upkeep, in both a physical and monetary sense. They do not have to be stored in the same environment as real donor bodies, allowing for easier and cheaper storage facilities and, most importantly, they can be used multiple times (Richardson et al., 2021). Whilst a real donor body can be classed as a "single use" material which can be dissected only once (although it can be used further in the form of prosections, etc), a synthetic body can be used over consecutive seasons with multiple groups, because it can be reassembled after each use. Potentially, this could link in with the findings from the previous question: medical and biomedical students should have priority over real donor bodies, but other relevant subjects could use synthetic bodies as a useful study aid if access to a donor body is not possible. However, this relies on non-medical and biomedical fields having the funds available to purchase a synthetic body.

Another issue, raised by five respondents, was the use of animal components in the creation of semi synthetic bodies, which use animal organs inside a synthetic structure. The recurring comment was that human individuals had consented to be used for educational purposes after death,

whilst animals had not. For example, respondent 195 commented that the use of animal components in semi synthetic bodies is "morally wrong". Unlike humans, other animals, both living and dead, are classed as a "tradeable commodity" (Kaw et al., 2016), and in the case of semi synthetic bodies it could be fairly argued that a student is dissecting an animal merely housed inside a different shell.

Alongside the ethical issues of using donor bodies in teaching, there are also practical issues, including transportation, chemical preservation, and storage (Brenner et al., 2003; Brenner, 2014). Additionally, substances hazardous to the health of living individuals (Brenner, 2014; Wilk et al., 2020) must be used to preserve donor bodies, thus requiring a specific environment for their processing, storage, and dissection. For example, an open and well-ventilated area is essential when dissecting a donor body due to the overpowering odour omitted by cutting into the preserved flesh (Bhat et al., 2019). Fully synthetic bodies such as the SynDaver (SynDaver, 2021), comprised of plant and polymer fibres, produced without the use of hazardous or toxic material, could be a counter to this.

Overall, the results presented here, as well as in literature, suggest that professionals and students working with human remains see value in the use of synthetic and semi synthetic bodies for the purposes of teaching. However, there are obvious ethical and educational issues with using semi synthetic alternatives. This suggests that whilst there are financial and variational limitations to using synthetic bodies, they may present a viable and more ethical alternative to semi synthetic versions and, in some cases, real donor bodies, according to the resources available in each case. That being considered, as the response seen by the majority of respondents still suggests that if there is access to a real donor body, then this should be used.

Replacement of human bones with replicas

The final question provided similar results to the previous, with a significant difference between the responses of the male and female groups, but with no significant variation between age categories. The difference noted between gender categories saw a mean score for males of 1.18, females of 1.01, and for gender fluid of 1.54. Even within the context of significant variation between male and female response, the consensus is that real human bones should be used for teaching, rather than replicated material with the majority of data – 67.5% – held in categories 1 (least strongly – skills would be lost by only using casts) and 2 (Less strongly) whilst only 8.3% was held in categories 4 (Strongly) and 5 (Most strongly – casts should be used instead of real bones).

This has also been noted in the additional comments. In total, 47 comments referred to the importance of using real bones over replicas for study, with 38 made by students and archaeology or heritage professionals who have experience of handling human bone. However, within these comments there was a further consensus that replica bone should be used initially to build an understanding of skeletal anatomy (i.e., identifying bones and their features). This applies mainly at a non-specialised, undergraduate level. However, with more advanced students, studying towards a specialisation, respondent comments suggested that casts are not always appropriate. Unfortunately, this could mean that some archaeologists without post-graduate qualifications could have little to no experience of handling real human bones before they first begin fieldwork, suggesting that real bones should still play a part to some degree within undergraduate study.

One of the repeated comments was of taphonomic damage – the alteration of bone over time depending on both environmental and human-based factors (Sorg, 2019). For example, Respondent 337 believed that students should become accustomed to studying real bones in order to understand any fragmentation and/or degradation that they may experience. The bones of an individual can alter dramatically depending on the environment of internment and any post-depositional interaction. This should be considered in teaching, and cannot be reflected effectively through replicas. Similarly, Respondent 62 believed that it was essential to have experience of handling human bones before beginning any fieldwork as an archaeologist in order to understand types of damage. Respondent 70 concurred,

believing that students need to handle human bones in order to be able to distinguish them from animal bones and to understand their fragility during excavation – something noted in past literature (Johnson, 1994).

Eighteen respondents also commented on the variation of human bones, which are specific to each individual. There are numerous metric and, more importantly in this instance, non-metric or discrete traits, seen in some individuals as singular or multiple characteristics (White and Folkens, 2005; Mays, 2010). The worries projected by these respondents were unanimous; when replacing real bones with polyresin copies, instances of individual variation could be lost. In particular, Respondent 313 focused on paleopathology (bone disease), and stated that real bones should be used for teaching, so students can understand normal variation before attempting to "identify pathological or atypical changes". It is vital to understand whether a characteristic is a non-metric trait, taphonomic damage or evidence of pathology as this is a core component of biological profiling across all anatomical, archaeological, and forensic fields (e.g. Roberts and Manchester, 1995; Mays, 2010).

Interestingly, Respondent 321 believed that replicated bones should be substituted for real ones within a public display setting; but, for teaching individuals who want to specialise in human remains, they should have access to real bones. This respondent also pointed out that the use of real human bone as a teaching material can help strengthen the protocols of ethical practice by thoroughly informing students about the material with which they are working. In fact, several institutions have begun to replace human skeletal material with replica bones. For example, when the remains of Richard III were uncovered in 2012, it was always the intention to re-inter them. However, his bones were scanned using CT equipment and then 3D printed, allowing for a copy to be put on display whilst his actual remains were interred in Leicester cathedral (Levitt, 2016). Technology has now advanced to the point that it is possible to 3D print bone to act as a graft in a living person (Xilloc, 2021). Given that this type of printing has to be precise in order to serve a living individual, it seems the use of 3D printed bones for the purposes of teaching could provide more than just a basic understanding of skeletal anatomy.

Replicated bones are now more readily available, with numerous online outlets selling them, from low quality plastic items to high quality 3D printed replicas. High end replications, such as those created by Bone Clones (2021) are much more detailed, encompassing a range of individual and pathological features. These are created using real human bones and are cast with enough precision to preserve fine details such as muscle attachment sites and nutrient foramina (Bone Clones, 2021). Created from polyurethane resin and hand stained to appear more realistic, these replicas have been cast from a number of individuals in order to demonstrate differing non-metric traits and pathologies. In fact, the page dedicated to replica skulls showcases multiple types or trauma from human impact as well as various diseases and ailments. One survey respondent liked the idea of casts to show trauma: Respondent 188 focussed heavily on different types of traumas which might not be readily available within skeletal collections, but which could be substituted with the use of casts. The most economic set-back of highly detailed items such as Bone Clones is the cost. Whilst institutions may obtain human remains from excavation work or from other such facilities, replicated bones must be purchased.

Limitations

Several limitations have been noted within this study. One of the methods of distribution was a female-led social media group, accounting for a greater number of female respondents. Also, the survey was sent out through several professional email lists and social media groups, but also distributed through a personal social media account. This accounts for the greater number of professional respondents as opposed to public. Were this study to be undertaken again, having greater access to the public could allow for a more even split in the data.

CONCLUSION

Despite some variations between groups, the results of the survey and subsequent statistical

analysis show a clear opinion that the use of human remains as a teaching resource is ethical. Whether in the form of a donor body or skeletal material, there is the overwhelming opinion that it is ethical to use real human remains to enhance the education of students, with the majority of respondents feeling more at ease with the use of real material as opposed to synthetic, and especially semi synthetic in regard to created material. However, while these seemed to be a general ethical consensus there was some contention regarding the issue of consent. Moreover, it must be remembered that the analysis conducted here focussed on the British population. The findings presented here may thus not apply within different cultures and societal groups. Future research would thus be well served conducting similar surveys amongst different groups, considering different factors such as nationality, ethnic background, and religion.

ACKNOWLEDGEMENTS

Thanks go to all survey participants who allowed for the generation the project's data. Along with the teaching staff at Sheffield MTU for their advice and input. But most importantly, to the individuals who donate their bodies to further the education of others.

Notes on Contributors

Georgina Goodison - contributed to all aspects of the manuscript including writing, reviewing, data analysis, and conception, as well as being the main writer on the first draft. Christopher Aris - contributed to all aspects of the manuscript including writing, reviewing, data analysis, and conception.

Ethical Compliance Statement

Before beginning research, ethical approval was sought and granted by the University of Sheffield in order to gather data from professionals and the general public.

REFERENCES

BAUCHNER H, VINCI RJ (2001) What have we learnt from the Alder Hey affair? *BMJ: Brit Med J,* 322: 309-310.

BHAT D, CHITTOOR H, MURUGESH P, BASAVANNA PN, DODDAIAH S (2019) Estimation of occupational formaldehyde exposure in cadaver dissection laboratory and its implications. *Anat Cell Biol,* 52(4): 419-425.

BONE CLONES (2021) Only Mother Nature does it better. *Bone Clones Inc*. URL: https://boneclones.com/ [accessed 14th August 2021].

BONNEY H, BEKVALAC J, PHILLIPS C (2020) Human remains in museum collections in the United Kingdom. In: Squires K, Errickson D, Márquez-Grant N (eds). *Ethical Approaches to Human Remains: A Global Challenge in Bioarchaeology and Forensic Anthropology*. Switzerland: Springer International Publishing, pp 211-237.

BRENNER E, MAURER H, MORIGGL B, POMAROLI A (2003) The human cadaver as an educational tool – classification and comparison with other educational tools. *Ann Anat,* 185(3): 229-230.

BRENNER E (2014) Human body preservation – old and new techniques. *J Anat,* 224(3): 316-344.

BURR JA, WINTER RC, HEYERDAHL-KING I, WARREN MA, REDMAN AK, NICHOLLS O (2019) A qualitative study of how students learn from human cadavers. *Eur J Anat,* 23(6): 447-452.

CAIN T (2017) Getting under the skin. *Wellcome Collection.* URL: https://wellcomecollection.org/articles/WXXZUyoAAJpKfPOq [accessed 20th July 2021].

COATES S (2021) Population estimates by ethnic group and religion, England and Wales: 2019. *Office for National Statistics.* URL: file:///C:/Users/wiggl/Downloads/Population%20estimates%20by%20ethnic%20group%20and%20religion,%20England%20and%20Wales%202019.pdf [accessed 25th July 2021].

DAVIS CR, BATES AS, ELLIS H, ROBERTS AM (2013) Human Anatomy: Let the students tell us how to teach. *Anat Sci Educ,* 7(4): 262-272.

DCMS (2004) Guidance for the Care of Human Remains in Museums. *Department for Culture, Media and Sport.* URL: https://assets.publishing.service.gov.uk/government/uploads/system/uploads/attachment_data/file/906601/GuidanceHumanRemains11Oct.pdf [accessed 25th July 2021].

ENGLISH HERITAGE (2009) Research into Issues Surrounding Human Bones in Museums. *English Heritage.* URL: https://historicengland.org.uk/content/docs/research/opinion-survey-results-pdf/ [accessed 10th August 2021].

FLETCHER A, ANTIONE D, HILL JD (2014) *Regarding the Dead: Human Remains in the British Museum.* London: British Museum Press.

GAZI A (2014) Exhibition Ethics – An overview of major issues. *J Conservation Museum Studies*. URL: https://www.jcms-journal.com/articles/10.5334/jcms.1021213/ [accessed 14th August 2021].

GHOSH SK (2017) Paying respect to human cadavers: We owe this to the first teacher in anatomy. *Ann Anat,* 211: 129-134.

HAD (2021) Statement of Intent. *Honouring the Ancient Dead.* URL: https://www.honour.org.uk/statement-of-intent/ [accessed 14th August 2021].

HANSMAN H (2015) Med school students can play "operation" with these synthetic cadavers. *Smithsonian Magazine.* URL: https://www.smithsonianmag.com/innovation/med-school-students-can-play-operation-with-these-synthetic-cadavers-180957328/ [accessed 10th September 2021].

HILLIER ML, BELL LS (2007) Differentiating human bone from animal bone: a review of histological methods. *J Forensic Sci,* 52(2): 249-263.

HTA (2020) Human Tissue Act 2004. *Human Tissue Authority.* URL: https://www.hta.gov.uk/guidance-professionals/hta-legislation/human-tissue-act-2004 [accessed 20th April 2021].

HTA (2021) About the HTA. *Human Tissue Authority.* URL: https://www.hta.gov.uk/about-hta [accessed 20th April 2021].

JENKINS T (2008) Dead bodies: The changing treatment of human remains in British museum collections and the challenge to the traditional model of the museum. *Mort*, 13(2): 105-118.

JOHNSON JS (1994) Consolidation of archaeological bone: a conservation perspective. *J Field Archaeol,* 21(2): 221-233.

JONES DG (2016) The public display of plastinates as a challenge to the integrity of anatomy. *Clin Anat,* 29(1): 46-54.

KAW A JONES, DG, ZHANG M (2016) The use of animal tissues alongside human tissue: Cultural and ethical considerations. *Clin Anat,* 29(1): 19-24.

LAPORTE C (2014) Ethics of displaying human remains in museums. *Institute for Cultural Practices – The University of Manchester.* URL: https://culturalpractice.wordpress.com/2014/11/26/ethics-of-displaying-human-remains-in-museums-by-caitlin-laporte/ [accessed 25th July 2021].

LEVITT S (2016) Displaying replica bones and skeletons. *Honouring the Ancient Dead.* URL: https://www.honour.org.uk/displaying-replica-bones-and-skeletons/ [accessed 14th August 2021].

LOHMAN J, GOODNOW K (2006) *Human Remains and Museum Practice.* London: UNESCO.

LOUKAS M, HANNA M, ALSAIEGH N, SHOJA MM, TUBBS RS (2011) Clinical anatomy as practiced by ancient Egyptians. *Clin Anat,* 24(4): 409-415.

MACDONALD H (2005) Human Remains: *Dissection and its Histories.* London: Yale University Press.

MAYS S (2010) *The archaeology of human bones.* (2nd ed). Oxford: Routledge.

MAZHAR MA, QAZI S, KHERALLAH S, ALDALATI A, ALTINAWI B, AZOUZ H, AHMAD JH, GANGULY P (2014) Identifying rare human anomalies through students directed dissection at Alfaisal University: Case Report. *Austin J Anat,* 1(4): 1018.

MCMENAMIN PG, MCLACHLAN J, WILSON A, MCBRIDE JM, PICKERING J, EVANS DJR, WINKELMANN A (2018) Do we really need cadavers anymore to learn anatomy in undergraduate medicine? *Med Teach,* 40(10): 1020-1029.

MDU (2021) Storing and disposing of human skeletons and material. *The MDU.* URL: https://www.themdu.com/guidance-and-advice/guides/storing-and-disposing-of-human-skeletons-and-material [accessed 14th August 2021].

MITCHELL PD, BOSTON C, CHAMBERLAIN AT, CHAPLIN S, CHAUHAN V, EVANS J, FOWLER L, POWERS N, WALKER D, WEBB H, WITKIN A (2011) The study of anatomy in England from 1700 to the early 20th century. *J Anat,* 219(2): 91-99.

NAGPRA (2021) Facilitating Respectful Return. *NAGPRA – Native American Graves Protection and Repatriation Act.* URL: https://www.nps.gov/subjects/nagpra/index.htm [accessed 10th August 2021].

PAPA V, VACCAREZZA M (2013) Teaching Anatomy in the XXI Century: new aspects and pitfalls. *Scientific World,* 2013: 310348-5.

PARKER PEARSON M (2003) *The archaeology of death and burial.* Sutton Publishing Limited, Gloucestershire.

RICHARDSON NS, ZWAMBERG D, MCFALL K, ANDREWS DM, GREGORY D (2021) Exploring the utility and student perceptions of synthetic cadavers in an undergraduate human anatomy course. *Anat Sci Educ,* 14(5): 605-614.

ROBERTS CA, MANCHESTER K (1995) *The Archaeology of Disease.* 3rd ed. Cornell University Press, New York.

ROBERTS CA (2009) *Human remains in archaeology: a handbook*. Oxford: Information Press.

SAYER D (2010) *Ethics and Burial Archaeology.* Gerald Duckworth & Co Ltd., London.

SORG MH (2019) Differentiating trauma from taphonomic alterations. *Forensic Sci Int,* 302: 109893.

STANDRING S (2016) A brief history of topographical anatomy. *J Anat*, 229: 32-62.

SWAIN H (2002) The ethics of displaying human remains from British archaeological sites. *Public Archaeology,* 2(2): 95-100.

SYNDAVER (2020) Our History. *SynDaver: Beyond Human.* URL: https://syndaver.com/history/ [accessed 20th August 2021].

TARLOW S, BATTELL LOWMAN E (2018) *Harnessing the Power of the Criminal Corpse.* Cham: Palgrave Macmillan.

THE BRITISH MUSEUM (2021) Human Remains. *The British Museum.* [Viewed 25th July 2021]. URL: https://www.britishmuseum.org/our-work/departments/human-remains.

THOMAS DP (2006) Thomas Vicary, barber-surgeon. *J Med Biogr,* 14(2): 84-89.

TRELEASE RB (2016) From chalkboard, slides, and paper to e-learning: How computing technologies have transformed anatomical sciences education. *Anat Sci Educ,* 9(6): 583-602.

VON HAGENS G (2014) *Body Worlds: the original exhibition.* Heidelberg: Arts and Sciences Exhibitions and Publishing GmbH.

WELLCOME COLLECTION (2018) Full policy on care of human remains in museums and galleries. *Wellcome Collection.* URL: https://wellcomecollection.org/pages/WyjY_SgAACoALCmH [accessed 25th July 2021].

WHITE TD, FOLKENS PA (2005) *The Human Bone Manual.* Elsevier Academic Press, London.

WILK R, LIKUS W, HUDECKI H, SYGULA M, RÓŻYCKA-NECHORITIS A, NECHORITIS K (2020) What would you like to print? Students' opinions on the use of 3D printing technology in medicine. *PloS One,* 15(4): e0230851.

XILLOC (2021) CT-bone: real bone from the 3D printer. *Xilloc.* URL: https://www.xilloc.com/ct-bone/ [accessed 14th August 2021].

Bibliometric and visualized analysis of global research on technology in anatomy education from 1987 to 2021

Yunus E. Kundakcı[1], Emre Atay[2]

[1] Department of Physiotherapy and Rehabilitation, Faculty of Health Sciences, Afyonkarahisar Health Sciences University, Afyonkarahisar, Turkey

[2] Department of Anatomy, Faculty of Medicine, Afyonkarahisar Health Sciences University, Afyonkarahisar, Turkey

SUMMARY

While anatomy has been taught by means of traditional methods for centuries, today anatomy education methods are developing with various digital educational resources. Therefore, determining the trends of publications on the use of technology in anatomy education can provide a roadmap for future studies on this topic. This study aims to conduct a bibliometric analysis of the documents about technology in anatomy education. Using the bibliometric analysis method, 437 documents between 1987 and 2021 were included in the study. Publications in journals indexed in Web of Science were reviewed in terms of the country, journal, citation, year, author, keywords, co-authorship, co-occurrence, and co-citation. The H-index value of the publications was 47, and the total number of citations was 8501. The publications highlight an exponential increase in the last few years, as well as the prominence of a particular journal and countries such as the USA, England or Australia. Wilson TD was the most prolific author in the field. According to the co-occurrence analysis, it is observed that the terms "gross anatomy education", and "medical education" are frequently used by the authors. In the last few years, 3D printing, virtual reality, augmented reality and social media were selected in anatomy education. This study identified the main research hotspots related to the use of technology in anatomy education. The findings can also help provide new directions and ideas for future research.

Key words: Anatomy education – Bibliometric study – Technology

INTRODUCTION

Anatomy is an important branch of basic medical sciences. It is also of great importance, as it includes the scientific and terminological foundations of medicine and other health disciplines (Moxham and Plaisant, 2014). It is possible to encounter anatomy education at almost all levels of the health education system (Estai and Bunt, 2016; Schaefer et al., 2019; Zargaran et al., 2020). In order to teach anatomy effectively, many researchers, especially anatomy educators, have been

Corresponding author:
Yunus Emre Kundakcı. Department of Physiotherapy and Rehabilitation, Faculty of Health Sciences, Zafer Saglik Kulliyesi, 2078th Street, No. 3, Afyonkarahisar, Turkey. Phone: +90 272 246 28 34; Fax: +90 272 246 28 69. E-mail: y.emre.kndkc@gmail.com

Submitted: January 11, 2023. **Accepted:** February 16, 2023

https://doi.org/10.52083/HNNY3374

developing various theories and contributing to the literature by introducing new evidence-based applications for many years (Scott, 1993; Singh et al., 2019). In the Web of Science (WoS) alone, there are 4356 documents between 1975 and2019 that contain the keyword "anatomy education" (Petekkaya et al,. 2021).

Many alternative education methods are used in the presentation of anatomy education. Methods such as face-to-face learning, books, atlas, dissection, prosection, plastination, video, online resources, social media, 3D models, augmented reality and virtual reality are among the methods used to teach anatomy effectively (Iwanaga et al., 2021). Comparative research on the advantages and disadvantages between traditional methods and newer and more technological methods tends to increase. Anatomy teaching methods and resources used to help provide educational material have evolved significantly in recent years (Hulme and Strkalj, 2017). Today, more innovative and interactive teaching strategies and techniques which sare student-centred rather than cadaver-based are becoming popular. These techniques are problem-based, self- or team-based learning, as well as computer-assisted learning, videos, simulations and 3D images in anatomy education (Singh et al., 2019; Turney, 2007). Due to the rapid progress of technology and the increasing need for e-learning, it is important to explore the potential of technology in anatomy education. All technologically realized innovations provide medical students with accessible and standardized anatomy teaching (Zargaran et al., 2020).

The first and most important basis for acquiring adequate knowledge and skills in anatomy is for students to concentrate and engage in learning anatomy (Kumar and Singh, 2020). At this point, studies show that educational approaches made using active and engaging learning strategies in anatomy education can improve student participation and interaction are highlighted (Eleazer and Scopa, 2018; Singh et al., 2019). In recent years, with the increasing ease of access to innovations such as 3-D printers, virtual reality and augmented reality, innovative anatomy education models have been developed. In anatomy laboratories, materials consisting of 2D plastic and atlas models are replaced by 3D virtual reality models that provide a deeper understanding of anatomy with today's technology (Falah et al., 2014). However, there is still uncertainty about the various materials and techniques used for anatomy education and the methods to provide optimal teaching (Zargaran et al., 2020).

Bibliometric analysis provide a different perspective in reflecting developments in various fields of scientific research (Petekkaya et al., 2021). This analysis is a useful method to objectively measure the current status and international scientific impact of a particular topic (Van Raan, 2003). At the same time, it succinctly and intelligibly presents to researchers and readers the general trends in their field of research. Visualization of Similarities viewer (VOSviewer) is a specially designed software tool that creates and visualizes bibliometric maps, thereby demonstrating the structural and dynamic aspects of scientific research areas (Mas-Tur et al., 2021). The accumulated knowledge of most scientists during the historical development of anatomy has led to a detailed anatomy database (Bahsi and Bahsi, 2019). Advances in anatomy education are the topic of many research articles, reviews, scientific meetings (Estai and Bunt, 2016; Iwanaga et al., 2021; Singh et al., 2019). For this reason, bibliometric, scientometric and altmetric analyses related to this current issue may also be useful (Petekkaya et al., 2021). Currently, there is a lack of research on the current situation, trends, hotspots and evaluation of the future appearance regarding the innovations brought by technology in anatomy education. With the innovations offered by technological developments, new evidence-based approaches to learning and teaching are being designed for students in the field of medicine and health sciences. Studies on anatomy education and technology are increasing in order to reveal effective learning methods.

This study aims to conduct a bibliometric analysis of documents related to anatomy education and technology using the WoS database. Until 2021, we present the trends of current publications on the subject in areas such as authors, keywords and countries to relevant researchers.

MATERIALS AND METHODS

Study design

This bibliometric study was conducted using documents published in indexed in the Web of Science (https://www.webofscience.com/). The datasets collected via WoS were obtained on December 20, 2021. All bibliometric analyses were completed by conducting them through the files downloaded on this date.

Data search and collection

In this study, data were collected through the Web of Science Core Collection database. The science of anatomy can potentially be covered by many journals in the fields of medicine, health, biology and biomedicine. Therefore, data collection was not attributed to the scope of any particular journal, and interdisciplinary research cutting across multiple fields and extending to related areas were also included in the analyses. All document types (article, proceeding paper, book chapter, etc.), countries, languages, data categories were included without going to any exclusion. We selected the words to search as TS = (technology OR virtual reality OR augmented reality OR 3D OR video OR social media OR internet) AND anatomy education. The first publication in the WoS database is obtained in 1987. A total of 438 documents were obtained by December 20, 2021, without restricted time parameters. Since the publication date of a document is 2022, a total of 437 documents were included in the research between 1987 and 2021. In addition, the authors checked for duplication in the documents. The accuracy of data such as titles, countries, journals, or authors were confirmed by the researchers, and the analyses were performed.

Data analysis and visualization

The datasets were downloaded from the database in "plain text file" format and Microsoft Excel program was used for descriptive results. Bibliometric analysis were performed, and network visualization maps were created using the VoSviewer package program (Van Eck and Waltman, 2010). The analyses were made on the basis of the number of publications and citations by year, the most prolific authors and journals, frequently used keywords, bibliographic coupling including co-citations of the authors, and co-authorship (Mas-Tur et al., 2021).

Bibliometric Analysis

With bibliometric analysis, it is possible to profile the relevant publications on a particular scientific research topic. Qualitative and quantitative changes of the subject can be determined, and trends within a discipline can be determined. This analysis consists of the application of some kind of statistical methods (De Bakker et al., 2005). Mas-tur et al. (2021) reported that analyses by using this method can rely on a variety of calculations (number of citations or number of publications by author, institution or country, keyword occurrence or co-occurrence, or co-authorship). Whether it is regarding a publication, author collaborations, a journal, or popularity on a topic, researchers can benefit from such systematic methods of revealing the influence of literature and scientific trends. Thus, bibliometric studies provide an opportunity to evaluate national and international cooperation on leading issues (De Bakker et al., 2005; Duque Oliva et al., 2006).

Visualization of Similarities viewer (VOSviewer)

VOSviewer is a software tool for creating and visualizing bibliometric networks such as journals, researchers or publications (LIUPost, 2021). VOSviewer uses the VOS mapping method. Depending on the matching method, images with citation, bibliographic matching, co-citation, or co-authoring relationships can be created. In this study, VOSviewer's network visualization and overlay visualization map type method were applied (Hebebci, 2021).

The VOSviewer clustering algorithm uses the smart local moving algorithm. This algorithm works based on clustering topics, marking and classifying each cluster with a different colour. A cluster consists of closely related nodes. Each node in a network is assigned to a cluster. The number of clusters is determined by a resolution parameter. The higher its value, the greater the number of clusters. VOSviewer uses colours to indicate the cluster to which a node is assigned.

Items are indicated by a label and, by default, a circle. The size of the circles and the size of the number of font occurrences of the label, and the colours represent the clusters. The distance between the two circles reveals the similarity and relationship between them (Van Eck and Waltman, 2010; Van Eck and Waltman, 2014).

In order to empirically determine the matches with the highest frequency in the data set examined in this study, some threshold values were determined for the terms that should be included in the cluster numbers (such as minimum 2 documents for network map including country, at least twenty citations for author co-authorship and co-citation analyses, author keywords used at least ten times, etc.).

Table 1. Top 20 most cited documents in Web of Science.

Authors	Article Title	Citations*	Total link strength**
Sugand et al. (2010)[b]	The Anatomy of Anatomy: A Review for Its Modernization[1]	484	132
McMenamin et al. (2014)[a]	The Production of Anatomical Teaching Resources Using Three-Dimensional (3D) Printing Technology[1]	294	61
Nicholson et al. (2006)[a]	Can virtual reality improve anatomy education? A randomised controlled study of a computer-generated three-dimensional anatomical ear model[2]	236	18
Estai and Bunt (2016)[b]	Best teaching practices in anatomy education: A critical review[3]	226	117
Moro et al. (2017)[a]	The Effectiveness of Virtual and Augmented Reality in Health Sciences and Medical Anatomy[1]	200	72
Preece et al. (2013)[a]	"Let's Get Physical": Advantages of a physical model over 3D computer models and textbooks in learning imaging anatomy[1]	197	58
Lim et al. (2016)[a]	Use of 3D printed models in medical education: A randomized control trial comparing 3D prints versus cadaveric materials for learning external cardiac anatomy[1]	173	29
Jaffar (2012)[a]	YouTube: An emerging tool in anatomy education[1]	158	16
Petersson et al. (2009)[a]	Web-Based Interactive 3D Visualization as a Tool for Improved Anatomy Learning[1]	146	33
Pereira et. ak (2007)[a]	Effectiveness of using blended learning strategies for teaching and learning human anatomy[2]	135	41
Barry et al. (2016)[a]	Anatomy Education for the YouTube Generation[1]	121	39
Yammine and Violato (2015)[a]	A meta-analysis of the educational effectiveness of three-dimensional visualization technologies in teaching anatomy[1]	117	108
Ghosh (2017)[b]	Cadaveric Dissection as an Educational Tool for Anatomical Sciences in the 21st Century[1]	116	140
Khor et al. (2016)[b]	Augmented and virtual reality in surgery-the digital surgical environment: applications, limitations and legal pitfalls[4]	114	10
Khot et al. (2013)	The relative effectiveness of computer-based and traditional resources for education in anatomy[1]	110	64
Kucuk et al. (2016)[a]	Learning Anatomy via Mobile Augmented Reality: Effects on Achievement and Cognitive Load[1]	106	66
Trelease (2016)[b]	From Chalkboard, Slides, and Paper to e-Learning: How Computing Technologies Have Transformed Anatomical Sciences Education[1]	103	160
Davis et al. (2014)[a]	Human Anatomy: Let the Students Tell Us How to Teach[1]	96	100
Codd and Choudhury (2011)[a]	Virtual Reality Anatomy: Is it Comparable with Traditional Methods in the Teaching of Human Forearm Musculoskeletal Anatomy?[1]	93	76
McBrid and Drake (2018)[a]	National survey on anatomical sciences in medical education[1]	90	20

Document Type: [a] Article; [b] Review.
Journal: [1] Anatomical Sciences Education; [2] Medical Education; [3] Annals of Anatomy; [4] Annals of Translational Medicine.
* Number of citations in the Web of Science database.
** Total link strength calculated by selecting a minimum number of 2 citations in VoSviewer.

Research ethics

The study protocol was approved by the Clinical Research Ethics Committee of the university (Number: 2021/491).

RESULTS

Overview of Publications on Anatomy education and technology

This study included 437 documents in total. It was determined that the majority of the documents were published in journals within the scope of Science Citation Index Expanded (366, 83.75%). According to Web of Science Categories, the top 5 categories were listed as follows: Education Scientific Disciplines (262, 59.95%), Anatomy Morphology (57, 13.04%), Radiology Nuclear Medicine Medical Imaging (24, 5.49%), Imaging Science Photographic Technology (21, 4.81%), and Surgery (21, 4.81%). The H-index of the documents was 47, the total number of citations was 8501 (6279 without self-citations). The majority of document types were articles (326; 74.6%). The first 20 documents with the most citations are shown in Table 1. The network map containing these documents (having minimum of 90 citations) was presented in Fig. 1. The documents with the highest number of citations and total link strength, respectively, included: "The Anatomy of Anatomy: A Review for Its Modernization" and "From Chalkboard, Slides, and Paper to e-Learning: How Computing Technologies Have Transformed Anatomical Sciences Education".

Publication Year

In the WoS database, the years 1987, 1994, 1999, 2000, 2005 and 2006 included a document. The years 2003 and 2004 included two documents. The majority of documents were published in the last 3 years: 2021 (78; 17.85%), 2020 (70, 16.02%) and 2019 (62; 14.19%). Top 3 citing years were as follows: 2021 (2025; 23.82%), 2020 (1934, 22.75%) and 2019 (1321; 15.54%) (Fig. 2).

Publication Countries

It was determined that a total of 60 countries contributed to the literature on anatomy education and technology. The first 10 of these are listed in Table 2. The United States was the country with the highest production with 125 (28.60%) documents followed by UK and Australia with 61 (13.96%) and 53 (12.13%), respectively. The forty countries with more than two publications linked to other countries and six clusters are shown in Fig. 3. The United States (35577) and England (25157) were the countries with the highest total link strength.

Publication Authors and Journals

There were a total of 1556 authors in documents on anatomy education and technology. The average number of documents per author was 0.28. Wilson TD was the author with the highest production, with 13 (2.98%) documents followed by Seo JH and Chytas D, with 9 (2.59%) and 8 (1.83%), respectively. The network map of the co-authorship analysis with authors with a minimum of 20

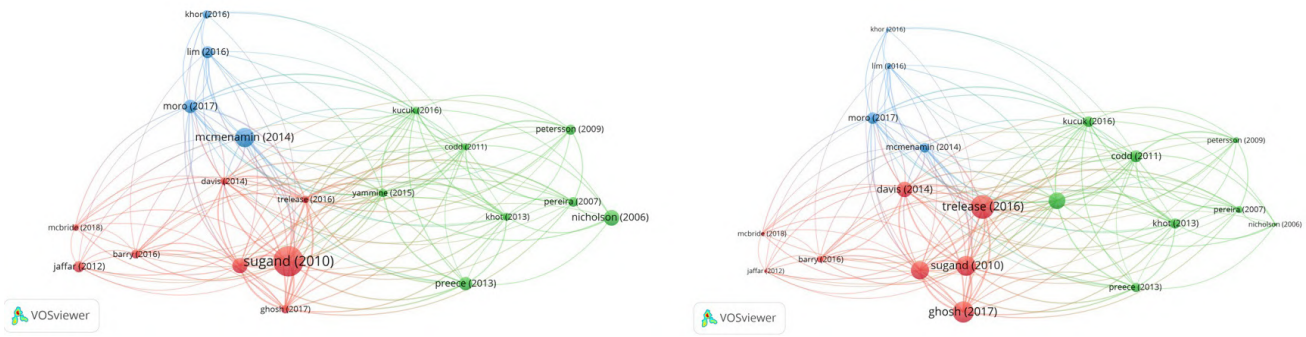

Fig. 1.- Network maps by citation and total link strength of the top 20 publications. 20 publications in 3 clusters. On the left, as the number of citations increases, the size of the circle increases. On the right, the total link strength increases as the size of the circles increases.

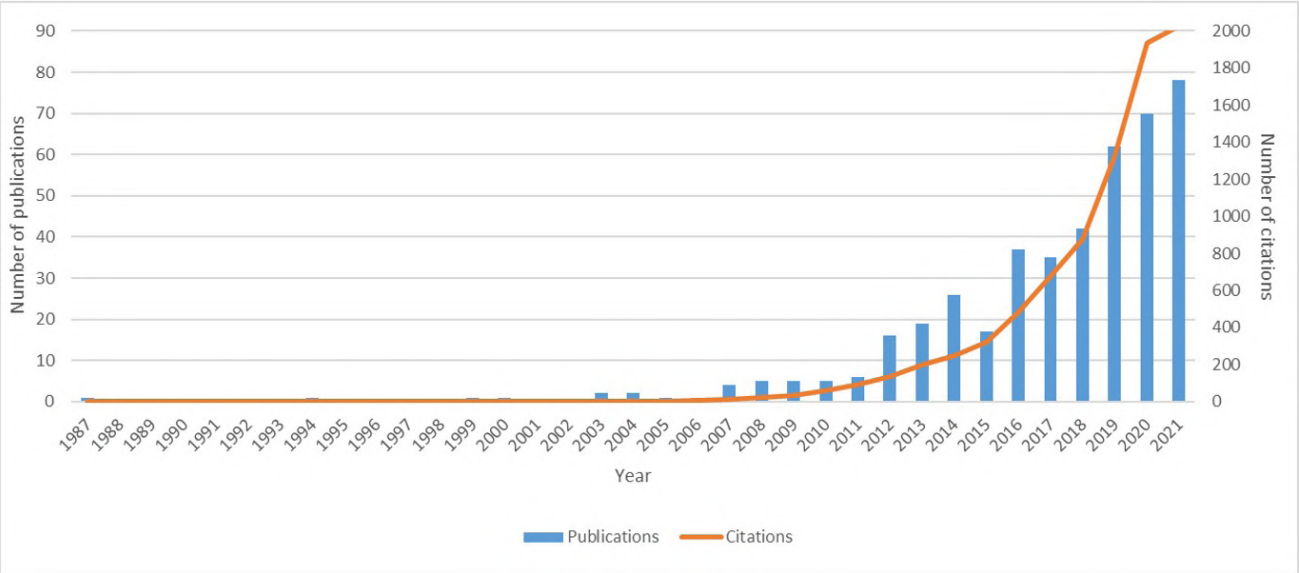

Fig. 2.- Change in the number of publications and citations of documents on "anatomy education and technology" in WoS by year.

Table 2. Top 10 countries of documents on anatomy education and technology.

Rank	Country	Frequency	% of 437	Citations / Documents (up 2021)	H-Index	Total link strength*
1	United States	125	28.60	17.66	25	35577
2	England	61	13.96	28.87	20	25157
3	Australia	53	12.13	29.72	17	19859
4	Canada	42	9.61	27.95	18	19455
5	Germany	22	5.03	18.50	11	7059
6	China	17	3.89	9.94	6	4122
7	Turkey	17	3.89	9.82	6	4288
8	Netherlands	16	3.66	10.44	9	9297
9	Scotland	14	3.20	8.57	5	4260
10	Ireland	13	2.98	18.23	6	3856

* Minimum number of documents of country: 2

citations are shown in Fig. 4A. Accordingly, 31 authors who met the threshold were distributed in 6 different clusters.

Co-citation analysis was also performed to reveal the most cited authors. When the minimum number of citations for an author was set to 20, 104 authors met this threshold and 3 clusters were distributed. Drake RL, Trelease RB, and Mayer RE were the authors with the highest total link strength, with 2776, 2157, and 1849, respectively (Fig. 4B).

The top ten journals with the highest number of documents are shown in Table 3. Anatomical Sciences Education (208, 47.6%) was the journal with the most publications.

Author keywords

Co-occurrence of keywords in 437 documents on anatomy education and technology was sent to VOSviewer for analysis and visualization, and 1190 keywords were formed. Twenty-seven keywords used at least ten times by the authors are in Table 4; the co-occurrence overlay and network visualization maps of these keywords are presented in Figures 4C and 4D, respectively. In the last few years, "COVID-19", "social media",

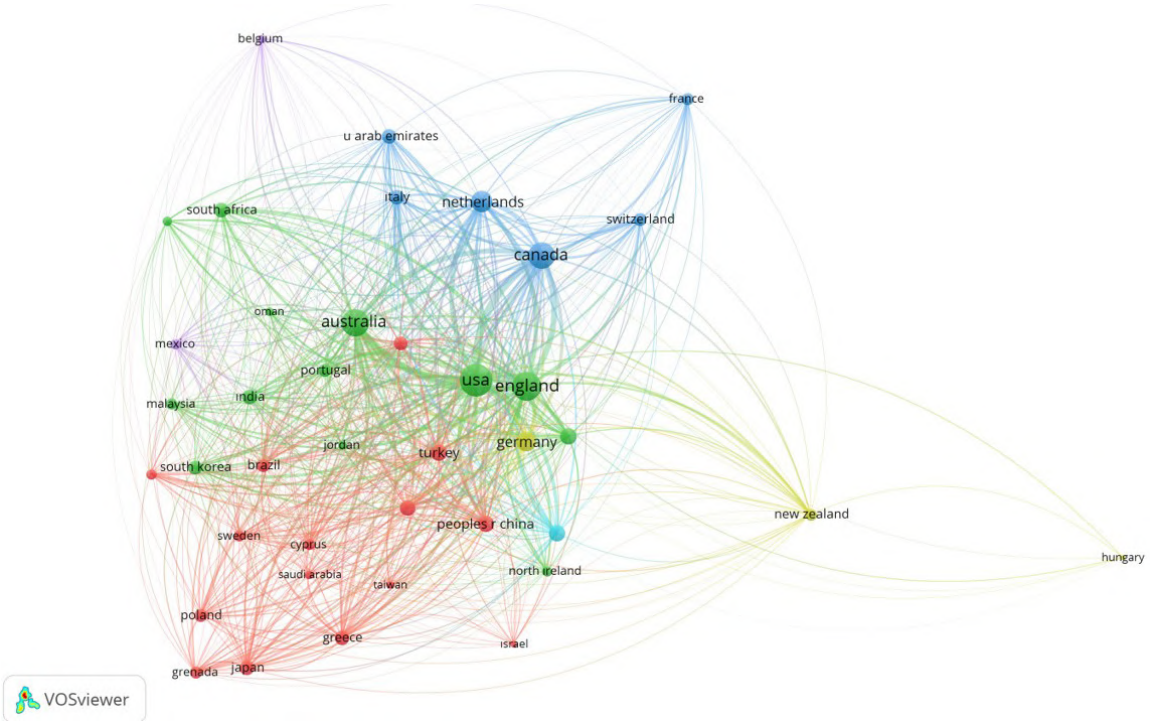

Fig. 3.- Network map with 40 countries in 6 clusters by setting the threshold to minimum 2 documents. As the size of the circles increases, the total number of links increases. More connections between different nodes indicate more cooperation between different countries.

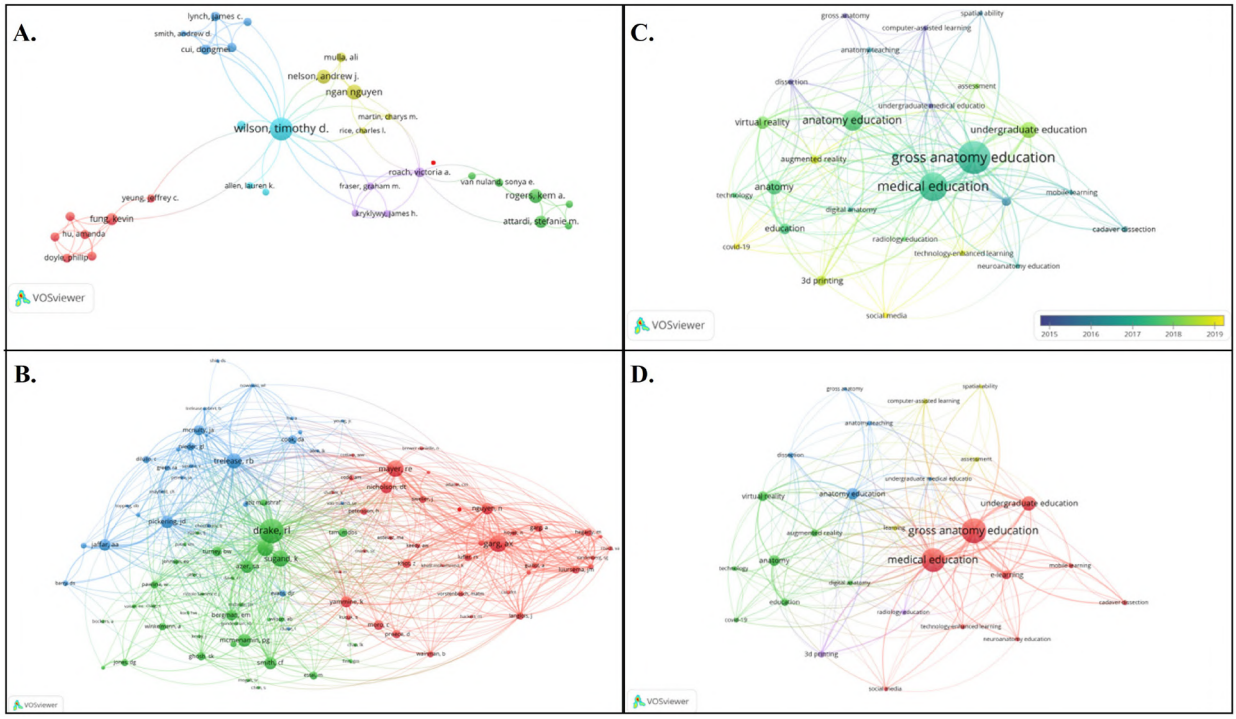

Fig 4.- A and B include maps of author co-authorship and co-citation analysis with VOSviewer. The size of each circle indicates the citations of articles produced by the author. The distance between any two circles indicates the relationship of co-authoring links, and the thickness of the link line indicates the strength of the link. **A.** Author co-authorship analysis. 442 authors met minimum of twenty citations threshold criteria and 31 of them are connected. Red cluster (7 items); green cluster (6 items); blue cluster (5 items); yellow cluster (5 items); purple cluster (4 items); turquoise cluster (4 items). **B.** Author co-cited analysis. 104 authors met minimum of twenty citations threshold criteria and are connected. Red cluster (39 items); green cluster (36 items); blue cluster (29 items). **C.** VOSviewer co-occurrence overlay visualization mapping of most frequent author keywords (minimum of 10 occurrences) in Anatomy education and Technology research from 1987 to 2021. Keywords in blue appeared earlier than that in yellow. **D.** VOSviewer co-occurrence network visualization mapping of most frequent author keywords (minimum of 10 occurrences) in Anatomy education and Technology. Twenty seven keywords were collected in 5 clusters. The large circles represent keywords with high link strength.

Table 3. Journals with publication titles on the topic.

Rank	Journals	Frequency	% of 437
1	Anatomical Sciences Education	208	47.6
2	Advances in Experimental Medicine and Biology	18	4.11
3	Clinical Anatomy	15	3.43
4	Faseb Journal	13	2.98
5	Medical Sciences Educator	11	2.52
6	International Journal of Morphology	9	2.06
7	Journal of Anatomy	8	1.83
8	Surgical and Radiologic Anatomy	7	1.60
9	Annals of Anatomy	6	1.37
10	BMC Medical Education	6	1.37

Table 4. Author keywords used at least ten times

Rank	Keywords	Occurrences	Total link strength
1	Gross anatomy education	176	322
2	Medical education	143	301
3	Anatomy education	88	103
4	Undergraduate education	60	141
5	Anatomy	54	92
6	Virtual reality	44	81
7	Education	34	56
8	3d printing	32	52
9	E-learning	27	74
10	Augmented reality	24	52
11	Cadaver dissection	14	29
12	Anatomy teaching	13	26
13	Dissection	13	33
14	Social media	13	25
15	Assessment	12	32
16	COVID-19	12	28
17	Technology	12	28
18	Technology-enhanced learning	12	30
19	Computer-assisted learning	11	31
20	Gross anatomy	11	16
21	Learning	11	31
22	Mobile learning	11	30
23	Neuroanatomy education	11	28
24	Radiology education	11	33
25	Undergraduate medical education	11	21
26	Digital anatomy	10	30
27	Spatial ability	10	21

"technology-enhanced learning"," undergraduate education", "3d printing" and "augmented reality" were the frequently used keywords by the authors (Fig. 4C). In Fig. 4D, these keywords that appeared more than ten times are included and classified into five clusters in the map: cluster 1 (gross anatomy education, medical education, undergraduate education, e-learning, cadaver dissection, social media, technology-enhanced learning, mobile learning and neuroanatomy education, in red); cluster 2 (anatomy, virtual reality, education, augmented reality, COVID-19, technology and digital anatomy, in green); cluster 3 (anatomy education, anatomy teaching, dissection, gross anatomy and undergraduate medical education, in blue); cluster 4 (assessment, computer-assisted learning, learning and spatial ability, in yellow), cluster 5 (3d printing and radiology education, in purple).

DISCUSSION

The rapid growth of the scientific community in recent years has made it necessary to show the research habits, trends and effects of a topic through scientific data in many respects (Ji et al., 2021). In this study, anatomy education and technology studies were analysed based on bibliometric and visualization methods to reveal the current state of technology use in anatomy education worldwide. The top publications, the researchers, publishers, countries and keywords were presented in order to examine the best teaching practices in the field of anatomy and to show the change of these practices with the developing technology.

The inclusion of modern and alternative approaches in the education process is an indispensable element of the education sector (Kurt et al., 2013). A number of developments were observed in the teaching resources used in anatomy education in the world at the beginning of the 21st century. The methods of teaching and learning anatomy have been extended with new tools and supports (Duparc et al., 2019). In this study, it was clearly observed that the popularity of publications related to technology in anatomy education has increased in recent years. These results suggest that anatomy education continues to be improved with technology-based materials. In fact, it was confirmed in our study that about half of the publications on the topic were published in the last three years and the number of citations made in these years constituted approximately 60% of all years. The increasing need for online education during the pandemic may also have had an impact on the increase in publications. The COVID-19 pandemic, which caused the interruption of face-to-face education in all forms of education, has also had tremendous effects on anatomy education (Iwanaga et al., 2021). In this process, as technology allows for students, educators added educational dissection videos to distance learning, students were encouraged to watch videos from social media such as YouTube, and universities acquired digital resources that support online learning (Franchi, 2020; Pather et al., 2020). The fact that the keywords used by the authors in our study in recent years are words such as COVID-19 and social media supports this situation.

Many years ago, many famous anatomists and practitioners in history, such as Vesalius, travelled along Europe's largest universities and contributed to the exchange of anatomical knowledge (Duparc et al., 2019). Today, information exchange can be monitored between authors, institutions and countries through simple software. A previous study reported the most influential countries in the world in the field of anatomy education as the United States, England and Australia, respectively. In this previous study, it was stated that these three countries have 70% of anatomy education publications (Kurt et al., 2013). The results in our study were similar to the findings of this previous study. Moreover, our study showed that these productive countries often cooperate with different countries. It can be predicted that these countries will come to the fore more than other countries in shaping the future of anatomy education. Another study, examining the publications of countries in the field of educational technology, reported the ten most productive countries as the United States, England, Taiwan, Australia, Netherlands, Canada, Turkey, Greece, Singapore and Germany, respectively (Hsu et al., 2013). As a matter of fact, as seen in the previous study, it is seen that the leading countries in the field of edu-

cational technologies were among the most effective and productive countries in our study (United States, England, Australia, Netherlands, Canada, Turkey and Germany). Advances in educational technologies of countries may have also affected publications about technology in anatomy education. We also emphasize that due to the educational policies and practices of each country or related industry developments, technology in terms of anatomy education between countries can be applied to different research programs and the current study results have a general perspective.

One of the most interesting publications on anatomy education is "*The Anatomy of Anatomy: A Review for Its Modernization*" (Sugand et al., 2010). Since its publication, it has been cited many times by other researchers. Despite frequent citations from this study, it was not in the first place in the current study in terms of total link strength. This indicates that the high number of citations may not always contain high links to other studies. A time effect occurring in terms of citation and link data may also have affected the findings. It might be more helpful to look at the download number when some kind of time effect maths added. Respectively by Trelease (2016) and Ghosh (2017), "*From Chalkboard, Slides, and Paper to e-Learning: How Computing Technologies Have Transformed Anatomical Sciences Education*" and "*Cadaveric Dissection as an Educational Tool for Anatomical Sciences in the 21st Century*" showed higher links with other work (Ghosh, 2017; Trelease, 2016). These 3 publications were published in Anatomical Sciences Education, which is one of the respected journals in the field of anatomy, as well as about half of the publications on anatomy education and technology in the current study. The main explanation for this situation can be explained by the content of the journal, the compatibility relationship between the publication, the author and the journal. Researchers will follow a significant part of the publications that will shape the future about anatomy education, which probably includes technological materials, through these current journals.

The publications on technology in anatomy education have increased due to the use of digital technologies in the field of education as in every field and the limitation of face-to-face education due to pandemic conditions. However, educators should pay attention to the use of technology in anatomy education. It is too early to accept that technology will be useful in anatomy education. Randomized controlled studies are still needed to show which method or methods are effective (Singh et al., 2019). Quality and bias-free studies can enable anatomy educators to understand which technology to use and when to use them. It may be beneficial to match such emerging and developing digital technologies with the learning characteristics of individuals in anatomy education (Pringle and Rea, 2018).

The author keywords are an important part of the literature and can be used to reflect research points in a particular field (Qin et al., 2020). At this point, in a previous study investigating digital technologies in anatomy education by creating various keywords, it was determined that 3D virtual reality models were the most common and effective digital technology used, followed by internet-based resources and computer-assisted learning (Pringle and Rea, 2018). In the recent past, videos, computer aided teaching methods, multimedia media resources, plastic anatomical models and the use of plastination were frequently used in the past in terms of anatomy education (Estai and Bunt, 2016; Hulme and Strkalj, 2017; Ogunranti, 1987). In our study, besides the keywords containing education, keywords such as virtual reality, 3D printing and E-learning were the keywords at the forefront of technology. The keywords suggest that the technologies of anatomy education were becoming increasingly widespread and important.

In our study, it was seen that the authors who focus on anatomy education continue to use keywords such as "technological" and "cadaver dissection" or just "dissection". This indicates that an effective anatomy learning and teaching methodologies are still discussed in the literature. Although new trends in anatomical education are introduced, not all universities or training centres can meet these approaches. A curriculum plan that includes different combinations of anatomy teaching approaches is highly institution-specific. The cost of any method to be chosen may be much more important at this point. In a recent

study, dissection, plastinated specimens, simulation, virtual dissection tables, plastic models and computer-aided teaching/learning methods were ranked from expensive to economical, respectively (Chumbley et al., 2020). In fact, it is a fact that, besides the high cost of using cadavers, there are many disadvantages such as cadaver supply, transportation, storage, short-term usability and psychological stress (Sahin and Cavus, 2019). At this point, perhaps computers will be preferred more by students and educators because they are advantageous in terms of both time and cost.

Contrary to studies stating that cadaver-based approaches are losing their effectiveness in anatomy education today (Singh et al., 2019; Turney, 2007), one of the keywords frequently used in our study is "cadaver dissection". Our findings were in line with a previous study. The top-ten keywords featured in our current study reflect the link between technology and anatomy teaching. Immediately after these came "cadaver dissection". This situation still points to the importance of traditional cadaver-based methods. Kurt et al. (2013) reported similar findings. Although the use of all these new and technologically developed methods has reduced both the time required for education and the cost of education, traditional cadaver teaching continues to be the preferred learning resource for medical students today. In addition, teaching based on prosection and plastination is more suitable for students of dentistry, pharmacy and related health sciences (Estai and Bunt, 2016). Anatomy knowledge is necessary in all invasive or non-invasive evaluation and treatment applications, especially in human surgical interventions (Turney, 2007). Therefore, it requires the best design of the anatomy curriculum in medical education. In our study, the keywords "cadaver dissection" and "dissection" had links with medical anatomy education in particular. These results suggest that the technological methods researched in anatomy education reflect the increasing search for alternatives due to the problems experienced with cadavers all over the world. As a matter of fact, recent research has emphasized that technological interventions and modern teaching methods should be preferred as an adjunct to or complementary to cadaver teaching in standardized medical curriculum (Kurt et al., 2013, Kumar and Singh, 2020; Zargaran et al., 2020).

The present study has some limitations. Since the study included results from only one database, publications related to the topic in other databases could not be evaluated. In addition, bibliometric indicators are limited to assessing the impact of research within the scientific community, and newer studies are disadvantaged here due to limited interaction. On the other hand, this study reveals the relationships between previous studies on anatomy education and technology, and provides an opportunity to identify common relationships in themes such as authors, countries, keywords of some frequently cited research and compilation publications. It also adds a different perspective to researchers by presenting a bibliometric methodology about studies on anatomy education and technology (Pringle and Rea, 2018; Zargaran et al., 2020) and the general trends of publications in recent years. It has been found that the publications on technology in anatomy have increased, especially the anatomy curriculum in medical faculties, and 3D printing, virtual reality, augmented reality and social media content are included. Reviewing this study while planning new studies on this specific topic may provide convenience to researchers, especially in terms of quickly evaluating cooperation between authors, publications and countries. For all these reasons, we think that the results of this study contain information that will guide researchers who are interested in anatomy education.

ETHICS APPROVAL

The study protocol was approved by the Clinical Research Ethics Committee of the university (Number: 2021/491).

AVAILABILITY OF DATA AND MATERIAL

The datasets used and/or analysed during the current study are available at the following URL: https://www.webofscience.com/wos/woscc/summary/536c467b-47e5-498d-ad8f-9fbffa51e612-1a1923e0/times-cited-descending/1

CONTRIBUTIONS

YEK and EA contributed to the study conception and design. Material preparation, data collection and anal-

ysis were performed by YEK. The first draft of the manuscript was written by YEK, and all authors commented on previous versions of the manuscript. All authors read and approved the final manuscript.

REFERENCES

BAHŞI I, BAHŞI (2019) "Teşrih-ül Ebdan ve Tercümânı Kıbale-i Feylesûfan": the first illustrated anatomy handwritten textbook in Ottoman-Turkish medicine. *Surg Radiol Anat,* 41(10): 1135-1146.

CHUMBLEY SD, DEVARAJ VS, MATTİCK K (2021) An approach to economic evaluation in undergraduate anatomy education. *Anat Sci Educ*, 14(2): 171-183.

DE BAKKER FG, GROENEWEGEN P, DEN HOND F (2005) A bibliometric analysis of 30 years of research and theory on corporate social responsibility and corporate social performance. *Bus Soc*, 44(3): 283-317.

DUPARC F, GRIGNON B, KACHLIK D (2019) History in anatomy education. *Surg Radiol Anat*, 41(10): 1101-1102.

DUQUE OLIVA EJ, CERVERA TAULET A, RODRÍGUEZ ROMERO C (2006) A bibliometric analysis of models measuring the concept of perceived quality inproviding internet service. *Innovar*, 16(28): 223-243.

ELEAZER CD, SCOPA KELSO R (2018) Influence of study approaches and course design on academic success in the undergraduate anatomy laboratory. *Anat Sci Educ,* 11(5): 496-509.

ESTAI M, BUNT S (2016) Best teaching practices in anatomy education: A critical review. *Ann Anat,* 208: 151-157.

FALAH J, KHAN S, ALFALAH T, ALFALAH SF, CHAN W, HARRISON DK, CHARISSIS V (2014) Virtual Reality medical training system for anatomy education. *Science and Information Conference*, IEEE, 752-758.

FRANCHI T (2020) The impact of the Covid-19 pandemic on current anatomy education and future careers: a student's perspective. *Anat Sci Educ,* 13(3): 312-315.

GHOSH SK (2017) Cadaveric dissection as an educational tool for anatomical sciences in the 21st century. *Anat Sci Educ,* 10(3): 286-299.

HEBEBCI MT (2021) The bibliometric analysis of studies on distance education. *Int J Technol Educ*, 4(4): 796-817.

HSU YC, HUNG JL, CHING YH (2013) Trends of educational technology research: More than a decade of international research in six SSCI-indexed refereed journals. *Educ Technol Res Dev,* 61(4): 685-705.

HULME A, STRKALJ G (2017) Videos in anatomy education: history, present usage and future prospects. *Int J Morphol*, 35(4): 1540-1546.

IWANAGA J, LOUKAS M, DUMONT AS, TUBBS RS (2021) A review of anatomy education during and after the COVID-19 pandemic: Revisiting traditional and modern methods to achieve future innovation. *Clin Anat*, 34(1): 108-114.

JI P, JIN J, KE ZT, LI W (2022) Co-citation and co-authorship networks of statisticians. *J Bus Econ Stat,* 40(2): 469-485.

KUMAR R, R SINGH (2020) Model pedagogy of human anatomy in medical education. *Surg Radiol Anat,* 42(3): 355-365.

KURT E, YURDAKUL SE, ATAÇ A (2013) An overview of the technologies used for anatomy education in terms of medical history. *Procedia Soc Behav Sci,* 103: 109-115.

LIUPOST (2021) Bibliometrics: Tools and Software. Available at: https://liu.cwp.libguides.com/c.php?g=225325&p=4966525.

MAS-TUR A, ROIG-TIERNO N, SARIN S, HAON C, SEGO T, BELKHOUJA M, PORTER A, MERIGÓ JM (2021) Co-citation, bibliographic coupling and leading authors, institutions and countries in the 50 years of Technological Forecasting and Social Change. *Technol Forecast Soc Change,* 165: 120487.

MOXHAM BJ, O PLAISANT (2014) The history of the teaching of gross anatomy - how we got to where we are. *Eur J Anat,* 18: 219-244.

OGUNRANTI J (1987) Video technology in integrated anatomy education. *J EducTelev,* 13(1): 63-67.

PATHER N, BLYTH P, CHAPMAN JA, DAYAL MR, FLACK NAMS, FOGG QA, GREEN RA, HULME AK, JOHNSON IP, MEYER AJ, MORLEY JW, SHORTLAND PJ, ŠTRKALJ G, ŠTRKALJ M, VALTER K, WEBB AL, WOODLEY SJ, LAZARUS MD (2020) Forced disruption of anatomy education in Australia and New Zealand: an acute response to the Covid-19 pandemic. *Anat Sci Educ,* 13(3): 284-300.

PETEKKAYA E, KARADAĞ M, DOKUR M (2021) Bibliometric and altmetric analysis of publications examining education methods in realm of anatomy. *Eur Res J,* 7(4): 391-408.

PRINGLE Z, P REA (2018) Do digital technologies enhance anatomical education? *Practice Evidence Scholarship Teach Learn Higher Educ,* 13(1): 2-27.

QIN F, DU J, GAO J, LIU G, SONG Y, YANG A, WANG H, DING Y, WANG Q (2020) Bibliometric profile of global microplastics research from 2004 to 2019. *Int J Environ Res Public Health,* 17(16): 5639.

SAHIN T, CAVUS N (2019) Education in the digital age: technological trends in anatomy education. *Folklor/Edebiyat,* 25(97): 31-46.

SCHAEFER AF, WILSON AB, BARGER JB, AZIM HM, BROKAW JJ, BROOKS WS (2019) What does a modern anatomist look like? Current trends in the training of anatomy educators. *Anat Sci Educ*, 12(3): 225-235.

SCOTT T (1993) How we teach anatomy efficiently and effectively. *MedTeach,* 15(1): 67-75.

SINGH K, BHARATHA A, SA B, ADAMS OP, MAJUMDER, MAA (2019) Teaching anatomy using an active and engaging learning strategy. *BMC Med Educ,* 19(1): 1-8.

SUGAND K, ABRAHAMS P, KHURANA A (2010) The anatomy of anatomy: a review for its modernization. *Anat Sci Educ,* 3(2): 83-93.

TRELEASE RB (2016) From chalkboard, slides, and paper to e learning: How computing technologies have transformed anatomical sciences education. *Anat Sci Educ,* 9(6): 583-602.

TURNEY BW (2007) Anatomy in a modern medical curriculum. *Ann R Coll Surg Engl,* 89(2): 104-107.

VAN ECK NJ, WALTMAN L (2010) Software survey: VOSviewer, a computer program for bibliometric mapping. *Scientometrics,* 84(2): 523-538.

VAN ECK NJ, WALTMAN L (2014) Visualizing Bibliometric Networks. In: Ding Y, Rousseau R, Wolfram D (eds). *Measuring scholarly impact: Methods and practice*. Springer, Cham, pp 285-320.

VAN RAAN A (2003) The use of bibliometric analysis in research performance assessment and monitoring of interdisciplinary scientific developments. *TATuP-Zeitschrift Technikfolgenabschätzung Theorie Praxis,* 12(1): 20-29.

ZARGARAN A, TURKI MA, BHASKAR J, SPIERS HVM, ZARGARAN D (2020) The role of technology in anatomy teaching: striking the right balance. *Adv Med Educ Pract,* 11: 259-266.